PRAIRIE PLANT RESPONSES TO CLIMATE CHANGE IN THE PACIFIC NORTHWEST

by

PAUL BARTON REED

A DISSERTATION

Presented to the Environmental Studies Program
and the Division of Graduate Studies of the University of Oregon
in partial fulfillment of the requirements
for the degree of
Doctor of Philosophy

June 2021

DISSERTATION APPROVAL PAGE

Student: Paul Barton Reed

Title: Prairie Plant Responses to Climate Change in the Pacific Northwest

This dissertation has been accepted and approved in partial fulfillment of the requirements for the Doctor of Philosophy degree in Environmental Sciences, Studies, and Policy by:

Bitty Roy	Chairperson
Scott Bridgham	Advisor
Lucas Silva	Core Member
Lauren Hallett	Core Member
Laurel Pfeifer-Meister	Core Member
Bart Johnson	Institutional Representative

and

Andy Karduna	Interim Vice Provost for Graduate Studies

Original approval signatures are on file with the University of Oregon Division of Graduate Studies.

Degree awarded June 2021

DISSERTATION ABSTRACT

Paul Barton Reed

Doctor of Philosophy

Environmental Sciences, Studies, and Policy

June 2021

Title: Prairie Plant Responses to Climate Change in the Pacific Northwest

Understanding how plants respond to climate change is of paramount importance since their responses can affect ecosystem functions and patterns of biodiversity. At the population level, climate change may alter phenology or demographic performance, causing a shift in where a species can persist. Despite being necessary to predict geographic range shifts, the effects of climate change on populations across large spatial gradients are not well understood. At the community level, changes to biotic interactions can amplify or counteract direct climatic effects and drive changes in plant community composition. Although plant community responses to climate change have been studied extensively, significant questions remain about the underlying mechanisms that drive those responses. These challenges make it difficult to predict the effects of future climate change on ecosystems.

Prairies in the western Pacific Northwest are critically endangered ecosystems whose flora may be exceptionally vulnerable to the effects of climate change. As a result, there is growing urgency to understand how plants will respond to climate change in this system. My dissertation addresses these challenges and concerns using a climate manipulation experiment embedded within a latitudinal climate gradient in the western Pacific Northwest. The studies presented herein provide novel information about prairie

plant phenological, demographic, and community responses to changes in temperature, moisture, and other factors. In Chapter II, I investigate how changes in temperature and moisture affect flowering times and temporal patterns of vegetation growth across a latitudinal gradient. In Chapters III and IV, I model the demographic performance of a suite of 14 native species, including six perennials (Chapter III) and eight annuals (Chapter IV). Several of these species are range-limited, providing novel insight about the differential responses to climate change within versus beyond current range boundaries. Finally, Chapter V explores the direct and indirect pathways of climate-driven community change and expands our mechanistic understanding of the factors underlying plant community composition. Throughout these chapters, I infer how plant responses to climate change may affect regional prairie conservation and restoration efforts in the future.

This dissertation includes previously published and unpublished coauthored material.

CURRICULUM VITAE

NAME OF AUTHOR: Paul Barton Reed

GRADUATE AND UNDERGRADUATE SCHOOLS ATTENDED:

University of Oregon, Eugene, OR
University at Buffalo, Buffalo, NY

DEGREES AWARDED:

Doctor of Philosophy, Environmental Sciences, Studies, and Policy, 2021, University of Oregon
Bachelor of Science, Biological Sciences, 2015, University at Buffalo

AREAS OF SPECIAL INTEREST:

Population Ecology
Community Ecology
Conservation
Restoration
Demographic Modeling
Botany
Global Change Ecology

PROFESSIONAL EXPERIENCE:

Graduate Research Fellow, University of Oregon, 2015-2021

Graduate Teaching Fellow, University of Oregon, 2015-2017, 2020-2021

Research Assistant, Haznedaroğlu Lab, Department of Civil, Structural, and Environmental Engineering, University at Buffalo, 2013

Research Assistant, Jacobs Lab, Department of Microbiology and Immunology, University at Buffalo, 2012-2013

GRANTS, AWARDS, AND HONORS:

USDA-NIFA Postdoctoral Fellowship, 2021-2023

General University Scholarships, University of Oregon, 2020, 2019

Soderwal Environmental Studies Travel Fund, University of Oregon, 2019

Graduate Evolutionary Biology and Ecology Students Summer Travel Award, 2019

Donald Wimber Conference Travel Award, Department of Biology, University of Oregon, 2018

Clarence and Lucille Dunbar Scholarship, University of Oregon, 2016

NSF Graduate Research Fellowship Program Honorable Mention, 2015

Honors College Research and Creativity Fund, University at Buffalo, 2014

President's Circle Study Abroad Scholarship, University at Buffalo, 2014

Undergraduate Study Abroad Fund, University at Buffalo, 2015

NSF Research Experience for Undergraduates Program, University at Buffalo, 2013

Wegmans Employee Scholarships, Wegmans Food Markets, Inc., 2012-2015

PUBLICATIONS:

Reed, P.B., Bridgham, S.D., Pfeifer-Meister, L.E., Peterson, M.L., Johnson, B.R., Roy, B.A., Bailes, G.T., Nelson, A.A., Morris, W.F., and Doak, D.F. (In press). Climate warming threatens the persistence of a community of disturbance-adapted native annual plants. *Ecology*.

Peterson, M.L., Bailes, G., Bridgham, S.D., Hendricks, L., Johnson, B.R., Pfeifer-Meister, L., **Reed, P.B.**, Shriver, R., Waddle, E., Wroton, H., Doak, D.F., Roy, B., and Morris, W.F. (2021). Latitudinal gradients in population growth do not reflect demographic responses to climate. *Ecological Applications*, *31*(2), e02242.

Reed, P.B., Peterson, M.L., Doak, D.F., Morris, W.F., Pfeifer-Meister, L.E., Roy, B.A., Johnson, B.R., Bailes, G.T., Nelson, A.A. and Bridgham, S.D. Climate manipulations differentially affect plant population dynamics within versus beyond northern range limits. *Journal of Ecology*, *109*(2), 664-675.

Reed, P.B., Pfeifer-Meister, L.E., Roy, B.A., Johnson, B.R., Bailes, G.T., Nelson, A.A., Boulay, M.C., Hamman, S.T., and Bridgham, S.D. (2019). Prairie plant phenology driven more by temperature than moisture in climate manipulations across a latitudinal gradient in the Pacific Northwest, USA. *Ecology and Evolution*, *9*(6), 3637–3650.

ACKNOWLEDGMENTS

This body of work was made possible through the tremendous guidance and patience from my colleagues, co-authors, and mentors. First, I would like to thank my primary advisor, Dr. Scott Bridgham, for training me as an ecologist and challenging me to excel as a researcher. I also thank my advisors Dr. Bitty Roy, Dr. Laurel Pfeifer-Meister, and Dr. Bart Johnson. In particular, I thank Bitty for teaching me how to become a botanist, Laurel for always providing clarity and seeing the bigger picture, and Bart for his careful, thorough edits on my writing. I thank Dr. Megan Peterson, Dr. William Morris, and Dr. Daniel Doak for their immense roles in teaching me about plant population demography. Their generous help and patience provided me with the tools I needed to conduct complex demographic analyses. I also thank my committee members, Dr. Lauren Hallett and Dr. Lucas Silva, for providing dissertation advice and encouraging me to apply for the postdoctoral fellowship that I was recently awarded. All my mentors provided unwavering support and guidance throughout my dissertation, for which I am grateful. Finally, I would like to thank my family and friends for the unending support and encouragement.

My dissertation would not have been complete without the collective assistance of many colleagues and field assistants, including: Graham Bailes, Aaron Nelson, Dr. Matthew Krna, Kathryn Nock, Megan Sherritt, Laura McCullough, Annelise Rue-Johns, Leah Thompson, Xing Wu, Aimee Okotie-Oyekan, Hannah Assour, and Holden Jones. In particular, Graham, Aaron, and Matthew were invaluable colleagues who helped me implement experiments and curate much of the data. I thank Peg Boulay and the students of the Environmental Leadership Program and Dr. Sarah Hamman and the AmeriCorp

volunteers with the Center for Natural Lands Management for their work collecting flowering phenology data. I also thank the Siskiyou Field Institute, The Nature Conservancy, and Capitol Land Trust for accommodating our research experiment on their properties. This research was supported by the National Science Foundation's Macrosystems Biology Program, award # 1340847, the Office of Science (Biological and Environmental Research), U.S. Department of Energy, grant # DE-FG02-09ER604719, and the University of Oregon.

TABLE OF CONTENTS

Chapter Page

LIST OF FIGURES

Figure Page

CHAPTER V

LIST OF TABLES

CHAPTER I

INTRODUCTION

As of the decade 2006-2015, anthropogenic climate change has caused an increase in the mean global surface temperature of nearly 1.0°C relative to pre-industrial levels (IPCC 2018). To date, rising temperatures have had well-documented plant ecological effects, including shifts to the timing of biological events [phenology] (Cleland et al. 2007), species' range distributions (Chen et al. 2011), and community compositions (Walther 2010). By the end of the 21st century, climate change models project an additional temperature increase of ~1.0-4.0°C, depending on emissions scenarios (IPCC 2014). Increasing precipitation variability and extreme events such as droughts are likely (Dai 2013, Pendergrass et al. 2017). These projected changes in climate may have major ecological implications, including the continued decline in global biodiversity and negative effects on ecosystem services (Pereira et al. 2010). To predict the ecological implications of future climate change, it is critical to understand plant responses at both the population and community levels.

At the population level, demographic vital rates (i.e., survival, growth, and reproduction) determine where a species can persist. For plant species, climate is a major driver of broad distributional patterns across latitudinal and elevational gradients (MacArthur 1972, Thomas 2010). As the climate changes, demographic performance may decline in some populations, necessitating a range shift in order to persist (Rehm et al. 2015). However, the effects of climate change on demographic performance within versus beyond current range boundaries are not well understood. Since dispersal can be a

major limitation for plants in their ability to keep pace with climate change (Hargreaves et al. 2014, Bayly and Angert 2019), management intervention may be necessary to save some species from disappearing (Vitt et al. 2010). Since management plans generally attempt to optimize benefits for a suite of native species (Wang et al. 2020), a key question is whether demographic responses can be generalized for multiple species.

Population demographic performance is also intrinsically linked to individual-level phenology. For example, premature flowering could negatively affect reproduction by leading to frost damage (Inouye 2008) or creating mismatches with pollinators (Miller-Rushing et al. 2010). Therefore, climate-driven shifts in the timing of key biological events could manifest in consequences at the plant population level. Nevertheless, how temperature and/or moisture regimes control phenological responses are not well understood. This is especially the case when considering multiple populations across large spatial gradients.

Climate effects on individual species scale up to the plant community level and can result in changes to the compositional makeup of a community. Plant functional group composition is a key determinant of ecosystem functions and services (Kremen 2005, McLaren and Turkington 2010). For example, the ratio of native to introduced species is relevant in an ecosystem valued for its biodiversity, while the ratio of perennial to annual species can have important implications for carbon storage and nutrient cycling (Koteen et al. 2011, Miller et al. 2011). While demographic studies can reveal individual species' responses to climate change, the situation becomes more complex at the community scale. Climate change can affect multiple functional groups simultaneously, resulting in changes to biotic interactions within the community. Changes to biotic

interactions can alter competitive dynamics for limiting resources such as moisture, nutrients, or space (Brooker 2006). To date, a major challenge in predicting plant community responses to climate change has been identifying the mechanisms underlying that change. Are changes driven by direct effects, such as temperature, or by indirect pathways, such as competition for limiting resources? Predicting community trajectories and diversity under future climates must start with understanding the direct and indirect pathways of plant community change.

Pacific Northwest Prairies

Prairies in the western Pacific Northwest (PNW) are extremely fragile ecosystems. Historically, these prairies were dominated by a diversity of native bunchgrasses and forbs and were abundant throughout the Klamath Mountains and the Willamette Valley-Puget Trough-Georgia Basin ecoregions (Dennehy et al. 2011, Dunwiddie and Bakker 2011). Native Americans maintained these prairies through frequent burning, as they provided food and other important resources (Boyd 1999). Following Euro-American settlement in the mid-1800's, fire suppression, land conversion, and the establishment of non-native species have contributed to the loss and modification of native prairies (Dennehy et al. 2011). Today they are considered critically endangered ecosystems, with <10% of original prairie habitat remaining (Noss et al. 1995). Those which remain are now largely dominated by introduced cool-season pasture grasses (Sinclair et al. 2006). As a result, many concerted efforts exist to conserve and restore native prairie biodiversity to the landscape (Dunwiddie and Bakker 2011).

The western PNW has a Mediterranean-type climate, characterized by its mild, wet winters and warm-to-hot, dry summers (Kottek et al. 2006). Models for the PNW

project a temperature increase of 2.5-5°C by the 2080s, with changes to precipitation being less certain (Mote and Salathé 2010, Dalton and Fleishman 2021). In general, the seasonality of the Mediterranean-climate system is expected to amplify, with winters becoming wetter and summers becoming drier. Drought potential may rise due to increasing evaporative demands, particularly in the valley lowlands (Jung and Chang 2012) where these prairies occur. Such climatic changes have the potential to exacerbate the decline of the native prairie ecosystem and jeopardize ongoing conservation and restoration efforts. As a result, there is growing urgency to understand plant responses to climate change in this system.

Dissertation Research

The overall objective of my dissertation is to examine how climate change affects plant ecology in Pacific Northwest prairies. More specifically, I seek to determine (1) the climatic controls over phenological shifts at both the population and community levels, (2) the population-demographic responses to climate change for a suite of native species near or beyond their northern range limit, and (3) the causal pathways underlying climate-driven change in functional group composition and species diversity. The intention of this research is two-fold: first, to advance the fields of population and community ecology using a cutting-edge climate manipulation experiment to model demographic performance and community dynamics, and second, to inform future restoration and management efforts of local prairie ecosystems in the face of climate change.

The entirety of my dissertation research came from the Heating of Prairie Systems (HOPS) experiment. HOPS was a climate manipulation experiment that existed at three

sites across a 520 km latitudinal climate gradient in the western PNW. The overarching objective of the HOPS experiment was to subject native prairie species to current and future climatic conditions and test whether demographic responses differed across the latitudinal gradient. The design of the experiment lent itself well to examining plant phenology and community dynamics, as well.

The HOPS experiment had 20 plots per site, divided into five replicates each of four climate treatments. The climate treatments consisted of a control (ambient temperature and precipitation), drought (annual precipitation reduced by 40%), warming (canopy temperatures increased by +2.5°C), and warming + irrigation (temperatures increased by +2.5°C and also irrigated with additional precipitation to ameliorate a warming-induced drying effect). The 40% drought was designed to represent an "extreme" event, as determined by the Precipitation Trends and Manipulation tools from Drought-Net (Lemoine et al. 2016). The +2.5°C warming was consistent with regional expectations for the end of the century (Mote and Salathé 2010).

Prior to plot establishment, all three sites were dominated by introduced perennial pasture grasses. Plots were established in early 2015 using a combination of herbicide application, mowing, and raking, followed by seeding with a consistent mix of 29 grass and forb species native to PNW prairies. Plots were subsequently reseeded in fall 2015, 2016, and 2017 with 14 native prairie species which became the focal species for the demography studies. These 14 focal species were composed of eight annuals and six perennials.

Chapter II of my dissertation is entitled "Prairie plant phenology driven more by temperature than moisture in climate manipulations across a latitudinal gradient in the

Pacific Northwest, USA" and is published in the journal *Ecology and Evolution* (2019). This publication is coauthored by me, Laurel E. Pfeifer-Meister, Bitty A. Roy, Bart R. Johnson, Graham T. Bailes, Aaron A. Nelson, Margaret C. Boulay, Sarah T. Hamman, and Scott D. Bridgham. In 2017 and 2018 of the HOPS experiment, we measured changes in flowering times and the seasonality of canopy biomass growth and senescence in response to our climate treatments. We asked whether phenological responses would differ in direction and/or magnitude at sites across the latitudinal gradient, and whether changes to soil temperature or moisture would be more predictive of responses.

Chapter III is entitled "Climate manipulations differentially affect plant population dynamics within versus beyond northern range limits" and is published in the *Journal of Ecology* (2021). This publication is coauthored by me, Megan L. Peterson, Laurel E. Pfeifer-Meister, William F. Morris, Daniel F. Doak, Bitty A. Roy, Bart R. Johnson, Graham T. Bailes, Aaron A. Nelson, and Scott D. Bridgham. In this publication, we focused on demographic data of the six perennial focal species in the HOPS demography experiment (2016-2018). Of these six perennials, two are "range-restricted," such that their current northern range limits occur south of at least one of the experimental sites. These two species were therefore planted both within and beyond their current ranges. We expected that population growth rates (for all species) would increase from south to north and that the range-restricted species would be able to establish populations when planted beyond their current ranges. Additionally, we expected warming and drought to decrease demographic performance within current ranges, but to be neutral or beneficial for the range-restricted species when planted beyond their current ranges.

Chapter IV is entitled “Climate warming threatens the persistence of a community of disturbance-adapted native annual plants” and is coauthored by me, Scott D. Bridgham, Laurel E. Pfeifer-Meister, Megan L. Peterson, Bart R. Johnson, Bitty A. Roy, Graham T. Bailes, Aaron A. Nelson, William F. Morris, and Daniel F. Doak. This manuscript focuses on demographic data of the eight annual focal species in the HOPS demography experiment (2016-2018) and uses three additional years of data (2010-2012) from a previous iteration of HOPS for a more comprehensive dataset. In this study, we replaced discrete climate treatments with continuous measures of temperature and moisture variables, and categorized plot preparation and management actions into three disturbance categories. For these eight annual species, we asked (1) How does demographic performance vary across a range of current and future climatic conditions? (2) Do these species exhibit similar patterns in population growth rates across climatic space? and (3) How important is the role of disturbance in determining performance and modulating climatic effects?

Chapter V is entitled “Introduced annuals mediate climate-driven community change in Mediterranean prairies of the Pacific Northwest, USA” and is coauthored by me, Laurel E. Pfeifer-Meister, Bitty A. Roy, Bart R. Johnson, Graham T. Bailes, Aaron A. Nelson, and Scott D. Bridgham. This study uses community cover data and continuous measures of temperature, moisture, and soil nitrogen availability from the HOPS experiment (2017-2019). We used structural equation models to examine how abiotic drivers (i.e., temperature, moisture, and nutrients) control plant functional group cover, and how these groups in turn determine overall diversity. We expected warming to favor introduced annuals at the expense of other functional groups and for overall diversity to

decline. In particular, we expected temperature to have strong direct effects on introduced annuals but for climatic effects on other groups to be primarily mediated through the increase in competitive pressure from introduced annuals for soil resources such as moisture and nitrogen.

Chapter VI summarizes the results of the preceding chapters (II-V) and discusses implications for future research.

CHAPTER II

PRAIRIE PLANT PHENOLOGY DRIVEN MORE BY TEMPERATURE THAN MOISTURE IN CLIMATE MANIPULATIONS ACROSS A LATITUDINAL GRADIENT IN THE PACIFIC NORTHWEST, USA

From Reed, P. B., Pfeifer-Meister, L. E., Roy, B. A., Johnson, B. R., Bailes, G. T., Nelson, A. A., Boulay, M. C., Hamman, S. T., & Bridgham, S. D. (2019). Prairie plant phenology driven more by temperature than moisture in climate manipulations across a latitudinal gradient in the Pacific Northwest, USA. *Ecology and Evolution*, 9(6), 3637-3650.

Contributions

P. B. Reed analyzed the data and wrote the manuscript. L. E. Pfeifer-Meister, B. A. Roy, B. R. Johnson, S. D. Bridgham, and P. B. Reed designed the experiment. G. T. Bailes and A. A. Nelson curated the NDVI data. M. C. Boulay and S. T. Hamman facilitated data collection by supporting field assistants. All authors contributed to data collection and provided valuable contributions during the revision process.

Introduction

Plant phenology, the timing of key events in plant life cycles, is shifting with climate change (Cleland, Chuine, Menzel, Mooney, & Schwartz, 2007; Menzel *et al.*, 2006; Parmesan & Yohe, 2003). Shifts have been observed at the individual species level (Fitter & Fitter, 2002; Whittington, Tilman, Wragg, & Powers, 2015), as well as for entire plant communities (Sherry *et al.*, 2007; Theobald, Breckheimer, & Hille Ris

Lambers, 2017), through both observational and manipulative studies. At the plant population level, the first appearance of flowers as well as the timing of peak flowering have important consequences for reproductive success and population viability. Phenological shifts in flowering may create asynchronies among interacting species (Yang & Rudolph, 2010), potentially disrupting mutualisms such as pollination or seed dispersal (Rafferty, Caradonna, & Bronstein, 2015), or result in mismatches with favorable environmental conditions, increasing the potential for detrimental events such as frost damage (Inouye, 2008). Shifts in phenology may also alter demographic vital rates and influence range distributions, which in turn can have large implications for patterns of biodiversity and species extinctions or persistence (Chuine & Beaubien, 2001; Miller-Rushing, Høye, Inouye, & Post, 2010; Parmesan & Yohe, 2003). At the community level, changes to the timing of seasonal biomass growth and senescence can affect processes such as primary productivity, carbon cycling, and competition (Cleland *et al.*, 2007; Tang *et al.*, 2016).

Despite ample evidence of recent phenological shifts, the controls of future shifts are not well understood. Temperature is typically viewed as one of the strongest controls of plant phenology, although other abiotic factors such as photoperiod and moisture can also exert influences (Moore, Lauenroth, Bell, & Schlaepfer, 2015; Rathcke & Lacey, 1985). Phenological events tend to advance with warming and are generally thought to be delayed with drought (Menzel *et al.*, 2006; Wolkovich *et al.*, 2012), although there are conflicting reports regarding the latter (Bernal, Estiarte, & Peñuelas, 2011; Cui, Martz, & Guo, 2017). While most studies have focused on temperature, moisture may be a stronger control than temperature for late-flowering species (Moore & Lauenroth, 2017), and is

especially critical in water-limited ecosystems (Crimmins, Crimmins, & David Bertelsen, 2010; Diez *et al.*, 2012). In Mediterranean climate regions, which are characterized by pronounced cool/wet and warm/dry seasons, moisture becomes increasingly limiting during the latter part of the growing season. Water availability thus becomes a critical factor, and moisture manipulation has been shown to affect plant phenology within Mediterranean regions (Bernal *et al.*, 2011; Hänel & Tielbörger, 2015). Moisture has even been shown to have greater influence on phenology than temperature in some cases, depending on the phenological event (Peñuelas *et al.*, 2004). However, a 60-year observational study of 29 plant species in Spain suggests temperature is the primary driver of changes in phenology in that Mediterranean region (Gordo & Sanz, 2010). The influence of biotic interactions (e.g., competition) on phenology is largely unknown outside the findings of Wolf *et al.* (2017) that plant diversity can affect phenology through its effects on soil temperature, nutrients, and moisture.

Globally, Mediterranean regions contain some of the most imperiled habitat and have among the greatest risks for biodiversity loss (Klausmeyer & Shaw, 2009; Sala *et al.*, 2000). Much of the US Pacific Northwest (PNW) has a Mediterranean climate (Kottek, Grieser, Beck, Rudolf, & Rubel, 2006), and models for the PNW predict ~3°C temperature increases by the end of the 21st century, with increasingly warmer, wet winters and hotter, drier summers including greater drought potential during the growing season (Mote & Salathé, 2010; Jung & Chang, 2012). Native prairie ecosystems in this region have dwindled to <10% of their historic extent and most are highly degraded (Noss, Laroe, & Scott, 1995; Crawford & Hall, 1997; UFWS, 2010) because of land-use change, altered fire regimes and invasive species (Bachelet *et al.*, 2011). Climate change

may further exacerbate the perturbations affecting these ecosystems, causing species range shifts or contractions, declining populations, or altering biogeographic patterns (Pfeifer-Meister *et al.*, 2013, 2016). Considering the vulnerability of prairie species and communities within this region, it is thus imperative to explore the implications of changing temperature and moisture patterns on prairie plant phenology and abundances, so managers and regulators can plan and adapt practices and policies.

Several studies have demonstrated the robustness of integrating manipulative experimentation with natural climate gradients to identify climate change effects on species, communities, and ecosystems (Dunne, Harte, & Taylor, 2003; Dunne, Saleska, Fischer, & Harte, 2004; Frenne *et al.*, 2013; Pfeifer-Meister *et al.*, 2013). However, this approach has been underutilized for phenological studies (but see Henry & Molau, 1997; Dunne *et al.*, 2003; Prieto *et al.*, 2009), especially considering that latitude may influence the magnitude or sensitivity of responses to climate change (Parmesan, 2007; J. Prevéy *et al.*, 2017). Additionally, manipulative experiments designed to study climate change effects on phenology often impose extensions of the growing season via snow removal, temperature increases, or moisture manipulations (Bernal *et al.*, 2011; Peñuelas *et al.*, 2004; Rosa *et al.*, 2015; Tielbörger *et al.*, 2014; Whittington *et al.*, 2015) but rarely are designed to manipulate both temperature and moisture, despite potentially confounding effects (Wolkovich *et al.*, 2012).

Here, we manipulated both temperature and soil moisture in three prairies across a 520 km latitudinal Mediterranean climate gradient within the PNW to examine the responses of plant phenology at both the population and community levels. At the population level, we focused on the flowering times of eight native, range-restricted focal species that we

planted within and beyond their current ranges. Additionally, as we discovered that many species had very low survival (limiting our sample size for the flowering phenology data), we also examined how site and climate impacted their abundances. At the community scale we focused on the seasonality of growth and senescence of canopy biomass. We asked: (1) How will the phenology of individual species, as well as prairie plant communities, respond to climate change across a latitudinal gradient? (2) Will range-restricted species' phenological responses and flowering abundances differ in direction and/or magnitude when planted within versus beyond their current northern range limits? And, (3) will changes to soil temperature or moisture be more predictive of phenological responses?

Materials and Methods

Site Descriptions:

The study was conducted at three sites from southwestern Oregon to central-western Washington in the Pacific Northwest (PNW) (Appendix A: Figure S2.1, Table S2.1). The southern site is in the Klamath-Siskiyou ecoregion of southwestern Oregon, the central site is at the southern end of the Willamette Valley ecoregion in western Oregon, and the northern site is in the Puget Trough ecoregion of central-western Washington (U.S. EPA, 2011). There is a strong climate gradient from north to south, with the northern site experiencing the coolest mean annual temperatures and most mesic summer soil moistures, the central site experiencing intermediate temperatures and soil moisture, and the southern site experiencing the warmest mean annual temperatures and driest soils in the summer (Pfeifer-Meister *et al.*, 2013, 2016) (Appendix A: Table S2.1, Figure S2.2).

Experimental Design:

At each site, 20 circular plots (7.1 m^2) were randomly assigned to one of four climate treatments with five replicates each: control (ambient temperature and precipitation), warming (canopy temperature raised by 2.5°C), warming with additional precipitation (warming + ppt; plots irrigated to fully offset a warming-induced drying effect), and drought (annual precipitation reduced by 40%). The southern and central sites were part of a previous experiment from 2010-2012 with a different set of treatments consisting of control, warming by 2.5°C, increased precipitation intensity by 20%, and warming by 2.5°C + increased precipitation intensity by 20% (Pfeifer-Meister *et al.*, 2013, 2016; Reynolds *et al.*, 2015). However, the precipitation intensity treatments had almost no effect on either plant or ecosystem responses since most of the additional water was applied during the wet season (Pfeifer-Meister *et al.*, 2013, 2016; Reynolds *et al.*, 2015). Thus, the current experiment has the same control and warming treatments at the two southernmost sites, but the enhanced precipitation intensity plots became the drought plots, and the warming plus enhanced precipitation intensity plots became the warming + ppt plots of the current experiment. The northern site was newly established for this experiment.

Warming treatments were achieved using six 2000-W infrared heaters per plot, as described in Pfeifer-Meister *et al.* (2013). The warming + ppt plots used an automated sprinkler system (with rainwater collected on site) designed to irrigate these plots for 30 minutes each night that the volumetric water content was below 95% of the control plot average. The drought treatment used a common fixed rain-out shelter design, with clear acrylic shingles (MultiCraft Plastics, Eugene, OR) covering 40% of the plot area to

prevent 40% of annual rainfall from reaching the plot. The acrylic material has high light transmittance, reducing microclimatic impacts such as shading concerns or temperature buffering (Gherardi & Sala, 2013; Yahdjian & Sala, 2002). The 40% reduction in annual precipitation represents an "extreme" drought, consistent with a one-in-100-year event for the three sites, determined using the Precipitation Trends and Manipulation tools from Drought-Net (Lemoine, Sheffield, Dukes, Knapp, & Smith, 2016). Drought treatments were installed in February 2016, all warming treatments initiated by summer 2016, and irrigation initiated during summer 2016. Heaters were turned off in August and September 2017 at all three sites due to fire hazard. We used dataloggers to record continuous canopy temperature, soil temperature (at 10 cm depth) and volumetric water content (to 30 cm depth) within each plot. To compare soil moisture across sites with considerably different soil characteristics, we calculated soil matric potentials as described in Saxton and Rawls (2006). See Appendix A: Figure S2.2 for data on soil temperature and matric potential in plots during the study. Due to heater malfunctions in one of the central-site warming plots for a period of the 2017 growing season, we excluded data from this plot for phenological analyses occurring during that time.

Between October 2014 – January 2015, all plots at the southern and central sites were mowed and raked while the new northern plots were treated with Glyphosate 2% (a total of three times) to remove standing biomass. By February 2015, all plots were seeded with a common mix of 29 native grass and forb species found in PNW prairies (Pfeifer-Meister *et al.*, 2013). Additionally, in fall of both 2015 and 2016, we seeded between 80-200 seeds per species of 14 range-restricted species within each plot for the purposes of a separate demography experiment. These species were selected for having medium to high

fidelities to upland prairies with geographic range distributions within the PNW (~41–50° latitude). Due to low establishment of six of these 14 species at all sites, only eight were used as focal species in this study (Table 2.1). For each species and site, we used seeds from the nearest available source population. Four species (*Collinsia grandiflora*, *Festuca roemeri*, *Microseris laciniata*, and *Plectritis congesta*) had unique sources for each site; the remaining four species (*Achyracheana mollis*, *Plagiobothrys nothofulvus*, *Ranunculus austro-oreganus*, and *Sidalcea malviflora*) had single sources for all sites.

Focal Species	Abbreviation	Family	Growth Habit	Duration	Approximate Northern Range Limit
Achyrachaena mollis Schauer	ACHMOL	Asteraceae	Forb	Annual	~43°N
Collinsia grandiflora Douglas ex Lindl.	COLGRA	Plantaginaceae	Forb	Annual	~50°N
*Festuca roemeri**	FESROE	Poaceae	Grass	Perennial	~50°N
Microseris laciniata (Hook.) Sch. Bip. ssp. laciniata	MICLAC	Asteraceae	Forb	Perennial	~50°N
Plagiobothrys nothofulvus A. Gray	PLANOT	Boraginaceae	Forb	Annual	~46°N
Plectritis congesta (Lindl.) DC.	PLECON	Valerianaceae	Forb	Annual	~50°N
Ranunculus austro-oreganus L.D. Benson	RANAUS	Ranunculaceae	Forb	Perennial	~43°N
Sidalcea malviflora (DC.) A. Gray ex Benth. ssp. virgata (Howell) C.L. Hitchc.	SIDMAL	Malvaceae	Forb	Perennial	~46°N

Table 2.1. Characteristics of the eight focal species analyzed for flowering phenology observations. *Note: Variety *roemeri* Yu. E. Alexeev at the central and northern sites; variety *Klamathensis* B.L. Wilson at the southern site.

Phenology Data:

From April – mid-June 2017, we collected flowering and abundance data on our eight focal species on a weekly (central and northern sites) or biweekly (southern site) basis. For each forb species, we tallied the total number of open flowers (defined by the presence of exposed stamens or stigmas) within each plot. For the lone grass species (*F. roemeri*), we tallied the total number of reproductive stalks containing spikelets (hereafter

considered flowers). For all species, we recorded the total number of flowering individuals. From these observations, we identified the first flowering dates (FFD) and peak flowering dates (PFD) for each species in each plot. Additionally, we calculated temperature sensitivities (change in days per °C) for each species at each site as: (phenological event date$_{i,\ warm}$ – phenological event date$_{ambient\ avg}$) / ΔT, where ΔT is the difference in temperature between the warmed and ambient plots, or 2.5°C.

At the community level, we regularly measured the phenology of the canopy biomass from November 2016 – August 2018 by determining the amount of live green vegetation using a handheld Crop Circle ACS-430 sensor (Holland Scientific Inc.), which calculates the normalized difference vegetation index (NDVI) from measurements taken above each plot canopy. NDVI is an index of "greenness" on a scale of -1 to 1, with increasing values indicating a greater quantity of live biomass (Pettorelli *et al.*, 2005). For each plot, we calculated the date of peak biomass (maximum NDVI), date of senescence, and rate of senescence for both 2017 and 2018, and the length of the growing season from fall 2017 through summer 2018. We did not include the previous growing season length since we lacked regular NDVI measurements in fall 2016. For the date of senescence, we chose the first date following peak biomass at which the NDVI was ≤ 80% of the peak. We calculated the rate of senescence as the slope (ΔNDVI/days) for the three sampling points with the greatest decline in NDVI. For the southern site in 2018, we only used two sampling points because senescence was so rapid that three sampling points would not have been linear. Lastly, we calculated the length of the growing season as the difference in days between the fall 2017 green-up (the first date following the summer 2017 minimum at which the NDVI was ≥ 125% of the minimum) and the end of

the season (the 2018 date of senescence). This timeframe represents a full growing season in this Mediterranean climate system, as vegetation growth commences with the return of the fall rains and ceases with the return of the summer drought.

Statistical Analyses:

All analyses used R version 3.3.2 (R Core Team, 2016). Site and climate treatment effects on flowering phenology were determined by analysis of variance (ANOVA), whereas significant differences among sites and climate treatments within sites were tested using Tukey's post-hoc comparisons. Because the control and drought treatments never differed for either FFD or PFD ($p \geq 0.19$) and the warming and warming + ppt treatments only marginally differed for PFD for one species ($p = 0.07$; all other cases $p \geq 0.15$), we collapsed the climate treatments into two temperature categories: ambient (control and drought) and warming (warming and warming + ppt) and reran analyses. Due to site x warming interactions, we tested for site effects using ambient plots only. Within sites, we tested for an effect of warming using two tailed t-tests. PFD data for *C. grandiflora* at the northern site were excluded due to an overwhelmingly large sample size (> 500 plants per plot) which made it logistically impossible to count flowers during its peak growing period.

To test for site and climate treatment impacts on flowering abundances, we ran generalized linear models for each species, testing for the best fit among Poisson, negative-binomial, and zero-inflated models by comparing Akaike information criterion (AIC). We selected the model with the lowest AIC value and tested for goodness-of-fit with a chi-square test. Finally, we identified significant effects using likelihood-ratio chi-

square tests. When a significant site x climate treatment interaction was present, we repeated this process within each site to test for climate treatment effects.

We analyzed multi-year NDVI variables (date of peak biomass, date of senescence, and rate of senescence) with repeated measures ANOVAs with site and climate treatment as between-subject effects and year as a within-subject effect. Following significant year interactions, we tested these variables (and 2018 growing season length) within years against site, climate treatment, and their interaction with ANOVAs. Additionally, to test for differences in NDVI on sampling dates across the duration of measurement, we conducted repeated measures ANOVAs with sampling date as a within-subject effect. We used logit-transformations to improve normality and Greenhouse-Geisser corrections when sphericity was violated. Following site x date interactions, we conducted repeated measures ANOVAs within each site. Lastly, following date x climate treatment interactions, we performed one-way ANOVAs on each date. Again, we found no differences between the control and drought treatments and between the warming and warming + ppt treatments for any of these analyses ($p > 0.10$), so we collapsed to the two ambient and warming categories and reran all NDVI analyses.

Using plot-level environmental data, we tested for trends in phenology response variables to soil temperature and moisture variables within and across sites. We excluded FFD and PFD data for *M. laciniata* and *R. austro-oreganus* since these species only survived at a single site. We calculated annual environmental variables using the durations 15-Jul-2016 – 15-Jul-2017 for 2017 phenology variables and 15-Jul-2017 – 15-Jul-2018 for 2018 phenology variables. For temperature variables, we used mean annual

(MAT), mean winter (MWT; 1-Dec – 28-Feb), and mean spring (MST; 1-Mar – 31-May) soil temperatures. For soil moisture variables, we looked at the annual number of days below wilting point (-1,500 kPa; DBWP); the mean annual matric potential (MAMP; adjusted to account for wilting point so any value < -1,500 became -1,500); and the date of first wilting point (DFWP). Strong correlations among the three temperature variables as well as the three soil moisture variables made it inappropriate to include all variables in multiple regression. Instead, for each response variable, we created 15 total models: each combination of one temperature variable with one moisture variable (nine models), and each temperature and each moisture variable alone (six models). Then for each response variable, we used the MuMIn package (Barton, 2018) to compare and rank each model using the small-sample-size corrected version of Akaike Information Criterion (AICc). Here, we report models that would be deemed equivalent based on a $\delta AICc < 2$. However, we do not report two parameter models if their AICc score was greater than a model that included only one of its parameters to maintain parsimony in interpretation. Following model ranking, we compared relative variable importance values to identify the most important explanatory variable for each response variable. These values are calculated by taking the sum of the Akaike weights (ω) over all models that include the explanatory variable (Burnham & Anderson, 2002). While there can be cases of over-interpreting relative variable importance values (Galipaud, Gillingham, David, & Dechaume-Moncharmont, 2014), it is nonetheless a reliable method if the only goal is simply to identify the single most important explanatory variable relative to all others.

Results

Reproductive Plant Abundances:

Site had a strong effect on focal species' abundances. In general, the number of reproductive plants increased dramatically from south to north (Figure 2.1; Appendix A: Table S2.2). To a lesser extent, climate treatment also affected the number of reproductive plants, but effects varied considerably by species and were generally idiosyncratic within sites (Figure 2.1; Appendix A: Table S2.2). Several species had small or nonexistent reproductive populations at certain sites, within certain climate treatments, or a combination; *R. austro-oreganus* and *M. laciniata* did not survive to reproduce at all at either the southern or central sites, nor did *F. roemeri* at the southern site. These abundance constraints ultimately hindered our ability to analyze all aspects of the flowering phenology data.

		Southern				Central				Northern			
		C	D	W	WP	C	D	W	WP	C	D	W	WP
WS	PLECON	9	4	5	0	102	80	37	32	56	57	33	45
HRL	COLGRA	0	0	0	0	9	14	1	2	644	336	449	215
	FESROE	0	0	0	0	5	4	5	5	7	9	3	5
	MICLAC	0	0	0	0	0	0	0	0	10	10	6	3
IRL	SIDMAL	8	11	3	2	1	0	1	1	22	24	24	25
	PLANOT	0	0	0	0	7	4	1	1	0	3	0	0
LRL	RANAUS	0	0	0	0	0	0	0	0	2	6	6	4
	ACHMOL	1	1	0	1	2	4	1	1	3	15	6	12

Figure 2.1. Median abundances of reproductive plants across the four climate treatments at each site. Shading is scaled independently for each species; darker corresponds to greater median abundances under that treatment and site, lighter corresponds to lesser median abundances. C = control, D = drought, W = warming, WP = warming + ppt. Northern range-limit groups: WS = Widespread, HRL = highest northern range limit (~50°N), IRL = intermediate northern range limit (~46°N), LRL = lowest northern range limit (~43°N; see Table 2.1).

Flowering Phenology:

In general, warming advanced both first (FFD) and peak (PFD) flowering dates at all sites. FFD advanced under warming for four of five species at the southern site, three of five species at the central site, and all eight species at the northern site (Figure 2.2a;

Appendix A: Table S2.3). A fourth species at the central site, *P. congesta*, also flowered seven days earlier in all warming plots compared to all ambient plots (Figure 2.2a); however, *P. congesta* did not exhibit any variability in FFD among the warming plots (n = 9) nor the ambient plots (n = 10), so we were unable to perform statistical tests on this species at this site. PFD advanced under warming relative to ambient temperature for three of five species at the southern site, four of six species at the central site, and all seven species with PFD data at the northern site (Figure 2.2b; Appendix A: Table S2.4).

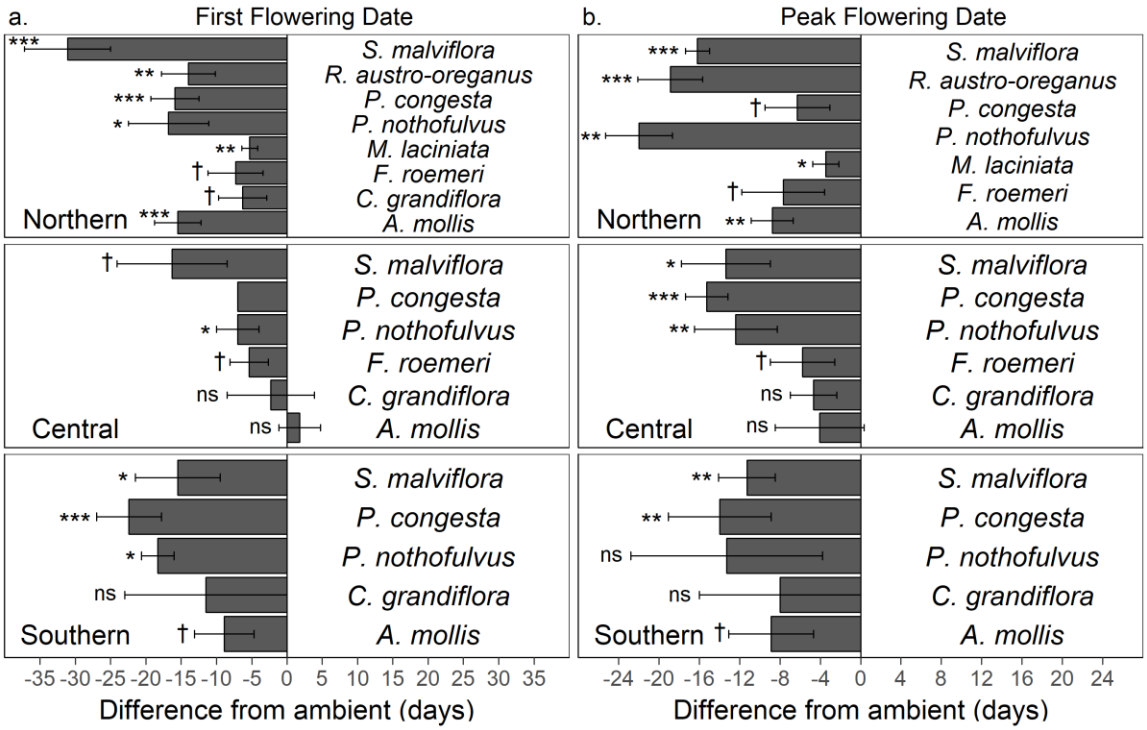

Figure 2.2. Mean difference ± standard error between warmed and ambient plots for (a) first flowering date (FFD) and (b) peak flowering date (PFD) at each site. Negative value indicates an advancement with warming. Significance codes: p > 0.1 = ns, p < 0.1 = †, p < 0.05 = *, p < 0.01 = **, p < 0.001 = ***; two-tailed t-tests. *P. congesta* FFD could not be tested statistically because it did not exhibit any variability among the warming plots (n = 9) nor the ambient plots (n = 10).

Under ambient temperatures, FFD and PFD varied by species across the latitudinal gradient (Figure 2.3). Of the annual species, *C. grandiflora* flowered earliest in

the southern site, but *A. mollis, P. nothofulvus,* and *P. congesta* all flowered earliest at the central site. There was no effect of site on FFD for the two perennial species, *F. roemeri* and *S. malviflora* (Figure 2.3a; Appendix A: Table S2.3). Four species, *A. mollis*, *F. roemeri, P. congesta,* and *S. malviflora,* reached PFD latest in the northern site. *C. grandiflora* followed a similar trend, reaching PFD earlier at the southern site compared to the central site, but this could not be tested due to a lack of variance. One species, *P. congesta,* reached PFD earliest at the central site. Site did not significantly affect PFD for *P. nothofulvus* (Figure 2.3b; Appendix A: Table S2.4). For temperature sensitivity, *A. mollis* exhibited greater sensitivity in FFD at the northern site compared to the central ($p = 0.003$), *P. nothofulvus* at the southern site compared to the central ($p = 0.091$), *P. congesta* at both the southern and northern sites compared to the central ($p \leq 0.036$), and *S. malviflora* at the northern site compared to both the southern and central ($p \leq 0.052$; Appendix A: Table S5, Figure S3). PFD temperature sensitivity did not differ by site for any species ($p > 0.10$; Appendix A: Table S2.5, Figure S2.3).

We identified the most likely model(s) of temperature and moisture explanatory variables from 2016-2017 for FFD and PFD of each species (excluding *M. laciniata* and *R. austro-oreganus*) (Appendix A: Table S6). For FFD, the most important predictors were mean winter temperature for *F. roemeri*, *P. nothofulvus,* and *S. malviflora*, mean spring temperature for *A. mollis* and *P. congesta*, and mean annual matric potential for *C. grandiflora* (Table 2.2; Appendix A: Figure S2.4). For PFD, the most important predictors were the same as for FFD for *A. mollis, P. nothofulvus,* and *S. malviflora*; for *C. grandiflora* and *F. roemeri,* the date of first wilting point, and for *P. congesta* the mean annual temperature became the most important predictors (Table 2.2; Appendix A:

Figure S2.5). For all species, temperature variables were negatively related to flowering dates; higher temperatures resulted in earlier flowering.

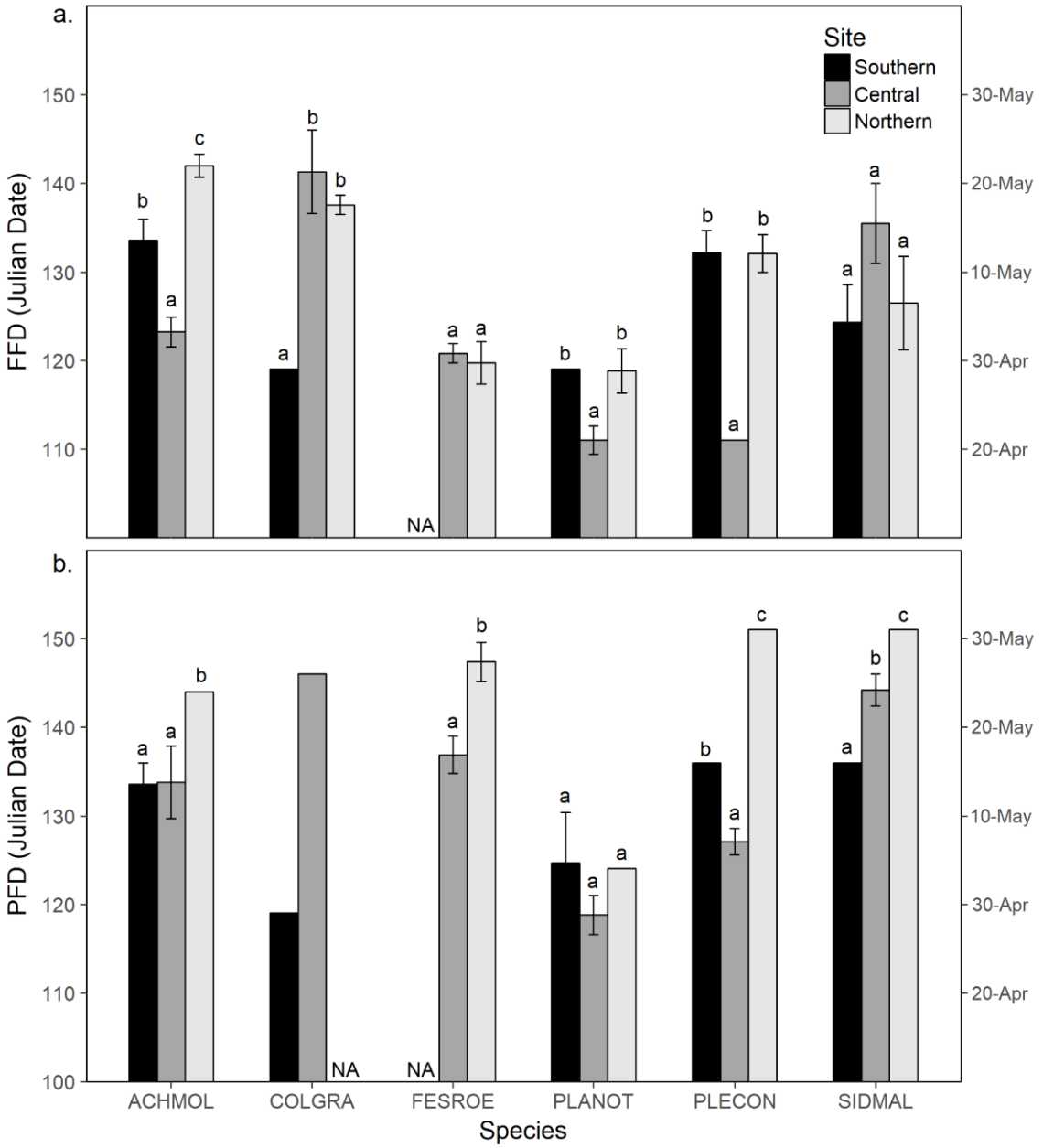

Figure 2.3. (a) First flowering date (FFD) and (b) peak flowering date (PFD) across sites, using ambient plots (due to significant site x warming interactions). Different letters indicate significant or marginal differences within a species ($p < 0.1$; Tukey's post-hoc comparisons). *C. grandiflora* was not tested statistically for PFD at the northern site (see methods).

Phenology of Community Biomass:

Across all plots, peak biomass was reached 20.6 ± 4.3 days earlier under warming than under ambient temperatures, regardless of site or year (mean difference ± standard error; $p < 0.001$; Appendix A: Table S2.7). Peak biomass occurred earliest in the south, with the southern site reaching its peak 29.8 ± 5.3 days earlier than the central site and 38.6 ± 5.3 days earlier than the northern site (Figure 2.4, vertical dashed lines; $p < 0.001$).

Contrary to the results for peak biomass, the effect of warming on the date of senescence varied by site and year (site x warming and warming x year interactions: $p < 0.05$; Appendix A: Table S7). In 2017, senescence occurred 10.5 ± 3.5 and 12 ± 5.6 days earlier under warming compared to ambient at the southern and central sites, respectively ($p \leq 0.049$). Warming did not affect the 2017 date of senescence at the northern site ($p = 0.172$; Figure 2.4, vertical dotted lines). In ambient plots, 2017 senescence occurred earliest in the south, with the southern site declining 12 ± 5.5 days earlier than the central site ($p = 0.09$) and 17.1 ± 5.5 days earlier than the northern site ($p = 0.012$). In 2018, senescence occurred 16.2 ± 4.3 days earlier under warming compared to ambient, regardless of site ($p < 0.001$; site x warming interaction: $p = 0.288$). The southern site senesced 20.3 ± 5.3 days earlier than the central site, which senesced 17.9 ± 5.3 days earlier than the northern site (Figure 2.4, vertical dotted lines; $p \leq 0.003$).

The effect of warming on the rate (i.e., the slope) of senescence was also dependent on site and year (site x warming and site x year interactions: $p \leq 0.087$; Appendix A: Table S7), with a greater rate of senescence under warming (-0.013 ± 0.001 Δ NDVI day^{-1}) compared to ambient (-0.011 ± 0.001 Δ NDVI day^{-1}) at the central site in 2017 ($p = 0.029$), but no treatment differences for either the southern or northern sites in

2017 or any site in 2018 ($p \geq 0.134$). In ambient plots in 2017, the rate of senescence was greater in the south (-0.017 ± 0.001 Δ NDVI day^{-1}) than both the central (-0.011 ± 0.001 Δ NDVI day^{-1}) and northern sites (-0.010 ± 0.001 Δ NDVI day^{-1}; $p < 0.001$).

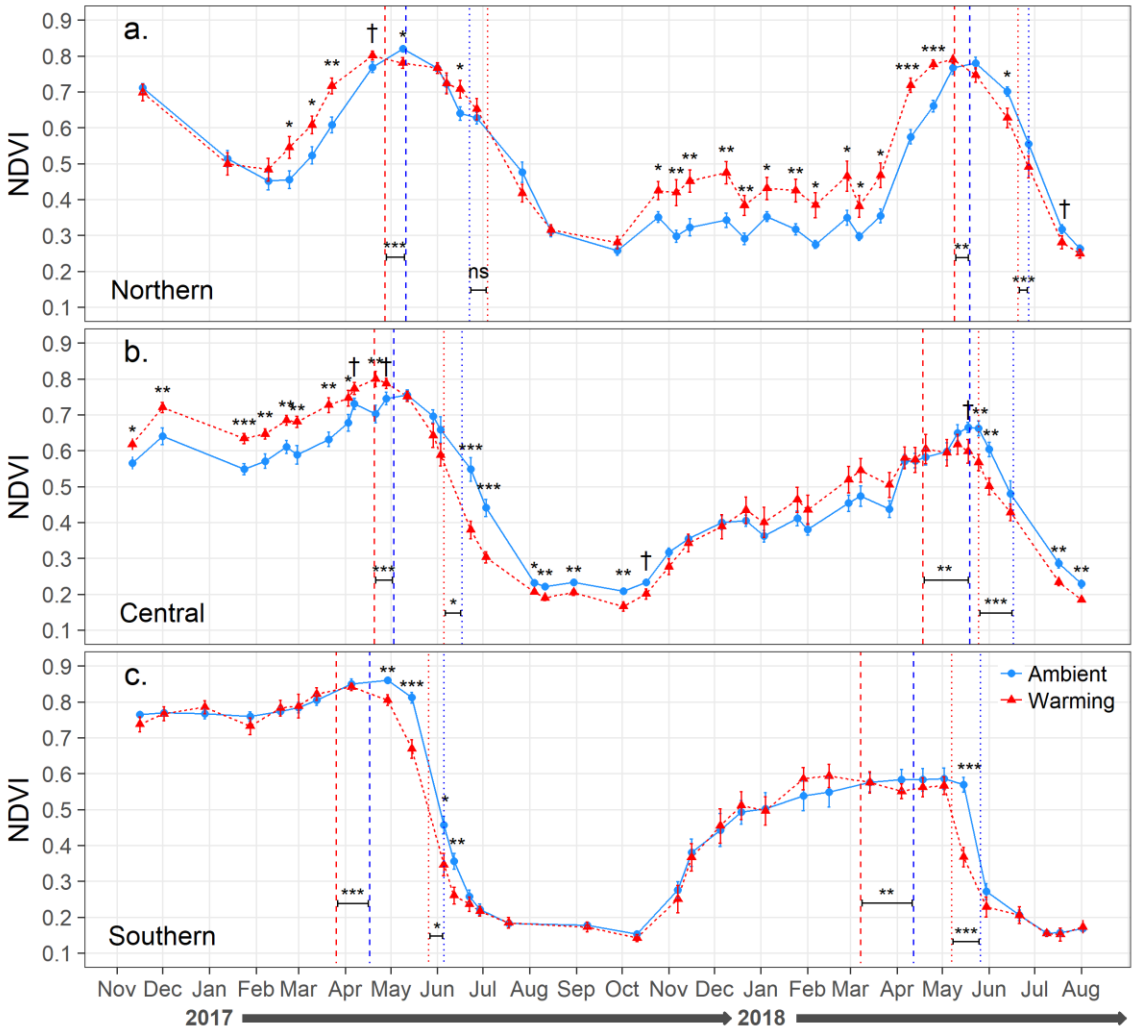

Figure 2.4. Normalized difference vegetation index (NDVI) of the ambient plots (control and drought) and warming plots (warming and warming + ppt) at each of the three sites from November 2016 to August 2018. Dates of peak biomass are shown with vertical dashed lines and dates of senescence with vertical dotted lines for both 2017 and 2018 (warming in red, ambient in blue). Significance codes: $p < 0.1$ = †, $p < 0.05$ = *, $p < 0.01$ = **, $p < 0.001$ = ***; two-tailed t-tests following repeated measures ANOVAs to examine warming effects within each date.

Similarly, in 2018 across all plots, senescence rate was again greater in the south (-0.018

± 0.001 Δ NDVI day^{-1}) than both the central (-0.011 ± 0.001 Δ NDVI day^{-1}) and northern sites (-0.011 ± 0.001 Δ NDVI day^{-1}; $p < 0.001$).

Phenology Variable	MAT	MWT	MST	MAMP	DFWP	DBWP
FFD (2017)						
ACHMOL	0.007	0.010	**0.983**	0.168	0.160	0.157
COLGRA	0.155	0.148	0.150	**0.638**	0.228	0.129
FESROE	0.067	**0.690**	0.124	0.207	0.516	0.109
PLANOT	0.010	**0.967**	0.022	0.148	0.158	0.137
PLECON	0.000	0.000	**1.000**	0.272	0.655	0.069
SIDMAL	0.007	**0.962**	0.021	0.195	0.195	0.221
PFD (2017)						
ACHMOL	0.460	0.011	**0.528**	0.234	0.337	0.135
COLGRA	0.239	0.177	0.125	0.292	**0.705**	0.003
FESROE	0.556	0.065	0.362	0.091	**0.688**	0.066
PLANOT	0.000	**0.999**	0.001	0.150	0.460	0.113
PLECON	**0.948**	0.000	0.052	0.138	0.829	0.014
SIDMAL	0.001	**0.993**	0.007	0.540	0.408	0.048
NDVI (2017+2018):						
Date of peak biomass	**1.000**	0.000	0.000	0.247	0.573	0.090
Date of senescence	**0.997**	0.000	0.003	0.593	0.108	0.295
Rate of senescence	0.745	0.123	0.036	**0.823**	0.170	0.007
GSL (2018)	**0.970**	0.001	0.030	0.459	0.160	0.381

Table 2.2. Relative variable importance values (highest value in bold) for each phenology response variable (FFD = first flowering date, PFD = peak flowering date, GSL = growing season length). Temperature variables: MAT = mean annual temp, MWT = mean winter temp, MST = mean spring temp; moisture variables: MAMP = mean annual matric potential, DFWP = date of first wilting point, DBWP = days below wilting point.

The effect of warming on NDVI value depended on site and date, with warming effects shifting from overall negative (suppressing biomass relative to ambient) to positive (increasing biomass relative to ambient) from south to north (Figure 2.4). At the southern site, warming suppressed biomass or was neutral. Suppression occurred from late April to mid-June in 2017 and again in May 2018, during the periods of senescence in both years (Figure 2.4c; warming x date interaction: $p < 0.001$). At the central site,

warming increased biomass from November 2016 through April 2017. By the end of June 2017, there was a shift to warming-induced biomass suppression, which continued until mid-October 2017, and again from mid-May 2018 to the end of sampling in August (Figure 2.4b; warming x date interaction: $p < 0.001$). At the northern site, warming increased biomass from late February to mid-April 2017, then in mid-June, and again from late-October 2017 to May 2018. Warming suppressed biomass relative to ambient for only one sampling date in 2017 (9-May) and only two dates in 2018 (13-June and 19-July) (Figure 2.4a; warming x date interaction: $p < 0.001$).

The effect of warming on the 2018 growing season length was also dependent on site (site x warming interaction: $p = 0.076$). Warming resulted in a net reduction in the southern site growing season length by 20.5 ± 6.1 days ($p = 0.004$) and in the central site growing season length by 21.6 ± 9.4 days ($p = 0.037$). There was no effect of warming on the northern site growing season length ($p = 0.965$). Under ambient conditions, the southern site had the shortest growing season (198.8 ± 4.2 days; $p < 0.001$) while the central (232.7 ± 4.2 days) and northern sites (238.4 ± 4.2 days) did not significantly differ from one another ($p = 0.615$).

For all four NDVI phenology variables, every candidate model (seven total) included mean annual temperature, while mean annual matric potential appeared in one candidate model for each variable (four models) (Appendix A: Table S6). Thus, mean annual temperature was the most important predictor for three of the four response variables (date of peak biomass, date of senescence, and 2018 growing season length), while mean annual matric potential was the most important for the rate of senescence (Table 2.2; Appendix A: Figure S2.6).

Discussion

We found that changes in temperature are likely to be more impactful than changes in precipitation on many aspects of plant phenology in PNW prairies, given the expectations for potential future climatic conditions in the region. Multiple lines of evidence supported this conclusion: first, temperature variables had the highest relative importance values for 12 of 16 phenological observations (both population and community-levels) modeled against an equal number of temperature and moisture predictor variables. Furthermore, none of the population or community-level variables had different responses to control (ambient temperature and precipitation) versus drought (ambient temperature and -40% precipitation), nor did warming (+2.5°C and reduced soil moisture) ever differ from warming + ppt (+2.5°C and ambient soil moisture).

Our 2.5°C increase in temperature in the warming treatments reflects expected future temperatures for the region, with models projecting ~3°C increase by the end of the 21st century (Mote & Salathé, 2010). Precipitation projections for the PNW are less certain, but generally predict an enhanced seasonality of wetter autumns and winters and drier summers, with a small (1-2%) overall increase in annual precipitation (Mote & Salathé, 2010). Thus, our 40% reduction in annual precipitation in the drought treatment is more extreme than current predictions, yet it did not affect the phenological variables we assessed. This may be at least partly because our drought treatment had little measurable impact on soil moisture except during the beginning (i.e., fall) and end (i.e., late spring) of the growing season (Appendix A: Figure S2.2; see discussion below). Furthermore, the fact that the effects of our warming + ppt treatment did not differ from those of warming alone directly implicates the importance of increasing temperature.

While the warming treatment was accompanied by a strong decrease in soil moisture (Appendix A: Figure S2.2), the warming + ppt treatment decoupled warming from the indirect effect of reducing soil moisture, indicating that the experimental effects we observed were indeed due to increasing temperature.

It is important to place our results that changes in temperature are likely to be more impactful than changes in soil moisture under future climate in the context of a Mediterranean climate system. Many prairie plants that are adapted to Mediterranean climates limit the timing of their reproductive events to the spring, prior to the extremely water-limited summer months. Plant growth and canopy development follow a similar trend. Thus, we propose that plants adapted to a Mediterranean climate are predisposed to temperature regulation for many aspects of their phenology. Our soil moisture data provide evidence that PNW Mediterranean ecosystems are buffered against large relative changes in precipitation during much of the year. From late fall to early spring, rain was frequent enough that the soils remained near saturation point (0 kPa) regardless of climate treatment. Over the summer, however, drought severity was so extreme that the soils remained well below permanent wilting point (-1,500 kPa), also regardless of treatment. These observations held true for both 2017 and 2018, which were relatively wet and dry years, respectively, for the southern and central sites, and relatively wet and average years for the northern site. From August 2016 – August 2017, precipitation for our southern, central, and northern sites was 163%, 119%, and 132%, respectively, of the 30-year averages from 1981-2010, while from August 2017 – August 2018, precipitation was 78%, 74%, and 106% of average, respectively (PRISM). Despite this high interannual variability in precipitation, we still saw the strong influence of temperature on

community-level phenology across years, even though annual mean temperatures during this time were no greater than ± 0.5°C of the 30-year averages for each site (PRISM). Thus, climate change would need to considerably alter the *timing* of future wet/dry seasons (i.e., substantially delaying the first rains or advancing the summer drought), rather than simply the magnitude of total precipitation, for moisture regime changes to meaningfully impact the timing of many phenological events in this system.

It is also important to note that different phenological events are likely to have different mechanistic triggers, especially in a Mediterranean climate system in which high temperatures are asynchronous with the wet season. For example, Peñuelas *et al.* (2004) found precipitation to be less influential than temperature on leaf-unfolding and flowering date events yet found a stronger influence for precipitation on fruiting events in a Mediterranean shrubland in the Iberian Peninsula. Additionally, the timing of the fall green-up in PNW prairies appears to be strongly controlled by the return of the rainy season. Indeed, we did not analyze fall 2017 green-up with our own NDVI data because it occurred in most plots as soon as soil matric potential returned to above wilting point in mid-October 2017, so there was not enough variation to analyze (Appendix A: Figure S2.2; Figure 2.4). Thus, it is possible that some later phenological events could be influenced by changes in moisture, although most events in this system tend to occur at times when temperature is more limiting.

At the population level in 2017, all eight of our focal species experienced some degree of advancement in first flowering dates (FFD) and peak flowering dates (PFD) with warming. Warming treatments advanced FFD from 2.1 days per °C (*M. laciniata* at the northern site) to 12.4 days per °C (*S. malviflora* at the northern site), with a total

mean advancement of 5.3 days per °C across species and sites. PFD advancements ranged from 1.4 days per °C (*M. laciniata* at the northern site) to 8.8 days per °C (*P. nothofulvus* at the northern site), with a total mean advancement of 4.7 days per °C. These values fall very much in line with evidence and predictions from other studies suggesting flowering times advance on average at a rate of ~2 – 7.5 days per °C (Amano, Smithers, Sparks, & Sutherland, 2010; Menzel *et al.*, 2006; Moore & Lauenroth, 2017; Wolkovich *et al.*, 2012). Furthermore, our results are consistent with those of a recent long-term (57 year) dataset on 115 plant species in Oregon's Willamette Valley which found that spring phenological events advanced by 5-7 days per °C (Lindh, McGahan, & Bluhm, 2018). While the flowering data we present includes only one season, we have supplemental evidence that bolster our conclusions from independent undergraduate projects for 2016 and 2018 at our central site and for 2016 at our southern site. In 2016, the three species studied at the southern site flowered first under warming compared to the ambient temperature plots (Kanner, McCullough, & Nock, 2017), while at the central site, seven of nine species flowered first under warming (ELP 2016 Team, *unpublished data*). In 2018 at the central site, low flowering-plant abundances largely led to non-significant findings, although *S. malviflora* and *P. congesta* flowering times advanced under warming (ELP 2018 Team, *unpublished data*). Thus, the flowering phenology results presented here have largely been consistent during other years of this experiment.

Some studies have found that phenological temperature sensitivity is greater at higher latitude (J. Prevéy *et al.*, 2017), whereas others have found the opposite (Wang, Ge, Dai, & Tao, 2015) or no effect (Parmesan, 2007; Wolkovich *et al.*, 2012). We did not find consistent evidence for any type of latitudinal trend in temperature sensitivity across

our sites. Of the four instances in which we found significant site effects, two cases (FFD for *A. mollis* and *S. malviflora*) exhibited greater sensitivity at the northern site, but two other cases (FFD for *P. nothofulvus* and *P. congesta*) exhibited greater sensitivity at the southern site.

We also did not find particularly strong evidence for a consistent directionality along the latitudinal gradient in the flowering times of these species under ambient temperatures. Latitude is known to impact flowering times, and we expected to see species reach flowering in ambient plots later moving from south to north, due to natural differences in the climate across this gradient. However, our environmental data indicate that the central site was slightly warmer than the southern site for much of the growing season between April – June 2017 (Appendix A: Figure S2.2), despite the southern site being warmer on average across the year. Thus, spring temperatures did not quite follow the latitudinal gradient, which may have contributed to these results. Furthermore, our findings across sites need to be interpreted cautiously since the southern site was not sampled with the same frequency as the central and northern sites, and we had unique seed sources across sites for *C. grandiflora*, *F. roemeri*, and *P. congesta.* Populations from different latitudes may differ in their phenologies based on unique evolutionary responses to growing season cues (Olsson & Agren, 2002), which may also contribute to the lack of a latitude effect on temperature sensitivity for at least the species with seeds sourced uniquely for each site.

Advances in flowering times have important implications for species' individual fitness, interactions with other species, and the assemblages of plant communities. Shifts in flowering times may desynchronize associations with pollinators, leading to lower

reproductive capacity for the host plant and cascading effects at other trophic levels (Forrest & Miller-Rushing, 2010; Miller-Rushing *et al.*, 2010; Rafferty *et al.*, 2015). In our imperiled prairies, *S. malviflora* is a known nectar source for the Fender's blue butterfly (*Icaricia icarioides fenderi* [Macy]), and both *C. grandiflora* and *P. congesta* are known host plants of the Taylor's checkerspot butterfly (*Euphydryas editha taylori*), two federally listed endangered species (Schultz, Hammond, & Wilson, 2003; Schultz *et al.*, 2011). If phenological shifts are strong enough to cause asynchronies between these butterflies' lifecycles and the growth and flowering of these and other key plant species, there could be dramatic implications for these butterflies' recovery. Moreover, phenological shifts in plants of interest to prairie restoration may affect the ability of practitioners to successfully accomplish common activities such as burning (Hamman, Dunwiddie, Nuckols, & Mckinley, 2011) or targeted weed control (Dennehy *et al.*, 2011). Conservation and restoration practitioners will likely need to develop adaptive strategies and plans that consider phenological shifts in order to continue meeting management goals (Bachelet *et al.*, 2011).

While we show that the flowering times of native prairie species are likely to advance with warming, our finding that their abundances were higher at our northern site relative to our southern may be more critical. Even after multiple years of seeding identical quantities into our plots, only a few species were able to successfully establish populations across the entire gradient, a theme that we have observed in the past (Pfeifer-Meister *et al.* 2013) and that has persisted in 2018 (*unpublished data*). Our southern site had very few reproductive individuals for any range-limited focal species, apart from *S. malviflora*. This suggests that factors affecting establishment are currently hindering

populations at this site, despite all species being within their current ranges at that location. Previous experiments have demonstrated that this site has high nutrient availability and levels of productivity that do not differ from our central site (Pfeifer-Meister *et al.*, 2013, 2016; Reynolds *et al.*, 2015). Instead, it seems likely that the extreme summer temperatures and the early-onset of summer drought experienced in that region (Appendix A: Figure S2.2) make it exceptionally difficult for these species to establish from seed. Contrary to results at the southern site, most of our species established relatively high abundances of reproductive individuals under ambient conditions at our northern site, with the exceptions of *P. nothofulvus*, *R. austro-oreganus*, and *A. mollis.* Interestingly, at least *R. austro-oreganus* and *A. mollis* were most abundant in the north under warming, warming + ppt, and drought, and this site is beyond these species' current northern range limits. Unexpectedly, these species struggled to achieve reproduction when planted at sites within their current ranges yet had no such constraints when planted north of their current range, suggesting they may need to shift their ranges northward to persist. In general, the less extreme climatic conditions and the longer growing seasons to the north seem to be more favorable for the fitness of all eight species, irrespective of their current ranges. These findings have implications for understanding species range distributions under future climates, and in a parallel demography experiment, we are actively assessing population projections for these and six additional species across this gradient. Furthermore, these findings confirm the importance of considering climate change when attempting to select proper seed sources for rare species restoration and recovery (Havens *et al.*, 2015), and when selecting which species to include in restoration projects (Bachelet et al 2011).

At the community scale, we found live plant biomass (NDVI) to be affected by warming in the following ways: consistent suppression at both the southern and central sites during the late spring to summer of both relatively wet (2017) and dry (2018) years, and suppression at the northern site during the summer of an average rainfall year (2018). However, we also found positive effects of warming at the central site during the winter and spring of the wet year (2017) and at the northern site during the winter, spring and fall of both wet and average years. Thus, for the central and northern sites, there appear to be interactions between the effect of warming and annual rainfall on live biomass across parts of the year, a phenomenon that has been previously documented (Mueller *et al.*, 2016; Zelikova *et al.*, 2015). At the southern site, however, this interaction is absent; warming is consistently negative. The impacts of future climate change on aboveground prairie biomass thus appear to depend substantially on the position of each site across a latitudinal gradient of increasingly severe Mediterranean drought.

Furthermore, we saw a warming-induced reduction of the 2018 growing season length at both the southern and central sites but a neutral effect at the northern site. Growing season lengths at higher northern latitudes (> 45°N) are reported to be increasing with global warming (Ibáñez *et al.*, 2010; Tucker *et al.*, 2001), yet the results from our northern site (~47°N) show no effect, at least in 2018. Gordo and Sanz (2009) reported increases in growing season lengths with warming in another Mediterranean climate system (Spain), which they attributed to large advancements in spring leaf-unfolding dates and smaller advancements in autumn leaf-falling dates. The contractions in growing season lengths at our southern and central sites likely reflect the fact that warming considerably advanced the date of senescence at these two sites, whereas it only

caused a small advancement at the northern site (Figure 2.4). Cui *et al.* (2017) also found contractions in growing season length in their Canadian prairie systems but attributed their findings to moisture limitations and not warming. Because we lacked NDVI data from fall 2016, we were unable to encapsulate the entirety of the 2017 growing season. However, considering the 2017 date of senescence advanced with warming at the southern and central sites, it is likely that warming would have also reduced the length of the 2017 growing season at these two sites. Contrarily, there may have been either a neutral or slight positive effect of warming on the 2017 growing season length at the northern site, considering its senescence date was unaffected by warming.

Shifts in the phenology of canopy biomass may have implications for community dynamics and ecosystem processes. Changes to growing season lengths are known to affect water cycling, rates and amount of carbon sequestration, and nutrient uptake from the soil (Ibáñez *et al.*, 2010). Shorter growing seasons could reduce annual productivity, thus lessening current rates of CO_2 sequestration (Cleland *et al.*, 2007). Additionally, shifting community biomass phenology may provide chances for exotic species to seize on resource opportunities previously unavailable to them, increasing the potential for community invasions (J. S. Prevéy & Seastedt, 2014). Moreover, these phenological shifts could lead to greater fire hazard during the dry season. In our experiment, we saw cases of biomass increasing with warming in the winter, meaning there could be a greater accumulation of herbaceous fuels. When this is followed by an earlier date of senescence, warming may be expected to cause both an earlier and more extreme fire season in the US west (Westerling, Hidalgo, Cayan, & Swetnam, 2006).

Overall, our study offers substantial evidence that future changes in temperature may have great influence on the timing of many key plant phenological events in a Mediterranean climate system and that effects due to changes in soil moisture may be buffered from even large changes in the amount of precipitation so long as the timing and duration of the rainy season is unchanged. We observed a strong influence of temperature on flowering phenology in eight native plant species both within and beyond their current geographic ranges, as well as for canopy biomass phenology at the community scale. Additionally, we found that the majority of our eight focal species are experiencing considerable reductions in their abundances near or south of their northern range limits, suggesting that the clock is ticking on their ability to persist within their current ranges.

CHAPTER III

CLIMATE MANIPULATIONS DIFFERENTIALLY AFFECT PLANT POPULATION DYNAMICS WITHIN VERSUS BEYOND NORTHERN RANGE LIMITS

From Reed, P. B., Peterson, M. L., Pfeifer-Meister, L. E., Morris, W. F., Doak, D. F., Roy, B. A., Johnson, B. R., Bailes, G. T., Nelson, A. A., & Bridgham, S. D. (2021). Climate manipulations differentially affect plant population dynamics within versus beyond northern range limits. *Journal of Ecology*, 109, 664-675.

Contributions

P. B. Reed analyzed the data and wrote the manuscript. All authors contributed to the design of the experiment. P. B. Reed, L. E. Pfeifer-Meister, B. A. Roy, B. R. Johnson, G. T. Bailes, A. A. Nelson, and S. D. Bridgham contributed to data acquisition, while M. L. Peterson, W. F. Morris, and D. F. Doak provided valuable guidance and intellectual support. All authors contributed to the review process and gave final approval for publication.

Introduction

With ongoing climate change, many species will need to shift their geographic ranges to persist. Indeed, multiple species have already shifted poleward and/or to higher elevations to track favorable climatic conditions (Chen, Hill, Ohlemuller, Roy, & Thomas, 2011; Parmesan, 2006; Parmesan & Yohe, 2003; Thomas, 2010), although the magnitudes and patterns of range shifts vary substantially across taxa (MacLean &

Beissinger, 2017). Range shifts have widespread consequences for ecosystem services (Pecl et al., 2017; Walther, 2010), and, if species are unable to shift their ranges rapidly enough, may further exacerbate biodiversity losses (Dawson, Jackson, House, Prentice, & Mace, 2011). Anticipating such effects must start with better predictions of how climate change will impact populations across species' geographic ranges.

Species range distributions are controlled by a complex set of factors including dispersal ability (Sexton, Mcintyre, Angert, & Rice, 2009), biotic interactions (Araújo & Rozenfeld, 2014; Louthan et al. 2015), and tolerance of abiotic conditions, with climate often assumed to be the primary driver of broad distributional patterns across latitudinal and elevational gradients (MacArthur, 1972; Thomas, 2010). The overall effect of climate on population dynamics is driven by its composite effects on different vital rates (i.e., survival, growth, fecundity, and recruitment). As temperatures increase, populations towards the warmer edges of a range may decline due to decreasing performance in one or more vital rates, leading to localized extinctions and potential range contractions at their trailing edges (Lesica & Crone, 2017; Panetta, Stanton, & Harte, 2018; Sheth & Angert, 2018). At the same time, climatic conditions near or beyond the cooler edge of a range may become increasingly favorable with warming (Rehm, Olivas, Stroud, & Feeley, 2015), leading to range expansions or shifts. Recent evidence, however, suggests that populations throughout a species range, not just at the warmer edges, may be at risk of decline if populations are locally adapted to climate (Peterson, Doak, & Morris, 2018). Demographic studies that can predict whether populations will decline or disappear towards the warmer range edges and/or expand at the cooler range edges are necessary to predict whether and how ranges will shift with future climate change.

Complicating the population-level effects of climate change are potentially opposing positive or negative effects on different vital rates, termed demographic compensation, which can buffer populations against perturbations (Doak & Morris, 2010; Villellas, Doak, García, & Morris, 2015). For example, Peterson et al. (2018) found that opposing survival and growth responses of the alpine plant *Silene acaulis* to warming contributed to the species' ability to persist across its range, while Oldfather & Ackerly (2019) found that inverse relationships in rates such as adult survival and germination contribute to stable population growth across a microclimate gradient in the alpine plant *Ivesia lycopodioides*. While demographic compensation may theoretically allow for a species to persist in its current range in the face of climate change, the presence of compensation does not guarantee long-term persistence, as extreme years may exceed a threshold at which the vital rates benefitting from climate change are outweighed by those being hindered (Doak & Morris, 2010; Sheth & Angert, 2018). Instead, species may be faced with a situation in which demographic compensation manages to slow the rate of decline but not rescue populations altogether.

To effectively address how climate change will impact populations across geographic ranges and whether species will need to shift their ranges to persist, manipulative experiments across environmental gradients are critical (Dunne, Saleska, Fischer, & Harte, 2004; Pfeifer-Meister et al., 2013). In particular, incorporating transplants of species to locales beyond their current limits allows for the direct testing of whether such species have the capacity to establish a population and persist beyond their current range limits (Baer & Maron, 2018; Gaston, 2009; Hargreaves, Samis, & Eckert, 2014). Since studies documenting changes in only one or a few demographic parameters

can be misleading (Gaston, 2009), experiments that use population models to integrate the combined effects of climate across the entire life cycle are most compelling in this regard.

Previously (2010-2012), we used a fully factorial warming (+2.5°C) and precipitation (+20%) experiment at three sites spanning a latitudinal climate gradient of increasing temperature and summer drought severity from north to south in the Pacific Northwest (PNW), USA to study the vital rates of 12 native prairie species planted within and beyond their northern range limits (Pfeifer-Meister et al., 2013). Our key finding was that warming decreased recruitment within but not beyond a species' current range. However, this earlier study did not last long enough to allow perennial species to mature and thus could not be used to calculate overall population growth rates. Furthermore, the effect of warming was confounded by a strong reduction in soil moisture that is typical of warming treatments (Rustad et al., 2001). Here, we updated this experimental design with a drought treatment (-40% annual precipitation) replacing the minimally impactful +20% precipitation treatment, and a warming plus precipitation treatment that added enough moisture to offset the drying effect of warming. We measured vital rates and, using integral projection models (IPMs), calculated the population growth rates for six perennials, including two "range-restricted" species whose northern range limits occur within our study area, from 2016-2018 at three experimental sites (the same southern and central sites as in Pfeifer-Meister et al. (2013) and a new northern site). IPMs have become widely adopted given their ability to accommodate both discrete and continuous states in projecting population dynamics, and there are many useful examples in the literature describing their implementation and methods (Ellner & Rees, 2006; Merow et

al., 2014; Rees, Childs, & Ellner, 2014). To our knowledge, this is the first study incorporating both climate manipulations and a latitudinal climate gradient to conduct full-scale demographic modeling of multiple species planted both within and beyond their northern limits. In this study we ask:

1. Do prairie plant population growth rates change over a latitudinal gradient within their current range limits? Is warming and/or drought detrimental to populations within their ranges?
2. Are the range-restricted perennial species capable of establishing when planted north of their cooler edges? Is warming and/or drought benign for such pioneering populations?
3. Which vital rates contribute most substantially to climatic effects on population dynamics? Is there evidence of demographic compensation buffering population responses to climate change?

We hypothesized that, due to climate warming in the recent past, population growth rates will increase from south to north, and that the range-restricted species will be capable of establishing when planted at sites north of their current leading edges. Within species' current ranges, we expected warming and/or drought to decrease population growth rates relative to controls, but to be neutral or beneficial for populations of the range-restricted species that establish at the sites north of their ranges. Lastly, where there are no effects of climate treatments on population growth rates, we expected some species to show evidence of demographic compensation.

Materials and Methods

Experimental design:

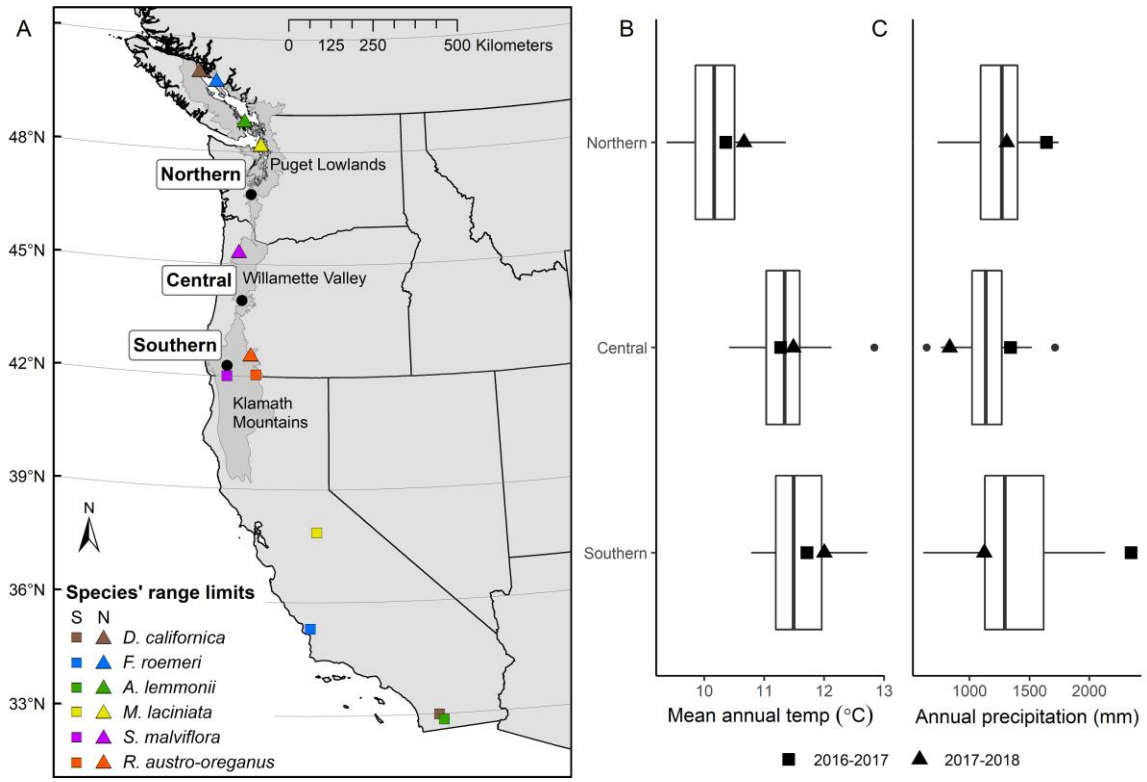

Figure 3.1. (A) Map of the southern, central, and northern experimental sites (black dots) and the southernmost and northernmost known populations (squares and triangles, respectively) of the six perennial focal species west of the Cascade and Sierra mountain divides. See Appendix B: Supplemental Methods for details regarding species' range limits. From north to south, the Puget Lowland, Willamette Valley, and Klamath Mountain ecoregions are highlighted in dark grey. (B) Mean annual temperatures and (C) annual precipitation over the period 1981-2010 (boxplots) and during the two annual transitions of this study (symbols) using the annual interval of 15-Jul to 14-Jul (data obtained from PRISM: http://www.prism.oregonstate.edu/). This annual interval was chosen as it encapsulates an entire growing season beginning before the onset of fall green-up and ending just after wilting point is reached.

The experiment took place from 2015 to 2018 at three sites across a 520 km latitudinal Mediterranean climate gradient in the PNW, USA (Figure 3.1). Each site contained 20 plots (each 7.1 m^2) randomly assigned to one of four climate treatments: control (ambient temperature and precipitation), drought (ambient temperature with annual precipitation reduced by 40%), warming (canopy temperature raised by 2.5°C with ambient precipitation), and warming + precipitation (canopy temperature raised by

2.5°C and irrigated to offset a warming-induced drying effect). Complete details about climate treatment implementation can be found in Appendix B: Supplemental Methods.

The southern and central sites had an experimental legacy from 2010-2012 (Pfeifer-Meister et al., 2013, 2016), with some adult individuals of the focal species remaining from the previous experiment (which we included when collecting data in the current experiment), while the northern site was newly established in 2015. Between October 2014 and January 2015, plots at the southern and central sites were mowed and raked, while the northern plots were treated with herbicide (2% Glyphosate) three times to reduce the thick cover of introduced pasture grasses (a typical prairie restoration technique in the PNW). In January 2015 to establish similar baseline communities, we seeded all plots with a consistent mix of 29 native grass and forb species found in PNW prairies (including our focal species; Appendix B: Table S1).

Our demographic study centered on six focal perennial species (Table 3.1; see Appendix B: Supplemental Methods for more detailed descriptions). All species were selected for having medium to high fidelity to upland prairies with their northern range limits occurring within the PNW (42~50°N) and their southern limits occurring below the latitude of our southernmost site (Figure 3.1; see Appendix B: Supplemental Methods for determining species' range limits). In fall 2015, 2016, and 2017, for each focal species and plot, we sowed 25 seeds into each of eight 5.5 cm diameter plastic rings, using different rings each year (for a total of 200 seeds per species per plot per year, with two exceptions: 150 seeds within six rings per plot for *Ranunculus austro-oreganus* in 2015 due to seed quantity limitations, and 250 seeds within five rings per plot for *Achnatherum lemmonii* in 2017 due to space limitations). To allow for local adaptation, we used the

nearest available seed sources for each site (Appendix B: Table S2). Due to low rates of germination with strong site differences in the field (see results), we also conducted a greenhouse germination experiment in fall 2018 with field-collected soil to test whether these results were the consequence of soil differences across sites (see Appendix B: Supplemental Methods).

Perennial Species	Family	Growth Habit	S-limit Lat	N-limit Lat	N-limit Region†
Ranunculus austro-oreganus L.D. Benson	Ranunculaceae	Forb	42.05°	42.60°	KM
Sidalcea malviflora (DC.) A. Gray ex Benth. ssp. *virgata* (Howell) C.L. Hitchc.	Malvaceae	Forb	42.00°	45.35°	WV
Microseris laciniata (Hook.) Sch. Bip.	Asteraceae	Forb	37.85°	48.21°	PL
Achnatherum lemmonii (Vasey) Barkworth var. *lemmonii*	Poaceae	Grass	32.84°	48.84°	WD
*Festuca roemeri**	Poaceae	Grass	35.30°	49.90°	PL
Danthonia californica Bol.	Poaceae	Grass	32.99°	50.13°	WC

Table 3.1. Descriptions of the six focal species. S-limit and N-limit Lats give the latitudes of the southernmost and northernmost known populations, respectively, within the species' contiguous ranges west of the Cascade and Sierra mountain divides. We determined whether a species is within or beyond its current range at our three experimental sites based on these values (see "Determining species' range limits" in Appendix B: Supplemental Methods for details). *Variety *roemeri* Yu. E. Alexeev at the central and northern sites; variety *Klamathensis* B.L. Wilson at the southern site. †KM = Klamath Mountains; WV = Willamette Valley; PL = Puget Lowlands; WD = widespread and disjunct; WC = widespread and common.

Lastly, to implement a treatment to examine the effect of aboveground competition on species' responses to the climate treatments, we initiated a biomass removal treatment in winter to early spring of 2017. In half of each plot, we reduced the presence of non-focal species with a combination of weeding and clipping. However, we found it impossible to conduct this treatment regularly and consistently throughout the growing season at all three sites, so we abandoned the treatment near the end of the 2017 growing season. To account for a potential treatment effect in 2017 or a legacy effect in 2018, we included a biomass removal treatment in our vital rate models.

Demographic data and analyses:

In 2016, 2017, and 2018, we marked and measured each individual in the plots and tracked them through subsequent years. To quantify germination and seedling survival, we conducted 2-4 censuses each winter-spring of the rings into which seeds had been added, counting the number of germinants and marking seedlings for subsequent tracking. During the final census of each spring, we recorded each existing plant's survival or death from the previous year and measured size and reproduction. To estimate the number of seeds each reproductive individual produced, we collected data on the number of flowers or spikelets per plant, the fraction of flowers becoming fruits, and the number of seeds per fruit. In some cases, for seed production, we only had data from a single site and/or a single year to provide estimates, as well as from a few natural populations in areas surrounding our study sites. Details on specific size and reproduction data collected for each species can be found in Appendix B: Supplemental Methods. We then modeled all vital rates as functions of climate treatments and, where appropriate, plant size, and then used IPMs to integrate vital rates into estimates of population growth rates for each annual transition for each level of the experimental treatments. Using these IPMs, we conducted life table response experiments (LTREs) to identify the contributions of grouped vital rates to differences in λ between treatments and controls (Caswell, 1989).

All the following analyses were conducted using R version 3.3.2 (R Core Team, 2016). We modeled the probabilities of binomial responses (survival, reproduction, fruit to flower ratio (for *Sidalcea malviflora*), and germination) using generalized linear mixed models with binomial error distribution and logit-link functions. We modeled mean

growth and variance in growth (the squared-residuals of the growth model) using general linear mixed models, and various reproductive output parameters (flowers/spikelets per plant, seeds per flower/spikelet, etc.) with either general linear mixed models or generalized linear mixed models with Poisson error distribution (Gaussian if responses were based on averaged values, Poisson if total counts; see species descriptions in Appendix B: Supplemental Methods). We treated adult survival, reproduction, mean adult growth, growth variance, and flowers/spikelets per plant as size-dependent vital rates, using both linear and quadratic effects of size. We used the lme4 package (version 1.1-17; Bates et al., 2015) for mixed models, treating plot (or population for data from natural populations) as a random effect, except in one circumstance (*A. lemmonii* adult survival) in which we lacked enough data to include a random effect.

For each species and most vital rates (see Appendix B: Table S3 for exceptions), we built two global models: a climate global model (using the climate treatment variable with four levels: control, drought, warming, and warming + precipitation) and a warming global model (collapsing the climate treatment into two temperature categories: ambient (control and drought) and warming (warming and warming + precipitation)). We used this collapsed warming treatment (in addition to the full climate treatment) because preliminary data exploration and evidence from previous experiments at these sites suggest changes in temperature have a stronger influence than changes in moisture on plant responses in this system (Pfeifer-Meister et al., 2013; Reed et al., 2019) and we gained degrees of freedom in doing so.

Both global models included all possible two-way interactions (and all possible main effects) involving site, climate or warming treatment, year, and plant size (for size-

dependent vital rates), plus a quadratic size term ($size^2$), and the main effect of the biomass removal treatment or a site x biomass removal treatment interaction for 2017/2018 germination (which could support such an interaction). We modeled 2016 germination separately from 2017/2018 since the sites did not have all climate treatments initiated yet. If a species had a constant failed response (e.g., no survival or reproduction) in a binomial vital rate at a given site, we dropped that site from that vital rate model to avoid a singular-fit issue (six sites dropped out of 73 possible cases; see Notes column in Appendix B: Table S3). Using the 'dredge' function from the MuMIn package (Barton, 2018), for both global models we compared all nested models with AICc and identified the best-fit model for each vital rate (Burnham & Anderson, 2004). On a few occasions, we removed quadratic size effects from models if they caused biologically unrealistic predictions towards the extremes of the size range. If the biomass removal treatment remained in the best-fit model for a vital rate, we used the non-weeded level when predicting that vital rate for the IPMs.

To synthesize the vital rate estimates into estimates of the population growth rate (λ), we built IPMs for each climate treatment at each site during both annual transitions. We did not fit an IPM at sites where we could not estimate the main effect of that site in one or more vital rate models for a species (e.g., if we were unable to estimate reproduction due to no individuals surviving to reproductive age). In our IPMs, we used plant size as our continuous state variable but included a discrete seedling stage. We set size limits to be just outside the maximum and minimum observed sizes across all sites, and discretized vital rate functions into 200 size bins using the midpoint rule (Easterling, Ellner, Dixon, & Mar, 2000; Ellner & Rees, 2006). We estimated growth probabilities of

adults and seedlings as the differences of the cumulative distribution function (CDF) at size bin boundaries (Dibner, Peterson, Louthan, & Doak, 2019). For seedlings surviving to the next year, we used distributions of possible sizes based on empirical CDFs fit to the parameters found in the best-fit seedling growth models (Appendix B: Table S3). We determined the predicted number of recruits produced by a reproductive individual at a given size as the product of the individual's reproductive output (total seeds: determined by its flower (or spikelet/etc.) production, the fruit to flower ratio (if applicable) and seeds per flower) and the germination rate. We calculated λ as the dominant eigenvalue of each discretized IPM matrix and estimated bias-corrected 95% confidence intervals for λ by resampling the coefficients of each vital rate function 1000 times using their means and covariance matrices and recalculating λ for each bootstrap replicate. We tested for statistical significance of a treatment effect on λ relative to the control by calculating the differences in λ between the treatment and control for each of the 1000 resamples and then calculating 95% confidence limits in those differences. A treatment has a significant effect on λ if those confidence limits do not overlap zero. The λ values we computed for each annual transition, as well as the vital rate contributions from LTREs (see following paragraph), are the asymptotic values that would be reached if the vital rate values during that transition remained constant.

Following bootstrap iterations of IPMs, we used the 'LTRE' function in the 'popbio' package (Stubben & Milligan, 2007) to determine the extent to which differences between climate treatments and controls in λ could be attributed to differences in the survival/growth (S/G) of seedlings, S/G of adults, or fecundity. We obtained the LTRE contributions for each element of the discretized S/G matrix and

fecundity matrix that constitute the IPM (e.g., approach two in (Griffith, 2017)). Sensitivities were evaluated midway between the treatment and control matrices (Caswell, 2001) and adult (non-seedling) contributions were summed over size bins. We utilized bootstrapped IPM matrices to estimate bias-corrected 95% confidence intervals in LTRE contributions. A contribution is significant when confidence intervals do not overlap zero. Evidence of demographic compensation under a climate treatment would exist if vital rates exhibited opposing contributions to differences in λ (Villellas et al., 2015).

Results

Population growth rates (λ) varied substantially across species, annual transitions, and sites (Figure 3.2). We were unable to fit an IPM at one or more sites for four of the six species due to their inability to establish a reproductive population (hereafter: 'establish') over the course of the experiment. This outcome was most common at the southern site, where only *R. austro-oreganus* and *S. malviflora* reached reproductive status. At the central and northern sites, two of the six species failed to establish (*Microseris laciniata* and *A. lemmonii* at the central site and *Danthonia californica* and *A. lemmonii* at the northern site). For the three species that established at more than one site, *R. austro-oreganus* and *Festuca roemeri* exhibited increasing λ from south to north while *S. malviflora* performed lowest at the central site, where it naturally occurs (Figure 3.2). In all but one case within current ranges, the warming treatments had neutral to significantly negative effects on λ relative to the controls (Figure 3.2: green backgrounds; Appendix B: Table S3.4). The lone exception was a positive effect under warming for *D. calfornica* in 2016-2017, but this switched to a negative effect in 2017-2018. In contrast,

the warming treatments had neutral to significantly positive effects on λ at sites beyond the northern

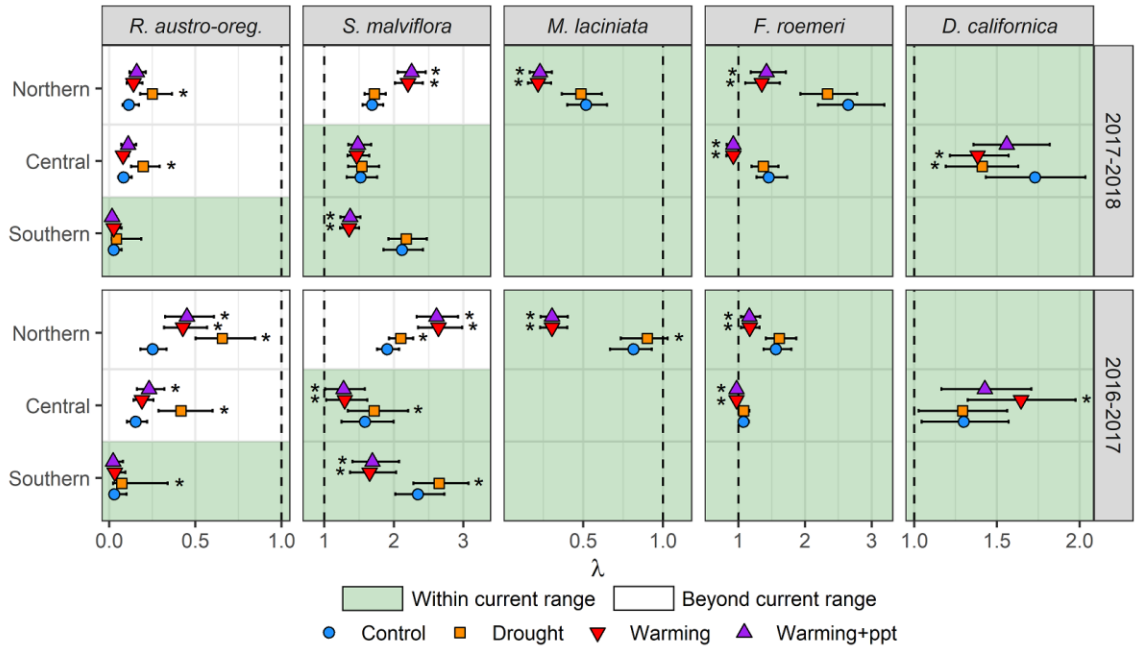

Figure 3.2. Population growth rates (λ) under climate treatments (control, drought, warming, and warming + ppt) for five perennial species at the southern, central, and northern experimental sites for 2017-2018 and 2016-2017. Species are arranged from left to right in ascending order of northern range limit. Lack of λ values at a given site for a species indicates that we did not fit an integral projection model (IPM) because the species did not establish a reproductive population. *Achnatherum lemmonii* is excluded entirely from the figure since we could not fit an IPM at any site. λ values are depicted with bias-corrected 95% confidence intervals obtained by resampling the coefficients of each vital rate function 1000 times using their covariance matrices. We tested for statistical significance of a treatment effect on λ relative to controls, as indicated by *, by calculating the differences in λ between the treatment and control for each of the 1000 resamples and then calculating 95% confidence limits in those differences (see Table S3.4). λ overlapping 1.0 (dashed line) = estimated stable population, λ < 1.0 = estimated declining population and λ > 1.0 = estimated growing population. Note the differing scales across species.

limits of the two range-restricted species, *R. austro-oreganus* and *S. malviflora* (Figure 3.2: white backgrounds; Appendix B: Table S3.4). In general, the warming and warming + precipitation treatments had similar effects on λ relative to the controls. The drought treatment had neutral to significantly positive effects whether within or beyond ranges for

R. austro-oreganus and *S. malviflora*, and a single significantly positive and negative effect within ranges for *M. laciniata* and *D. californica*, respectively (Figure 3.2; Appendix B: Table S3.4). Overall, negative effects of the warming treatments within current ranges were of greater magnitude and more frequent than those of the drought treatment.

LTREs revealed the extent to which differences between climate treatments and controls in the survival/growth (S/G) of seedlings, S/G of adults, and/or fecundity contributed to differences in λ. We found no consistent evidence for demographic compensation: in most cases, a given climate treatment affected all three sets of vital rates in the same direction relative to control (i.e., all positive or all negative contributions; Figure 3.3). While the LTREs provide contributions of grouped vital rates, in many cases only one of the vital rates within a group (e.g., only seedling survival OR growth, not both) was involved in the contribution. Specific vital rate results can be found in the Supporting Information (best-fit model results: Appendix B: Figures. S3.1-S3.16; best-fit model structures: Table S3.3; best-fit model coefficients: Table S3.5).

The inability of most species to establish populations at one or more sites was mostly driven by extremely low rates of germination and seedling survival. Despite sowing thousands of seeds per species per site during each fall of 2015, 2016, and 2017, few germinated and survived to adulthood. Across all species, these critical early-life vital rates were significantly lower where species failed to establish compared to where species successfully established (logistic regressions, $P < 0.001$ for both germination and survival). All species except *S. malviflora* had significantly lower germination at the southern site relative to the remaining two sites (Figure 3.4A).

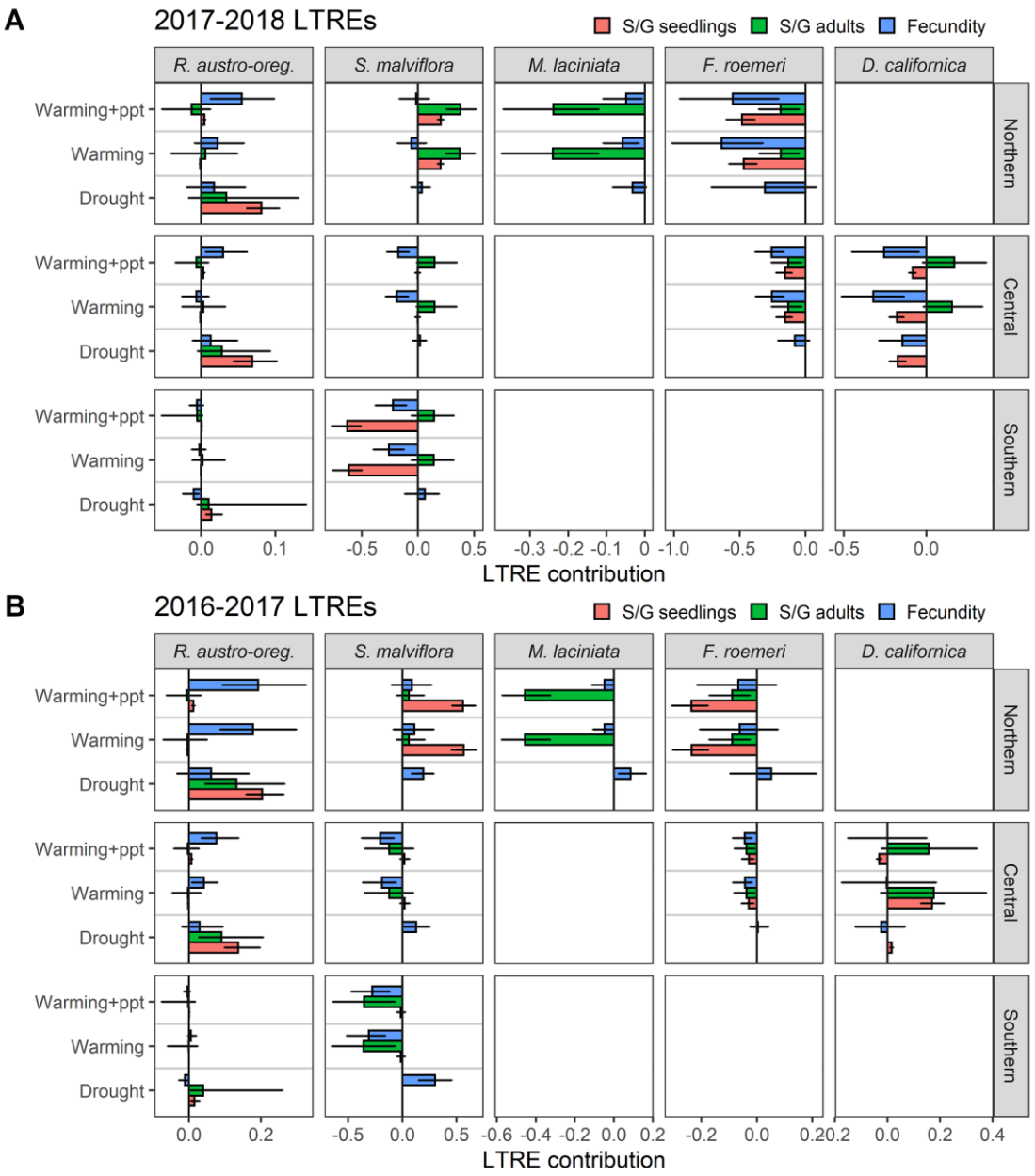

Figure 3.3. Life table response experiment (LTRE) results for (A) 2017-2018 and (B) 2016-2017 to determine the extent to which differences in population growth rates (λ) between each climate treatment (drought, warming, or warming + ppt) and the controls can be attributed to differences in the survival/growth (S/G) of seedlings, S/G of adults, or fecundity. Where a species lacks data at a given site due to failed establishment, we could not conduct an LTRE. *Achnatherum lemmonii* is excluded entirely from the figure since it failed to establish at any site. Contributions of each vital rate group are depicted with bias-corrected 95% confidence intervals by utilizing bootstrapped IPM matrices generated by resampling the coefficients of each vital rate function 1000 times using their covariance matrices. A vital rate group has a significant contribution towards a treatment's effect on λ relative to the control if its confidence interval does not overlap zero. Note the differing scales across species and annual transitions.

In the greenhouse germination study, we also found significant differences in germination across the soils from the three sites. However, only for *F. roemeri* did the southern soil have the lowest greenhouse germination rate (Figure 3.4B), so there was no consistent evidence that this site's soil was inhibitory for germination. In general, germination rates were considerably higher or comparable in the greenhouse relative to the field (Figure 3.4A, B; note the different scales), except for *D. californica* in the central soil (considerably lower than its germination rate in the field).

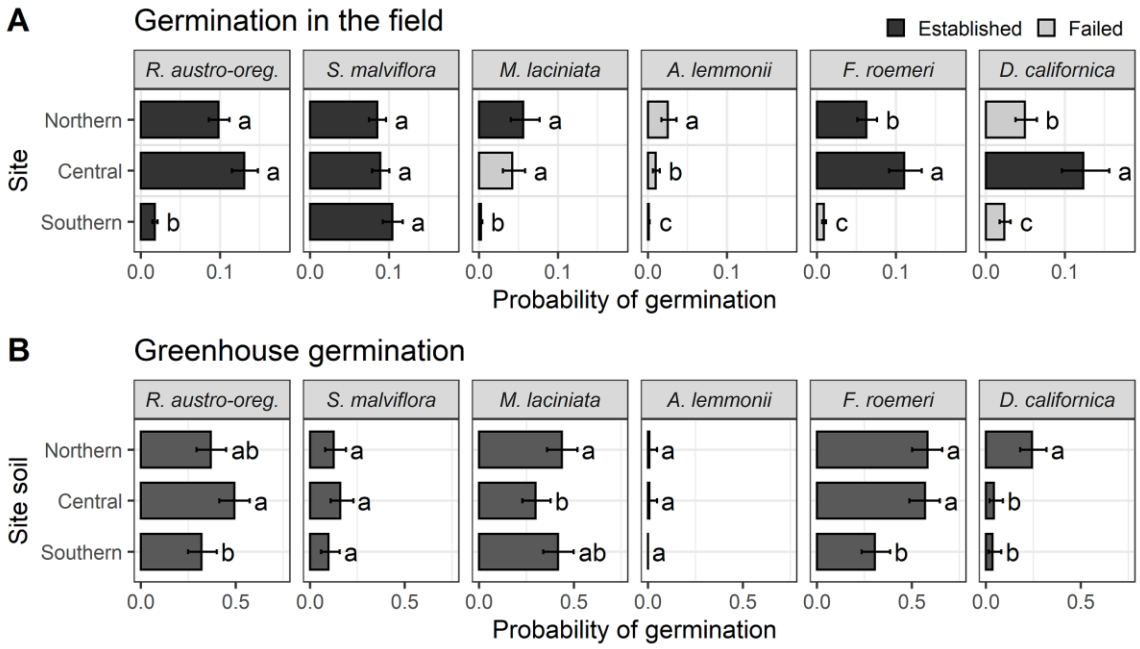

Figure 3.4. (A) Species' site-wide germination rates across years and treatments, where lowercase letters indicate significant differences among sites ($P < 0.05$) unique to each species. (B) Greenhouse germination rates in fall 2018 for each species by experimental site soil. Lowercase letters indicate significant differences between site soils for a species. Bars show estimated marginal means ± 95% confidence intervals. Note the different scales on the x-axis.

Discussion

In this study, we examined the population dynamics of six native perennials under experimental climate change within their northern range limits, as well as beyond the northern limits for two of the species. We found evidence suggesting that these species

may become increasingly vulnerable to decline within their current ranges due to warming. Contrarily, for the two range-restricted species also planted beyond their northern limits, projected changes in climate may benefit such pioneering populations. These findings support the expectation that species' ranges will shift with climate change.

Population growth rates for two species, *R. austro-oreganus* and *F. roemeri,* exhibited a latitudinal pattern, increasing from south to north. Annual temperatures in the PNW have already risen by ~0.8°C during the 20th century and the rate of increase has been accelerating (Abatzoglou, Rupp, & Mote, 2014; P. Mote, 2003), indicating that warmer temperatures may have caused these leading edge-trailing edge patterns in this system. The results of our climate treatments support this: a consistent result (with one exception) was that the warming treatments only decreased λ at sites within species' current ranges and increased λ at the sites beyond the northern limits of the two range-restricted species. This was also consistent with the prior experiment, in which warming reduced recruitment within but not beyond current ranges (Pfeifer-Meister et al., 2013). Increasing temperatures at sites within ranges generally caused these sites to become *less* hospitable, whereas increasing temperatures (and reduced precipitation) at sites beyond ranges caused those sites to become *more* hospitable. These circumstances may be attributed to direct physiological/thermal tolerance thresholds being surpassed (within ranges) or met (beyond ranges) (Angert, Sheth, & Paul, 2011; Peterson, Doak, & Morris, 2019), or by changes to biotic interactions causing greater competition (within ranges) or facilitation (beyond ranges) (Ettinger & HilleRisLambers, 2017).

Interestingly, since the negative effects of the warming treatments on λ within current ranges were of greater magnitude and more frequent than that of the drought

treatment (which had only a single negative effect), warming itself, rather than reduced soil moisture, appears to be driving the demographic decline in this system. We have previously found that warming also had a greater influence than moisture on these and other species' phenological responses to climate change (Reed et al., 2019), and we observed a similar response for soil respiration (Reynolds, Johnson, Pfeifer-Meister, & Bridgham, 2015). It seems that these phenomena are a function of the region's Mediterranean climate system, in which very wet soils occur throughout the winter and very dry soils throughout the summer until the onset of fall rains. Thus, there is only a narrow window in the spring growing season during which plants are negatively affected by changes in precipitation up to a 40% drought. Given the predicted rise in temperatures for the PNW (P. W. Mote & Salathé, 2010), these species will face increasingly difficult demographic pressures within their current ranges.

We also discovered that most species failed to establish reproductive populations at one or more sites regardless of climate treatment. Extremely low rates of germination and seedling survival drove this lack of establishment, which was especially pronounced in the southern site, where four of the six species could not establish and five of the six had their lowest rates of germination. Importantly, with the exception of *D. californica*, which was not included in the original experiment, these species also had an additional three years (2010-2012) for establishment to take place at the southern and central sites from the previous experimental legacy (Pfeifer-Meister et al., 2013), yet still failed to establish in most cases in the south.

Our greenhouse germination data suggests that soil conditions may be partially implicated in the failed establishment for *F. roemeri* in the south, but not for the other

species, which germinated just as well in the southern soil as they did in the soil(s) from where they could establish in the field. Instead, an inability to cope with the biotic community present may have contributed to the poor recruitment at this site. Shortly after reestablishing this experiment, our southern site became dominated by exotic annual grasses (Reed et al., *unpublished data*). Changes in species interactions, such as an increase in competition, can contribute to localized extinctions or demographic decline (Cahill et al., 2012; Olsen, Töpper, Skarpaas, Vandvik, & Klanderud, 2016). This appears to be the case at our southern site, where the rapid shift towards a dense cover of annual grasses coincided with low recruitment and, consequently, an inability to establish for most of our focal species. The invasive annual grasses which came to dominate (e.g., *Bromus tectorum*, *Bromus hordeaceus*, and *Vulpia myuros*) are winter-annual species, reaching full maturity early in the growing season (January to April), during the period of germination for most of our focal perennials. Thus, the perennial germinants likely experienced a strong competitive disadvantage relative to the winter-annual grasses, which were able to use up resources before the perennial germinants had an opportunity. This shift towards annual grass dominance also occurred between 2010-2012 and may become increasingly common in PNW prairies with hotter, drier conditions (Pfeifer-Meister et al., 2016), suggesting that recruitment challenges for these native perennials may become more commonplace.

Given our results, expectations under future climate change for the two range-restricted species, *R. austro-oreganus* and *S. malviflora*, differ considerably. Despite establishing populations at all three sites and the climate treatments being generally beneficial for populations outside its range, *R. austro-oreganus* exhibited consistently

poor demographic performance ($\lambda << 1$). This suggests that even if *R. austro-oreganus* could disperse beyond its range, it may face many challenges in maintaining viable populations. This species is endemic to a single county in southwestern Oregon and may be especially vulnerable in the future. *S. malviflora*, in contrast, exhibited high demographic performance ($\lambda >> 1$) across all three sites, with higher population growth rates in the south and north relative to the central site. Natural populations of this species are much less common in southern Oregon relative to the Willamette Valley, so its population growth rates being lowest at our central site suggests a possible role of enemy escape for this species at the southern and northern sites (Mlynarek et al., 2017). Indeed, *S. malviflora* is known to be affected by seed weevil larvae (*Macrorhoptus* ssp., among others) in the Willamette Valley (Young-Mathews, 2012), and we observed evidence of weevil damage at our central site but not at the southern and northern sites (B. Roy, *pers. obs.*). Although the IPMs consistently predicted $\lambda > 1$ for *S. malviflora*, the warming treatments did significantly reduce λ at the southern and central sites, suggesting it may only take a few extreme years to drive populations towards decline. At the northern site, beyond its range, populations exhibited high performance, especially under the warming treatments. Thus, if *S. malviflora* can disperse north of the Willamette Valley, our experimental results suggest that it may be capable of persisting.

Across their current ranges in this experiment, *M. laciniata* and *A. lemmonii* both seem vulnerable to decline. Nearest its northern limit, *M. laciniata* populations experienced considerable reductions in λ under warming, and at the southern and central sites, failed to establish altogether due to extremely poor recruitment. Data collected from four natural populations across part of its range from 2015-2018 support these

suggestions of vulnerability, as early-season senescence and high rates of herbivory caused poor demographic performance in all populations (P. Reed, *unpublished data*). *A. lemmonii* failed to establish at all in our experiment, with extremely low germination observed both in the field as well as in our greenhouse germination study. Low germination success can be indicative of inbreeding depression, which is often greater in species with isolated populations (Richards, 2000). While we consider *A. lemmonii* 'widespread' across the PNW, its populations are small (a few hundred plants) and markedly disjunct, suggesting inbreeding depression may be a factor leading to its decline.

While *Festuca roemeri* exhibited leading edge-trailing edge patterns in this experiment, data from natural populations of *A. lemmonii, F. roemeri,* and *D. californica* collected between 2015-2018 show an opposing pattern of λ decreasing from south to north (Peterson et al., *unpublished data*). However, that study also showed that local performance of those natural populations decreases with warmer, drier conditions, suggesting that factors other than climate (e.g., habitat quality, biotic interactions) may control the natural latitudinal patterns in λ, but that climate change will still negatively impact populations across their ranges. Thus, these species may be vulnerable to population decline and range contractions with climate change, and their future viability may well depend on an increase in performance for their northern peripheral (leading edge) populations, as well as their potential to disperse to newly suitable habitats.

Demographic compensation has been hypothesized as a mechanism which can 'buffer' populations from a perturbation (e.g., climate change), potentially rescuing them from decline (Doak & Morris, 2010). Using a life table response experiment analysis, we

found little evidence for demographic compensation in our focal species. However, we caution that our results are not entirely conclusive: survival and growth are two commonly opposing vital rates (Peterson et al., 2018), but our methods only considered their combined contribution, and also did not examine potentially opposing responses across size classes. Thus, we may be underestimating the cases of compensation. Whether compensation will rescue species in the coming decades as warming continues is unanswered, although other studies suggest it is unlikely (Doak & Morris, 2010; Sheth & Angert, 2018).

While our study provides strong evidence that climate change will alter demographic performance within and, for two species, beyond northern range limits, there are a few notable caveats. First, the three-year study period is relatively short compared to the lifespan of these perennial plants, so it is possible that reproductive populations could establish given more time. Notably here, however, most species (all but *D. californica*), actually had six years of potential establishment at the southern and central sites (given the previous experiment). Second, the patterns we observed were often driven by germination and seedling survival, but these early-life vital rates may have low impact on λ relative to adult performance. Given relatively low adult sample sizes for some vital rates and species (Appendix B: Table S3), we lacked complete estimates of adult performance in some cases. Regarding the low germination in this experiment, it is also possible that the seeds are only dormant and thus still viable (Trask & Pyke, 1998). However, if true, our evidence suggests germination might be restricted to rare "optimal" years. If the frequency of optimal years is too low to compensate for seed loss due to biotic and abiotic factors, the net result would still be decreasing

demographic performance. Lastly, other site factors not related to climate, including the biotic communities (see above discussion), disturbance history, and soil characteristics, may be potentially relevant in the responses we observed.

Conclusions

To our knowledge, this study was the first to construct complete demographic models of multiple perennial species planted within and beyond their northern range limits under a climate manipulation experiment embedded within a latitudinal gradient. Overall, our findings imply that some native perennial prairie species in the PNW are at risk of decline with climate change, and that these species may need to shift their ranges to persist in the future. Population decline within ranges appears to be driven by warming in this Mediterranean climate system. Increased temperature tended to reduce population growth rates within but not beyond northern range limits, and poor demographic performance within ranges was often attributable to low germination and seedling survival.

Our findings have important management implications. The low establishment rates of these perennial species suggest that transplanting larger plants may be a more effective strategy than seed sowing for restoration practitioners hoping to reestablish or manage populations under climate change (Wallin, Svensson, & Lönn, 2009), particularly for areas that experience a shift towards winter-annual grass dominance with climate change. Beyond their current range limits, species may be capable of establishing populations if they can disperse to suitable habitats. Indeed, our two range-restricted perennials are capable of establishing north of their ranges (and even outperforming when compared to their current ranges), and evidence from other transplant studies suggest that

this is a relatively common phenomenon (Baer & Maron, 2018; Hargreaves et al., 2014; Norton, Firbank, Scott, & Watkinson, 2005; Prince & Carter, 1985; Samis & Eckert, 2009). Thus, dispersal limitation may be a critical factor in the persistence of many species in the future, especially considering the potential for further landscape fragmentation. In managing for native biodiversity, these implications beg the questions: should restoration practitioners consider 'restoring' based on future range suitability? Is assisted migration a viable option for protecting vulnerable species? The best answers to these questions depend upon a species' capacity to adapt to climate change (Dawson et al., 2011), its potential for expansion outside its current range, and the value society chooses to place on protecting biodiversity. This ethical dilemma may become increasingly important to debate as climate change continues to threaten species' persistence.

CHAPTER IV

CLIMATE WARMING THREATENS THE PERSISTENCE OF A COMMUNITY OF DISTURBANCE-ADAPTED NATIVE ANNUAL PLANTS

Contributions

This chapter is co-authored by Paul B. Reed, Scott D. Bridgham, Laurel E. Pfeifer-Meister, Megan L. Peterson, Bart R. Johnson, Bitty A. Roy, Graham T. Bailes, Aaron A. Nelson, William F. Morris, and Daniel F. Doak. I was responsible for leading the data collection, analyses, and writing of this manuscript. Daniel F. Doak prepared the climate data. All authors designed the experiment, contributed to the review process, and gave final approval for publication.

Introduction

Managing vulnerable species in a rapidly changing environment is a major conservation challenge. Because many species are believed to be at risk of decline with climate change (Pereira et al. 2010, Moritz and Agudo 2013, Román-Palacios and Wiens 2020), an increasingly important task is to predict how demographic performance will be affected by future climatic conditions, as well as what other factors could be managed to mitigate climate effects. This leads to two important questions for conservation: Under what climatic conditions can species exhibit stable or increasing populations? And, how do non-climatic effects such as disturbance alter population growth rates, potentially providing a way to mitigate climate change effects via local management?

Management of vulnerable plant populations, even before anthropogenic climate change became a complicating threat, has relied on understanding the factors most

important in controlling local population growth rates. Disturbance is often a critical component to successfully establishing and maintaining a population (Connell and Slatyer 1977, Palmer et al. 1997, Macdougall and Turkington 2007). This is especially true for annual plants, which tend to be early-successional species and are therefore frequently limited by competition (Bazzaz 1979, Tilman 1990, Rees and Long 1992). Annuals are also subject to dramatic fluctuations in population size (Nunney 2002) and may be especially vulnerable to climate change (Morris et al. 2008). However, no studies to our knowledge have examined the controls of climate and disturbance together on the demographic success of a suite of co-occurring annual plants. It is critical to identify what factors have similar effects on co-occurring species to inform community-wide management in the face of climate change. While many conservation and restoration plans attempt to optimize benefits for a suite of native species (Wang et al. 2020), doing so successfully requires an understanding of the extent to which demographic responses are generalizable.

Furthermore, while climate change may prove detrimental for species within portions of their current geographic ranges, it may also open the possibility for range shifts that support long-term persistence (Pfeifer-Meister et al. 2013, Rehm et al. 2015, Reed et al. 2021). But because the ability to track favorable climatic conditions may be limited by dispersal (Loarie et al. 2009, Hargreaves et al. 2014, Bayly and Angert 2019, Cruzan and Hendrickson 2020, Pagel et al. 2020), vulnerable plants may require intentional translocations to newly suitable sites (Vitt et al. 2010). To justify such actions, it is important to understand how species will perform across climate gradients under projected climate change.

Experimentation provides a robust means to relate species' demographic performance to the effects of climate and disturbance. In particular, experimental manipulations that impose a range of current and future climatic conditions across multiple sites can disentangle the role of climate from local site factors (Dunne et al. 2004, Villellas et al. 2019), and identify the degree to which population growth rates might change under future (relative to current) conditions. In addition, field manipulations focused on multiple species can give insights into the generality of climate responses, as well as other factors limiting population growth rates. While single species studies have provided many insights into limiting factors, a key question is whether they can be generalized to multiple species.

Here, using six years of data from two climate manipulation experiments spanning four sites across a latitudinal gradient, we examined the relationship between climate and demography for a suite of eight annual plant species native to prairie habitat in the western Pacific Northwest (PNW), USA. While our experiments were principally designed to focus on climate manipulations, we were also able to address how management-driven disturbance conditions shaped demographic performance.

Of the eight annual species we studied (Table 4.1; see Appendix C: Supplemental Methods for species' descriptions), five have current northern range limits that occur south of at least one of our experimental sites (Figure 4.1). These five species were therefore planted both within and beyond their current ranges. All eight species are important members of imperiled PNW prairie ecosystems (Noss et al. 1995), which have become the focus of many regional conservation and restoration efforts (Dunwiddie and Bakker 2011). PNW prairies were historically widespread, in part due to frequent burning

by Native Americans (Boyd 1999). Following Euro-American settlement, fire suppression, land conversion, and the establishment of non-native species have contributed to the loss and modification of PNW prairie ecosystems (Dennehy et al. 2011). Native annual species, in particular, have suffered tremendous declines, and many have become locally extirpated from most remaining prairie fragments (Dunwiddie et al. 2014). Deliberate reintroductions are often necessary to restore this functional group to the landscape.

Species	**Family**	**Exp**
Plectritis congesta (Lindl.) DC	Caprifoliaceae	Exp2
Collinsia grandiflora Lindl.	Plantaginaceae	Both
Clarkia purpurea (W. Curtis) A. Nelson & J.F. Macbr.	Onagraceae	Both
Plagiobothrys nothofulvus A. Gray	Boraginaceae	Exp2*
Aristida oligantha Michx.	Poaceae	Both
Achyrachaena mollis Schauer	Asteraceae	Both
Thysanocarpus radians Benth.	Brassicaceae	Both*
Navarretia pubescens (Benth.) Hook. & Arn.	Polemoniaceae	Both

Table 4.1. The eight focal species in descending order of northern range limit (see Figure 4.1). All species have southern range limits in California. "Exp" column: *P. congesta* and *P. nothofulvus* were only planted in the second experiment (Exp2), while all other species were planted in both experiments. **P. nothofulvus* and *T. radians* were also not planted in fall 2015 (see Methods).

Ongoing climate change may further threaten these ecosystems (Bachelet et al. 2011), as regional precipitation is expected to become more variable and mean annual temperature is expected to rise by ~3°C by the end of the 21st century (Mote and Salathé 2010). Indeed, previous studies from our climate manipulation experiments suggest that warming will be detrimental for native perennial species within their current geographic range limits (Pfeifer-Meister et al. 2013, Reed et al. 2021), cause a greater risk of introduced annual grass invasions (Pfeifer-Meister et al. 2016), and shift native species'

flowering and growth phenology (Reed et al. 2019). To understand how climate and disturbance will affect populations for this suite of native annual species, we asked:

1. How does demographic performance, and thus population growth rate, vary across a range of current and future climatic conditions?
2. Do species exhibit similar patterns in population growth rates across climatic space? Does being within versus beyond current northern limits affect performance?
3. How important is the role of disturbance in determining performance and modulating climate effects on these annual species?

Methods

Study sites and experimental design:

This study combines six years of data from two experiments (Exp1: 2010-2012; Exp2: 2016-2018) that occurred across four sites spanning a 520 km latitudinal Mediterranean-climate gradient in the western PNW (Figure 4.1). The southern and central sites were used during both Exp1 and Exp2 while the northern 2 site replaced the northern 1 site between experiments since the northern 1 site was no longer available. Summer drought severity increases from north to south across this gradient. The 30-year normal (1981-2010) mean annual temperatures are 10.6°C, 10.5°C, 11.4°C, and 12.3°C at the northern 2, northern 1, central, and southern sites, respectively, while mean annual precipitation is 1240 mm, 1196 mm, 1134 mm, and 1434 mm, respectively (PRISM Climate Group). However, the southern site receives the greatest proportion of its precipitation in the early growing season (November – March) and is generally much drier than the other sites in the spring and summer (Reynolds et al. 2015). All sites are

located within PNW prairie habitat and were dominated by introduced perennial grasses prior to plot establishment. Treatments were discontinued at the southern and central sites during the gap years between Exp1 and Exp2.

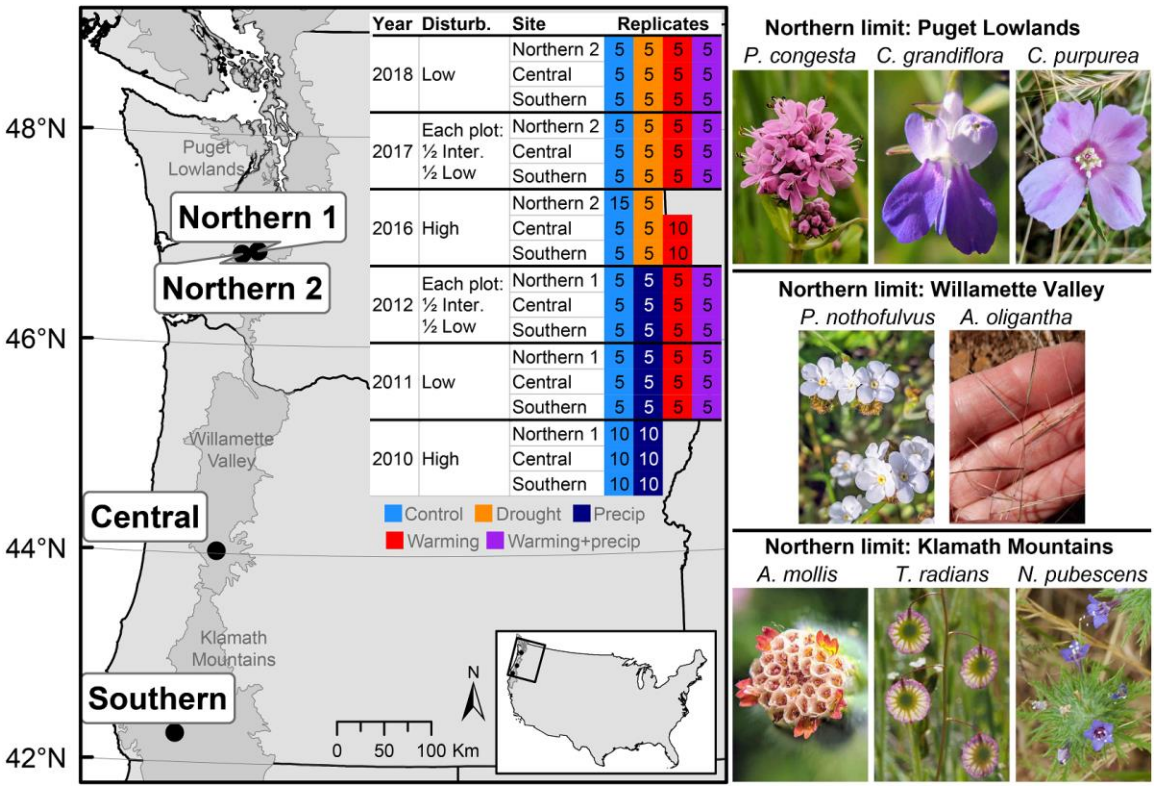

Figure 4.1. On the left: map of the four experimental sites in the western Pacific Northwest, USA, with inset table describing the disturbance conditions, sites, and climate treatment plot replicates for each year of the experiments (Exp1: 2010-2012, Exp2: 2016-2018; see Methods). There were 62 unique year x site x climate treatment combinations and 360 replicates in total. On the right: the eight focal species grouped by their current northern-range-limit regions (full species names given in Table 4.1). The Klamath Mountain species are within their current ranges only at the southern site; the Willamette Valley species are within their current ranges at the southern and central sites; the Puget Lowland species are within their current ranges at all four sites. Photo of *A. oligantha* by Ed Alverson; all other photos by Paul Reed and Bitty Roy.

Each site contained 20 plots of 7.1-m^2 that required heavy disturbance, prior to both experiments, to reduce existing vegetation and establish baseline starting communities. In late 2009 and 2015, plots were mowed, raked, and treated with herbicide (2% Glyphosate and grass-specific Poast). These events created ample open space for the

2010 and 2016 growing seasons, which are hereafter referred to as 'high disturbance' conditions (Figure 4.1). Following the 2009 disturbance, we sowed the southern, central, and northern 1 plots with an establishment mix of 19 native prairie species (Pfeifer-Meister et al. 2013), and, following the 2015 disturbance, we sowed the southern, central, and northern 2 plots with an establishment mix of 29 native prairie species (Reed et al. 2021). Beginning in year two of each experiment (2011 and 2017), rapid regrowth of non-native vegetation resulted from minimal plot maintenance (hereafter: 'low disturbance' conditions). This regrowth was moderately controlled in half of each plot in 2012 and 2017 by implementing an 'intermediate disturbance' treatment (see below).

Each plot was assigned to a climate manipulation treatment. For Exp1, these were control (ambient temperature and precipitation), precip (+20% precipitation within the 2 week interval in which it occurred), warming (+2.5-3°C), and warming + precip (+2.5-3°C and +20% precipitation). Because we found the +20% precipitation treatment to have minimal effects and the warming treatment to be confounded by a reduction in soil moisture in other studies (Pfeifer-Meister et al. 2013, 2016), we modified treatments prior to Exp2. In Exp2, the climate treatments were control, drought (-40% precipitation), warming (+2.5°C), and warming + precip (automatically irrigated to fully offset the warming-induced drying effect). See Appendix C: Supplemental Methods for a complete description of all climate treatments. Although there were differences in the warming + precip treatments of Exp1 and Exp2, we group them together in our figures for simplicity. Thus, we define five broad climate treatments overall (control, drought, precip, warming, and warming + precip). Due to logistical constraints with heating and irrigation, some treatments had delayed starting dates, resulting in uneven treatment replicates during

some years (Figure 4.1; Appendix C: Supplemental Methods). Within each plot, we continuously logged canopy temperature and soil volumetric water content over the course of each experiment. However, also due to logistical constraints, this did not begin until several months into each experiment.

To monitor germination and survival of focal species, we planted 200 seeds per species per plot (25 seeds into eight 5.5-cm diameter subplot rings) in the fall prior to each experiment year, with a few exceptions. Neither *Plectritis congesta* nor *Plagiobothrys nothofulvus* were planted during Exp1, and neither *P. nothofulvus* nor *Thysanocarpus radians* were planted in fall 2015. Additionally, for *T. radians*, we only sowed 80 seeds in fall 2016 and 70 seeds in fall 2017 (10 seeds into eight and seven subplot rings, respectively) due to seed quantity limitations. To account for local adaptation, we used the nearest available seed sources for each site.

Because we observed very low recruitment one year into both experiments, we implemented an 'intermediate disturbance' treatment in half of each plot in the winter-spring of 2012 and 2017. This intermediate disturbance consisted of weeding and clipping any non-focal species to reduce their aboveground biomass. This resulted in only a moderate reduction in competitors compared to the high disturbance conditions of 2010 and 2016, based on our visual assessment of the amount of open space created. However, there was a noticeable reduction in non-focal species biomass compared to the plot halves not receiving the treatment, as well as the entire plots during the low disturbance-only years of 2011 and 2018. Thus, both experiments (and all four sites) imposed high, intermediate, and low disturbance conditions.

Demographic data:

We quantified three vital rates each experiment year: germination, survival (from germination to flowering), and per-capita seed production. Between winter and spring, we conducted 2-4 censuses of each plot to count the number of germinants from the previous fall's planting. We thinned germinants in overcrowded subplots and corrected survival estimates for thinning. We aggregated germination and survival counts to the plot or the half-plot level (for 2012 and 2017). In 2018, we estimated germination from the seedbank by returning to subplot rings seeded in fall 2016 and fall 2015 to count second and third year germinants, respectively.

Per-capita seed production (collected during the final spring censuses) was estimated differently for Exp1 and Exp2. In Exp2, we counted plant-level fruit and/or seed production on all or a subset of the individuals in a plot, harvesting a subset of fruits for the species which were too difficult to directly count seeds in the field. However, in Exp1, we harvested fruits from a known number of plants and combined these into a single sample (per plot), and then counted the total number of seeds (per plot) to estimate mean seeds per plant. Because we lacked plant-level seed production for Exp1, we calculated the mean number of seeds per plant for each year at the plot level for both experiments.

Analysis overview:

Since we combined results from different sites, years, and experimental treatments into a single analysis, we needed to create common data currencies. We did so by categorizing plot preparation and management actions into three disturbance groups (noted above and in Figure 4.1), and by replacing categorical climate treatments with continuous measures of temperature, precipitation, and composite variables (actual

evapotranspiration and climatic water deficit). We then considered regression models that accounted for site, disturbance, and continuous climate covariates. In addition to allowing us to combine data from two experiments into a single, robust analysis, by regressing vital rates on actual climate variables (rather than taking an ANOVA approach with categorical treatments), we can (in future work) better project the effects of future changes in those climate variables.

However, this approach also meant that we could not account for interactions among sites and years, or random effects within years that were not related to interannual differences in climate. We attempted to address this with a random year effect, but year was partially confounded with site and disturbance and there were unequal sample sizes among sites. This often resulted in poor model fit with unrealistic estimates for some site and year combinations.

Since we could not account for interactions among sites and years, the effects of disturbance and climate covariates may be overestimated due to excessively narrow standard errors on coefficient estimates. However, despite this caveat, we feel that our strategy made the best-possible use of our unique datasets. It allowed us to combine multiple years of data from manipulative climate treatments across four sites into a climate response surface based on temperature and moisture, which are the climate forcing variables of interest to the larger scientific community. We also did this for suite of eight plant species rather than focusing on a single species.

Analyses:

We conducted all analyses using R version 4.0.2 (R Core Team 2020). Because we noticed a strong decline in focal species' performance when disturbance was low, we

first ran an ANOVA-based analysis looking at the effects of disturbance and site. Using mixed models, we ran logistic regressions on germination, survival, and recruitment into the reproductive class (total survival from planting to reproduction, or the product of germination and survival). Since we lacked plant-level seed data for Exp1 and thus could not use a Poisson-family generalized linear model, we ran linear models of the log-transformed mean number of seeds per plant (plus a small constant 0.1 since some means were zero) weighted by the number of plants per plot used to calculate the means. We treated site, disturbance, and their interaction as fixed effects and plot as a random effect (to account for repeated sampling across years) and tested for statistical differences among sites and disturbance levels using Tukey's post-hoc comparisons.

To test for relationships between vital rates and climate, we focused on environmental variables related to temperature, precipitation, and drought stress due to their documented relevance for PNW prairie plant performance (Pfeifer-Meister et al. 2016, Reed et al. 2019, 2021, Peterson et al. 2020). To accommodate missing plot-level data on canopy temperature and soil moisture, and to estimate how large-scale climate conditions will alter plant performance, we ran a series of analyses that translated treatment-specific, plot-level climatic data into predicted measures of mean temperature, total precipitation, and drought stress that correspond to PRISM (PRISM Climate Group) climate variables (Appendix C: Supplemental Methods). Briefly, using directly measured data from control plots, we first established the relationship between monthly site-level PRISM estimates of temperature and precipitation with plot-level canopy temperature and soil volumetric water content. Using this relationship, we then estimated PRISM values of temperature and precipitation for each climate treatment plot using their unique

temperatures and water contents. Finally, we used these estimates of temperature and precipitation to derive potential evapotranspiration (PET), actual evapotranspiration (AET – the amount of water removed by evaporation and transpiration) and climatic water deficit (CWD – PET minus AET), which were calculated using the Redmond 2019 R function using a modified Thornthwaite water balance model. For analyses of demographic rates, we aggregated monthly climate variables (mean temperature, total precipitation, AET, and CWD) into winter and spring seasonal values (November - February and March - June, respectively), since in the Mediterranean-type climate of the PNW these species generally germinate in the fall and winter, grow and reproduce in the spring, and senesce by the summer.

Using these seasonal values, we tested for climate effects on vital rates by fitting a series of mixed models that also accounted for site x disturbance effects and a random plot effect. We fit models that combined one temperature variable (winter or spring) with one moisture variable (winter or spring precipitation, AET, or CWD, excluding winter CWD since it was always zero), resulting in seven total climate variables (two seasons x four variables, minus winter CWD). We excluded models containing combinations of winter temperature with winter AET and spring temperature with spring CWD due to high collinearity. We included quadratic effects of climate to allow unimodal (hump-shaped) relationships between vital rates and climate, as it is reasonable to expect vital rates to peak at intermediate conditions. We incorporated temperature x precipitation interactions but not temperature x AET or temperature x CWD since temperature is directly incorporated into the calculations of AET and CWD.

We were unable to include climate x site or climate x disturbance interactions due to low within-site climate variation during the high-disturbance years (when not all climate treatments were operational yet), and limited data in later years when species' abundances were low. Including such interactions forced poor model fit with unrealistic predictions. Although this prohibited us from testing whether climate responses differed within versus beyond current ranges, we could still establish relationships between vital rates and the climate across the entire latitudinal gradient.

We identified the model with the best predictive performance for each vital rate using a *K*-fold cross-validation procedure (James et al. 2013, Tredennick et al. 2021), where $K = 5$. Stratifying by site, disturbance, and year, we randomly split the dataset into five groups (*folds*) and iteratively withheld one fold (20%) at a time to serve as an out-of-sample test set while the remaining four folds (80%) served as a training set. Within each loop, we fit all possible subsets of the series of models we wanted to examine, including two no-climate null models (one that accounted for site and disturbance effects and the other accounting for site only). For each model fitted to the training dataset, we made predictions on the out-of-sample test data and compared these predictions to observed values to calculate a mean-squared-error for each model within each fold. We then calculated the average mean-squared-error for each model across the five folds and considered the model with the lowest average mean-squared-error to have the best predictive performance. We then fit this "best" model formula to the entire dataset.

To estimate population growth rates (λ), we sampled 1000 random sets of our seven climate variables from a multivariate normal distribution based on their means and covariances across all sites and years of the study. We then predicted germination,

survival, and seed production for each site and disturbance level on that set of climate values using our models with the best predictive performance, and calculated λ as the product of the three predicted vital rates. To estimate uncertainty in each vital rate, we used the 'predictInterval' function from the merTools package (Knowles and Frederick 2020), using 2000 simulations to obtain 95% prediction intervals. We multiplied the three upper limits of the vital rates to get the upper prediction limit for λ, and the three lower limits of the vital rates to get the lower prediction limit for λ. We did not include a seedbank when calculating λ as our limited seedbank germination data suggested these rates were minimal (see Results).

To visualize λ as a function of climate, we performed a principal component analysis (PCA) on our measured climate data. Using a PCA was necessary since different vital rates could be explained by different combinations of the seven climate variables (e.g., a germination model may include winter temperature and winter precipitation, but the survival model includes spring temperature and spring CWD). Using the simulated set of multivariate climate values, we plotted smoothed contours of λ against PC1 and PC2 scores using a loess fit. We acknowledge that this loess-fit procedure adds a second dimension of uncertainty to our analyses. However, our goal with these analyses was to simply to visualize the best-estimated relationships between λ and climate, and not to estimate full uncertainty in these effects. Thus, we felt this was the simplest procedure to use and interpret.

Lastly, we also explored how climate and disturbance event frequency jointly determined each species' long-run (geometric mean) annual population growth rate. For

an annual plant with no seed bank living in an environment with stochastic disturbances, the long-run growth rate is given by:

$$\lambda_g = {\lambda_h}^{p_h(d)} {\lambda_i}^{p_i(d)} {\lambda_l}^{p_l(d)}$$

where λ_h, λ_i, and λ_l are the population growth rates in years of high, intermediate, and low disturbance conditions, respectively, and $p_h(d)$ $p_i(d)$, and $p_l(d)$ are the proportions of years with high, intermediate, and low disturbance conditions, which depend on the frequency of disturbance events, *d*. We assumed that high disturbance conditions prevail in a year with a disturbance event, intermediate conditions prevail in the first year post-disturbance event, and low disturbance conditions two or more years post-disturbance. We used a Markov model in which we calculated λ_g across disturbance event probabilities (*d*) ranging from 0 to 1 in increments of 0.02. The proportions of years with high, intermediate, and low disturbance conditions are then given by the dominant right eigenvector (normalized to one) of the Markov matrix that governs transitions between disturbance states (where columns represent the high, intermediate, and low disturbance conditions this year and rows represent the conditions next year, in the same order):

$$\begin{bmatrix} d & d & d \\ 1-d & 0 & 0 \\ 0 & 1-d & 1-d \end{bmatrix}$$

Because *P. nothofulvus* was not planted under high disturbance conditions, we assumed intermediate conditions in a disturbance event year and low disturbance conditions one or more years post-disturbance event.

Results

Recruitment was greatest under high disturbance for most species and sites (Figure 4.2A; site x disturbance: $p < 0.05$ for all species). *P. congesta* was the major

exception, having highest recruitment under intermediate disturbance regardless of site. Predicted recruitment was 11.0 ± 2.1% (mean ± 1 s.e.) across all species and sites under high disturbance but fell to just 3.9 ± 1.3% and 2.3 ± 0.8% under intermediate and low disturbance, respectively. Germination and survival, the two components of recruitment, exhibited similar responses to disturbance but significant differences were more common for germination (Appendix C: Figure S4.1). Most species also had greatest per capita seed production under high disturbance regardless of site, with seed counts often more than tenfold greater compared to intermediate and low disturbance (Figure 4.2B). Again, *P. congesta* (at the northern 2 site) was the major exception to this finding. Germination from the seedbank was mostly negligible, with high-end estimates of just 0.6% and 0.3% of the seeds germinating after two and three years in the seed bank, respectively, in 2018 across all species and sites (Appendix C: Table S4.1).

We established strong relationships between monthly PRISM estimates of temperature ($R^2 = 0.985$) and precipitation ($R^2 = 0.828$) from control plot canopy temperatures and soil volumetric water contents. When performing a PCA on our set of seven climate variables, the first two principal components accounted for 50.02% and 23.77% of the variance in the climate data, respectively (Figure 4.3). PC1 was mostly driven by variation in temperature (cooler to warmer from left to right), while PC2 generally reflected additional variation explained by moisture (drier to moister from bottom to top). Most of the climate-space variation was between the warmed and not-warmed treatments regardless of site, rather than among sites (Appendix C: Figure S4.2).

With the exception of *P. nothofulvus* seed production, the vital rate models with the best predictive performance included at least one climate term (Appendix C: Table

S4.2). In general, most of these models substantially reduced average mean-squared-error relative to the two no-climate null models (Appendix C: Table S4.3). Most vital rates predicted by temperature and/or climatic water deficit (CWD) had negative or unimodal

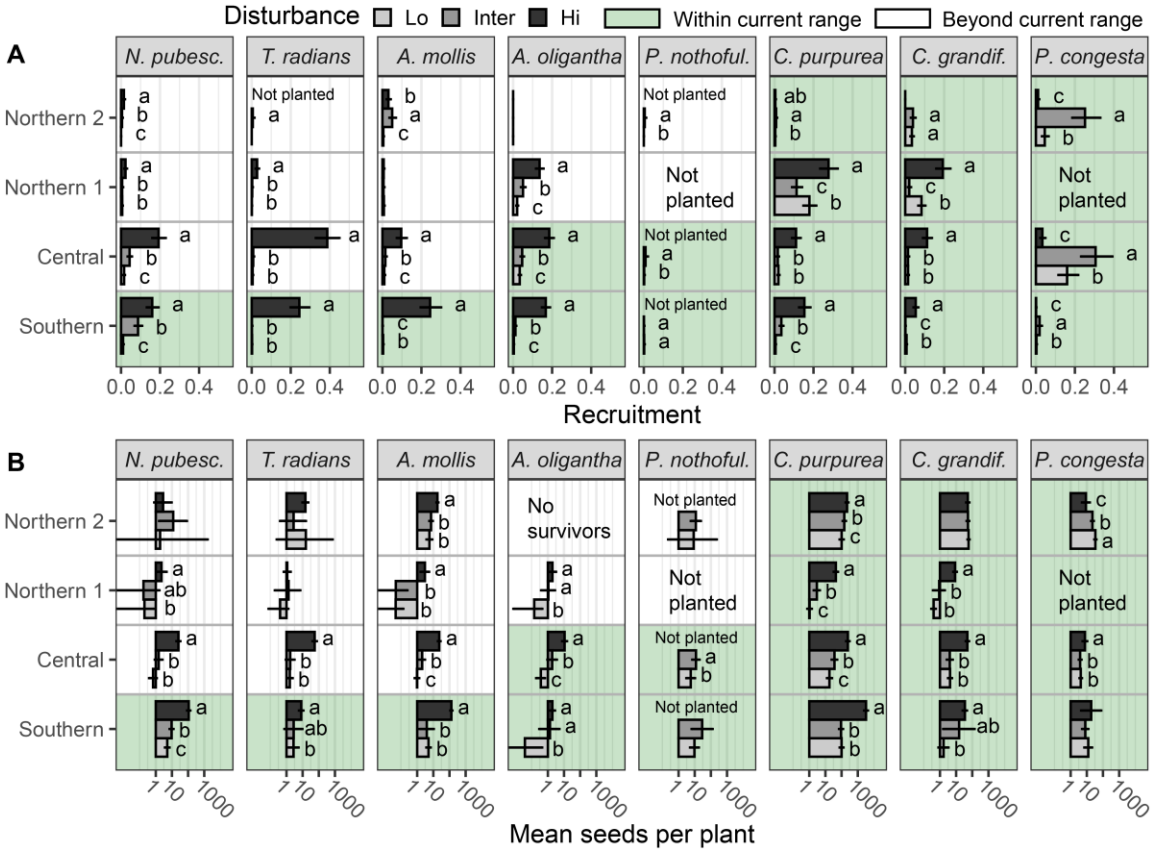

Figure 4.2. The role of disturbance (high, intermediate, low) on species' (A) recruitment (surviving plants per seed planted) and (B) seeds per surviving plant (note the log-scale axis). Bars show estimated marginal means ± 95% confidence limits. "High" disturbance includes all data from 2010 and 2016; "intermediate" disturbance includes all data from the plot halves receiving the intermediate disturbance treatments of 2012 and 2017; "Low" disturbance includes all data from 2011 and 2018, as well as all data from the plot halves that did not receive the intermediate disturbance treatments in 2012 and 2017 (see methods). Letters indicate significant differences ($p < 0.05$) between disturbance levels for a given site and species. Species are arranged from left to right in ascending order of northern range limit.

relationships with these variables, whereas relationships to precipitation and actual evapotranspiration (AET) were more variable (Appendix C: Figures S4.3-S4.10).

Although disturbance and site influenced the intercepts of vital rate-climate relationships, there was no consistent tendency for certain sites to support higher performance.

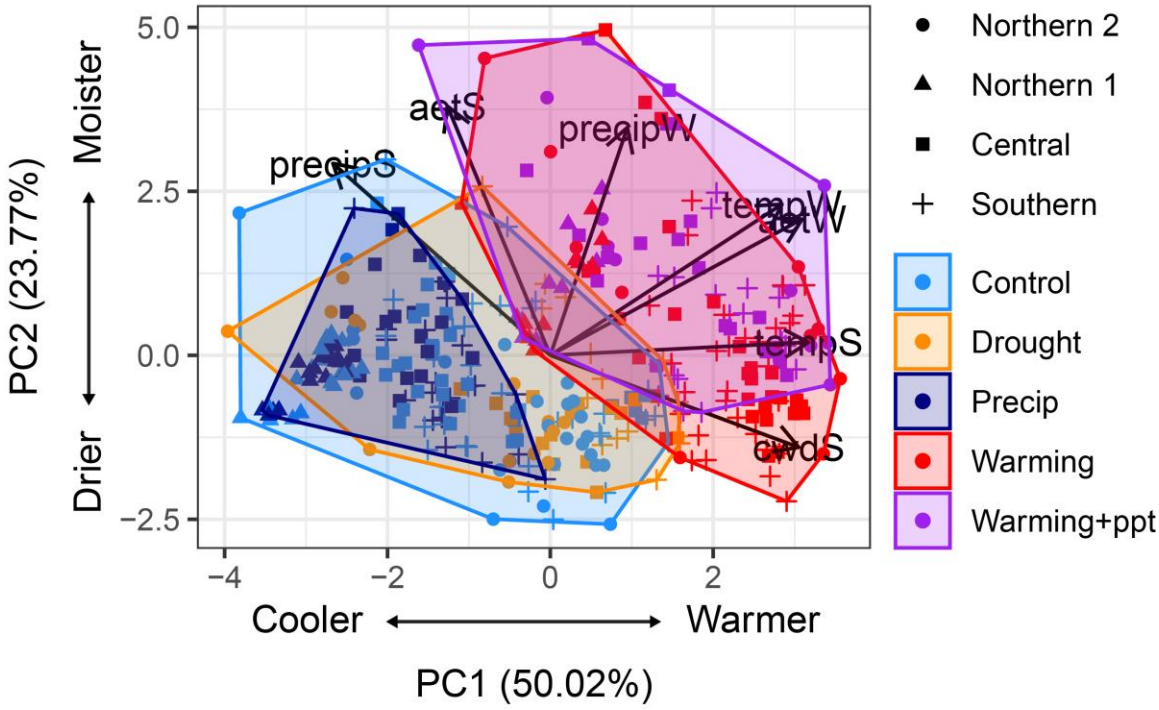

Figure 4.3. Principal components analysis of the seven climate variables used in the study, using all 360 unique replicates from Exp1 and Exp2. Polygons encapsulate the five broad climate treatments. 'temp' = mean temperature, 'precip' = total precipitation, 'aet' = total actual evapotranspiration, 'cwd' = total climatic water deficit; 'W' = winter, 'S' = spring. PC1 is primarily driven by temperature (cooler to warmer from left to right) while PC2 reflects additional variation explained by moisture (drier to moister from bottom to top). There is considerable separation in climatic space as a result of the warming treatments, regardless of site.

When integrating vital rate models into predicted population growth rates (λ), we observed a wide range in the magnitude of λ by species and disturbance (Figure 4.4: note each species' response is averaged across sites). However, with few exceptions, λ was << 1 under low disturbance but >> 1 under high disturbance. These patterns hold true at the 95% prediction limits (Appendix C: Figures S4.11, S4.12). The only exceptions were *P. congesta*, for which λ peaked at intermediate disturbance, and *Collinsia grandiflora*, which showed relatively weak effects of disturbance. λ also differed strongly by site, but

this effect did not appear to be a simple function of latitude (Appendix C: Figures S4.13-S4.15).

For most species, λ increased toward cooler climatic conditions (Figure 4.4: negative scores for PC1; note the colored polygons depicting the range of climatic conditions that occurred in each treatment). *Navarretia pubescens, T. radians,* and *P. nothofulvus* peaked at cooler, drier conditions while *Achyrachaena mollis, Clarkia purpurea, C. grandiflora,* and *P. congesta* peaked at cooler, moister conditions. *Aristida oligantha* was the major exception, as it increased toward warmer, drier conditions (Figure 4.4). Again, responses remain consistent at the 95% prediction limits (Appendix C: Figures S4.11, S4.12). These patterns become especially apparent when plotting log(λ) against PC1 (Figure 4.5; note each species is plotted under its optimal disturbance condition). Five of the eight species exhibit a steep decline in log(λ) once outside of ambient PC1 conditions, while *P. nothofulvus* and *P. congesta* exhibit more subtle, but consistent, decline. *A. oligantha* is the lone species to have log(λ) increase with PC1.

Lastly, the long-run annual population growth rate, calculated as a function of climate and disturbance frequency, revealed that more frequent disturbances would increase population growth rates for every species except *P. congesta* (Figure 4.6). With greater warming (increasing PC1), *N. pubescens, T. radians, A. mollis, P. nothofulvus, C. purpurea,* and *C. grandiflora* would all require more frequent disturbance to sustain population growth rates. In contrast, while *A. oligantha* would also benefit from more frequent disturbance, this would not be necessary for it to sustain its populations under future conditions.

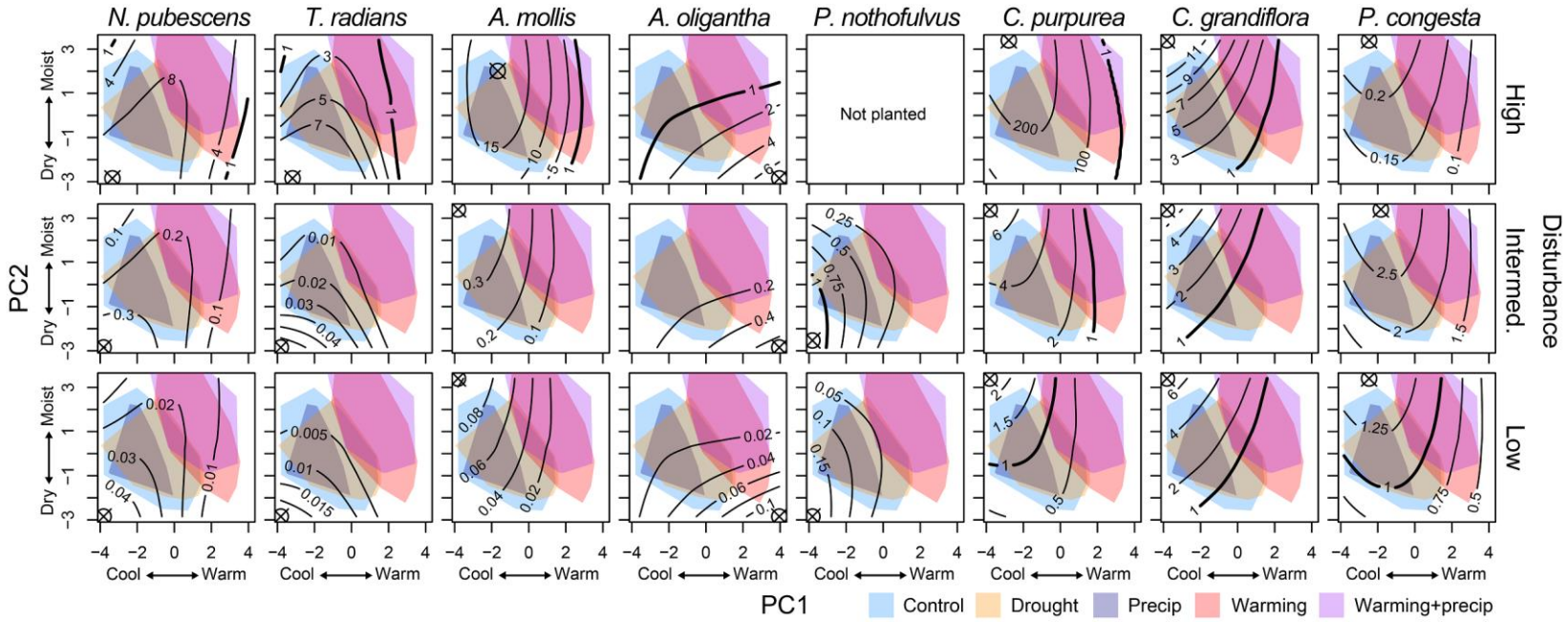

Figure 4.4. Contour plots of estimated population growth rates (λ) as a function of climate (PC1 and PC2) and disturbance (high, intermediate, and low) averaged across sites for each of the eight focal species. Climate is depicted as the first two principal components of all seven climate variables used in the study, with PC1 reflecting temperature (cooler to warmer left to right) and PC2 reflecting moisture (drier to moister bottom to top). Colored polygons depict the range of climatic conditions that occurred in each climate treatment over the course of the experiments. ⊗ indicates the location of highest λ.

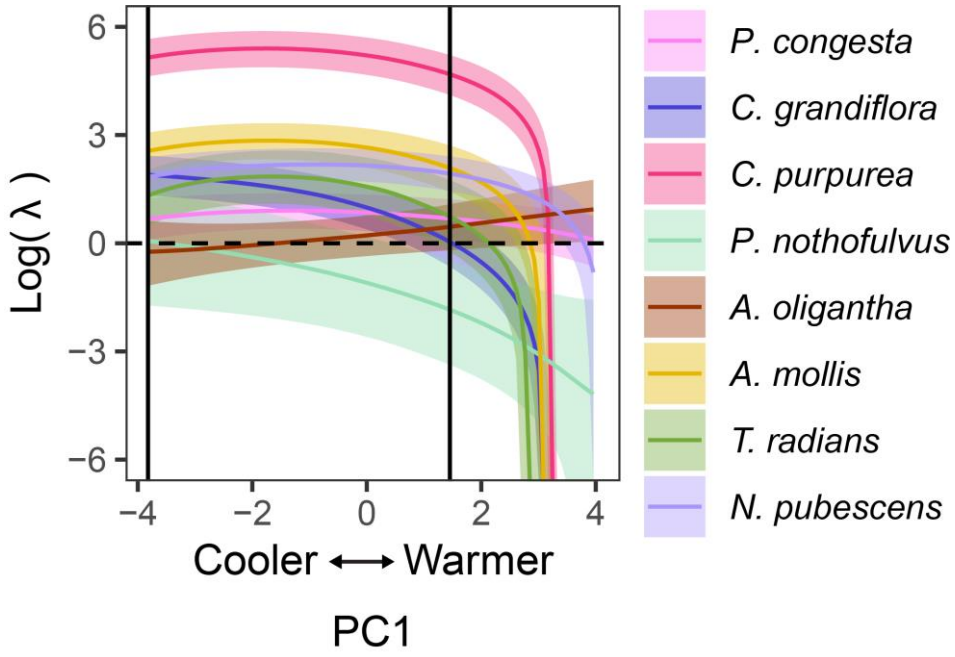

Figure 4.5. Log-transformed population growth rates (λ) of each species against PC1 (at PC2 = 0). Shaded bands indicate 95% prediction intervals. Dashed horizontal line at Log(λ) = 0 indicates a "stable" population. Black vertical lines identify the range of PC1 values in the control treatment plots across all sites and years.

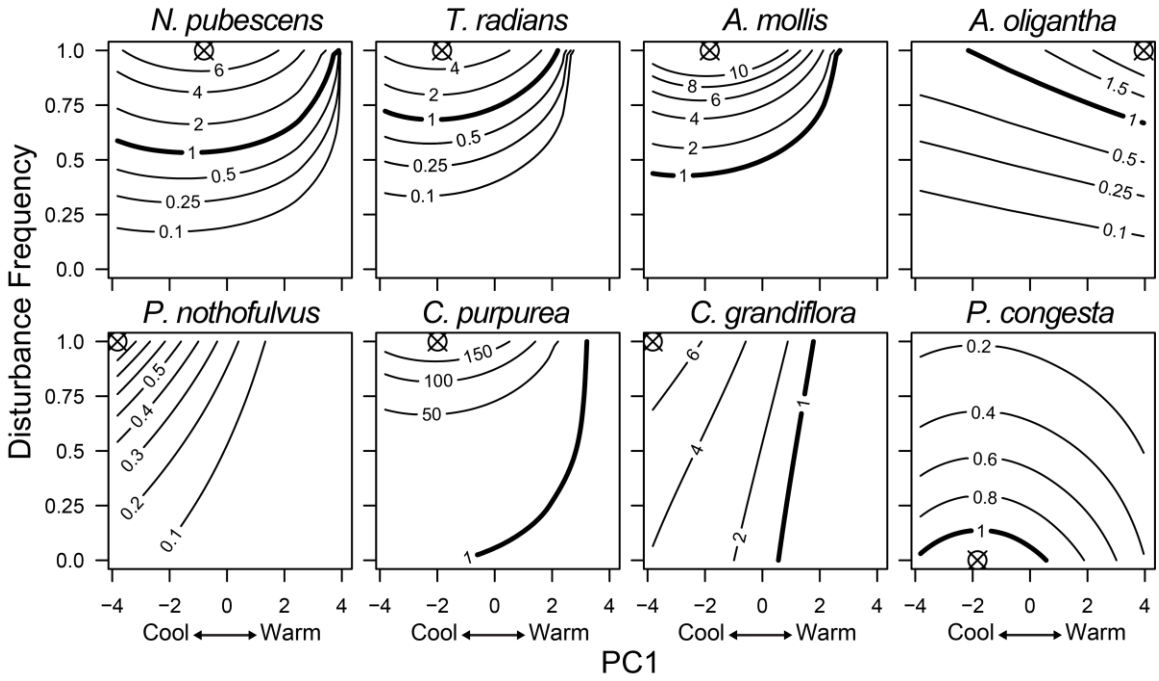

Figure 4.6. Contour plots of the long-run (geometric mean) annual population growth rate (λ) for each species as a function of climate (PC1) and disturbance frequency. Long-run population growth rates were calculated using Markov models (see Methods), assuming that high disturbance conditions prevail in a disturbance event year, intermediate conditions in the first year post-disturbance event, and low disturbance conditions two or more years post-disturbance event. For *P. nothofulvus*, which was not planted during a high disturbance year, we used intermediate conditions in a disturbance event year and low disturbance conditions one or more years post-disturbance event. ⊗ indicates the location of highest λ.

Discussion

We have shown how both disturbance and warming strongly drive the demographic performance of a suite of native annual species reintroduced to PNW prairies. We found evidence suggesting that most species' population growth rates decline precipitously following the initial boom of a major disturbance event, and that seven of the eight species have increasingly poor performance under future climatic conditions. While stressing the importance of implementing common prairie restoration disturbances such as fire, grazing, and mowing (Davison and Kindscher 1999) when managing annual plant populations, these results also warn that future warming may lead

to local extirpations despite best management practices. This is consistent with studies of very different systems (Bickford et al. 2010, Linares and Doak 2010, Montero-Serra et al. 2019), suggesting that although managing local demographic drivers may partially mitigate climate change effects, the impacts of climate change may overwhelm such efforts for many species.

Extremely few studies of the demographic drivers of plants have compared multiple species to ask whether responses can be generalized (but see Peterson et al. 2020, Reed et al. 2020). The observation that climate warming caused declining population growth rates was remarkably consistent across these eight species, with *A. oligantha*, a C4 grass (Adams and Wallace 1985) and our only C4 focal species, being the lone exception that exhibited the opposite response. This is perhaps unsurprising, given that C4 species generally reach highest dominance in warmer environments (Edwards and Still 2008). Given the projected increase in regional temperatures of ~3°C by the 2080s (Mote and Salathé 2010, Dalton and Fleishman 2021), *A. oligantha* may be poised to persist and even thrive in the future. Contrarily, the consistently negative responses to warming among the remaining species does not bode well for the future of native plant biodiversity in PNW prairies. It is estimated that the richness of native annuals in western Washington prairies has already declined from ~50% of the native flora in the early 1800s to ~18% today (Dunwiddie et al. 2014). As the climate shifts toward warmer conditions, these species may further drop out of communities and cause native diversity to decline (Pfeifer-Meister et al. 2016). Indeed, data at the community level show that native cover and diversity decline with increasing temperature and drought severity, while introduced annual cover increases (Reed et al., in prep).

The observation that warming caused declining demographic performance agrees with previous work on other PNW prairie species in these experiments (Pfeifer-Meister et al. 2013, Reed et al. 2021), as well as on a widespread mountain plant in Colorado (Panetta et al. 2018) and two North American tundra plants (Doak and Morris 2010). However, while some studies only report declining population growth rates at species' trailing edges (Lesica and Crone 2017, Sheth and Angert 2018), we found declining rates across a large latitudinal gradient, including near our species' leading (northern) edges. This echoes the warning of Peterson et al. (2018) that species may be at risk of decline throughout their geographic ranges. If declines in vital rates such as survival and fecundity are left unchecked, populations could be eliminated (Panetta et al. 2018). Although multi-year seedbanks may allow for some buffering, this decline may be more rapid for annual species, which, unlike perennials, are not also buffered by persistent adult stages (Morris et al. 2008).

Furthermore, several of these focal species have relatively restricted ranges along the west coast of the United States, only occurring from parts of California to southern Oregon (*N. pubescens, T. radians,* and *A. mollis*) or the Columbia River Gorge (*P. nothofulvus*). Range-restricted species may be more susceptible to warming (Parmesan 2006, Sheth and Angert 2014), and if a species becomes increasingly restricted, it may eventually become found only within microclimate refugia. In PNW prairies, key refugia habitats are known to be critical in supporting vulnerable species' persistence (Bachelet et al. 2011). However, such locations will likely not remain refugia in future climates (Ulrey et al. 2016).

Whether a species was planted within or beyond its current northern range limit did not appear to influence the magnitude of the site effect on demographic performance. Instead, the idiosyncratic site effects we document may be attributed to other local factors such as nutrients, soil characteristics, and the surrounding biotic communities. Unfortunately, we were unable to test whether the demographic responses to climate differed by site, as we did in Pfeifer-Meister et al. (2013) and Reed et al. (2020), since we lacked enough within-site climate variation during the important establishment years when competition was low. With such data, we may have observed opposing demographic responses such as warming being detrimental within but not beyond northern range limits (Reed et al. 2021). Although this could have hinted at the potential benefits of geographic range shifts, our results at least provide broad conclusions that these species are vulnerable.

Given the increasing urgency to intervene when species become vulnerable to climate change, the responses to disturbance observed here have important management implications. Without the presence of a substantial long-lived seed bank, most of these species appear to require the low-competition environments that followed major disturbance events. Intermediate levels of disturbance (i.e., weeding and clipping of non-focal species) often provided a boost relative to low disturbance conditions (i.e., minimal maintenance), but these were generally small effects. While disturbance can facilitate the spread of invasive species (Bradford and Lauenroth 2006, Lembrechts et al. 2016), it can also play an important role in managing vulnerable species by helping them to establish in new locations (Coates et al. 2006, Holl and Hayes 2006) or to maintain viable populations where currently found.

In these experiments, we introduced or reintroduced our focal species to degraded prairie sites where they are not otherwise currently found. While the strong disturbance events that preceded both experiments caused most of these species to initially exhibit a "boom" year, these were often followed up with "bust" years that were exacerbated by warming. The major exception was *P. congesta*, which did not appear to depend on intense disturbance events. For the other species, our evidence suggests that maintaining high disturbance frequencies (short return intervals) will be critical for successfully establishing and maintaining populations in the face of climate warming (Figure 4.6). Indeed, ecological and ethnographic evidence indicates that PNW prairies historically burned with a typical fire return interval of 1-2 years, driven by both natural ignitions and those set by Native Americans to manage prairie resources (Boyd 1999, Storm and Shebitz 2006). Frequent fire would thus have been a key to their more widespread distribution and greater abundance prior to Euro-American settlement (Dunwiddie et al. 2014). A return to such short disturbance intervals may be even more critical under projected climate warming. Although the nature of disturbances (e.g., burrowing mammals, floods, fire, etc.) may differ in other systems, we suspect that an interplay between climate change and altered disturbance in their effects on disturbance-adapted plants is likely to be common.

Despite compelling evidence for climate and disturbance as important demographic controls, there are a few remaining caveats. First, it is important to note that our contour plots of λ are meant to represent directional trends and the actual values should not be taken literally. Figure 4.4 is averaged across sites, which had very different and idiosyncratic effects on the magnitude of λ. True population growth rates of these

species would inevitably be site- and context-dependent, although we expect that the negative effects of warming would hold true in many cases. Second, our λ calculations do not account for intraspecific competition. Given that we only planted 200 seeds per species per plot in each year (and never had close to 100% germination), we believe that this force was negligible, especially relative to interspecific competition (given far greater cover from non-focal species). Lastly, it is possible that species were "hedging their bets" by delaying germination through the unfavorable years post-establishment (Gremer and Venable 2014). If this is the case, the species may have built adequate seed banks (through our continued seed addition) to have more "booms" in subsequent years. While second and third-year germination in 2018 suggest minimal seedbank activity (Appendix C: Table S1), this data was limited to a single low disturbance year and we cannot discount the possibility of continued seed dormancy. *C. purpurea* seed can remain viable after three years of dry lab storage, but its germination rate may be reduced by 50-60% at that point (Thomson et al. 2016). *P. congesta* is thought to lack dormancy (Young-Mathews 2012). Little else is known about dormancy potential in these native annual forbs or their longevity in the seedbank, other than the belief that their seedbanks are already depleted in most remaining prairie sites (Dunwiddie et al. 2014). In general, our finding that declining disturbance frequency could be a threat is unlikely to be changed by the inclusion of a seed bank.

In conclusion, we identified the important roles of warming and disturbance on the demographic performance of a suite of annual species native to Pacific Northwest prairies, seeded at multiple sites over multiple years. This type of comprehensive study using climate manipulations is exceedingly rare and provides a robust analysis of how

species may fare in future climatic conditions. While active management and intervention, including frequent disturbance, will be essential to lessen the risk of climate change for vulnerable annual plant populations, their long-term persistence may still be in jeopardy.

CHAPTER V

INTRODUCED ANNUALS MEDIATE CLIMATE-DRIVEN COMMUNITY CHANGE IN MEDITERRANEAN PRAIRIES OF THE PACIFIC NORTHWEST, USA

Contributions

This chapter is co-authored by Paul B. Reed, Laurel E. Pfeifer-Meister, Bitty A. Roy, Bart R. Johnson, Graham T. Bailes, Aaron A. Nelson, and Scott D. Bridgham. I was responsible for leading the data collection, analyses, and writing of this manuscript. All authors designed the experiment, contributed to the review process, and gave final approval for publication.

Introduction

Climate change is altering plant communities by promoting widespread invasions (Thuiller *et al.* 2008), reshuffling compositional assemblages (Pecl *et al.* 2017), and contributing to the loss of species diversity (Harrison *et al.* 2015). A major challenge to effectively managing plant communities is identifying the direct and/or indirect pathways by which these changes occur (Gornish & Tylianakis 2013; Avolio *et al.* 2015). For example, moisture, rather than temperature, could be the primary influence on plant community responses (Franklin *et al.* 2016), or vice versa. Biotic interactions can act as important intermediaries (Brooker 2006). Nutrient availability may be the driver of change but be dependent on climate (Brooks 2003). In many cases, the underlying mechanisms by which temperature, moisture, nutrients, and biotic interactions influence change in plant communities remain a black box.

There is debate whether direct or indirect effects dominate climate-driven plant community change. Theoretical evidence suggests that direct climatic effects are more important in some grassland plant communities (Chu *et al.* 2016), which has been corroborated through some empirical studies. For example, in a Kansas prairie, the direct effects of temperature had greater influence than species interactions on the population dynamics of ten forb species (Adler & HilleRisLambers 2008). However, alternative evidence highlights the important roles of indirect effects, given their potential to amplify or counteract direct effects (Adler *et al.* 2009).

Studies in California grasslands with Mediterranean-climate systems support both direct and indirect effects of climate on plant communities. For example, Levine *et al.* (2010) found that the precipitation responses of native annual forbs were minimally affected by the responses of their competitors. However, LaForgia *et al.* (2020) found that drought effects on native annual forbs (especially resource-acquisitive ones) were exacerbated when invasive winter-annual grasses were present, suggesting a strong mediation of climate through competition. Suttle *et al.* (2007) found that while extending the wet season initially boosted plant species richness, these effects were reversed once increased nutrient availability prompted a shift from forbs to winter-annual grasses, which suppressed other species through their litter accumulation. In prairie and grassland systems such as this, winter-annual invasives may amplify or counteract direct climatic effects on other functional groups by altering soil resources such as moisture or nitrogen (Prevéy & Seastedt 2014), potentially shifting competitive hierarchies in their favor (Everard *et al.* 2010).

The Pacific Northwest (PNW) of the United States is a Mediterranean-climate region defined by its mild, wet winters and warm-to-hot, dry summers (Kottek *et al.* 2006). Like many other Mediterranean-climate ecosystems, PNW prairies are critically endangered (Noss *et al.* 1995; Sala *et al.* 2000; Klausmeyer & Shaw 2009). Following Euro-American settlement, most prairies have been lost to land-use change or considerably altered by non-native plant invasions (Dunwiddie & Bakker 2011). While introduced winter-annual species achieved dominance in the hotter, drier California grasslands (Clary 2012), introduced perennial grasses were the primary invaders in the cooler, moister PNW (Sinclair *et al.* 2006). How climate change will alter these (and other Mediterranean-climate) plant communities is an important conservation question.

Models for the PNW project a temperature increase of at least 2.5°C by the 2080s (compared to 1970-1999), with changes in precipitation being less certain (Mote & Salathé 2010; Dalton & Fleishman 2021). In general, the seasonality of the Mediterranean-climate system is expected to become more extreme, with winters becoming wetter and summers becoming longer and drier. Increased precipitation variability and extreme events are likely (Pendergrass *et al.* 2017). Drought potential may rise due to increasing evaporative demands, particularly in the valley lowlands (Jung & Chang 2012), where many of these prairies occur.

Previous research by our group suggested that climate change will alter plant community composition and decrease diversity in PNW prairies (Pfeifer-Meister *et al.* 2016). In particular, experimental warming increased introduced annual cover, causing communities to become more similar to invaded grasslands in California. Although this was hypothesized to be due to a reduction in soil moisture, temperature and moisture

were confounded: adding +20% precipitation to warming did little to alleviate the warming-induced drying effects. Additionally, the role of introduced annuals in mediating climatic effects, or whether nutrient availability played any role, were unexplored. Thus, it is difficult to ascertain whether these climate-driven community changes can be primarily attributed to temperature, moisture, nutrients, or other factors.

Here, we built upon this previous research with three years of new data, decoupling the direct warming effects from their drying effect. We used structural equation modeling to examine the extent to which abiotic drivers (i.e., temperature, moisture, and nitrogen) controlled functional group cover, and how these groups in turn determined diversity, richness, and evenness. Utilizing a new climate manipulation experiment embedded at three sites across a latitudinal gradient, we asked the following two overarching questions: In a Mediterranean-climate system, (1) What are the direct and indirect effects of climate on the cover and diversity of prairie plant communities? (2) To what extent are warming effects mediated by introduced annuals, and what are the resulting effects on soil moisture and nitrogen?

We hypothesized that warming would favor introduced annual species at the expense of other functional groups and would thus negatively affect diversity. In particular, we expected a direct positive effect of temperature on introduced annual cover, as many of these species in this system are winter annuals (Dennehy *et al.* 2011) that may benefit from more favorable early growing-season conditions (Dunwiddie *et al.* 2014; Pfeifer-Meister *et al.* 2016). Concurrently, we expected increasing temperatures to reduce soil moisture, augmented by feedbacks from introduced annuals, whose rapid growth draws down available soil water (Prevéy & Seastedt 2014). We also expected a decline in

nitrogen (N) availability due to reduced soil moisture and greater uptake by introduced annuals, shifting the competitive hierarchy in their favor (Everard *et al.* 2010; Prevéy & Seastedt 2014). As a result, we expected the cover of later-growing functional groups (i.e., introduced perennials, native perennials, and native annuals) to decline with warming and drying, and for this to be primarily mediated through increasing competitive pressure by introduced annuals. Finally, we expected these changes to result in a decline in diversity, induced by losses in both richness and evenness.

Methods

Experimental design:

We conducted this study at three prairie sites spanning a 520-km latitudinal gradient across the western PNW, with sites selected to reflect the Mediterranean-climate gradient of increasing temperature and summer drought severity from north to south (Figure 5.1). We established twenty 7.1-m^2 plots per site in 2015 for a native plant demography experiment (Reed *et al.* 2021). The southern and central site plots had a legacy dating back to 2010-2012 (Pfeifer-Meister *et al.* 2013, 2016). Prior to plot establishment, sites were dominated by introduced perennial grasses, requiring herbicide application (2% Glyphosate (RoundUp) and 0.75% grass-specific Fusilade) and seeding with a diverse mixture of 31 native prairie species to establish the experiment (Pfeifer-Meister *et al.* 2013). Between late 2012 and early 2014, the southern and central plots were left fallow with no treatments or maintenance. In late 2014, a new northern site was added. At that point, all sixty plots were treated with herbicide and sown with the same mix of 29 native species, with additional sowing of 14 focal native species in fall 2015, 2016, and 2017 (Reed *et al.* 2021).

We established four climate treatments: control, drought, warming, and warming + irrigation (five plots per treatment per site). Controls experienced ambient temperature and precipitation, the drought treatment reduced annual precipitation by ~40%, and the warming treatments increased canopy temperature by approximately +2.5°C with infrared lamps. The warming + irrigation plots were irrigated with additional rainfall such that their soil volumetric water content matched the control plot average. All treatments began by September 2016 and both warming and warming + irrigation ceased in July 2018 (see Appendix D: Supplemental Methods for additional details).

Climate and nitrogen data:

Between fall 2016 and summer 2019, we continuously logged plot canopy and soil temperatures and soil volumetric water content aggregated to daily averages. Missing values due to equipment malfunction were interpolated (see Appendix D: Supplemental Methods). To compare moisture across sites with different soil characteristics, we calculated soil matric potential from volumetric water content, soil texture, and soil carbon (Saxton & Rawls 2006; see Appendix D: Supplemental Methods). Matric potentials are negative values where 0 kPa indicates saturation and -1500 kPa indicates permanent wilting point. In the Mediterranean climate of the PNW, active vegetation growth occurs mainly in the wet season, followed by several months of dormancy during the summer drought. Therefore, we aggregated soil temperature and moisture data to the growing season from October 1 – June 30 (Reed *et al.* 2019). We also investigated annual, winter, and spring seasonal values, but only report growing season here because trends were consistent.

We collected data on total inorganic nitrogen (N) availability (μg/10cm^2 strip/burial period) using Plant Root Simulator (PRS®) Probes (Western Ag, Saskatoon, SK, CAN). We buried four anion and four cation probes in each plot for four-month periods (fall, winter, and spring) between August 2016 and July 2018. We calculated the mean growing season N availability by averaging values across the three burial periods for 2017 (August 2016 – July 2017) and 2018 (August 2017 – July 2018) but lacked this data for 2019.

Plant community data:

In each spring 2017-2019, we measured plant cover at peak standing biomass (approximately mid-May, late-May, and mid-June at the southern, central, and northern sites, respectively) using the point intercept method (Elzinga *et al.* 1998). Using a 1-m^2 quadrat in a fixed location within each plot, we dropped 25 equally-spaced pins through the plant canopy. We counted each plant contact with a pin (hit) to the species level and multiplied hits by four (to scale to 100). Due to canopy layering, >100% cover occurred. We assigned a cover of 0.4% to species which were present in the quadrat but not hit by a pin. To determine the functional group covers, we assigned each species to an origin (native/introduced), duration (annual/perennial, with the few biennials assigned as annuals), and habit (grass/forb) by referring to the Consortium of Pacific Northwest Herbaria (https://www.pnwherbaria.org/data/search.php) and the USDA Plant Profiles (https://plants.usda.gov/) databases. Using the *vegan* package in R (Okansanen *et al.*, 2019), we calculated Simpson's index of diversity as:

$$1 - D = 1 - \sum_i^s p_i^2$$

where p_i is the relative cover of species *i* and *s* is the richness, or total number of species. Lastly, we calculated Simpson's evenness (Simpson 1949; Morris *et al.* 2014) as:

$$E = \frac{\frac{1}{\sum_i^s p_i^2}}{s}$$

Analyses:

Analyses

We conducted analyses using R version 4.0.2 (R Core Team, 2020). Due to repeated sampling of the plots, we ran all analyses using mixed models (lme4 package; Bates *et al.* 2015) with plot as a random effect. Marginal and conditional R^2 values were calculated based on Nakagawa *et al.* (2017), with R^2_m providing the variance explained by the fixed effect(s) alone and R^2_c providing the variance explained by both fixed and random effects. Because heaters and irrigation were turned off after July 2018, we excluded data from the warming and warming + irrigation plots in 2019 to prevent any legacy treatment effects from obscuring patterns.

To improve the normality of distributions for several variables, we used the following transformations. We transformed soil moisture using -log(1-matric potential) so that the transformed values stayed consistent with raw values (more negative = drier, less negative = moister). We used square root transformations for N availability and the cover of both introduced annuals and introduced perennials. For native perennial and native annual cover, we used a log transformation after adding a constant of 0.4% since these functional groups had 0% cover in some plots. Lastly, because diversity and evenness were proportional data, we used logit transformations (Warton & Hui 2011).

Differences in the abiotic variables (temperature, moisture, and N availability) were examined with ANOVA with site as a fixed effect followed by Tukey's post-hoc comparisons if site was significant ($p < 0.05$). We explicitly left site out as a predictor from all subsequent analyses because sites were chosen to represent a climate gradient and would obscure the continuous-data climate signals.

Using the piecewiseSEM package (Lefcheck 2016), we examined our *a priori* hypotheses with structural equation models (SEM), which linked together a series of multiple regressions fitted using lme4 with plot as a random effect. We investigated Pearson's correlation coefficients and checked for multicollinearity using variance inflation factors (VIFs). Concerns over multicollinearity were minimal since the greatest VIF was 3.4 (Table S1) and, in general, VIFs > 5 may indicate multicollinearity (James *et al.* 2013). We ran separate SEMs for diversity, richness, and evenness. Although we hypothesized that biotic effects would primarily occur through introduced annuals, we also accounted for the possibility of introduced perennials affecting the two native functional groups, since introduced perennials are already widely prevalent throughout this system and have strong competitive effects on native prairie species (Sinclair *et al.* 2006; Stanley *et al.* 2011).

We initially restricted SEMs to 2017 and 2018 since we lacked N availability data in 2019. After discovering minimal effects of N availability on functional group cover (see Results), we reran SEMs without this variable to include the 30 additional 2019 datapoints. The richness and evenness SEMs had poor model fit when only including the four functional groups as their predictors (see Results), so we also added direct effects of temperature and soil moisture on richness and evenness. To calculate indirect effects, we

multiplied the standardized coefficients of the significant paths that constituted the effect. Finally, we also ran independent bivariate regressions for visualization.

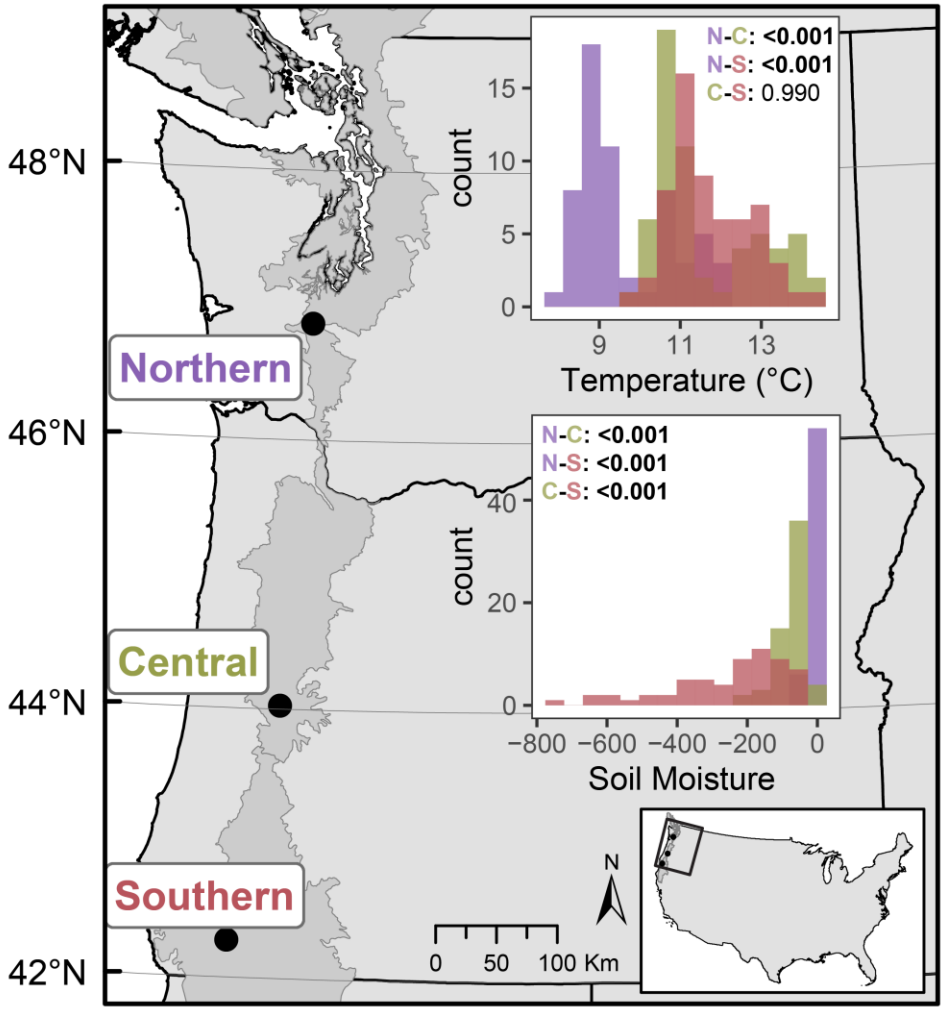

Figure 5.1. The southern, central, and northern experimental sites occur across a 520 km latitudinal climate gradient in the western Pacific Northwest, USA. Across all plots, site significantly affects mean growing season soil temperature (top histograms) and moisture (soil matric potential (kPa); bottom histograms). P-values of Tukey's post-hoc comparisons provided within histograms. Soil moisture was transformed prior to analyses (see Methods).

Results

Abiotic variables:

Across all treatments, mean growing season soil temperature, moisture, and N availability differed by site ($p < 0.001$). From north to south, average plot conditions

became warmer (northern: 9.8 ± 1.1°C (mean ± s.d.), central: 11.8 ± 1.4°C, southern: 11.9 ± 0.9°C) and drier (northern: -11.4 ± 10.8 kPa, central: -66.3 ± 44.7 kPa, southern: -239.0 ± 172.6 kPa), although the central and southern plots were not significantly different for temperature (Figure 5.1). Treatment-specific means in temperature and moisture differed by site and year (Appendix D: Figures S5.1, S5.2). Mean N availability was lowest in the central plots while the northern and southern plots did not significantly differ (Appendix D: Figure S5.3c). Soil moisture had strong, negative correlations with both introduced annual cover and temperature (Appendix D: Figure S5.4). N availability had a small, negative correlation with soil moisture, but no significant relationships with introduced annual cover or temperature (Appendix D: Figure S5.4).

Using SEM, we found that temperature significantly reduced soil moisture regardless of restricting to 2017 and 2018 data (-0.65 standardized estimated, $p < 0.001$, Appendix D: Figure S5.6, Table S5.2) or including 2019 data (-0.40 std. est, $p < 0.001$, Figure S5.2, Table S5.3). Introduced annual cover also contributed to a reduction in soil moisture (2017-2018: -0.20 std. est., $p = 0.011$, Appendix D: Figure S5.6; 2017-2019: -0.18 std. est., $p = 0.022$, Figure 5.2). N availability was negatively affected by soil moisture (-0.34 std. est., $p = 0.024$, Appendix D: Figure S5.6), but not directly by either temperature (0.09 std. est., $p = 0.519$) or introduced annual cover (-0.22, $p = 0.146$, Appendix D: Figure S5.6, Table S5.2).

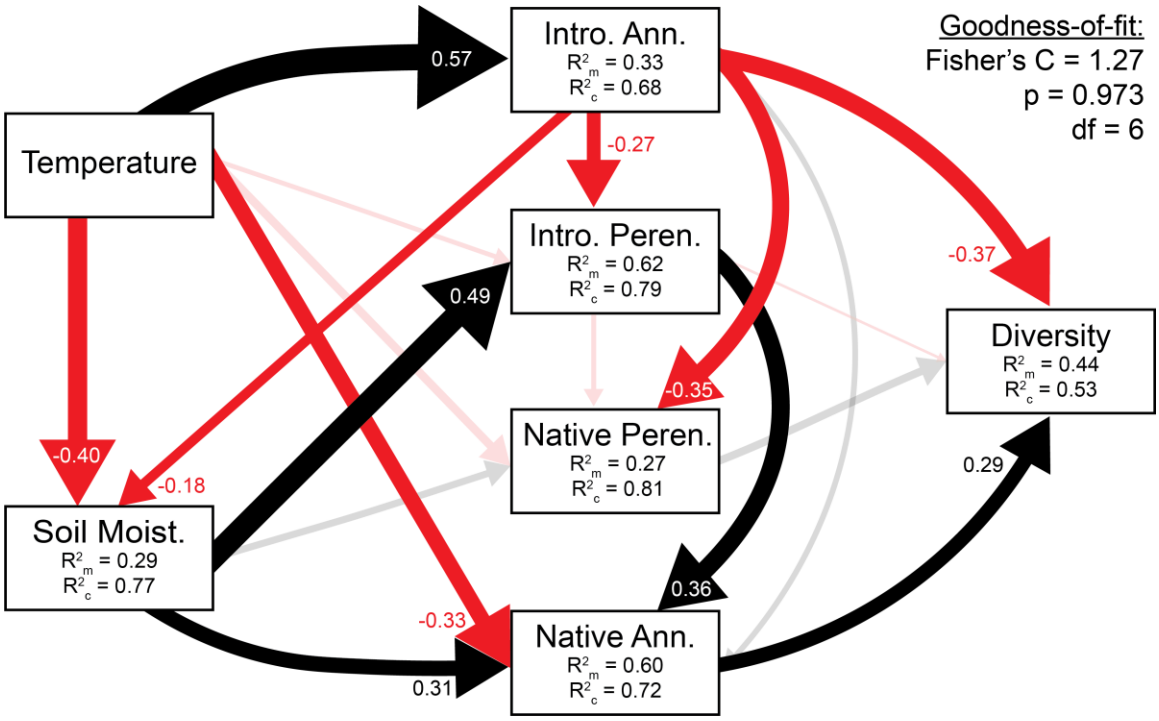

Figure 5.2. Structural equation model using 2017-2019 data to determine how climate controls functional groups and how functional groups control diversity. Values within/next to arrows are standardized estimates of coefficients and arrow thickness is scaled to their magnitude. Red = negative effects, black = positive effects, semi-transparent = non-significant effects ($p > 0.05$; Table S5.3). Within each response variable box (those at the receiving end of arrows), R^2_m provides the variance explained by the fixed effect(s) alone (boxes at the starting end of the arrows) and R^2_c provides the variance explained by both fixed and random effects (plot = random). "Moist." = Moisture, "Intro." = Introduced, "Peren." = "Perennials, "Ann." = Annuals.

Functional group cover:

Overall, introduced annuals averaged the greatest cover (505.4%, range: 0-1596.4%), followed by introduced perennials (228.3%, range: 0-900.8%), native perennials (121.0%, range: 0-564.8%), and native annuals (30.0%, range: 0-328.4%). Native annual, native perennial, and introduced perennial cover all had significant, positive correlations with one another but significant, negative correlations with introduced annual cover (Appendix D: Figure S5.5). Introduced annuals increased with temperature and had a negative relationship with soil moisture (Figure 5.3a,e), while the

other three functional groups all decreased with increasing temperature and increased with soil moisture (Figure 5.3b-g). There were no significant relationships between functional group cover and N availability (Appendix D: Figure S5.7a-d), nor did N availability ever act as a significant mediator in the SEMs (Appendix D: Figure S5.6; Table S2). Therefore, we focus on the SEMs which include 2019 data (and exclude N availability).

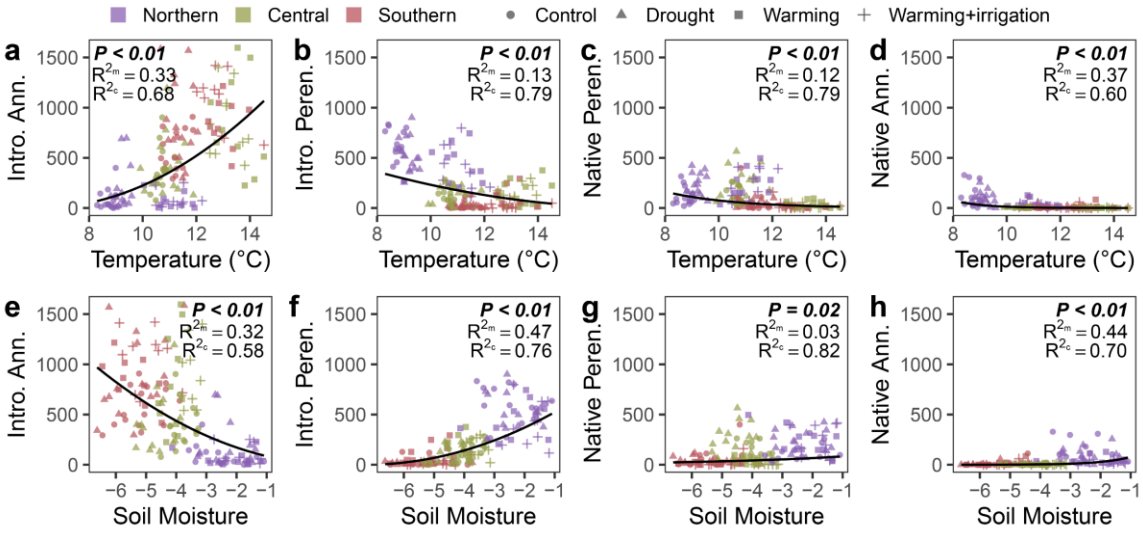

Figure 5.3. Bivariate regressions showing functional group cover against mean growing season soil temperature (a-d) and moisture (e-h), with plot as a random effect. Soil moisture = -log(1-matric potential). R^2_m (above) provides the variance explained by the fixed effect(s) alone and R^2_c (below) provides the variance explained by both fixed and random effects (plot = random).

We found the effects of temperature on introduced perennials and native perennials to be primarily mediated through its effects on introduced annuals and soil moisture (Figure 5.2). In particular, soil moisture had a positive effect on introduced perennials (0.49 std. est.), while introduced annuals had a negative effect (-0.27 std. est.), as well as an indirect effect (-0.09 std. est.) mediated through their effect on soil moisture. For native perennials, the only significant effect was a negative effect from introduced annuals (-0.35 std. est.). For native annuals, temperature and moisture had

direct negative (-0.33 std. est.) and positive (0.31 std. est.) effects, respectively, while the effects of introduced annuals on native annuals were mediated indirectly (-0.06 std. est.) through soil moisture (Figure 5.2).

Diversity, richness, and evenness:

Diversity declined with increasing temperature and increased with soil moisture (Figure 5.4a,d). It also declined with increasing introduced annual cover but increased with cover for the three other functional groups (Appendix D: Figure S5.8a-d). Using SEM, we found that introduced annual cover had a negative effect (-0.37 std. est.) and native annual cover a positive effect (0.29 std. est.) on diversity, while introduced perennial and native perennial cover had negligible effects (Figure 5.2; Appendix D: Table S5.3). There was a 45% reduction in predicted diversity from minimum to maximum introduced annual cover and a 31% increase from minimum to maximum native annual cover. The SEM for diversity had good model fit (goodness-of-fit: $p = 0.973$).

Like diversity, richness also declined with increasing temperature and increased with moisture (Figure 5.4b,e), whereas evenness was not affected by temperature and weakly declined with moisture (Figure 5.4c,f). Additionally, richness declined with increasing introduced annual cover but increased with cover for the three other functional groups (Appendix D: Figure S5.8e-h), whereas evenness only declined with increasing introduced annual cover (Appendix D: Figure S5.8i-l). Both richness and evenness SEMs had poor model fit when only including functional group cover as their predictors (goodness-of-fit: $p \leq 0.057$), so we added direct effects of temperature and moisture. For richness, soil moisture, native annual cover, and native perennial cover had positive

effects (0.51, 0.54, and 0.20 std. est., respectively; Appendix D: Figure S5.9a). Predicted richness increased from 6.5 to 24.5 species from minimum to maximum soil moisture. For evenness, introduced annual cover and soil moisture had negative effects (-0.65 and -0.35 std. est., respectively; Appendix D: Figure S5.9b).

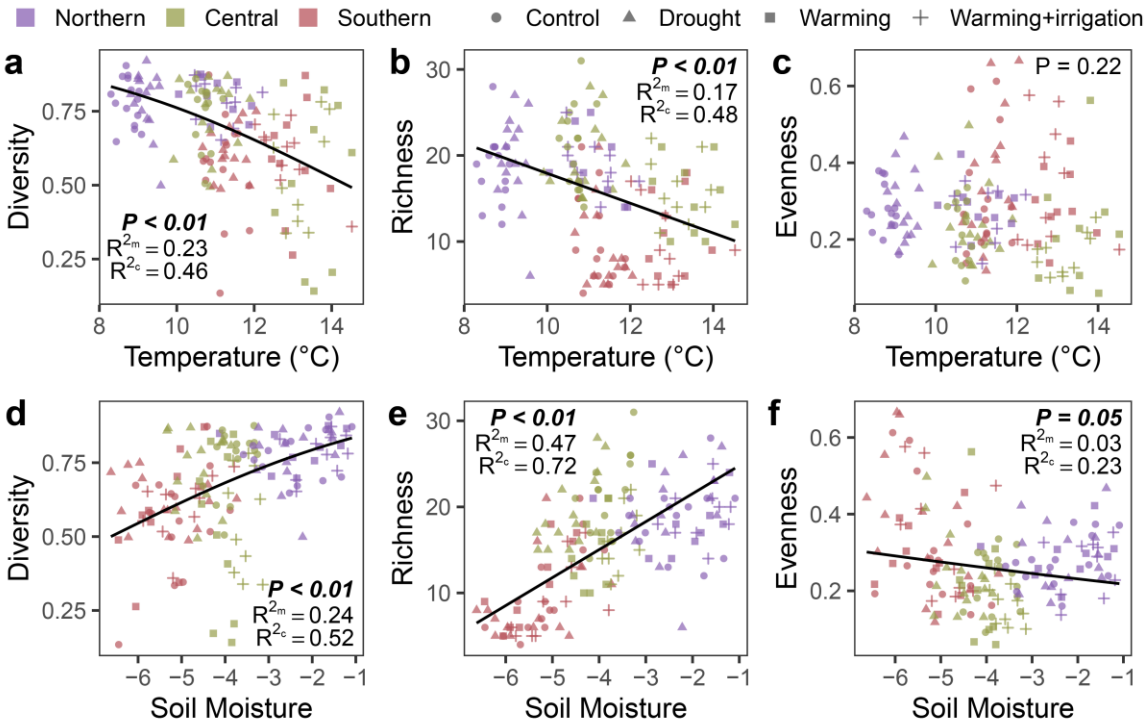

Figure 5.4. Bivariate regressions showing Simpson's index of diversity, richness, and evenness against mean growing season soil temperature (a-c) and moisture (d-f), with plot as a random effect. Soil moisture = -log(1-matric potential). R^2_m (above) provides the variance explained by the fixed effect(s) alone and R^2_c (below) provides the variance explained by both fixed and random effects (plot = random).

Discussion

A major challenge in community ecology is to tease apart the complex relationships behind climate-driven community change. This challenge may be best best-achieved using large-scale, multisite experiments analyzed with path-analytic approaches (Brooker 2006; Gornish & Tylianakis 2013). Using a climate manipulation experiment embedded at three Mediterranean-prairie sites across a latitudinal gradient in the PNW,

we used SEM and found that warmer conditions result in increasing cover of introduced annuals, along with subsequent declines in other functional groups and diversity. Our data not only confirm results from our previous study (Pfeifer-Meister *et al.* 2016), but identify the causal pathways underlying the observed climate-community relationships.

Our first hypothesis, that warmer conditions favor introduced annuals, was strongly supported. Indeed, we found a direct positive effect of temperature on introduced annual cover, which we suspect was due to the early winter-growth habits common to this group. The most abundant introduced annuals in our study, *Vulpia spp.* (*V. myuros* and *V. bromoides*), *Bromus spp.* (*B. hordeaceus* and *B. tectorum*), and *Trifolium subterraneum*, were orders of magnitude more common than other annuals (Appendix D: Figure S5.10) and are characterized as winter-growing, early-maturing species (USDA-Natural Resources Conservation Service 2012; USDA-NRCS 2014; Friddle 2018). Warming could be advantageous to such species by promoting growth during the early growing season (Cleland *et al.* 2006; Blumenthal *et al.* 2016), at a time when temperature is most limiting and the rest of the community is still largely dormant.

Whether this favoring of introduced annuals came at the expense of other functional groups (i.e., through competition for limiting resources) was partially supported. Invasive annual grasses such as *Bromus* can rapidly exploit and draw down soil water resources (Melgoza *et al.* 1990; Dyer & Rice 1999). These grasses generally reached peak flowering in our study by mid-April, whereas most other functional groups peaked around mid-May to mid-June (P. Reed, pers. obs.), when soil moisture became a critically-limiting resource (Appendix D: Figure S5.2). As corroborated by our SEMs, introduced annuals negatively affected soil moisture and soil moisture had strong effects

on introduced perennials and native annuals. Thus, one major mechanism of climate-driven community change in this system is through increasing competition for soil moisture. The most abundant introduced annuals, *Vulpia* and *Bromus,* are relatively drought-tolerant (USDA-Natural Resources Conservation Service 2012; USDA-NRCS 2014) and avoid the detriments of reducing soil moisture by completing their entire life cycle prior the onset of extreme summer drought. However, it is important to note that the direct negative effect of temperature on soil moisture was greater than that from introduced annuals, indicating that competition from this functional group amplifies, but does not entirely control, moisture limitation for the rest of the community.

We found minimal support for N limitation acting as an important intermediary in these community dynamics. Soil moisture is the transport medium for plant-available N (Everard *et al.* 2010), but we actually found a slightly negative relationship between N availability and soil moisture (Appendix D: Figure S5.4), driven by relatively high N availability at our driest (southern) site (Appendix D: Figure S5.3c). Legumes (e.g., *Trifolium* and *Vicia spp*.) were among the most common introduced annuals in this study (Appendix D: Figure S5.10), and *Trifolium subterraneum* was especially common at the southern site in 2017. Thus, increases in N-fixation may have offset decreases in N availability due to drier conditions. Alternatively, N availability could be controlled by other site-specific factors. Regardless, N availability did not affect the cover of introduced perennials, native perennials, or native annuals, and was poorly predicted by temperature, soil moisture, and introduced annual cover ($R^2_m = 0.07$, $R^2_c = 0.27$, Appendix D: Figure S5.6).

The direct effects of introduced annuals on the two perennial functional groups suggests that an additional competition mechanism is at play. In our parallel demography experiment, we speculated that poor recruitment among native perennials was driven by competition from introduced annual grasses (Reed *et al.* 2021). Poor recruitment ultimately led to fewer adult-stage individuals, hence the lower cover observed here. In a similar California grassland system, litter accumulation positively reinforces the biomass of introduced annual grasses to suppress native recruitment (Mariotte *et al.* 2017). Likewise, seedling establishing for both native and introduced perennials declined with increasing litter depth in our plots (Brambila *et al.,* unpublished data). Given that existing vegetation was initially removed from our plots, introduced perennials had to reestablish through the seedbank while native perennials came in via our seed additions. As warmer conditions promoted the rapid biomass growth of introduced annuals, they formed a dense cover early in the season (*Vulpia* and *Bromus spp.* often reaching 20+ hits per pin) coupled by a thick litter layer that remained the following season. Such conditions shade out young seedlings of slower-growing perennials during their critical establishment phase. Thus, an additional mechanism mediated by introduced annuals seems to be through increasing competition for space and light.

There was also a strong direct effect of moisture on introduced perennials. In California, introduced perennial grass cover is strongly correlated with proximity to the moist coastline (Clary 2012). Likewise, in PNW prairies, this functional group was highly successful at invading cool, moist sites (Sinclair *et al.* 2006). Although the land surrounding our plots at the driest (southern) site is dominated by introduced perennial grasses, the property is regularly irrigated from spring to summer (P. Reed, pers. obs.).

The strong effect of moisture on introduced perennials implies that, even in the absence of competitive pressure by introduced annuals, future moisture limitation may prove detrimental for this group. From a management perspective, any decline in a non-native functional group may appear desirable on the surface. However, some non-natives can play an important role relative to management objectives (Dunwiddie & Rogers 2017). For example, in PNW prairies, the introduced perennial forb *Plantago lanceolata* serves as a critical host for the endangered Taylor's checkerspot butterfly (Dunwiddie & Rogers 2017), and several other introduced perennial forbs provide important nectar resources for a variety of pollinators (Lindh 2018). Introduced perennial grasses provide important forage value for livestock throughout the region. Given the potential undesirability of a perennial-to-annual state transition (D'Antonio & Vitousek 1992), any perennial cover (whether native or introduced) may be worth preserving to some degree.

As for native annuals, the direct effects of temperature and moisture strongly support our parallel demography study which suggests that climate change will cause many native annuals to decline, regardless of competition (Reed *et al.*, in review). Although several species in that study were strongly disturbance-dependent, population growth rates rapidly deteriorated with warming even under favorable disturbance regimes (i.e., low competition). Importantly, the two most abundant native annuals in this study (*Collinsia grandiflora* and *Plectritis congesta*; Appendix D: Figure S5.10) were also the two least affected by disturbance in that demography study (Reed *et al.*, in review). Thus, their relatively high abundances may have influenced the negligible direct effect from introduced annuals.

Surprisingly, there was a positive effect from introduced perennials to native annuals (0.36 std. est., Figure 5.2). We included this pathway since introduced perennials have long been directly outcompeting native species in this system (Sinclair *et al.* 2006; Stanley *et al.* 2011). However, the positive relationships that we found between native annual, native perennial, and introduced perennial cover suggest that these three functional groups can coexist under common favorable conditions without inherent competitive exclusion (Appendix D: Figure S5.5). Therefore, we suspect that the significant positive arrow from introduced perennials to native annuals is actually correlative, rather than causative, since both functional groups were most common at the northern site, where cooler and moister conditions are the true underlying causes. Throughout PNW prairies, native annuals have already declined to an alarming degree (Dunwiddie *et al.* 2014). Our results suggest that this trend may continue with climate change, whether introduced annuals are present or not.

We found support for the hypothesis that diversity will decline with warmer and drier conditions (Harrison 2020). We found this to be driven mostly by changes in the two annual functional groups. Similar to California annual grasslands (Harrison *et al.* 2018), native annual cover was a strong factor contributing to richness. Soil moisture was also a strong driver of richness (Appendix D: Figure S5.9b), consistent with several grassland studies that find positive relationships between moisture and richness (Adler & Levine 2007; Hallett *et al.* 2014; Harrison *et al.* 2018). If soil water availability declines in the future (due to more frequent droughts, higher evaporative demand, and/or greater competition), native annuals may drop out of these communities, thereby reducing overall diversity through a decline in species richness.

Intriguingly, introduced annuals played a large role in affecting diversity not by their effects on richness, but by their strong negative effects on evenness (Appendix D: Figure S5.9). This result is consistent with a study conducted in a more arid sagebrush-grassland ecosystem, in which communities with more introduced annuals (e.g., *Bromus tectorum*) had lower evenness (despite higher richness) since only a few species dominated (Allen & Knight 1984). In our study, this phenomenon seems to be driven by fundamental differences between the central and southern sites. Introduced annuals were the most species-rich functional group (Appendix D: Figure S5.10), and most of their richness occurred at the central site. *Vulpia spp.* and *Bromus hordeaceus* tended to dominate in these plots (hence low evenness; Appendix D: Figure S5.8i), but the central plots were moist enough to maintain relatively high richness (Figure 5.4e). Richness plummeted under the driest conditions of the southern plots (Figure 5.4e). These conditions so highly favored *Vulpia spp.* and *Bromus hordeaceus* that there actually became a tipping point for evenness: cover was almost exclusively these two species, often in a roughly-equal split. This may explain why evenness was actually highest in the driest (southern) plots (Figure 5.4f). However, we caution that this evenness-moisture bivariate relationship was weak ($R^2_m = 0.03$; $R^2_c = 0.23$), and the total proportion of variance explained for evenness in its SEM remained relatively low ($R^2_m = 0.22$; $R^2_c = 0.41$). Overall, diversity appears poised to decline with climate change due to an increasing dominance by only a handful of introduced annuals.

While our large-scale experiment and SEM approach was a powerful way to identify the pathways by which climate alters plant communities, there are a few caveats. Separate from its effects on the aboveground community, climate change can also

directly and/or indirectly affect the soil seed bank (Ma *et al.* 2020), which we do not consider in this study. Additionally, there are likely bidirectional, causative relationships between variables (i.e., feedback loops) and missing pathways not considered in these models. However, given our previous evidence (Pfeifer-Meister *et al.* 2016), we feel our hypothesized model structure represents the most likely reality. Finally, our plots were relatively early-successional, 'restored' communities that were established following a clearing disturbance. It is quite possible that effects would be different in established, undisturbed communities, where priority effects exist (Corbin & D'Antonio 2004). However, this makes our results highly relevant for local prairie restoration efforts, which must consider the complex relationships between disturbance, invasives, and climate if they are to be successful.

In conclusion, while we found direct negative effects of warming and drying on extant vegetation (i.e., native annuals, native perennials, and introduced perennials), we also found that these effects were commonly amplified by increasing introduced annuals. These invaders directly benefit from warmer temperatures and seem to outcompete other functional groups for limiting resources such as moisture, space, and light. Thus, introduced annuals appear to be the only functional group in this system that are poised to prosper under warmer and drier conditions. Other groups and overall diversity will decline as a result of this shift in dominance and/or due to direct negative effects of climate change. Such changes will challenge land managers in their efforts to maintain species-rich and functionally-diverse prairie ecosystems for years to come.

CHAPTER VI

CONCLUSIONS

Future climate change is likely to have profound impacts on plant ecology at both the population and community levels. Changes to plant ecology will affect global patterns of biodiversity and may alter ecosystem functions and services. Prairies within the western Pacific Northwest are highly imperiled ecosystems (Noss et al. 1995), whose plant ecology may be exceptionally vulnerable to the effects of climate change (Bachelet et al. 2011). As a result, there is growing urgency to understand how plants will respond to climate change in this system, which my dissertation sought to address. Using a cutting-edge climate manipulation experiment at three sites across a latitudinal climate gradient (the HOPS experiment), we measured prairie plant phenological, demographic, and community responses to changes in temperature, moisture, and other factors. We modeled the demographic performance of a suite of native species and the pathways by which compositional changes occur. The results presented herein have important management implications and may be relevant for the future restoration of local prairie ecosystems in the face of climate change.

Chapter II investigated how changes in temperature and moisture affect flowering times and canopy biomass growth and senescence in 2017 and 2018. We found that warming generally exerted a stronger control than moisture manipulations on spring phenological events, despite the transition from temperature-limitation to moisture-limitation during spring months in this Mediterranean-climate system. Warming advanced flowering regardless of whether a species was within or beyond its current

range and advanced the date of peak community biomass regardless of site or year. Senescence of community biomass occurred earlier with warming in both years at the southern and central sites but only in 2018 for the northern site. The length of the growing season contracted due to warming at the southern and central sites but was unaffected at the northern site. Our results emphasize that future temperature changes may exert strong influence on plant phenological events, but that these shifts may not be consistent across the latitudinal range of prairies in the western Pacific Northwest.

While this study helped answer how prairie phenology will respond to future climates, questions remain about the implications of such responses. Will shifts in flowering time create a mismatch between plants and pollinators, or will pollinators exhibit a corresponding shift in their emergence and foraging behavior? What are the long-term implications of a shorter growing season on ecosystem services such as carbon storage or forage production? Future research should aim to address these important questions.

Chapter III investigated the demographic responses (i.e., germination, survival, growth, and reproduction) of six native perennial species to three years of the HOPS climate manipulation experiment (2016-2018). Of these six perennials, two are "range-restricted," such that their current northern range limits occur south of at least one of the experimental sites and were therefore planted both within and beyond their current ranges. We integrated vital rates into estimates of population growth rates (λ) using integral projection models. We found that establishment from seed (i.e., successful germination and seedling survival) was a major limitation to achieving a reproductive population in at least one site for most species. Warming negatively affected λ at sites within species' current ranges but warming and drought positively affected λ for the two range-restricted species at the sites beyond their current ranges. These results support

predictions of climate-driven range shifts: populations within current ranges are increasingly vulnerable to decline, while demographic performance beyond current ranges may increase with climate change.

Like Chapter III, Chapter IV also investigated demographic responses to the HOPS climate manipulation experiment but focused on the eight native annual species and included three additional years of data (2010-2012) from an earlier iteration of the experiment. Given that native annual species are thought to be highly disturbance-dependent (Dunwiddie et al. 2014), we also binned various plot preparation and management actions into disturbance-intensity categories to determine how effective disturbance could be in mitigating climate change effects. We found that disturbance strongly influenced demographic performance and that seven of the eight species had increasingly poor performance with warmer conditions. Importantly, most species exhibited precipitous declines in λ under warmer-than-ambient experimental conditions and may require more frequent disturbance intervention to sustain populations. These results highlight the urgency for adaptive management practices that facilitate their restoration or introduction to newly suitable locations. Frequent and intense disturbances are critical to reduce competitors and promote native annuals' persistence, but even such efforts may prove futile under future climate regimes.

By modeling the demography for a suite of species under a manipulative experiment embedded within a regional climate gradient, the studies in Chapter III and Chapter IV were novel and innovative in their approach. However, more can be done to better predict species' range distributions under future climates. In particular, future research with our collaborators will use these modeled vital rate-climate relationships in a regional landscape simulation to determine where across the landscape these species could persist based on future climatic

conditions. Is climate change likely to drive species toward extinction where they are currently found? If they colonize new locations outside of their current ranges, will they be capable of surviving and establishing populations? If the answer to the latter is yes, a key question will be whether the species are able to disperse to new locations rapidly enough. By coupling these simulations with landscape genetics studies designed to determine dispersal probabilities based on land cover and habitat connectivity, it will be possible to improve predictive accuracy for species' range distributions in the future.

Additionally, the results from Chapter IV beg the questions: what kinds of disturbance are successful at maintaining native annual populations? Can we restore them to working landscapes that feature regular disturbance (e.g., grazed lands)? Since Euro-American settlement and the cessation of frequent fire intervals (Boyd 1999), native annuals have suffered the worst declines of any functional group in Pacific Northwest prairies (Dunwiddie et al. 2014). Given that much of these prairies are now agricultural and pasture lands, there may be opportunities to integrate restoration with livestock grazing, which may provide a disturbance regime necessary for native annuals' persistence. It remains to be seen whether this could be a feasible strategy but represents a prime opportunity for future research.

Finally, Chapter V investigated how abiotic drivers (i.e., temperature, moisture, and nutrients) controlled plant functional group cover, and how these groups in turn determined overall diversity between 2017-2019. We found that warmer temperatures caused increased cover of introduced annuals, along with subsequent declines in other functional groups and diversity. Our results not only confirmed those from a previous study (Pfeifer-Meister et al. 2016), but identified the causal pathways underlying the observed climate-community relationships. While there were direct effects of temperature

and moisture on perennial vegetation, these effects were typically amplified by introduced annuals. Competition for moisture, rather than nitrogen, was a critical mechanism of community change in this seasonally water-limited Mediterranean-climate system. Diversity decline was driven by a loss in native annuals and increasing dominance by introduced annuals. Such changes to the plant community may challenge land managers in their efforts to maintain species-rich and functionally-diverse prairie ecosystems for years to come.

The results of this study help explain those from previous chapters and point toward an annualization of Pacific Northwest prairies under climate change. However, it is unknown how a regime shift from perennial to annual grass dominance will affect ecosystem services. As shown in Chapter V, one effect will likely be a decline in biodiversity. Another effect may a reduction in soil water availability due to the earlier seasonality of canopy biomass growth and senescence (Chapter II). In California grasslands, the introduced annual invasion of the 1800's is believed to have caused a major reduction in soil carbon storage (Koteen et al. 2011). Will the same phenomenon occur in this system? Furthermore, most remaining prairie habitat exists within a patchwork of managed agricultural systems that depend on key services such as reliable forage production and pollinator abundance. Therefore, future work should address the implications for ecosystem services of a perennial-to-annual state transition in Pacific Northwest prairies.

APPENDIX A

SUPPLEMENTARY INFORMATION FOR CHAPTER II

Supplemental Figures

Figure S2.1. Locations of the three sites from southwestern Oregon to central-western Washington along the interior valleys of the Pacific Northwest. The sites span a 520 km latitudinal Mediterranean climate gradient of increasingly warmer and drier growing seasons moving from north to south. Map data sourced from Esri, USGS, NOAA, and US Census Bureau.

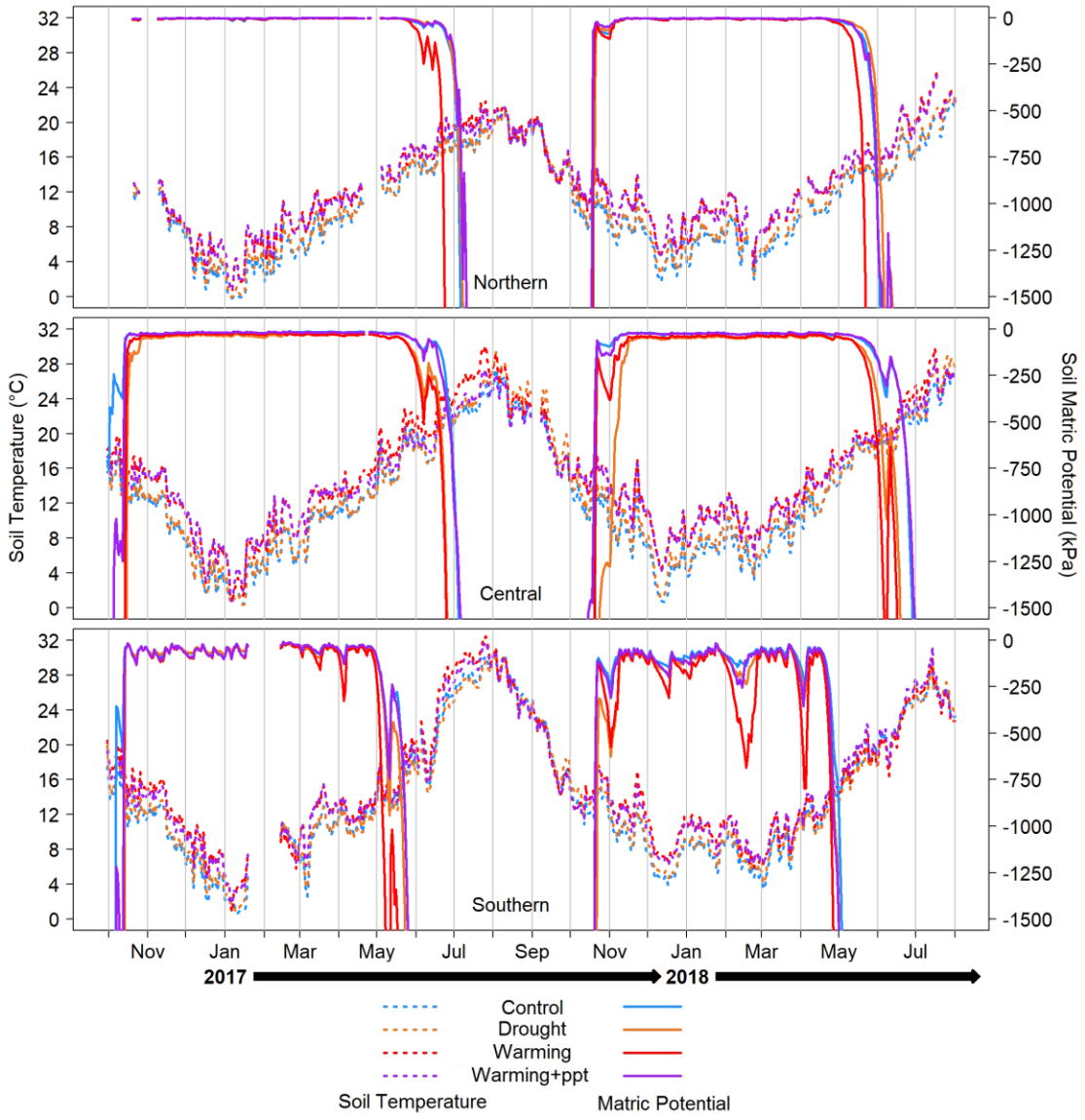

Figure S2.2. Mean daily soil temperature at 10 cm depth (left y-axis, dotted lines) and soil matric potential to 30 cm depth (right y-axis, solid lines) from Sept. 30, 2016 – Aug. 1, 2018 in the four climate treatments at each site. Note the earlier onset of summer drought (matric potential < -1500 kPa) and higher annual temperatures moving from north to south, and earlier summer drought in 2018 compared to 2017. Breaks in the data are due to equipment errors. Heaters were turned off from August – October 2017 at all three sites due to fire hazards.

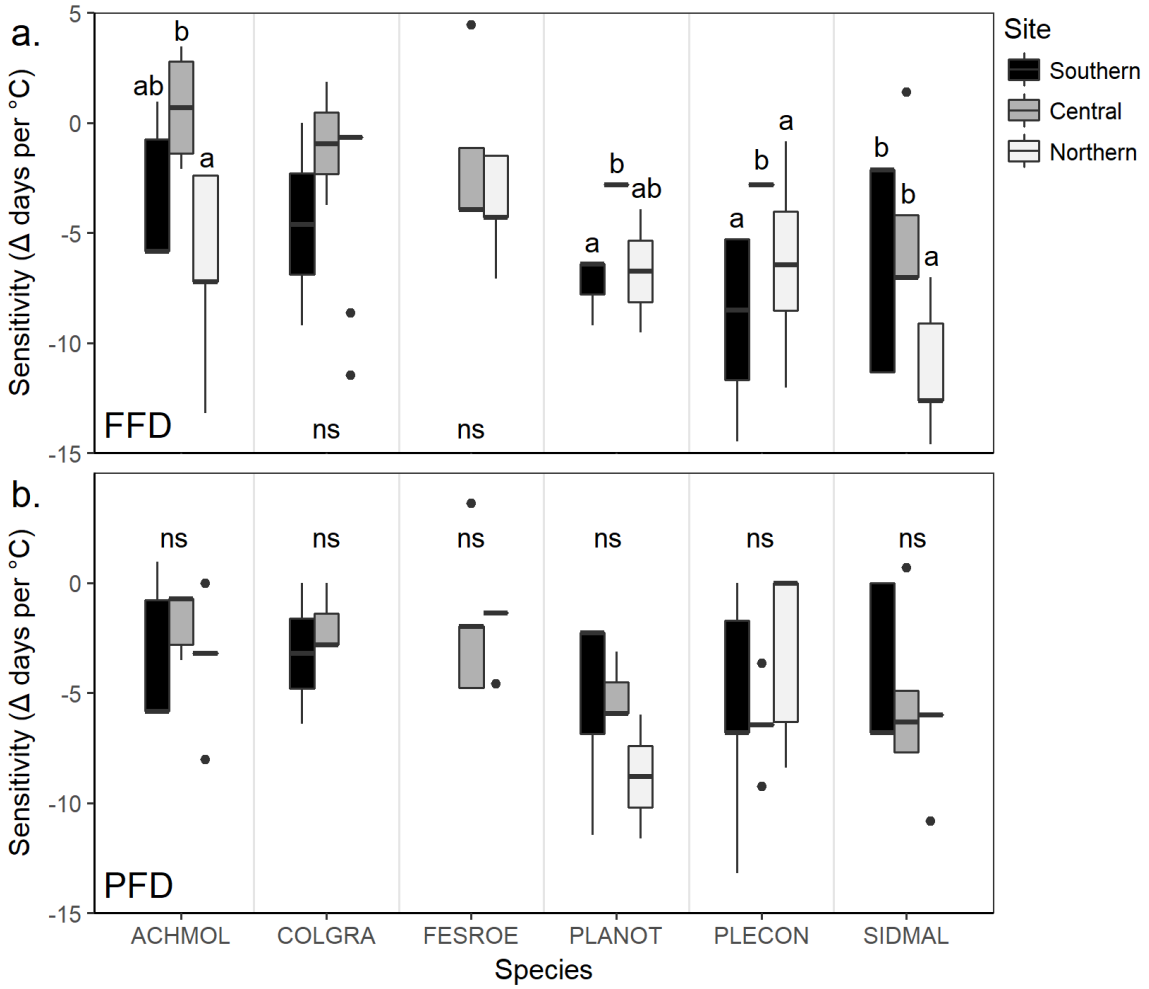

Figure S2.3. Temperature sensitivities between warmed and ambient plots for (a) first flower date (FFD) and (b) peak flower date (PFD) across sites. Different letters indicate significant or marginal differences between sites within a species ($p < 0.10$; Tukey's post-hoc comparisons); 'ns' = not significant.

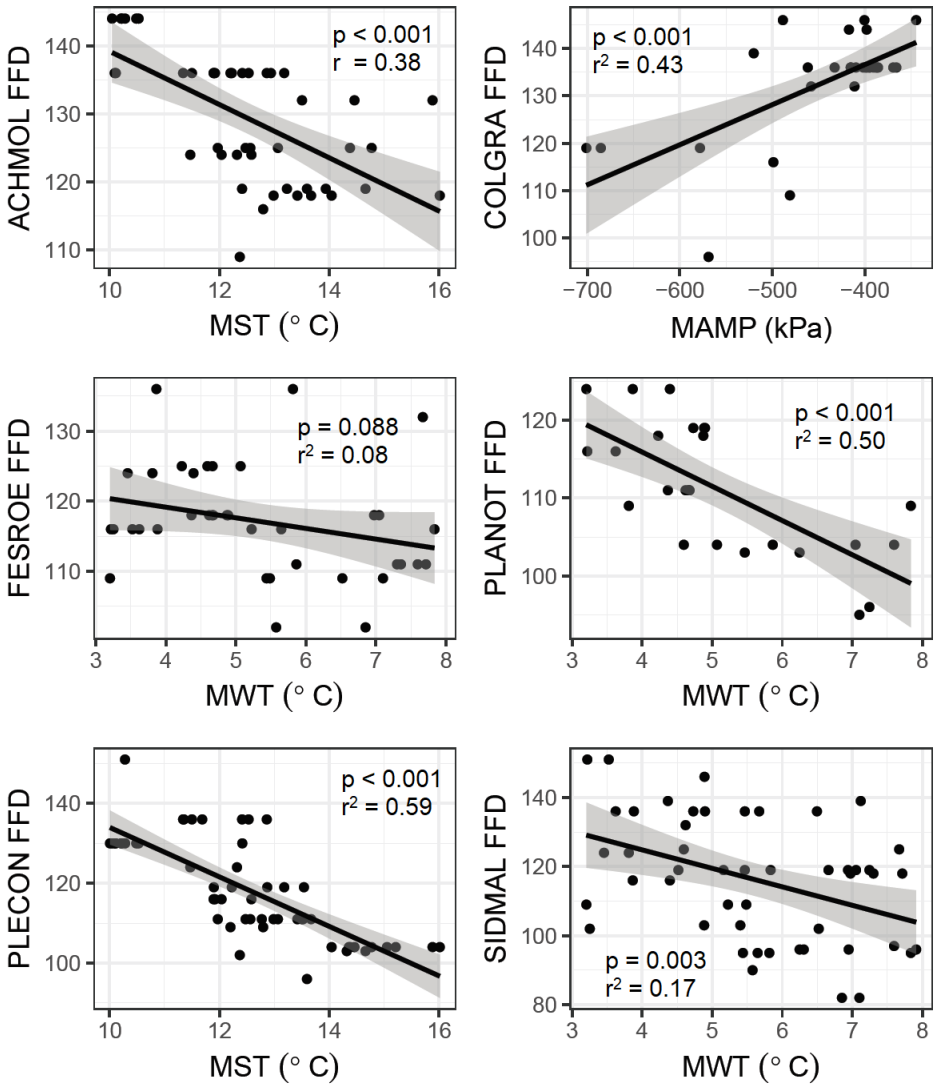

Figure S2.4. First flower dates (FFD) regressed against each species' most important predictor variable (Table 2.2). MST = 'mean spring temperature', MAMP = 'mean annual matric potential', MWT = 'mean winter temperature'.

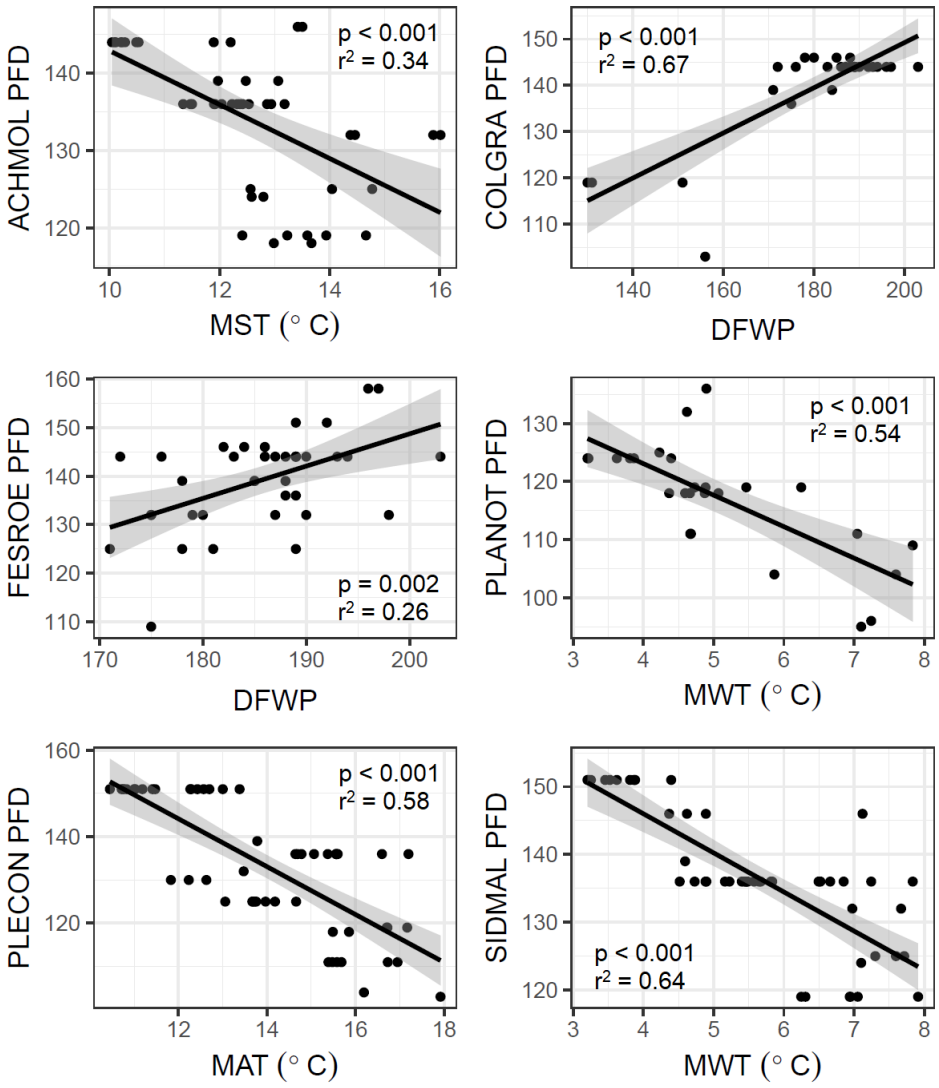

Figure S2.5. Peak flower dates (PFD) regressed against each species' most important predictor variable (Table 2.2). MST = 'mean spring temperature', DFWP = 'date of first wilting point', MWT = 'mean winter temperature', MAT = 'mean annual temperature'.

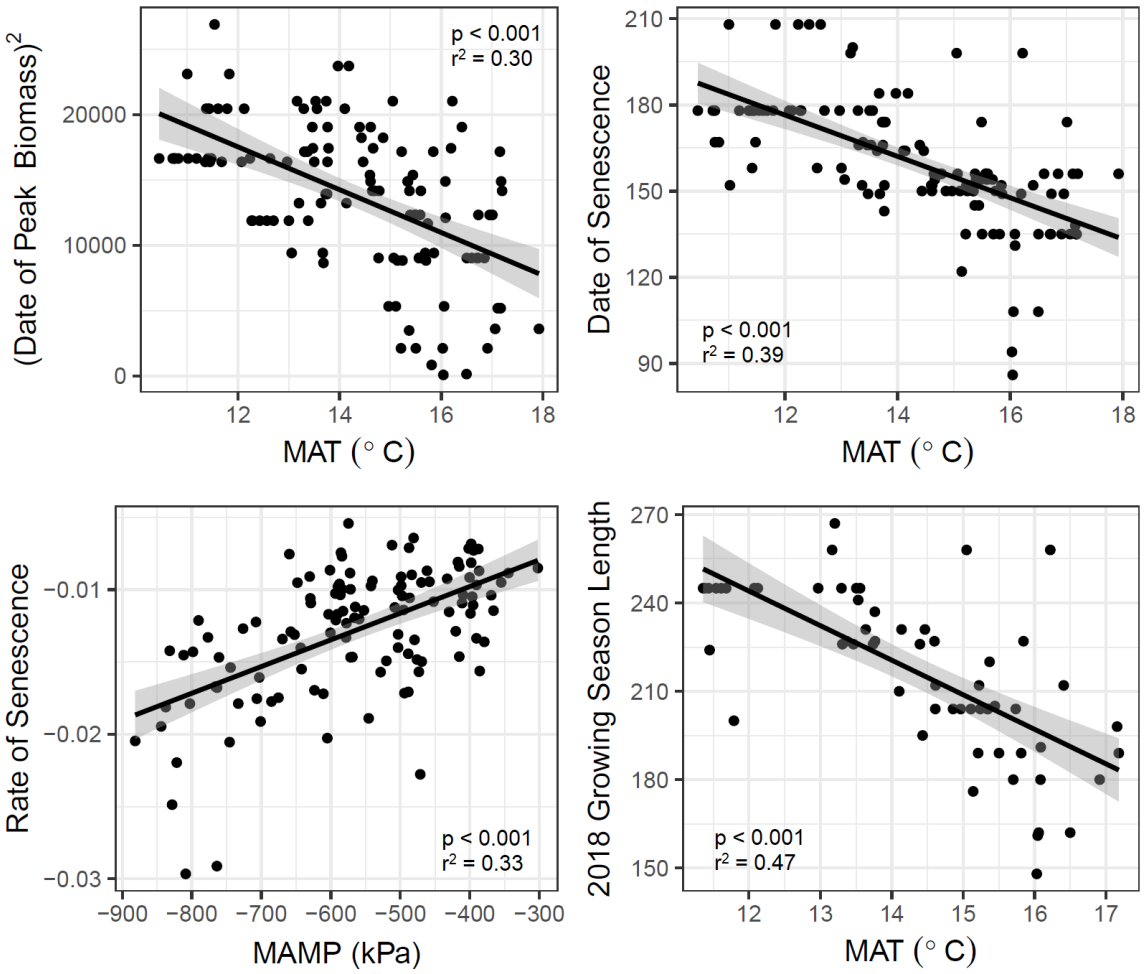

Figure S2.6. Community-level phenology variables each regressed against their most important predictor variable (Table 2.2). Date values are in Julian days; the date of peak biomass was squared to improve normality. MAT = 'mean annual temperature', MAMP = 'mean annual matric potential (adjusted)'.

Supplemental Tables

Table S2.1. Experimental site information. PRISM model is from the period 1981-2010 (http://www.prism.oregonstate.edu/). Soil taxonomy and series information: Natural Resources Conservation Service, United States Department of Agriculture (USDA), Web Soil Survey (http://websoilsurvey.nrcs.usda.gov/).

	Experimental Site		
	Southern	Central	Northern
Land Management	Siskiyou Field Institute	The Nature Conservancy	Capitol Land Trust
Latitude;	42.27811;	44.02615;	46.86415;
Longitude	-123.642278	-123.182171	-122.958918
Elevation (m)	394	165	79
Monthly Air Temp (°C) (PRISM)			
Mean	12.3	11.4	10.6
Max	20.2	17.3	15.9
Min	4.4	5.4	5.3
Annual Precipitation (mm) (PRISM)	1434	1134	1240
Fall (Sep-Nov)	316	293	363
Winter (Dec-Feb)	742	496	499
Spring (Mar-May)	331	275	288
Summer (Jun-Aug)	45	71	90
Soil			
Taxonomy	Loamy-skeletal, mixed, superactive, mesic Entic Ultic Haploxerolls	Very-fine, smectitic, mesic Vertic Haploxerolls	Medial, mixed, mesic Typic Haploxerands
Series	Takilma cobbly loam	Hazelair silty clay loam	Cathcart medial-loam pasture

Table S2.2. Likelihood Ratio (LR) χ^2 values, degrees of freedom (df), and p-values from analyses of abundances of reproductive plants of our eight focal species. 'Climate trt' indicates climate treatment, and '-' indicates not enough data to run a statistical test. Bold = significant at $p < 0.05$, italics = marginally significant ($p < 0.10$).

Abundances		**ACHMOL**		**COLGRA**		**FESROE**		**MICLAC**		**PLANOT**		**PLECON**		**RANAUS**		**SIDMAL**	
	df	LR X^2	*p*	LR X^2	*p*	LR X^2	*p*	LR X^2	*p*	LR X^2	*p*	LR X^2	*p*	LR X^2	*p*	LR X^2	*p*
Model Type		Negative Binomial		Negative Binomial		Poisson		Negative Binomial		Negative Binomial		Zero-Inflated Negative Binomial		Negative Binomial		Negative Binomial	
2-way Analysis of Deviance																	
Site	2	30.9	**<0.001**	1358	**<0.001**	1.5	0.227	-	-	15.5	**<0.001**	67.8	**<0.001**	-	-	333.6	**<0.001**
Climate Trt	3	9.5	**0.024**	5.2	0.156	4.1	0.252	-	-	14.2	**0.003**	2.3	0.513	-	-	0.8	0.854
Site x Climate Trt	6	13.2	**0.04**	22.9	**0.001**	2	0.574	-	-	4.5	0.605	20.9	**0.002**	-	-	29.3	**<0.001**
1-way Analysis of Deviance: within sites																	
Southern: Climate Trt	3	2.1	0.544	1.4	0.717	-	-	-	-	2.7	0.433	1.1	0.774	-	-	14.1	**0.003**
Central: Climate Trt	3	7.8	*0.051*	33.2	**0**	0.3	0.965	-	-	11.4	**0.01**	31.1	**<0.001**	-	-	2.6	0.462
Northern: Climate Trt	3	11.7	**0.008**	7	*0.073*	6.6	*0.086*	4.9	0.18	5.7	0.126	9.9	**0.019**	12.3	**0.007**	3.4	0.336

Table S2.3. Degrees of freedom (df) and p-values from ANOVAs and t-tests of first flower date (FFD) of our eight focal species. '-' indicates not enough data to run a statistical test. '#' indicates that tests for PLECON could not be run at the central site because there was no variance among all ambient plots nor among all warmed plots, Bold = significant at $p < 0.05$, italics = marginally significant ($p < 0.10$).

FFD		**ACHMOL**	**COLGRA**	**FESROE**	**MICLAC**	**PLANOT**	**PLECON**	**RANAUS**	**SIDMAL**
	df	*p*	*p*	*p*	*p*	*p*	*p*	*p*	*p*
2-way ANOVAs (using climate treatments)		Error df = 33	Error df = 18	Error df = 30	-	Error df = 14	Error df = 42	-	Error df = 37
Site	2	**0.001**	**<0.001**	0.351	-	0.491	**<0.001**	-	**0.02**
Climate Trt	3	**0.019**	0.172	**0.02**	-	**0.001**	**<0.001**	-	**<0.001**
Site x Climate Trt	6	**0.028**	0.214	**0.038**	-	0.244	**0.028**	-	0.262
2-way ANOVAs (using warming treatments)		Error df = 39	Error df = 24	Error df = 34	-	Error df = 20	Error df = 48	-	Error df = 43
Site	2	**0.001**	**<0.001**	0.405	-	0.507	**<0.001**	-	**0.01**
Warming	1	**0.001**	*0.075*	**0.013**	-	**<0.001**	**<0.001**	-	**<0.001**
Site x Warming	2	**0.006**	0.672	0.7	-	*0.084*	**0.005**	-	0.145
1-way ANOVAs (site effects, ambient plots)		Error df = 20	Error df = 12	Error df = 18	-	Error df = 15	Error df = 26	-	Error df = 21
Site	2	**<0.001**	**<0.001**	0.681	-	**0.017**	**<0.001**	-	0.437
1-way ANOVAs Southern		Error df = 9	-	-	-	Error df = 2	Error df = 11	-	Error df = 15
Climate Trt	3	*0.079*	-	-	-	*0.068*	**0.007**	-	0.143
1-way ANOVAs Central		Error df = 10	Error df = 2	Error df = 14	-	Error df = 8	#	-	Error df = 6
Climate Trt	3	0.952	0.928	0.17	-	0.189	#	-	*0.073*
1-way ANOVAs Northern		Error df = 14	Error df = 16	Error df = 16	Error df = 8	Error df = 4	Error df = 16	Error df = 13	Error df = 16
Climate Trt	3	**0.007**	*0.071*	**0.014**	*0.052*	0.118	**0.001**	**0.002**	**0.001**
t-tests: Southern		df = 9.1	df = 1	-	-	df = 2	df = 13	-	df = 17
Warming		*0.07*	0.5	-	-	**0.016**	**<0.001**	-	**0.018**
t-tests: Central		df = 9.3	df = 3.9	df = 16	-	df = 10	#	-	df = 8
Warming		0.585	0.725	*0.058*	-	**0.039**	#	-	*0.07*
t-tests: Northern		df = 12.2	df = 11	df = 18	df = 7	df = 6	df = 18	df = 15	df = 18
Warming		**<0.001**	*0.089*	*0.077*	**0.003**	**0.025**	**<0.001**	**0.002**	**<0.001**

Table S2.4. Degrees of freedom (df) and p-values from ANOVAs and t-tests of peak flower date (PFD) for each of our eight focal species. '-' indicates not enough data to run a statistical test. '@' indicates that PFD data for *C. grandiflora* at the northern site were excluded due to an overwhelmingly large sample size (> 500 plants per plot) which made it logistically impossible to count flowers during its peak growing period. Bold = significant at $p < 0.05$, italics = marginally significant ($p < 0.10$).

PFD		**ACHMOL**	**COLGRA**	**FESROE**	**MICLAC**	**PLANOT**	**PLECON**	**RANAUS**	**SIDMAL**
	df	*p*	*p*	*p*	*p*	*p*	*p*	*p*	*p*
2-way ANOVAs (using climate treatments)		Error df = 33	Error df = 18	Error df = 30	-	Error df = 14	Error df = 42	-	Error df = 37
Site	2	**<0.001**	**<0.001**	**0.002**	-	0.321	**<0.001**	-	**<0.001**
Climate Trt	3	**0.037**	**<0.001**	0.125	-	**0.003**	**<0.001**	-	**<0.001**
Site x Climate Trt	6	0.656	**<0.001**	0.825	-	0.183	0.173	-	0.543
2-way ANOVAs (using warming treatments)		Error df = 39	-	Error df = 34	-	Error df = 20	Error df = 48	-	Error df = 43
Site	2	**0.001**	-	**0.001**	-	0.328	**<0.001**	-	**<0.001**
Warming	1	**0.002**	-	**0.016**	-	**<0.001**	**<0.001**	-	**<0.001**
Site x Warming	2	0.606	-	0.72	-	0.422	*0.08*	-	0.325
1-way ANOVAs (site effects, ambient plots)		Error df = 20	-	Error df = 18	-	Error df = 15	Error df = 26	-	Error df = 21
Site	2	**0.022**	-	**0.003**	-	0.184	**<0.001**	-	**<0.001**
1-way ANOVAs Southern		Error df = 9	-	-	-	Error df = 2	Error df = 11	-	Error df = 15
Climate Trt	3	*0.079*	-	-	-	0.65	**0.032**	-	**0.005**
1-way ANOVAs Central		Error df = 10	Error df = 2	Error df = 14	-	Error df = 8	Error df = 15	-	Error df = 6
Climate Trt	3	0.868	0.506	0.41	-	**0.015**	**<0.001**	-	0.149
1-way ANOVAs Northern		Error df = 14	-	Error df = 16	Error df = 8	-	Error df = 16	Error df = 13	Error df = 16
Climate Trt	3	**0.032**	-	0.288	0.389	-	0.261	**<0.001**	**<0.001**
t-tests: Southern		df = 9.1	df = 1	-	-	df = 3.7	df = 5	-	df = 8
Warming		*0.07*	0.5	-	-	0.24	**0.041**	-	**0.004**
t-tests: Central		df = 8.7	df = 2	df = 16	-	df = 5.8	df = 17	-	df = 8
Warming		0.377	0.184	*0.091*	-	**0.008**	**<0.001**	-	**0.016**
t-tests: Northern		df = 9	-	df = 17	df = 7	df = 6	df = 9	df = 14.7	df = 8
Warming		**0.003**	-	*0.079*	**0.033**	**0.001**	*0.081*	**<0.001**	**<0.001**

Table S2.5. Degrees of freedom (df) and p-values from ANOVAs of temperature sensitivities (difference between warmed and ambient plots divided by 2.5°C) for first flowering date (FFD) and peak flowering date (PFD) across sites for six focal species.

Sensitivity (FFD)		**ACHMOL**	**COLGRA**	**FESROE**	**PLANOT**	**PLECON**	**SIDMAL**
	df	*p*	*p*	*p*	*p*	*p*	*p*
1-way ANOVAs (site effect on sensitivity)		Error df = 19	Error df = 12	Error df = 16	Error df = 5	Error df = 22	Error df = 22
Site	2	**0.004**	0.632	0.66	*0.086*	**0.002**	**0.013**
Sensitivity (PFD)		**ACHMOL**	**COLGRA**	**FESROE**	**PLANOT**	**PLECON**	**SIDMAL**
	df	*p*	*p*	*p*	*p*	*p*	*p*
1-way ANOVAs (site effect on sensitivity)		Error df = 19	Error df = 3	Error df = 16	Error df = 5	Error df = 22	Error df = 22
Site	2	0.353	0.652	0.675	0.561	*0.096*	0.322

Table S2.6. Candidate models to describe the phenology response variables (FFD = first flowering date, PFD = peak flowering date, GSL = growing season length). *K* = the number of parameters, AIC_c = small-sample-size corrected version of Akaike Information Criterion, δAIC_c = change in AIC_c, ω = Akaike's weight. Only models with $\delta AIC_c < 2$ are reported, and two-parameter models are not reported if they had an AIC_c less than a model including one of its parameters alone. Temperature variables: MAT = mean annual temp, MWT = mean winter temp, MST = mean spring temp; moisture variables: MAMP = mean annual matric potential (adjusted so values < -1,500 became -1,500), DFWP = date of first wilting point, DBWP = days below wilting point.

Phenology Variable	Model(s)	*K*	AIC_c	δAIC_c	ω	Adj. R^2
FFD (2017)						
ACHMOL	–MST	1	313.8	0.00	0.51	0.37
COLGRA	MAMP	1	220.2	0.00	0.35	0.41
FESROE	–MWT – DFWP	2	265.1	0.00	0.40	0.15
PLANOT	–MWT	1	171.9	0.00	0.54	0.47
PLECON	–MST – DFWP	2	374.2	0.00	0.44	0.66
	–MST – MAMP	2	375.9	1.76	0.27	0.65
SIDMAL	–MWT	1	418.0	0.00	0.38	0.16
PFD (2017)						
ACHMOL	–MST + DFWP	2	308.7	0.00	0.28	0.39
	–MAT	2	308.9	0.16	0.24	0.37
	–MST + MAMP	2	309.8	1.03	0.15	0.37
COLGRA	DFWP	1	198.2	1.79	0.14	0.66
FESROE	–MAT + DFWP	2	269.2	0.00	0.36	0.38
	–MST + DFWP	2	269.8	0.68	0.40	0.36
PLANOT	–MWT – DFWP	2	177.5	0.00	0.42	0.57
	–MWT	1	178.5	1.01	0.26	0.52
PLECON	–MAT + DFWP	2	384.0	0.00	0.82	0.71
SIDMAL	–MWT + MAMP	2	311.5	0.00	0.54	0.71
	–MWT + DFWP	2	312.1	0.55	0.41	0.70
NDVI (2017+2018):						
Date of peak biomass	–MAT + DFWP	2	2374.1	0.00	0.57	0.32
	–MAT + MAMP	2	2375.8	1.68	0.25	0.31
Date of senescence	–MAT + MAMP	2	1016.1	0.00	0.59	0.44
	–MAT – DBWP	2	1017.5	1.39	0.30	0.43
Rate of senescence	–MAT + MAMP	2	-1006.5	0.00	0.60	0.35
GSL (2018)	–MAT + MAMP	2	523.9	0.00	0.44	0.57
	–MAT – DBWP	2	524.2	0.29	0.38	0.57

Table S2.7. Results from statistical analyses of community-level phenology response variables. *Year effects within sites used ambient-only plots for date and rate of senescence.

		Date of peak biomass	**Date of senescence**	**Rate of senescence**	**Growing Season Length**
	df	*p*	*p*	*p*	*p*
3-Way Repeated Measures ANOVAs (2017 + 2018)		Error df = 108	Error df = 108	Error df = 108	
Site	2	**<0.001**	**<0.001**	**<0.001**	
Warming	1	**<0.001**	**0.002**	0.666	
Site x Warming	2	0.349	**0.023**	0.339	NA
Year	1	0.701	**0.002**	**0.009**	
Site x Year	2	*0.096*	0.187	**0.001**	
Warming x Year	1	0.288	**0.011**	0.574	
Site x Warming x Year	2	0.565	0.659	0.168	
1-Way Repeated Measures ANOVAs* (year effects within sites)		Error df = 19	Error df = 9*	Error df = 9*	
Southern: Year	1	0.164	**0.008**	**0.010**	NA
Central: Year	1	0.440	0.975	0.762	
Northern: Year	1	**0.019**	0.337	0.163	
2-way ANOVAs: 2018		Error df = 54	Error df = 54	Error df = 54	Error df = 54
Site	2	**<0.001**	**<0.001**	0.172	**<0.001**
Warming	1	**0.002**	**<0.001**	0.504	**0.008**
Site x Warming	2	0.408	0.288	0.908	*0.076*
1-way ANOVAs: 2018 (site effects, ambient plots)		NA	NA	NA	Error df = 27
Site	2				**<0.001**
2-way ANOVAs: 2017		Error df = 54	Error df = 54	Error df = 54	
Site	2	**<0.001**	**<0.001**	**<0.001**	
Warming	1	**<0.001**	0.317	0.894	NA
Site x Warming	2	0.623	**0.013**	**0.045**	
1-way ANOVAs: 2017 (site effects, ambient plots)		NA	Error df = 27	Error df = 27	NA
Site	2		**0.013**	**<0.001**	
t-tests: Southern 2018		NA	NA	NA	df = 14.4
Warming					**0.004**
t-tests: Central 2018		NA	NA	NA	df = 14.5
Warming					**0.037**
t-tests: Northern 2018		NA	NA	NA	df = 18.0
Warming					0.965
t-tests: Southern 2017		NA	df = 9.0	df = 17.9	NA
Warming			**0.015**	0.163	
t-tests: Central 2017		NA	df = 16.0	df = 17.9	NA
Warming			**0.049**	**0.029**	
t-tests: Northern 2017		NA	df = 16.0	df = 17.6	NA
Warming			0.172	0.881	

APPENDIX B

SUPPLEMENTARY INFORMATION FOR CHAPTER III

Supplemental Methods

Climate treatment implementation:

At the center of each plot we recorded canopy temperatures (using SI-121 infrared radiometers; Campbell Scientific, Logan, Utah, USA), soil temperatures (at 10 cm depth using 107-L thermistor probes; Campbell Scientific), and volumetric water contents (at 0-30 cm depth using CS616-L water content reflectometers; Campbell Scientific) and logged these data continuously with 30 min averages (via AM16/32B multiplexors connected to CR1000 dataloggers; Campbell Scientific). To achieve an increase in canopy temperatures for the warming and warming + precipitation plots by +2.5°C relative to ambient temperatures, we used six 2000-W infrared heaters per plot (Kalglo Electronics, Bethlehem, Pennsylvania, USA) and modulated their radiation output using the canopy temperatures recorded in control plots (Kimball et al., 2008). This temperature increase of +2.5°C relative to ambient temperatures is consistent with expectations for the region by the end of the 21st century (Mote & Salathé, 2010). To irrigate the warming + precipitation plots, we collected rainfall on polycarbonate sheets and stored it in cisterns. Each night that the volumetric water content of a warming + precipitation plot fell below 95% of the control plot average, an automated sprinkler system irrigated the plot for 30 minutes. With this irrigation design, we achieved soil matric potentials approximately equal to the ambient soil matric potentials of the control plots (see Figure S2 in Reed et al. (2019)). Lastly, we implemented our drought treatment with a fixed rainout shelter design, using clear acrylic shingles with high light transmittance (MultiCraft Plastics, Eugene, Oregon, USA) that covered and intercepted precipitation over 40% of the plot area. This 40% reduction in precipitation represents an "extreme" event for each the three sites, determined using the Precipitation Trends and Manipulation tools from Drought-Net (Lemoine, Sheffield, Dukes, Knapp, & Smith, 2016). The drought treatment was initiated in February 2016 at all sites, warming in February, January, and June 2016 at the southern, central, and northern sites, respectively, and irrigation for the warming + precipitation treatment in September 2016 at all sites. Due to fire hazard during the driest summer months, we turned heaters off in August and September 2016 and 2017. All treatments ceased in July 2018 at the end of the experiment.

Determining species' range limits:

We assigned species' latitudinal range limits based on recent recorded observations gathered from the Consortium of Pacific Northwest Herbaria (www.pnwherbaria.org/) and the Consortium of California Herbaria (https://ucjeps.berkeley.edu/consortium/) as of April 1, 2019, and corroborated these recordings with observations from field sites and/or consultation with regional experts. We defined species' current range limits as the latitudes of the northernmost and southernmost known populations within the species' contiguous ranges documented

within the last 50 years. Because our study area is westside lowland Pacific Northwest prairies, we restricted records to the west side of the Cascade and Sierra mountain divides. For the species with broader distributions (*Achnatherum lemmonii* and *Danthonia californica*), this excluded records from ecoregions that would substantially alter the climatic interpretation of a particular latitude.

For *Sidalcea malviflora ssp. virgata*, the northernmost population within its contiguous range exists at 45.35°N in the Willamette Valley of Oregon. There is a single, small, disjunct population existing >160 km further northern in Thurston County, Washington, but its status as a native or nonnative population is unclear (Hitchcock et al. 2018). Considering these facts, we assigned this species' northern limit as that northernmost population found in the Willamette Valley.

Species descriptions and measurements of size and reproduction:

Ranunculus austro-oreganus (Southern Oregon buttercup) is a perennial forb in the *Ranunculaceae* family endemic to a narrow range of the Klamath Mountain ecoregion of southwestern Oregon. To estimate size of adult *Ranunculus* in our experiment, we counted the total number of basal leaves and measured the length of the longest leaf. We then calculated size as the log-transformation of the number of basal leaves x length of the largest leaf. For reproduction, we counted the total number of flowers on reproductive individuals and modeled this as a generalized linear mixed model with Poisson error distribution. Using 2018 data from both natural *Ranunculus* populations as well as our plots, we counted the number of seeds present on fully matured flowers to estimate an average number of seeds produced per flower.

Sidalcea malviflora ssp. *virgata* (Rose checkermallow) is a perennial forb in the *Malvaceae* family native to prairie habitat in the Willamette Valley ecoregion of western Oregon. The species is gynodioecious with a strong taproot and trailing rhizomes. On adult *S. malviflora* plants in our experiment, we counted the total number of leaves (not including bracts) and measured the length and width of the largest leaf on each individual. We then calculated the area of the largest leaf and multiplied this by the number of leaves for our size variable, which we log-transformed for normality. To collect reproduction data, we counted the total number of flowering stems and counted the number of flowers on two random stems to generate an average flower count per stem. We then calculated the estimated total flower production for each reproductive individual, which we log-transformed and modeled as a general linear mixed model. In 2018 following flowering, we returned to a subset of tagged stems to count the number of fruits present and used these counts to estimate the fraction of flowers that become fruit. Lastly, we counted seeds in a subset of these fruits to calculate the average number of seeds produced per fruit at the site level.

Microseris laciniata (Cutleaf silverpuffs) is a perennial forb in the *Asteraceae* family native to prairie habitat from northern California to Washington, with its northern range occurring in the Puget Lowland ecoregion. We measured size on adult *M. laciniata* in our experiment in the same fashion as for *R. austro-oreganus* (above): calculating size as the log-transformed product of the number of basal leaves x length of the longest leaf. For reproduction, we counted the total number of inflorescences on each reproductive individual and modeled this as a generalized linear mixed model with Poisson error distribution. On a subset of inflorescences used as seed sources for the experiment in

2018, we counted seed scars to estimate the average number of seeds produced per inflorescence.

Achnatherum lemmonii var. *lemmonii* (Lemmon's needlegrass) is a perennial bunchgrass native to western North America, where it is relatively widespread but disjunct and uncommon. The species is drought-adapted and typically found in hotter, drier, rocky outcrop habitats. Its inflorescences produce spikelets containing chasmogamous (cross-pollinated) seeds. To measure size in adult *A. lemmonii* in our experiment, we measured the length and width of the bunchgrasses' basal mass as well as its center-die-back (CDB; area within the mass that may have experienced senescence) to calculate the basal area (cm^2) as: basal mass length x width – CDB length x width. We then log-transformed basal areas to improve normality of our size variable. We did not collect reproduction data on *A. lemmonii* since we had no reproductive adults establish in our plots.

Festuca roemeri (Roemer's fescue) is a perennial bunchgrass native to western Washington, Oregon, and northwestern California, with its northern range occurring in the Puget Lowland ecoregion. *F. roemeri* is relatively uncommon due to a lack of quality remnant prairies but is an important target for restoration in native prairie and oak habitat. Its inflorescences produce spikelets containing chasmogamous seeds. Our size variable for adult *F. roemeri* was also log-transformed basal area, measured and calculated the same way as described for *A. lemmonii* (above). To collect reproduction data, we counted the total number of inflorescences and counted the number of spikelets on two inflorescences to generate an average spikelet count per inflorescence. We then calculated an estimated total spikelet production for each reproductive individual, which we log-transformed and modeled as a general linear mixed model. Using inflorescences harvested in 2017 from natural *F. roemeri* populations we monitored in the region, we estimated the average number of seeds per spikelet.

Danthonia californica (California oatgrass) is a perennial bunchgrass native to wetland and upland prairie habitat in the western United States and Canada and is considered widespread and generally common across that range. Its inflorescences produce spikelets containing chasmogamous seeds as well as cleistogamous (self-pollinated) seeds concealed within the stems. Our size variable for adult *D. californica* was also log-transformed basal area, measured and calculated the same way as described for *A. lemmonii* and *F. roemeri* (above). To collect reproduction data, we counted the total number of inflorescences and counted the number of spikelets and flag leaves (correlated with cleistogamous seeds) on two inflorescences to generate average spikelet and flag leaf counts per inflorescence. We then calculated an estimated total spikelet production and number of flag leaves per reproductive individual, which were log-transformed and modeled as general linear mixed models. Like with *F. roemeri*, we used inflorescences harvested in 2017 from natural *D. californica* populations we monitored in the region to estimate the average number of chasmogamous seeds per spikelet and the number of cleistogamous seeds per flag leaf.

2018 greenhouse germination study:

Following the conclusion of the field experiment, we conducted a greenhouse germination study in 2018 to test whether the soils from the experimental sites (southern, central, and northern) led to site-level differences in germination. In August 2018, we

collected soil between 2.5-25 cm depth at each site and sifted the soils to remove rocks, large roots, and seeds. To accommodate plant growth within germination trays, we added perlite and acid-washed sand to the soils to achieve a soil:sand:perlite ratio of 2:1:1.

In September 2018, we planted 144 seeds of each focal species for each soil type in small-celled germination trays (one seed per cell planted several millimeters below the soil surface), using the same seed source for each species across soils. We then cold-stratified all germination trays for 30 days in a 4°C dark room, regularly moistening the soils with deionized water. Following cold stratification, we moved germination trays to a greenhouse where they were placed randomly under ambient light conditions for the first two weeks and then placed under grow-lights for 12 hours/day for the remainder of the experiment. Germination counts began at the first sign of germination for each species (during cold stratification for some species) and continued for the duration of the experiment (through December 2018).

To test for soil differences in germination for each species, we used generalized linear models with binomial error distribution and logit-link functions, tested for significance using analysis of deviance, and identified significantly different soils using Tukey's post-hoc tests. We conducted analyses using R version 3.3.2 (R Core Team, 2016).

Supplemental Figures

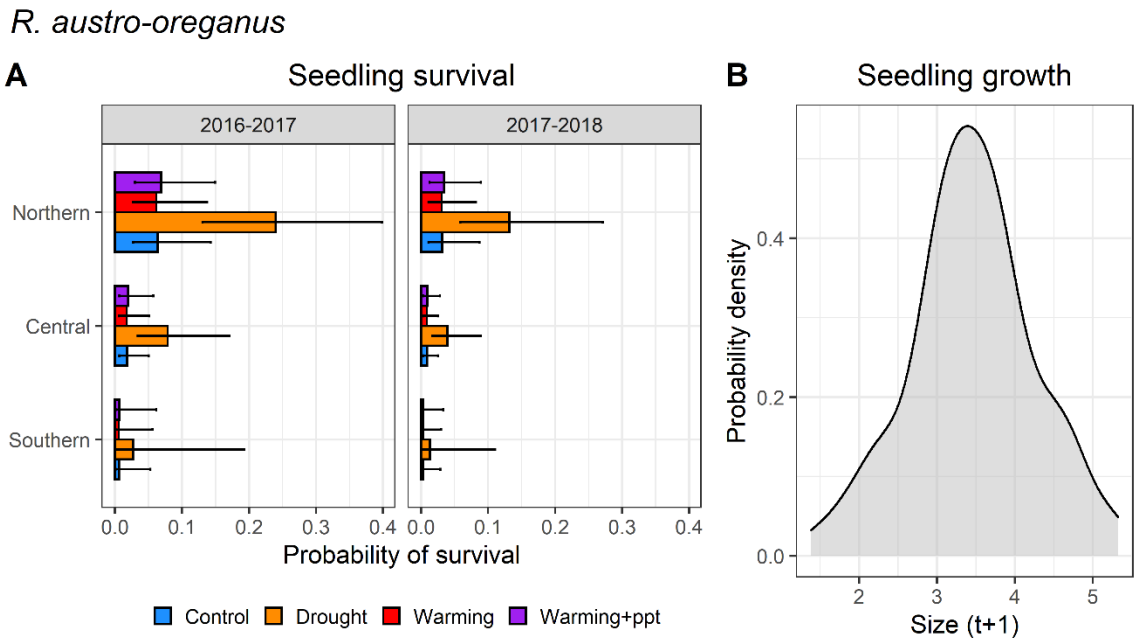

Figure S3.1. *Ranunculus austro-oreganus* seedling survival (A) and growth (B). (A) depicts model predictions (estimated marginal means ± 95% confidence intervals) for the best-fit model of seedling survival (Table S3). Because the biomass removal treatment was in the best-fit model, predictions shown here are for the control level of this treatment. (B) depicts the probability density function of seedling size distribution at time *t*+1 (the second year of the transition) across all data, as supported by the best-fit model for seedling growth (Table S3).

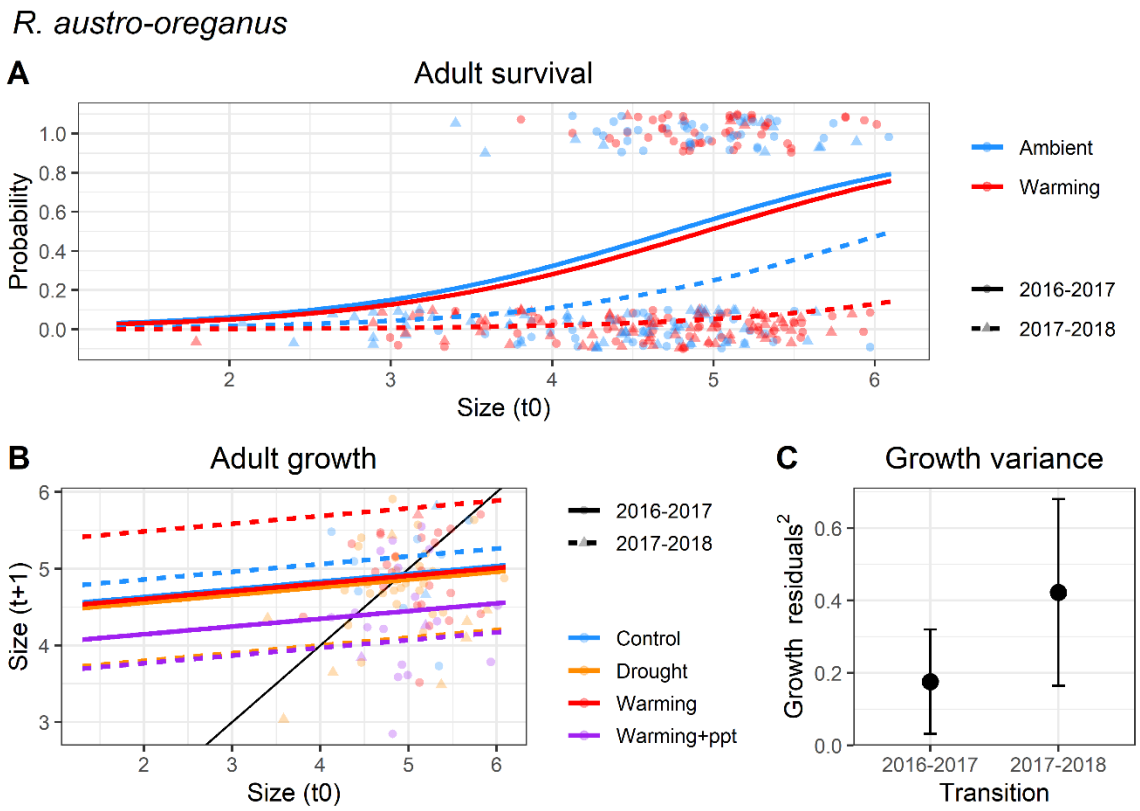

Figure S3.2. Model predictions based on the best-fit models (Table S3) for *Ranunculus austro-oreganus* adult survival (A), growth (B), and variance in growth (C; estimated marginal means ± 95% confidence intervals). Adult survival is depicted against plant size at time *t*0 (the first year of the transition), growth is plant size at time *t*+1 (the second year of the transition) against plant size at time *t*0, and growth variance is the squared-residuals of the growth model against the best-fit set of parameters. Survival and growth show true datapoints in the background (survival datapoints are jittered around 1.0 (survived) or 0.0 (died)). The solid black line in (B) indicates intercept = 0 and slope = 1; any point above this line indicates growth, anything below indicates shrinkage. Because the biomass removal treatment was in the best-fit model for growth variance (C), predictions shown here are for the control level of this treatment.

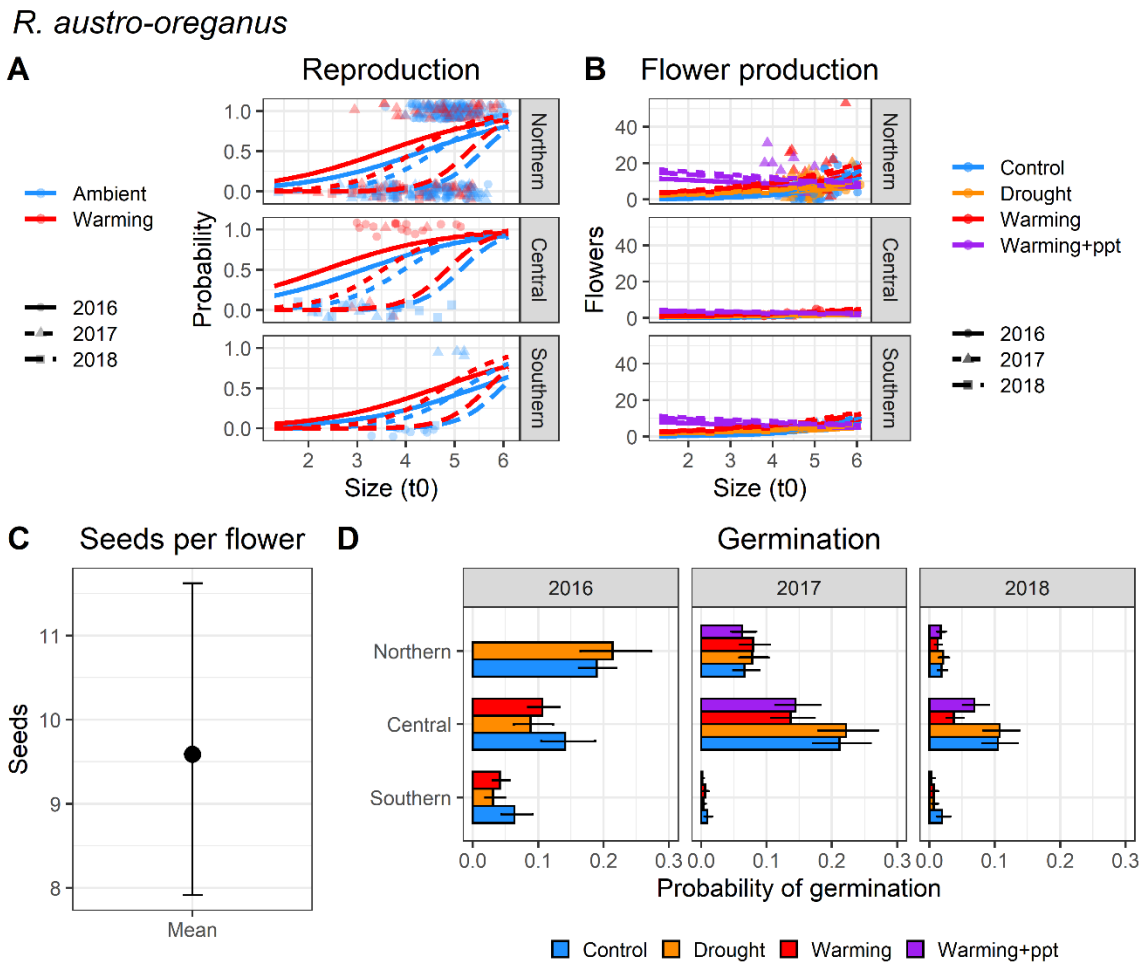

Figure S3.3. Model predictions based on the best-fit models (Table S3) for *Ranunculus austro-oreganus* fecundity vital rates (reproduction (A), flower production (B), seeds per flower (C), and germination (D); estimated marginal means ± 95% confidence intervals for (C) and (D)). The probability of reproducing (A) and flower production (B) are depicted against plant size at time *t*0 (year). Reproduction and flower production show true datapoints in the background (reproduction datapoints are jittered around 1.0 (flowering) or 0.0 (not flowering)). 2016 germination was modeled separately from 2017/2018 since not all climate treatments were initiated yet at the sites (see methods) and since 2016 germination was unnecessary for building the IPMs. Because the biomass removal treatment was in the best-fit model for 2017/2018 germination, predictions shown here are for the control level of this treatment.

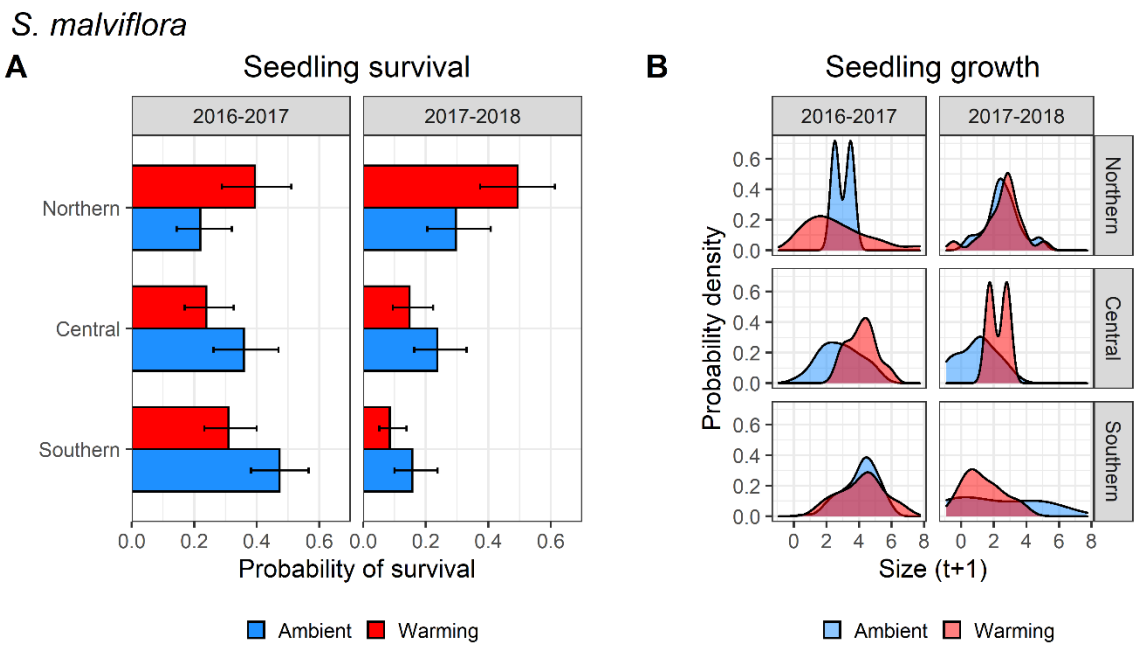

Figure S3.4. *Sidalcea malviflora* seedling survival (A) and growth (B). (A) depicts model predictions (estimated marginal means ± 95% confidence intervals) for the best-fit model of seedling survival (Table S3). Because the biomass removal treatment was in the best-fit model, predictions shown here are for the control level of this treatment. (B) depicts the probability density functions of seedling size distributions at time *t*+1 (the second year of the transition) for the control level of the biomass removal treatment under all other parameters supported by the best-fit model for seedling growth (Table S3).

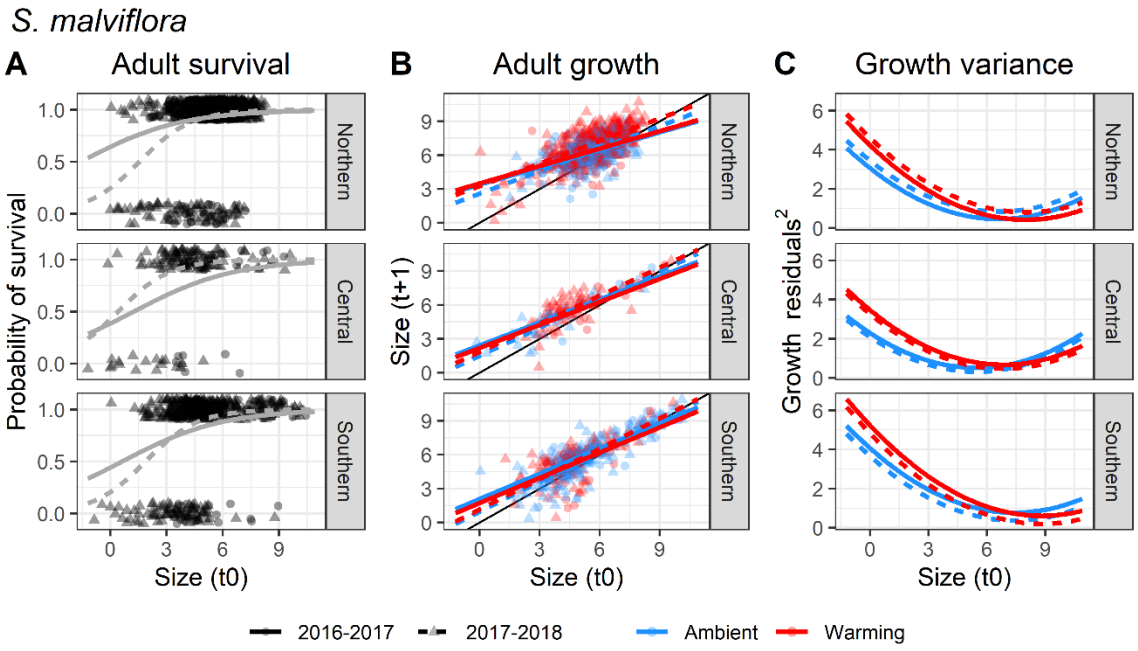

Figure S3.5. Model predictions based on the best-fit models (Table S3) for *Sidalcea malviflora* adult survival (A), growth (B), and variance in growth (C). Adult survival is depicted against plant size at time *t*0 (the first year of the transition), growth is plant size at time *t*+1 (the second year of the transition) against plant size at time *t*0, and growth variance is the squared-residuals of the growth model also against plant size at time *t*0. Survival and growth show true datapoints in the background (survival datapoints are jittered around 1.0 (survived) or 0.0 (died)). The solid black line in (B) indicates intercept = 0 and slope = 1; any point above this line indicates growth, anything below indicates shrinkage. Because the biomass removal treatment was in the best-fit model for survival (A), predictions shown here are for the control level of this treatment.

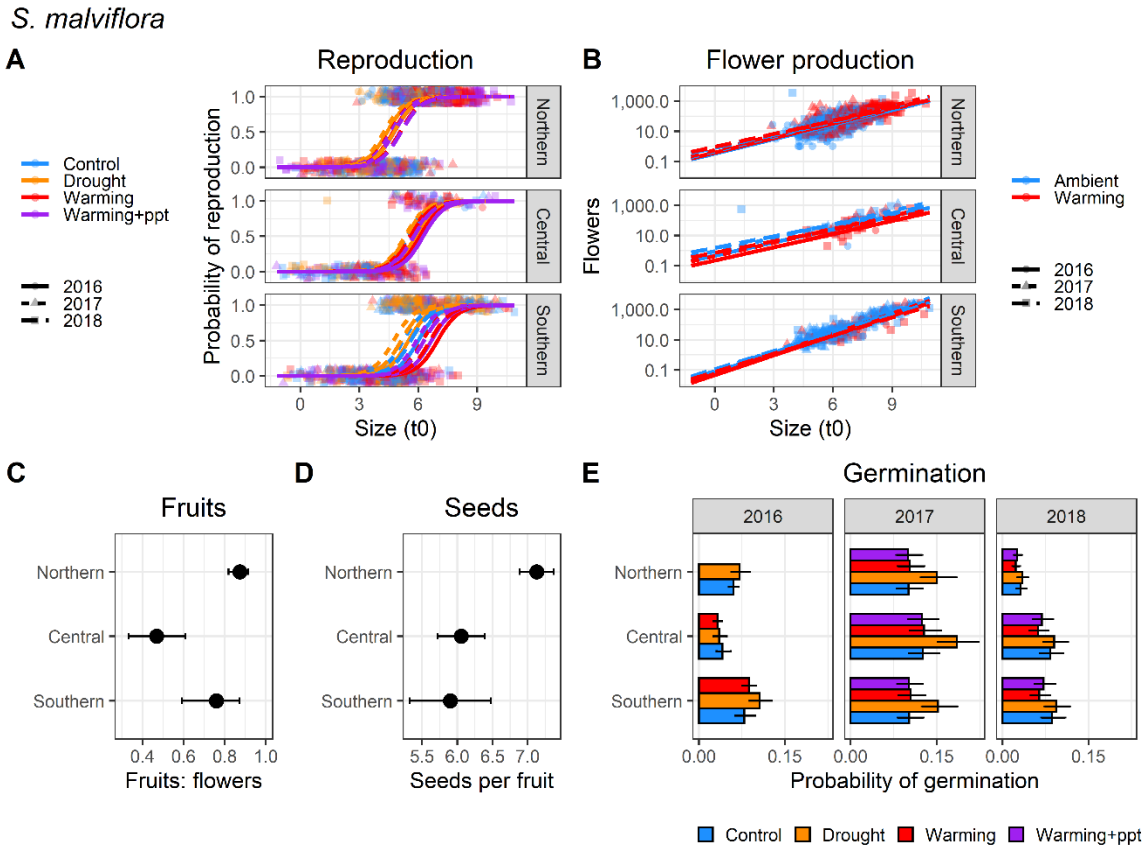

Figure S3.6. Model predictions based on the best-fit models (Table S3) for *Sidalcea malviflora* fecundity vital rates (reproduction (A), flower production (B), fruit to flower ratio (C), seeds per fruit (D), and germination (E); estimated marginal means ± 95% confidence intervals for (C), (D), and (E)). The probability of reproducing (A) and flower production (B) are depicted against plant size at time *t*0 (year). Reproduction and flower production show true datapoints in the background (reproduction datapoints are jittered around 1.0 (flowering) or 0.0 (not flowering)). 2016 germination was modeled separately from 2017/2018 since not all climate treatments were initiated yet at the sites (see methods) and since 2016 germination was unnecessary for building the IPMs. Because the biomass removal treatment was in the best-fit model for 2017/2018 germination, predictions shown here are for the control level of this treatment.

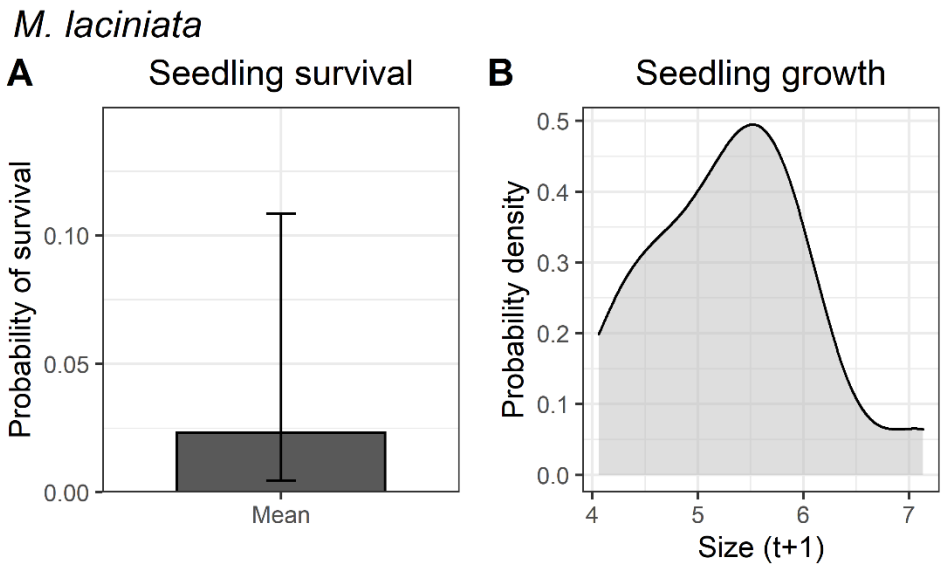

Figure S3.7. *Microseris laciniata* seedling survival (A) and growth (B). (A) depicts the model prediction (estimated marginal mean ± 95% confidence interval) for the best-fit model of seedling survival using data from the Central and Northern sites (Table S3). The southern site was not included in the model due to a constant response (no seedlings survived). (B) depicts the probability density function of seedling size distribution at time *t*+1 (the second year of the transition) across the Central and Northern sites as supported by the best-fit model for seedling growth (Table S3). Because no seedlings survived at the Southern site, it had no seedling growth data to include in this model.

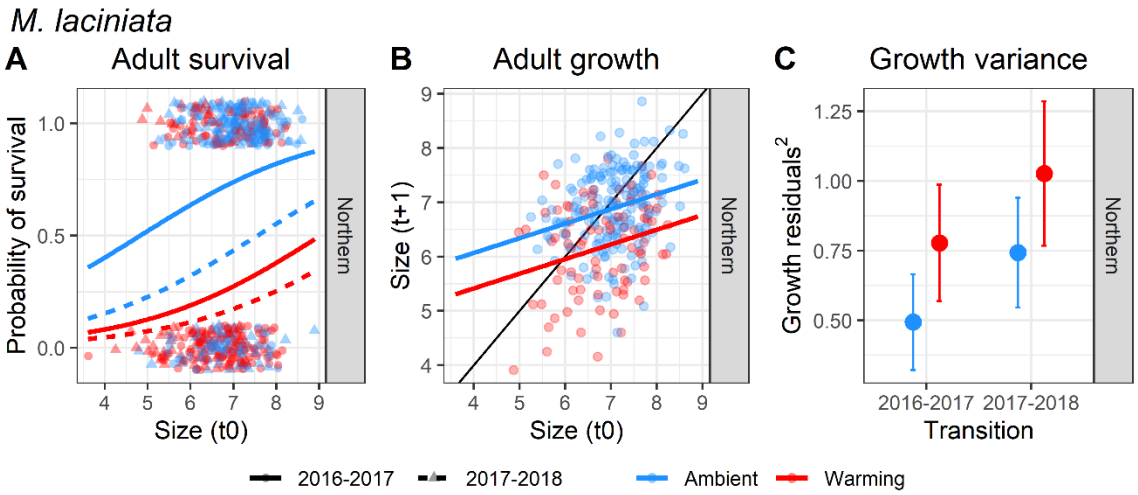

Figure S3.8. Model predictions based on the best-fit models (Table S3) for *Microseris laciniata* adult survival (A), growth (B), and variance in growth (C; estimated marginal means ± 95% confidence intervals). For adult survival, the Southern and Central sites were not included in the model due to no data (Southern site) and a constant response (no adults survived; Central site). For growth, neither the Southern nor Central sites had data. Survival is depicted against plant size at time *t*0 (the first year of the transition), growth is plant size at time *t*+1 (the second year of the transition) against plant size at time *t*0, and growth variance is the squared-residuals of the growth model against the best-fit set of parameters. Survival and growth show true datapoints in the background (survival datapoints are jittered around 1.0 (survived) or 0.0 (died)). The solid black line in (B) indicates intercept = 0 and slope = 1; any point above this line indicates growth, anything below indicates shrinkage. Because the biomass removal treatment was in the best-fit models for survival (A) and growth variance (C), predictions shown here are for the control level of this treatment.

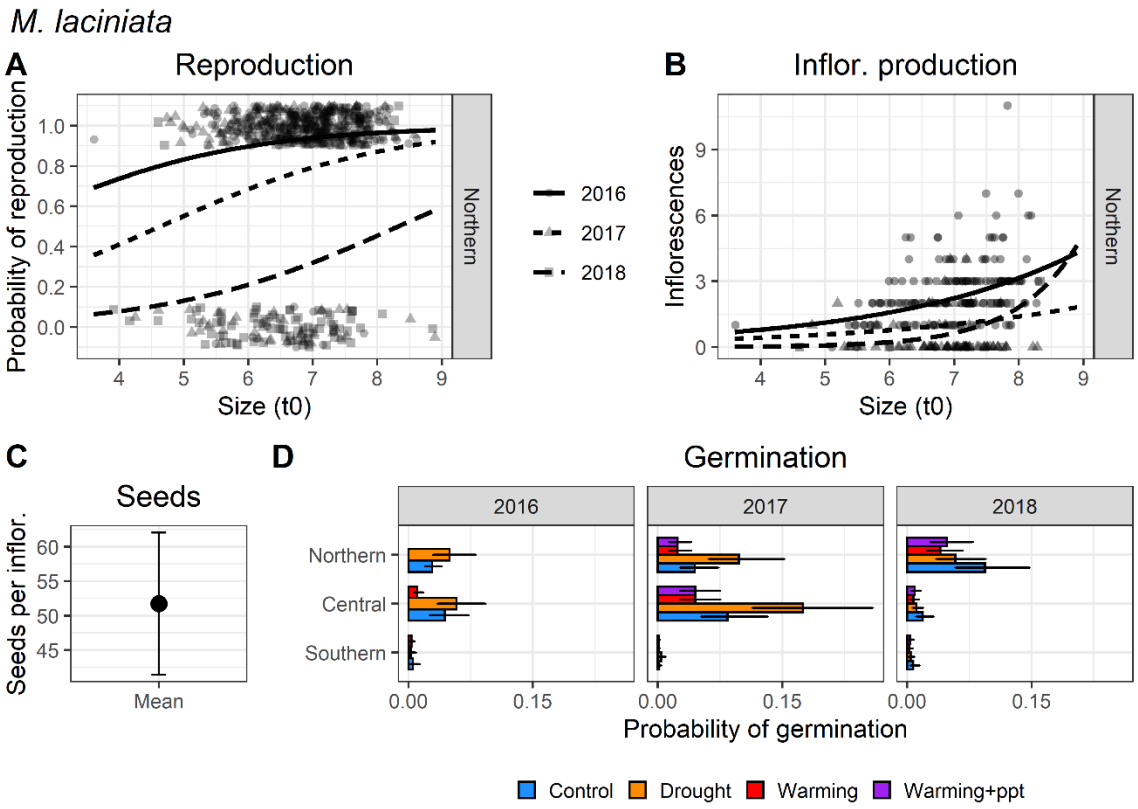

Figure S3.9. Model predictions based on the best-fit models (Table S3) for *M. laciniata* fecundity vital rates (reproduction (A), inflorescence production (B), seeds per inflorescence (C), and germination (D); estimated marginal means ± 95% confidence intervals for (C) and (D)). For reproduction, the Southern and Central sites were not included in the model due to no data (Southern site) and a constant response (no adults flowered; Central site). For inflorescence production, neither the Southern nor Central sites had data. The probability of reproducing (A) and inflorescence production (B) are depicted against plant size at time *t*0 (year). Reproduction and inflorescence production show true datapoints in the background (reproduction datapoints are jittered around 1.0 (flowering) or 0.0 (not flowering)). 2016 germination was modeled separately from 2017/2018 since not all climate treatments were initiated yet at the sites (see methods) and since 2016 germination was unnecessary for building the IPMs. Because the biomass removal treatment was in the best-fit models for reproduction, inflorescence production, and 2017/2018 germination, predictions shown here are for the control level of this treatment.

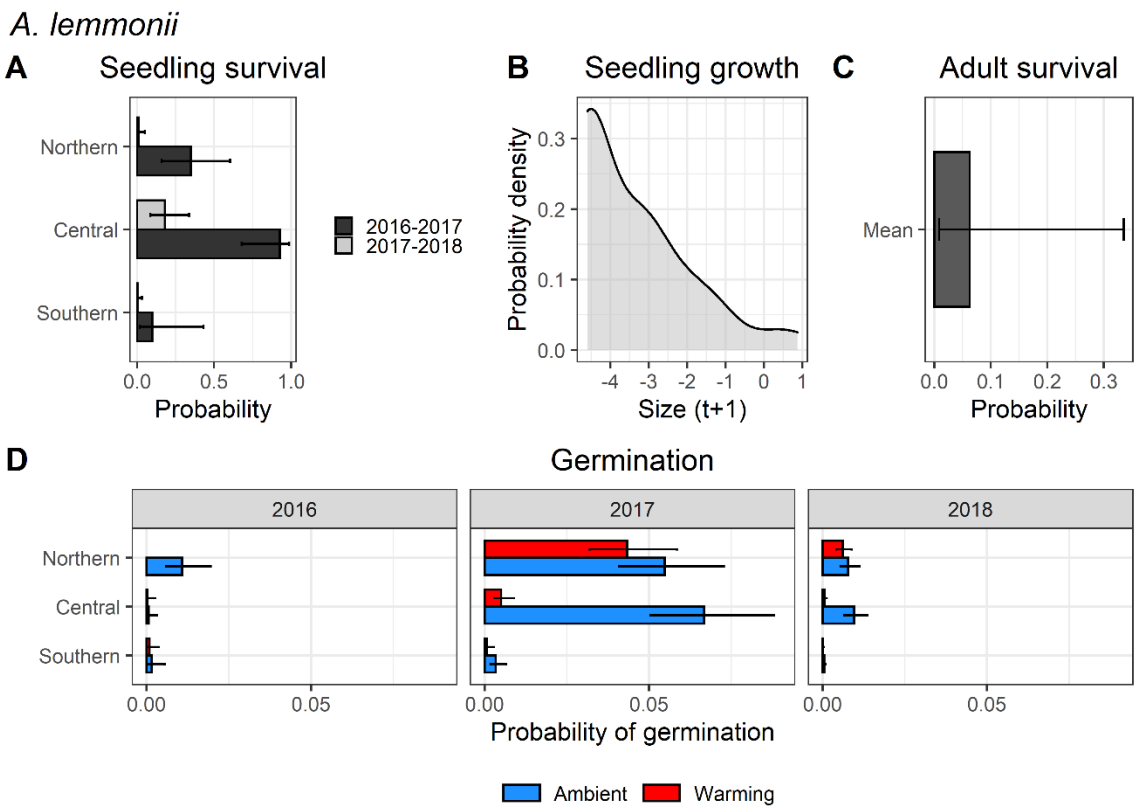

Figure S3.10. Model predictions based on the best-fit models (Table S3) for all measurable vital rates for *Achnatherum lemmonii*: seeding survival (A), seedling growth (B), adult survival (C), and germination (D). Seedling survival (A), adult survival (C), and germination (D) depict estimated marginal means ± 95% confidence intervals. Seedling growth (B) depicts the probability density function of seedling size distribution at time *t*+1 (the second year of the transition) across all data, as supported by the best-fit model for seedling growth. For adult survival, the Central site was not included due to no data. 2016 germination was modeled separately from 2017/2018 since not all climate treatments were initiated yet at the sites (see methods) and since 2016 germination was unnecessary for building the IPMs. Because the biomass removal treatment was in the best-fit models for seedling survival and 2017/2018 germination, predictions shown here are for the control level of this treatment.

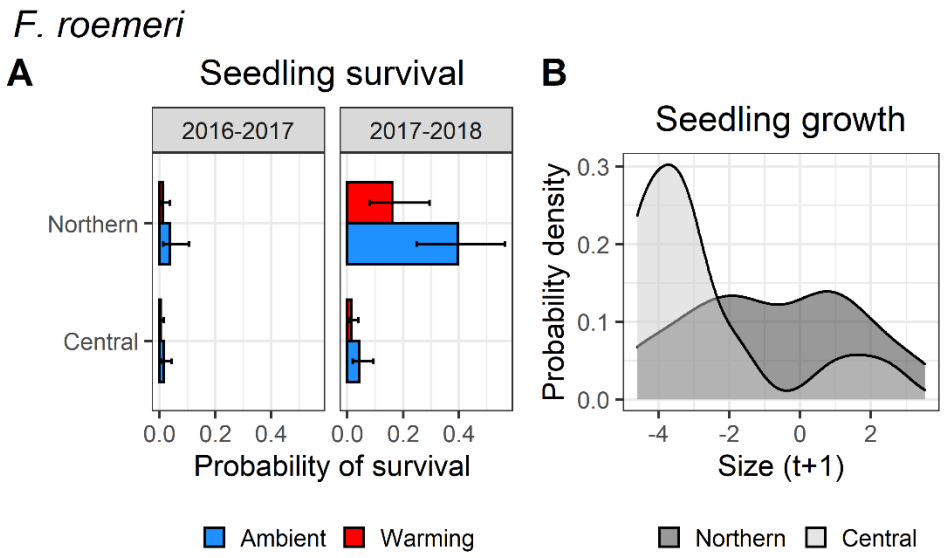

Figure S3.11. *Festuca roemeri* seedling survival (A) and growth (B). (A) depicts model predictions (estimated marginal means ± 95% confidence intervals) for the best-fit model of seedling survival at the Central and Northern sites (Table S3). The Southern site was not included in the model due to a constant response (no seedlings survived). Because the biomass removal treatment was in the best-fit model, predictions shown here are for the control level of this treatment. (B) depicts the probability density function of seedling size distribution at time *t*+1 (the second year of the transition) at the Central and Northern sites, as supported by the best-fit model for seedling growth (Table S3). The Southern sites was not included in the model due to no data.

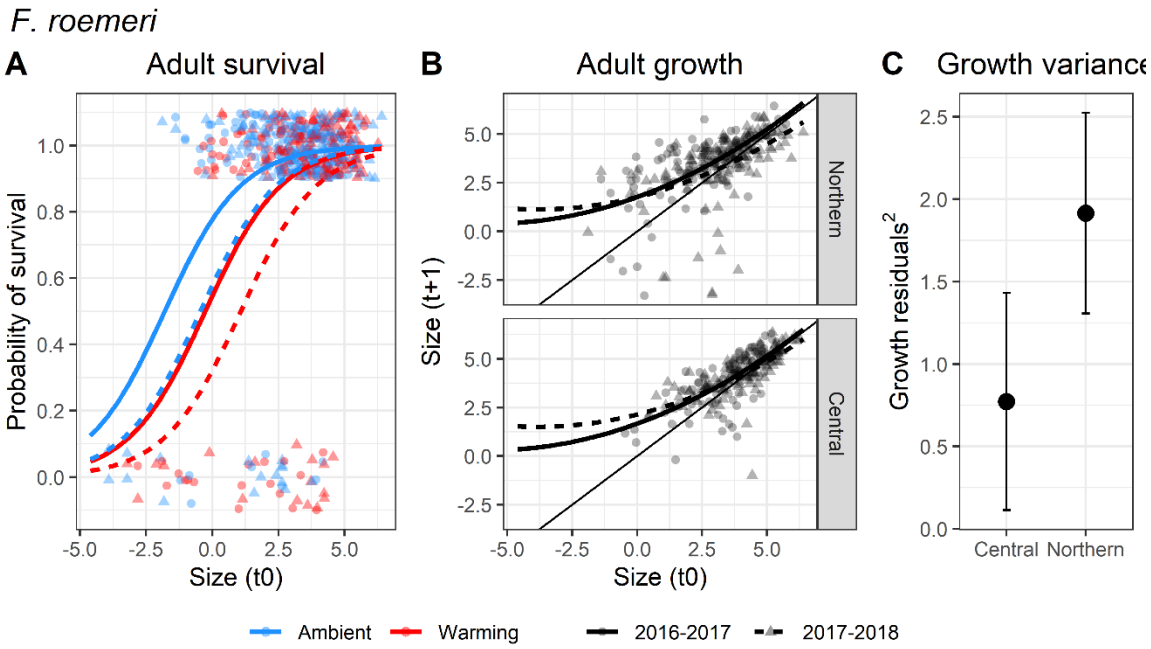

Figure S3.12. Model predictions based on the best-fit models (Table S3) for *Festuca roemeri* adult survival (A), growth (B), and variance in growth (C; estimated marginal means ± 95% confidence intervals). The Southern site was not included in any model due to no data. The best-fit model for adult survival did not include the site term so this data is pooled across both the Central and Northern sites. Survival is depicted against plant size at time *t*0 (the first year of the transition), growth is plant size at time *t*+1 (the second year of the transition) against plant size at time *t*0, and growth variance is the squared-residuals of the growth model against the best-fit set of parameters. Survival and growth show true datapoints in the background (survival datapoints are jittered around 1.0 (survived) or 0.0 (died)). The solid black line in (B) indicates intercept = 0 and slope = 1; any point above this line indicates growth, anything below indicates shrinkage. Because the biomass removal treatment was in the best-fit models for survival, predictions shown here are for the control level of this treatment.

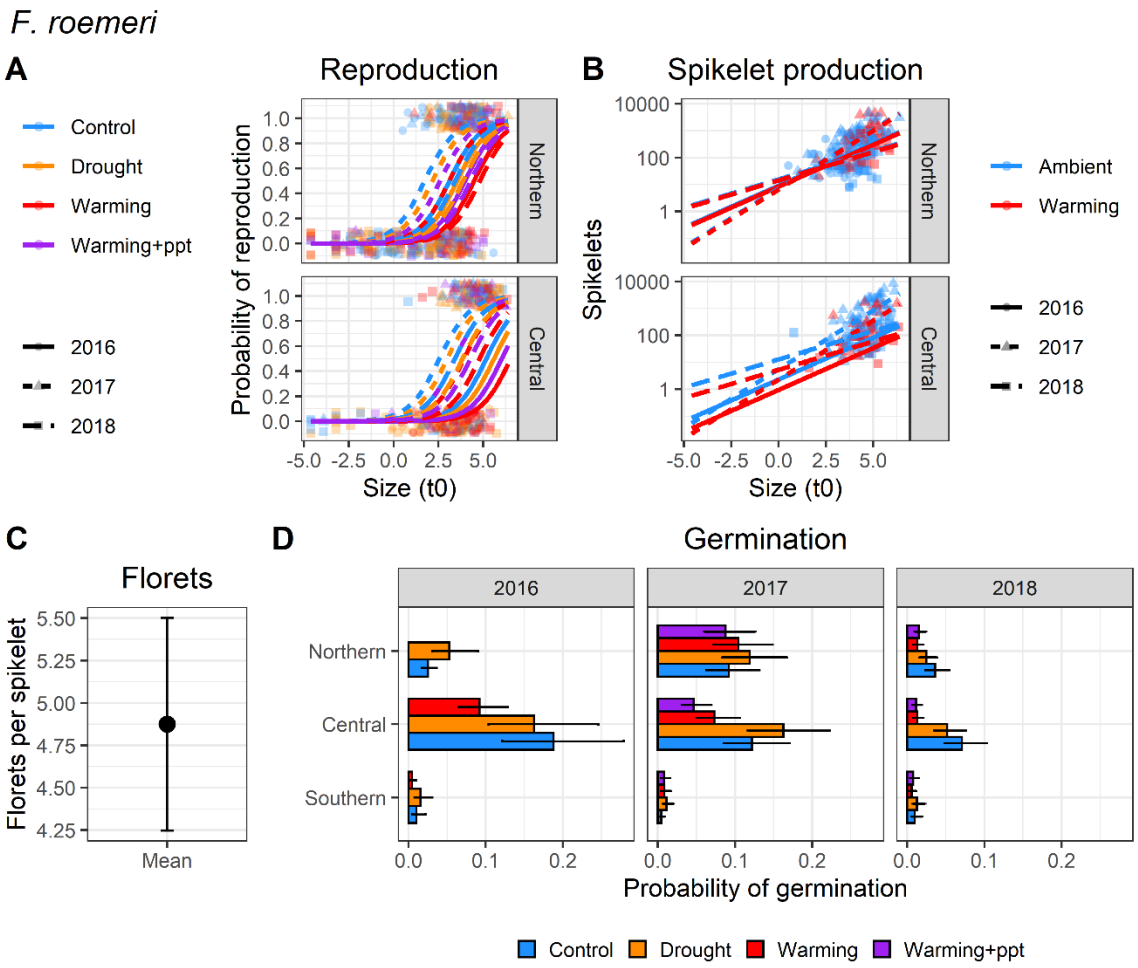

Figure S3.13. Model predictions based on the best-fit models (Table S3) for *F. roemeri* fecundity vital rates (reproduction (A), spikelet production (B), florets per spikelet (C), and germination (D); estimated marginal means ± 95% confidence intervals for (C) and (D)). For reproduction and spikelet production, the Southern site was not included in the models due to no data. The probability of reproducing (A) and spikelet production (B) are depicted against plant size at time *t*0 (year). Reproduction and spikelet production show true datapoints in the background (reproduction datapoints are jittered around 1.0 (flowering) or 0.0 (not flowering)). 2016 germination was modeled separately from 2017/2018 since not all climate treatments were initiated yet at the sites (see methods) and since 2016 germination was unnecessary for building the IPMs. Because the biomass removal treatment was in the best-fit model for 2017/2018 germination, predictions shown here are for the control level of this treatment.

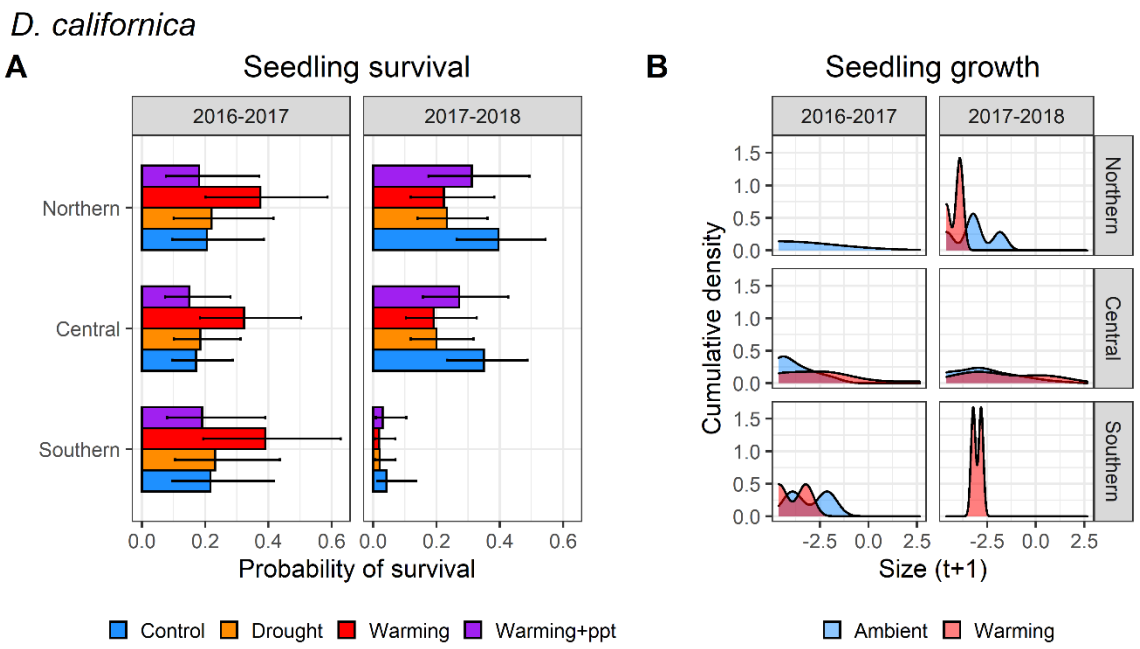

Figure S3.14. *Danthonia californica* seedling survival (A) and growth (B). (A) depicts model predictions (estimated marginal means ± 95% confidence intervals) for the best-fit model of seedling survival (Table S3). (B) depicts the probability density functions of seedling size distributions at time *t*+1 (the second year of the transition) for the control level of the biomass removal treatment under all other parameters supported by the best-fit model for seedling growth (Table S3).

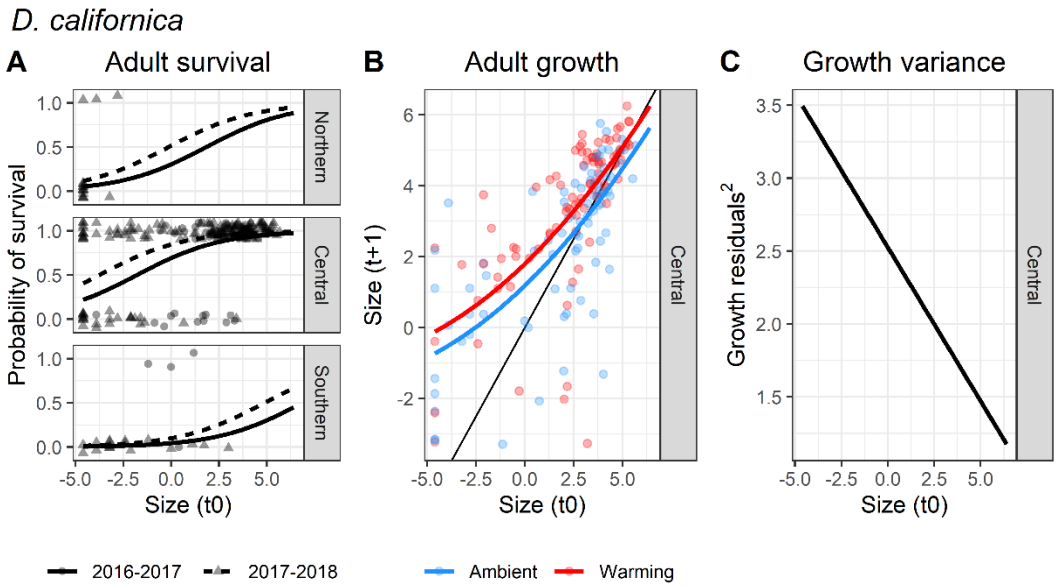

Figure S3.15. Model predictions based on the best-fit models (Table S3) for *Danthonia californica* adult survival (A), growth (B), and variance in growth (C; estimated marginal means ± 95% confidence intervals). For growth and growth variance, the Southern and Northern sites were not included in the models due to insufficient data. Adult survival is depicted against plant size at time *t*0 (the first year of the transition), growth is plant size at time *t*+1 (the second year of the transition) against plant size at time *t*0, and growth variance is the squared-residuals of the growth model also against plant size at time *t*0. Survival and growth show true datapoints in the background (survival datapoints are jittered around 1.0 (survived) or 0.0 (died)). The solid black line in (B) indicates intercept = 0 and slope = 1; any point above this line indicates growth, anything below indicates shrinkage.

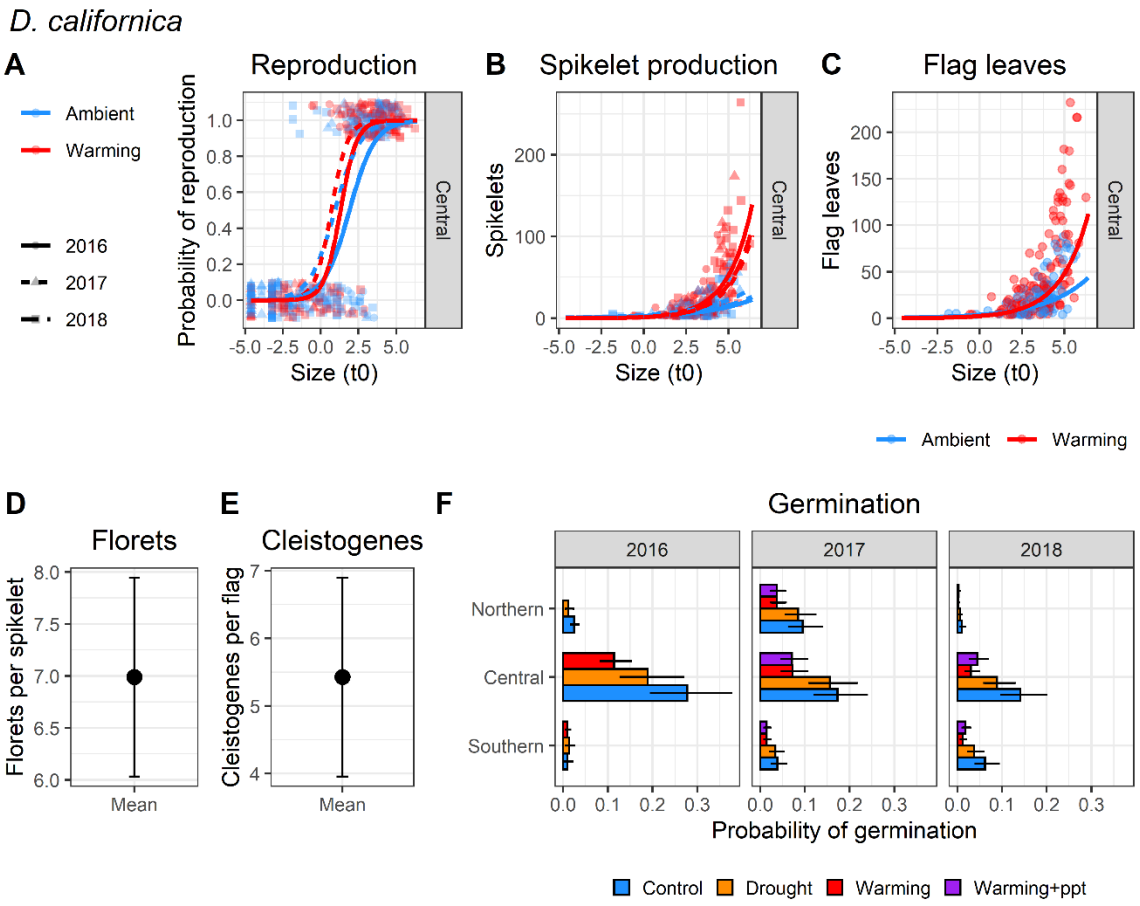

Figure S3.16. Model predictions based on the best-fit models (Table S3) for *Danthonia californica* fecundity vital rates (reproduction (A), spikelet production (B), flag leaves (C), florets per spikelet (D), cleistogenes per flag leaf (E), and germination (F); estimated marginal means ± 95% confidence intervals for (D), (E), and (F)). For reproduction, the Southern and Northern sites were not included in the models due to a constant response (no adults flowered). For spikelet production and flag leaves, the Southern and Northern sites were not included due to no data. The probability of reproducing (A), spikelet production (B), and flag leaves (C) are depicted against plant size at time *t*0 (year) and show true datapoints in the background (reproduction datapoints are jittered around 1.0 (flowering) or 0.0 (not flowering)). 2016 germination was modeled separately from 2017/2018 since not all climate treatments were initiated yet at the sites (see methods) and since 2016 germination was unnecessary for building the IPMs. Because the biomass removal treatment was in the best-fit model for 2017/2018 germination, predictions shown here are for the control level of this treatment.

Supplemental Tables

Table S3.1: The 29 native species, their seed sources, and seeding quantities used in broadcast-seeding of plots in January 2015 to establish similar starting communities. FBP = Friends of Buford Park; Frosty Hollow = wild collected by Steve Erikson; SBS = Siskiyou Biosurvey collected by Greg Carey and crew; WC = wild collected. Seeding dates: Southern = 1/23-24/2015; Central = 1/25/2015; Northern = 1/19/2015.

Species	Southern source	Southern quantity per plot	Central source	Central quantity per plot	Northern source	Northern quantity per plot
Achillea millefolium L.	SBS WC	0.3g	FBP nursery	0.5g	Frosty Hollow WC	0.8g
Achnatherum lemmonii (Vasey) Barkworth ssp. *lemmonii*	2010 experiment leftover	1.5g	FBP nursery	1.5g	City of Eugene nursery	1.5g
Achyrachaena mollis Schauer	WC Whetstone	0.75g	WC Whetstone	0.75g	WC Whetstone	0.75g
Acmispon americanus (Nutt.) Rydb.	SBS WC	0.3g	FBP nursery	0.3g	FBP nursery	0.3g
Acmispon parviflorus (Benth.) D.D.Sokoloff	SBS WC	0.5g	FBP nursery	0.5g	Frosty Hollow WC	0.5g
Agoseris grandiflora (Nuttall) Greene	SBS WC	0.07g	FBP nursery	0.07g	Ft. Lewis nursery	0.07g
Brodiaea coronaria (Salisb.) Engl. ssp. *coronaria*	SBS WC	0.08g	FBP nursery	0.12g	CNLM nursery	0.12g
Camassia quamash (Pursh) Greene ssp. *maxima* Gould	SBS WC	0.5g	FBP nursery/Heritage Seedlings mix	0.5g	Frosty Hollow WC	0.5g
Clarkia purpurea (Curtis) A. Nelson & J.F. Macbr.	SBS WC	0.3g	City of Eugene nursery	0.5g	City of Eugene nursery	0.5g
Collinsia grandiflora Lindl.	SBS WC	2g	Heritage Seedlings	2g	Heritage Seedlings	2g
Danthonia californica Bolander var. *americana* (Scribner) A.S. Hitchc.	SBS WC	4g w/ chaff	FBP nursery	2.2g	Frosty Hollow WC	2.2g
Daucus pusillus Michaux	SBS WC	0.05g	Spencer Butte WC	0.04g	Frosty Hollow WC	0.04g
Dichelostemma congestum (Sm.) Kunth	SBS WC	0.4g	FBP nursery/Heritage Seedlings mix	0.8g	Heritage Seedlings	0.8g
Drymocallis glandulosa Lindl. Rydb. var. *glandulosa*	SBS WC	0.6g	FBP nursery	0.6g	Frosty Hollow WC	0.6g
Eriophyllum lanatum (Pursh) J. Forbes var. *leucophyllum* (DC) W.R. Carter)	SBS WC	0.6g	FBP WC	0.6g	Frosty Hollow WC	0.6g
Festuca roemeri Y.V. Alexeev	SBS WC	1.5g w/ chaff	FBP nursery	0.8g	CNLM nursery	0.4g
Juncus occidentalis (tenuis)	SBS WC	0.5g	FBP nursery	0.5g	CNLM/Frosty Hollow mix	0.5g
Koeleria macrantha (Ledeb.) Schult.	SBS WC	0.6g	FBP nursery	0.6g	Frosty Hollow WC	0.6g
Lomatium nudicaule (Pursh) J.M. Coult. & Rose	SBS WC	1g	FBP nursery/Heritage Seedlings mix	0.7g	Heritage Seedlings	1g
Lomatium utriculatum (Nuttall) J.M. Coult. & Rose	SBS WC	0.15g	FBP nursery	0.15g	Frosty Hollow WC	0.15g
Lupinus bicolor Lindl. ssp. *bicolor*	SBS WC	0.5g	FBP nursery	0.15g	Frosty Hollow WC	0.15g
Microseris laciniata (Hook.) Sch. Bip. ssp. *laciniata*	SBS WC	2.5g w/ chaff	FBP WC	0.85g (clean)	CNLM nursery	0.85g (clean)
Plectritis congesta (Lindl.) DC. var. *congesta*	SBS WC	0.15g	FBP WC	0.15g	Frosty Hollow WC	0.15g
Prunella vulgaris L. var. *lanceolata* (W.P.C. Barton) Fernald	SBS WC	0.7g	City of Eugene/FBP mix	0.8g	Frosty Hollow WC	0.8g
Ranunculus austro-oreganus L.D. Benson	WC Table Rocks	1.1g	WC Table Rocks	1.1g	WC Table Rocks	1.1g
Sidalcea malviflora (DC.) A. Gray ex Benth. ssp. *virgata* (Howell) C.L. Hitchc.	City of Eugene nursery	5.15g	City of Eugene nursery	5.15g	City of Eugene nursery	5.15g
Thysanocarpus radians Benth.	WC Table Rocks	0.9g	WC Table Rocks	0.9g	WC Table Rocks	0.9g
Toxicoscordion venenosum (S.Watson) Rydb. *var. venenosum*	SBS WC	0.2g	FBP nursery	0.2g	Frosty Hollow WC	0.1g
Triteleia hyacinthina (Lindl.) Greene	SBS WC	0.04g	FBP nursery	0.04g	FBP nursery	0.04g

Table S3.2: The six focal species' seed sources used for seeding into germination rings in fall 2015, 2016, and 2017. *Variety roemeri Yu. E. Alexeev at the central and northern sites; variety Klamathensis B.L. Wilson at the southern site. SBS = Siskiyou BioSurvey; FBP = Friends of Buford Park; HS = Heritage Seedlings; CNLM = Center for Natural Lands Management.

Species	Year	Southern source	Central source	Northern source
Ranunculus austro-oreganus L.D. Benson	2015	SBS (Eagle Point, OR)	SBS (Eagle Point, OR)	SBS (Eagle Point, OR)
	2016			
	2017			
Sidalcea malviflora (DC.) A. Gray ex Benth. ssp. *virgata* (Howell) C.L.	2015	FBP (Eugene, OR)	FBP (Eugene, OR)	FBP (Eugene, OR)
	2016			
	2017			
Microseris laciniata (Hook.) Sch. Bip.	2015	SBS (Eagle Point, OR)	FBP (Eugene, OR)	CNLM (Olympia, WA)
	2016			
	2017			
Achnatherum lemmonii (Vasey) Barkworth var. *lemmonii*	2015	SBS (Eagle Point, OR)	FBP (Eugene, OR)	HS (Salem, OR)
	2016			FBP (Eugene, OR)
	2017			HS (Salem, OR)
Festuca roemeri *	2015	SBS (Eagle Point, OR)	FBP (Eugene, OR)	CNLM (Olympia, WA)
	2016			
	2017			
Danthonia californica Bol.	2015	SBS (Eagle Point, OR)	FBP (Eugene, OR)	CNLM (Olympia, WA)
	2016			
	2017			

Table S3.3: Best-fit vital rate models for the six focal species. For each species and most vital rates (see Notes for exceptions), two best-supported models were selected via 'dredging' based on AICc (one from a climate treatment-based global model and the other from a warming treatment-based global model as described in the methods). The best-fit model shown below is the model with the lower AICc between the two best-supported models. For adult growth, μ is the mean and σ^2 is the variance. We modeled 2016 germination separately from 2017/2018 since not all climate treatments were initiated yet at the sites (see methods) and since 2016 germination was not used in the IPMs. For consistency, we fit adult growth variance (σ^2) and 2016 germination using only one global model based on whether the climate or warming treatment was in the best-fit model for adult growth (μ) and 2017/2018 germination, respectively. N is the sample size for each species and vital rate used in model-fitting. δAICc = difference in AICc between best supported climate and warming treatment models. R^2_m and R^2_c = marginal and conditional R^2 values, respectively, for mixed models. * indicates an interaction with main effects also included in the model. BmsTrt = biomass removal treatment. See Table S5 for best-fit model coefficients. **Notes:**

[1] Climate and warming treatment global models reduce to same best-supported model.

[2] Only used climate treatment-based global model.

[3] Natural population data; no climate or warming treatment variable.

[4] Only used warming treatment-based global model.

Vital rate	N	Best-fit model	R^2_m	R^2_c	δAICc	Notes
Ranunculus austro-oreganus						
Seedling survival	1052	Site + Climate + Year + BmsTrt	0.244	0.357	4.4	
Seedling growth	77	Intercept-only	0.000	0.179		[1]
Adult survival	310	Year*Warming + Size	0.425	0.425	2.4	
Adult growth	93	μ: Climate*Year + Size	0.250	0.250	2.0	
		σ^2: Year + BmsTrt	0.100	0.225		[2]
Reproduction	393	Year*Size + Site + Warming	0.493	0.517	0.2	
Flower production	201	Climate*Size + Site + Year	0.624	0.729	8.7	
Seed set	132	Intercept-only	0.000	0.547		[3]
Germination (2017/2018)	24,000	Site*Year + Site*Climate + Climate*Year + Site*BmsTrt	0.397	0.407	4.1	
Germination (2016)	9,000	Site*Climate	0.135	0.159		[2]
Sidalcea malviflora ssp. virgata						
Seedling survival	2049	Site*Year + Site*Warming + BmsTrt	0.106	0.164	5.7	
Seedling growth	555	Site*Year + Site*Warming + BmsTrt	0.303	0.337	2.9	
Adult survival	1684	Site*Year + Size*Year + BmsTrt	0.252	0.333		[1]
Adult growth	1425	μ: Site*Size + Site*Year + Site*Warming + Year*Size + Warming*Year	0.618	0.629	6.5	
		σ^2: Site*Size + Site*Year + Size*Warming + $Size^2$ + BmsTrt	0.073	0.094		[4]

Vital rate	N	Best-fit model	R^2_m	R^2_c	δAICc	Notes
Sidalcea malviflora ssp. virgata						
Reproduction	2824	Site*Climate + Site*Year + Size	0.833	0.836	2.7	
Flower production	1513	Site*Size + Site*Year + Site*Warming + Year*Size	0.645	0.661	2.0	
Fruit set	136	Site	0.123	0.396		[3]
Seed set	740	Site	0.170	0.440		[1]
Germination (2017/2018)	24,000	Site*Year + Site*BmsTrt + Climate*Year	0.091	0.117	6.6	
Germination (2016)	12,000	Site*Climate	0.053	0.053		[2]
Microseris laciniata						
Seedling survival	246	Intercept-only	0.000	0.532		[1]; Southern not in model (constant response)
Seedling growth	16	Intercept-only	0.000	0.819		[1]; Southern not in model (no data)
Adult survival	526	Warming*Year + Size + BmsTrt	0.283	0.340	0.4	Southern (no data) and Central (constant response) not in model
Adult growth	260	μ: Warming + Size	0.224	0.224	4.0	Southern and Central not in model (no data)
		σ^2: Year + Warming + BmsTrt	0.062	0.062		[4]; Southern and Central not in model (no data)
Reproduction	647	Year + Size + BmsTrt	0.372	0.391		[1]; Southern (no data) and Central (constant response) not in model
Inflorescence production	517	Year*Size + BmsTrt	0.373	0.396		Southern and Central not in model (no data)
Seed set	15	Intercept-only				[3]; non-mixed model
Germination (2017/2018)	24,000	Site*Year + Climate*Year + Site*BmsTrt	0.479	0.548	45.5	
Germination (2016)	12,000	Site*Climate	0.249	0.310		[2]
Achnatherum lemmonii						
Seedling survival	197	Site + Year + BmsTrt	0.397	0.458		[1]
Seedling growth	40	Intercept-only	0.000	0.616		[1]
Adult survival	16	Intercept-only				Central not in model (no data); non-mixed model
Adult growth	1					Not modeled (insufficient data)
Reproduction	55					Not modeled (constant response)
Germination (2017/2018)	27,000	Site*Warming + Year + BmsTrt	0.541	0.560	10.0	
Germination (2016)	12,000	Site*Warming	0.302	0.483		[4]

Vital rate	N	Best-fit model	R^2_m	R^2_c	δAICc	Notes
Festuca roemeri						
Seedling survival	719	Site*Year + Warming + BmsTrt	0.404	0.467	3.4	Southern not in model (constant response)
Seedling growth	91	Site	0.125	0.333		[1]; Southern not in model (no data)
Adult survival	499	Warming + Year + Size + BmsTrt	0.332	0.439	3.6	Southern not in model (no data)
Adult growth	440	μ: Site*Year + Year*Size + $Size^2$	0.427	0.428		[1]; Southern not in model (no data)
		σ^2: Site	0.067	0.069		[1]; Southern not in model (no data)
Reproduction	817	Site*Year + Climate + Size	0.715	0.733	0.3	Southern not in model (no data)
Spikelet production	321	Site*Year + Site*Warming + Year*Size	0.494	0.517	6.5	Southern not in model (no data)
Florets per spikelet	68	Intercept-only	0.000	0.307		[3]
Germination (2017/2018)	24,000	Site*Climate + Site*Year + Climate*Year + Site*BmsTrt	0.337	0.368	8.1	
Germination (2016)	12,000	Site*Climate	0.313	0.372		[2]
Danthonia californica						
Seedling survival	947	Site*Year + Climate*Year	0.159	0.252	2.8	
Seedling growth	231	Site + Year + Warming + BmsTrt	0.269	0.431	2.9	
Adult survival	244	Site + Year + Size	0.449	0.657		[1]
Adult growth	172	μ: Warming + Size + $Size^2$	0.531	0.567	0.3	Southern and Northern not in model (no data)
		σ^2: Size	0.018	0.121		[1]
Reproduction	433	Warming*Size + Year	0.832	0.881	1.0	Southern and Northern not in model (constant responses)
Spikelet production	210	Year*Warming + Warming*Size	0.513	0.632	3.1	Southern and Northern not in model (no data)
Flag-leaf production	210	Warming*Size	0.485	0.621	0.8	Southern and Northern not in model (no data)
Florets per spikelet	180	Intercept-only	0.000	0.686		[3]
Cleistogamous seeds per flag leaf	420	Intercept-only	0.000	0.376		[3]
Germination (2017/2018)	24,000	Site*Year + Site*Climate + Site*BmsTrt	0.277	0.348	4.5	
Germination (2016)	12,000	Site*Climate	0.326	0.372		[2]

Table S3.4. Estimated population growth rates (λ) with 95% confidence limits (λ LCL = lower confidence limit; λ UCL = upper confidence limit) calculated by resampling the coefficients of each vital rate function 1000 times using their means and covariance matrices and recalculating λ for each bootstrap replicate. We tested for statistical significance of a treatment effect on λ relative to controls by calculating the differences in λ between the treatment and control (λtreatment - λcontrol) for each of the 1000 resamples and then calculating 95% confidence limits in those differences (Δλ LCL, Δλ UCL). A treatment has a significant effect on λ if the Δλ confidence limits do not overlap zero, as indicated by *.

Species	Annual Transition	Site	Climate treatment	λ	λ LCL	λ UCL	$\lambda_{treatment} - \lambda_{control}$	Δλ LCL	Δλ UCL	
R. austro-oreganus	2017-2018	Northern	Control	0.114	0.079	0.173				
R. austro-oreganus	2017-2018	Northern	Drought	0.251	0.181	0.365	0.137	0.067	0.227	*
R. austro-oreganus	2017-2018	Northern	Warming	0.141	0.103	0.193	0.027	-0.031	0.079	
R. austro-oreganus	2017-2018	Northern	Warming+ppt	0.159	0.118	0.212	0.045	-0.021	0.100	
R. austro-oreganus	2017-2018	Central	Control	0.084	0.053	0.130				
R. austro-oreganus	2017-2018	Central	Drought	0.197	0.127	0.293	0.113	0.057	0.191	*
R. austro-oreganus	2017-2018	Central	Warming	0.080	0.057	0.113	-0.004	-0.044	0.024	
R. austro-oreganus	2017-2018	Central	Warming+ppt	0.110	0.070	0.157	0.026	-0.015	0.062	
R. austro-oreganus	2017-2018	Southern	Control	0.026	0.011	0.072				
R. austro-oreganus	2017-2018	Southern	Drought	0.042	0.015	0.187	0.016	-0.001	0.126	
R. austro-oreganus	2017-2018	Southern	Warming	0.025	0.012	0.072	-0.001	-0.032	0.018	
R. austro-oreganus	2017-2018	Southern	Warming+ppt	0.017	0.007	0.042	-0.009	-0.053	0.003	
R. austro-oreganus	2016-2017	Northern	Control	0.252	0.182	0.334				
R. austro-oreganus	2016-2017	Northern	Drought	0.656	0.501	0.847	0.405	0.252	0.577	*
R. austro-oreganus	2016-2017	Northern	Warming	0.428	0.319	0.569	0.176	0.057	0.318	*
R. austro-oreganus	2016-2017	Northern	Warming+ppt	0.451	0.324	0.609	0.200	0.068	0.354	*
R. austro-oreganus	2016-2017	Central	Control	0.153	0.103	0.220				
R. austro-oreganus	2016-2017	Central	Drought	0.416	0.288	0.600	0.263	0.163	0.420	*
R. austro-oreganus	2016-2017	Central	Warming	0.190	0.142	0.256	0.037	-0.021	0.089	
R. austro-oreganus	2016-2017	Central	Warming+ppt	0.232	0.162	0.320	0.079	0.021	0.152	*
R. austro-oreganus	2016-2017	Southern	Control	0.029	0.011	0.101				
R. austro-oreganus	2016-2017	Southern	Drought	0.073	0.023	0.340	0.044	0.008	0.262	*
R. austro-oreganus	2016-2017	Southern	Warming	0.033	0.014	0.095	0.004	-0.055	0.032	
R. austro-oreganus	2016-2017	Southern	Warming+ppt	0.023	0.009	0.080	-0.006	-0.080	0.013	
S. malviflora	2017-2018	Northern	Control	1.687	1.552	1.849				
S. malviflora	2017-2018	Northern	Drought	1.721	1.580	1.882	0.034	-0.062	0.109	
S. malviflora	2017-2018	Northern	Warming	2.202	2.018	2.413	0.515	0.335	0.686	*
S. malviflora	2017-2018	Northern	Warming+ppt	2.254	2.058	2.460	0.567	0.378	0.755	*

Species	Annual Transition	Site	Climate treatment	λ	λ LCL	λ UCL	$\lambda_{treatment} - \lambda_{control}$	Δλ LCL	Δλ UCL	
S. malviflora	2017-2018	Central	Control	1.522	1.325	1.763				
S. malviflora	2017-2018	Central	Drought	1.540	1.343	1.789	0.018	-0.045	0.074	
S. malviflora	2017-2018	Central	Warming	1.464	1.335	1.648	-0.057	-0.258	0.167	
S. malviflora	2017-2018	Central	Warming+ppt	1.483	1.347	1.674	-0.039	-0.233	0.185	
S. malviflora	2017-2018	Southern	Control	2.118	1.854	2.419				
S. malviflora	2017-2018	Southern	Drought	2.178	1.923	2.475	0.060	-0.118	0.187	
S. malviflora	2017-2018	Southern	Warming	1.356	1.229	1.502	-0.761	-1.024	-0.483	*
S. malviflora	2017-2018	Southern	Warming+ppt	1.373	1.232	1.521	-0.744	-0.998	-0.472	*
S. malviflora	2016-2017	Northern	Control	1.903	1.763	2.075				
S. malviflora	2016-2017	Northern	Drought	2.099	1.929	2.276	0.196	0.090	0.294	*
S. malviflora	2016-2017	Northern	Warming	2.639	2.348	2.984	0.736	0.476	1.024	*
S. malviflora	2016-2017	Northern	Warming+ppt	2.612	2.327	2.925	0.709	0.474	0.996	*
S. malviflora	2016-2017	Central	Control	1.586	1.250	1.998				
S. malviflora	2016-2017	Central	Drought	1.715	1.339	2.206	0.129	0.012	0.256	*
S. malviflora	2016-2017	Central	Warming	1.295	1.028	1.622	-0.291	-0.586	-0.020	*
S. malviflora	2016-2017	Central	Warming+ppt	1.277	1.014	1.585	-0.309	-0.608	-0.035	*
S. malviflora	2016-2017	Southern	Control	2.345	2.021	2.727				
S. malviflora	2016-2017	Southern	Drought	2.651	2.281	3.074	0.306	0.153	0.461	*
S. malviflora	2016-2017	Southern	Warming	1.652	1.372	2.033	-0.694	-1.060	-0.362	*
S. malviflora	2016-2017	Southern	Warming+ppt	1.692	1.408	2.076	-0.653	-1.035	-0.334	*
M. laciniata	2017-2018	Northern	Control	0.517	0.401	0.650				
M. laciniata	2017-2018	Northern	Drought	0.485	0.366	0.617	-0.032	-0.084	0.003	
M. laciniata	2017-2018	Northern	Warming	0.216	0.155	0.299	-0.301	-0.449	-0.179	*
M. laciniata	2017-2018	Northern	Warming+ppt	0.228	0.165	0.305	-0.289	-0.429	-0.171	*
M. laciniata	2016-2017	Northern	Control	0.814	0.668	0.930				
M. laciniata	2016-2017	Northern	Drought	0.901	0.735	1.028	0.087	0.027	0.168	*
M. laciniata	2016-2017	Northern	Warming	0.304	0.230	0.401	-0.510	-0.641	-0.371	*
M. laciniata	2016-2017	Northern	Warming+ppt	0.304	0.234	0.403	-0.510	-0.642	-0.372	*
F. roemeri	2017-2018	Northern	Control	2.646	2.192	3.193				
F. roemeri	2017-2018	Northern	Drought	2.335	1.928	2.785	-0.311	-0.733	0.081	
F. roemeri	2017-2018	Northern	Warming	1.348	1.101	1.622	-1.298	-1.863	-0.896	*
F. roemeri	2017-2018	Northern	Warming+ppt	1.420	1.184	1.712	-1.226	-1.788	-0.829	*
F. roemeri	2017-2018	Central	Control	1.453	1.269	1.732				
F. roemeri	2017-2018	Central	Drought	1.371	1.195	1.601	-0.082	-0.212	0.029	
F. roemeri	2017-2018	Central	Warming	0.922	0.819	0.993	-0.531	-0.778	-0.341	*
F. roemeri	2017-2018	Central	Warming+ppt	0.922	0.821	0.990	-0.532	-0.780	-0.342	*
F. roemeri	2016-2017	Northern	Control	1.559	1.377	1.796				
F. roemeri	2016-2017	Northern	Drought	1.612	1.413	1.869	0.052	-0.097	0.219	
F. roemeri	2016-2017	Northern	Warming	1.167	1.038	1.318	-0.392	-0.581	-0.249	*
F. roemeri	2016-2017	Northern	Warming+ppt	1.162	1.035	1.326	-0.397	-0.576	-0.245	*
F. roemeri	2016-2017	Central	Control	1.073	1.009	1.156				
F. roemeri	2016-2017	Central	Drought	1.078	1.011	1.165	0.004	-0.024	0.042	
F. roemeri	2016-2017	Central	Warming	0.968	0.914	0.997	-0.105	-0.180	-0.051	*
F. roemeri	2016-2017	Central	Warming+ppt	0.968	0.913	0.997	-0.105	-0.182	-0.051	*
D. californica	2017-2018	Central	Control	1.731	1.434	2.036				
D. californica	2017-2018	Central	Drought	1.411	1.191	1.630	-0.320	-0.491	-0.167	*
D. californica	2017-2018	Central	Warming	1.383	1.217	1.572	-0.348	-0.631	-0.065	*
D. californica	2017-2018	Central	Warming+ppt	1.559	1.359	1.819	-0.171	-0.461	0.137	
D. californica	2016-2017	Central	Control	1.300	1.046	1.570				
D. californica	2016-2017	Central	Drought	1.292	1.027	1.563	-0.007	-0.103	0.085	
D. californica	2016-2017	Central	Warming	1.645	1.324	1.975	0.346	0.095	0.640	*
D. californica	2016-2017	Central	Warming+ppt	1.426	1.164	1.708	0.127	-0.109	0.361	

Table S3.5: Linear coefficients and standard errors (in parentheses) from the best-fit vital rate models (see Table S3 for best-fit model structures). Linear equations specified by the coefficients are inverse-logit transformed for binomial logistic regressions ('odds ratios') and exponentially transformed for Poisson regressions ('incidence rate ratios'). Vital rate column headers have footnotes (1, 2, 3) to specify model type (1 binomial logistic regression; 2 normal; 3 Poisson). Categorical predictor variables are listed with the factor level in brackets. Reference-level factors for each categorical predictor: BmsTrt = 'No Removal'; Climate = 'Control'; Site = 'Central'; Warming = 'Ambient'; Year = '2016' (for all rates except Germination; Year reference level = '2017' for Germination 2017/2018).

Ranunculus austro-oreganus										
Predictors	**Seedling survival** $_1$	**Seedling growth** $_2$	**Adult survival** $_1$	**Adult growth** μ_2	**Adult growth** σ^2_2	**Reproduction** $_1$	**Flower production** $_3$	**Seed set** $_3$	**Germ (17/18)** $_1$	**Germ (2016)** $_1$
(Intercept)	0.02 (0.54)	3.47 (0.11)	0.01 (1.20)	4.43 (0.60)	0.18 (0.07)	0.07 (1.65)	0.03 (0.62)	9.59 (0.10)	0.27 (0.14)	0.16 (0.17)
BmsTrt [Removal]	1.90 (0.26)				0.20 (0.08)				1.20 (0.07)	
Climate [Drought]	4.64 (0.51)			-0.08 (0.21)			10.13 (0.79)		1.06 (0.18)	0.59 (0.25)
Climate [Warming]	0.97 (0.58)			-0.03 (0.21)			14.74 (0.87)		0.59 (0.19)	0.72 (0.21)
Climate [Warming+ppt]	1.08 (0.58)			-0.49 (0.22)			111.08 (0.70)		0.63 (0.19)	
Site [Northern]	3.71 (0.43)					0.35 (0.59)	3.79 (0.29)		0.27 (0.21)	1.42 (0.20)
Site [Southern]	0.33 (1.14)					0.14 (0.94)	2.59 (0.45)		0.04 (0.33)	0.41 (0.27)
Size			2.70 (0.25)	0.10 (0.11)		2.32 (0.35)	2.15 (0.10)			
Warming [Warming]			0.82 (0.32)			1.95 (0.37)				
Year [2017]	0.48 (0.30)		0.26 (0.41)	0.23 (0.43)	0.25 (0.12)	0.03 (1.99)	1.42 (0.09)			
Year [2018]						0.00 (4.47)	1.29 (0.20)		0.44 (0.11)	
BmsTrt [Removal] * Site [Northern]									1.56 (0.12)	
BmsTrt [Removal] * Site [Southern]									1.03 (0.26)	
Climate [Drought] * Site [Northern]									1.12 (0.27)	1.97 (0.32)
Climate [Drought] * Site [Southern]									0.34 (0.41)	0.79 (0.41)
Climate [Warming] * Site [Northern]									2.05 (0.27)	
Climate [Warming] * Site [Southern]									1.04 (0.40)	0.88 (0.34)
Climate [Warming+ppt] * Site [Northern]									1.49 (0.27)	
Climate [Warming+ppt] * Site [Southern]									0.28 (0.51)	
Climate [Drought] * Size							0.62 (0.15)			
Climate [Warming] * Size							0.66 (0.17)			
Climate [Warming+ppt] * Size							0.42 (0.14)			
Climate [Drought] * Year [2017]				-0.99 (0.48)						
Climate [Drought] * Year [2018]									0.97 (0.15)	
Climate [Warming] * Year [2017]				0.65 (0.70)						
Climate [Warming] * Year [2018]									0.56 (0.18)	
Climate [Warming+ppt] * Year [2017]				-0.61 (0.59)						
Climate [Warming+ppt] * Year [2018]									1.00 (0.16)	
Site [Northern] * Year [2018]									0.60 (0.13)	
Site [Southern] * Year [2018]									4.77 (0.27)	
Size * Year [2017]						2.06 (0.43)				
Size * Year [2018]						4.52 (0.94)				
Year [2017] * Warming [Warming]			0.20 (0.75)							

Sidalcea malviflora ssp. virgata											
Predictors	**Seedling survival $_1$**	**Seedling growth $_2$**	**Adult survival $_1$**	**Adult growth μ_2**	**Adult growth σ^2_2**	**Reproduction $_1$**	**Flower production $_2$**	**Fruit set $_1$**	**Seed set $_2$**	**Germ (17/18) $_1$**	**Germ (2016) $_1$**
(Intercept)	0.56 (0.23)	3.33 (0.19)	0.63 (0.71)	2.41 (0.42)	2.30 (0.73)	0.00 (0.87)	-0.75 (0.66)	0.88 (0.29)	6.06 (0.16)	0.14 (0.12)	0.04 (0.16)
BmsTrt [Removal]	0.86 (0.10)		0.72 (0.16)		-0.17 (0.09)					1.16 (0.07)	
Climate [Drought]						1.17 (0.81)				1.59 (0.13)	0.85 (0.23)
Climate [Warming]						0.77 (0.61)				1.03 (0.14)	0.77 (0.20)
Climate [Warming+ppt]						0.55 (0.68)				0.99 (0.14)	
Site [Northern]	0.50 (0.34)	-0.82 (0.29)	2.88 (0.54)	0.96 (0.42)	0.76 (0.70)	9.45 (0.75)	-0.35 (0.60)	7.84 (0.36)	1.07 (0.19)	0.78 (0.13)	1.49 (0.18)
Site [Southern]	1.60 (0.29)	0.64 (0.23)	1.26 (0.56)	-0.33 (0.42)	1.77 (0.72)	0.90 (0.85)	-1.90 (0.64)	3.58 (0.49)	-0.15 (0.33)	0.79 (0.13)	2.01 (0.20)
Size			1.45 (0.10)	0.68 (0.06)	-0.65 (0.17)	6.75 (0.08)	0.67 (0.08)				
$Size^2$					0.06 (0.01)						
Warming [Warming]	0.56 (0.30)			-0.24 (0.23)	1.17 (0.37)		-0.75 (0.22)				
Year [2017]	0.56 (0.20)	-1.73 (0.27)	1.19 (0.77)	-0.92 (0.33)	-0.21 (0.41)	2.81 (0.75)	0.67 (0.50)				
Year [2018]						2.46 (0.72)	1.18 (0.47)			0.63 (0.11)	
BmsTrt [Removal] * Site [Northern]										1.57 (0.11)	
BmsTrt [Removal] * Site [Southern]										1.14 (0.10)	
Climate [Drought] * Site [Northern]						1.68 (0.85)					1.41 (0.28)
Climate [Drought] * Site [Southern]						2.18 (0.86)					1.63 (0.28)
Climate [Warming] * Site [Northern]						1.42 (0.71)					
Climate [Warming] * Site [Southern]						0.20 (0.73)					1.44 (0.25)
Climate [Warming+ppt] * Site [Northern]						1.79 (0.76)					
Climate [Warming+ppt] * Site [Southern]						0.50 (0.79)					
Climate [Drought] * Year [2018]										0.69 (0.12)	
Climate [Warming] * Year [2018]										0.70 (0.13)	
Climate [Warming+ppt] * Year [2018]										0.82 (0.13)	
Site [Northern] * Size				-0.16 (0.06)	-0.14 (0.10)		0.07 (0.07)				
Site [Southern] * Size				0.06 (0.06)	-0.23 (0.11)		0.34 (0.08)				
Site [Northern] * Warming [Warming]	4.13 (0.43)			0.34 (0.23)			0.90 (0.23)				
Site [Southern] * Warming [Warming]	0.89 (0.40)			-0.13 (0.25)			0.33 (0.26)				
Site [Northern] * Year [2017]	2.70 (0.30)	1.64 (0.36)	0.15 (0.61)	0.12 (0.25)	0.59 (0.43)	0.49 (0.80)	-0.30 (0.31)				
Site [Northern] * Year [2018]						0.21 (0.77)	-0.30 (0.29)			0.46 (0.12)	
Site [Southern] * Year [2017]	0.37 (0.30)	-0.49 (0.39)	0.28 (0.62)	-0.21 (0.26)	-0.20 (0.46)	1.52 (0.86)	-0.47 (0.33)				
Site [Southern] * Year [2018]						0.84 (0.83)	-0.71 (0.30)			1.32 (0.10)	
Size * Warming [Warming]					-0.16 (0.07)						
Size * Year [2017]			1.41 (0.12)	0.15 (0.04)			0.01 (0.06)				
Size * Year [2018]							-0.08 (0.05)				
Warming [Warming] * Year [2017]				0.57 (0.11)							

Microseris laciniata										
Predictors	**Seedling survival $_1$**	**Seedling growth $_2$**	**Adult survival $_1$**	**Adult growth μ_2**	**Adult growth $\sigma^2{}_2$**	**Reproduction $_1$**	**Inflorescence production $_3$**	**Seed set $_2$**	**Germ (17/18) $_1$**	**Germ (2016) $_1$**
(Intercept)	0.02 (0.83)	5.38 (0.29)	0.10 (1.06)	4.99 (0.45)	0.49 (0.08)	0.29 (1.02)	0.20 (0.38)	51.73 (4.81)	0.09 (0.26)	0.05 (0.27)
BmsTrt [Removal]			3.09 (0.22)		-0.23 (0.09)	2.01 (0.25)	1.20 (0.07)		1.30 (0.10)	
Climate [Drought]									2.32 (0.31)	1.34 (0.38)
Climate [Warming]									0.52 (0.33)	0.23 (0.38)
Climate [Warming+ppt]									0.52 (0.33)	
Site [Northern]									0.51 (0.26)	0.64 (0.32)
Site [Southern]									0.02 (0.47)	0.12 (0.55)
Size			1.61 (0.15)	0.27 (0.06)		1.77 (0.15)	1.41 (0.05)			
Warming [Warming]			0.13 (0.39)	-0.65 (0.10)	0.28 (0.10)					
Year [2017]			0.27 (0.31)		0.25 (0.09)	0.25 (0.32)	0.67 (0.81)			
Year [2018]						0.03 (0.35)	0.00 (1.99)		0.21 (0.17)	
Year [2018]										
BmsTrt [Removal] * Site [Northern]									1.31 (0.13)	
BmsTrt [Removal] * Site [Southern]									0.28 (0.41)	
Climate [Drought] * Year [2018]									0.26 (0.19)	
Climate [Warming] * Year [2018]									0.77 (0.21)	
Climate [Warming+ppt] * Year [2018]									0.94 (0.22)	
Site [Northern] * Climate [Drought]										1.33 (0.49)
Site [Southern] * Climate [Drought]										0.38 (0.87)
Site [Southern] * Climate [Warming]										2.93 (0.72)
Site [Northern] * Year [2018]									10.62 (0.17)	
Site [Southern] * Year [2018]									20.18 (0.43)	
Size * Year [2017]							0.95 (0.12)			
Size * Year [2018]							2.00 (0.27)			
Year [2017] * Warming [Warming]			2.05 (0.44)							

Achnatherum lemmonii					
Predictors	**Seedling survival $_1$**	**Seedling growth $_2$**	**Adult survival $_1$**	**Germ (17/18) $_1$**	**Germ (2016) $_1$**
(Intercept)	12.75 (0.92)	-3.32 (0.35)	0.07 (1.03)	0.07 (0.15)	0.00 (0.83)
BmsTrt [Removal]	2.86 (0.46)			1.35 (0.09)	
Site [Northern]	0.04 (0.82)			0.81 (0.20)	17.86 (0.86)
Site [Southern]	0.01 (1.35)			0.05 (0.37)	2.51 (1.00)
Warming [Warming]				0.07 (0.32)	0.50 (1.34)
Year [2017]	0.02 (0.94)				
Year [2018]				0.14 (0.12)	
Site [Northern] * Warming [Warming]				11.05 (0.38)	
Site [Southern] * Warming [Warming]				2.81 (0.85)	1.14 (1.63)

Festuca roemeri											
Predictors	**Seedling survival $_1$**	**Seedling growth $_2$**	**Adult survival $_1$**	**Adult growth μ_2**	**Adult growth σ^2_2**	**Reproduction $_1$**	**Spikelet production $_2$**	**Florets $_2$**	**Germ (17/18) $_1$**	**Germ (2016) $_1$**
(Intercept)	0.01 (0.58)	-2.73 (0.64)	3.47 (0.44)	1.67 (0.23)	0.77 (0.32)	0.00 (0.59)	0.83 (0.68)	4.87 (0.24)	0.14 (0.20)	0.23 (0.26)
BmsTrt [Removal]	1.99 (0.30)		1.67 (0.36)						2.33 (0.08)	
Climate [Drought]						0.60 (0.33)			1.40 (0.27)	0.84 (0.37)
Climate [Warming]						0.20 (0.37)			0.57 (0.28)	0.44 (0.33)
Climate [Warming+ppt]						0.36 (0.41)			0.35 (0.29)	
Site [Northern]	2.75 (0.74)	2.14 (0.75)		0.09 (0.16)	1.14 (0.43)	11.12 (0.48)	1.38 (0.38)		0.73 (0.29)	0.11 (0.33)
Site [Southern]									0.03 (0.43)	0.05 (0.47)
Size			2.00 (0.10)	0.48 (0.11)		3.23 (0.10)	0.72 (0.13)			
$Size^2$				0.04 (0.02)						
Warming [Warming]	0.29 (0.40)		0.35 (0.45)				-0.89 (0.24)			
Year [2017]	3.19 (0.58)		0.39 (0.35)	0.47 (0.34)		21.41 (0.44)	0.88 (0.79)			
Year [2018]						7.78 (0.43)	1.72 (0.86)		0.55 (0.11)	
BmsTrt [Removal] * Site [Northern]									0.69 (0.12)	
BmsTrt [Removal] * Site [Southern]									0.41 (0.25)	
Climate [Drought] * Site [Northern]									0.96 (0.39)	2.57 (0.51)
Climate [Drought] * Site [Southern]									1.81 (0.50)	1.81 (0.65)
Climate [Warming] * Site [Northern]							0.80 (0.32)		2.02 (0.39)	
Climate [Warming] * Site [Southern]									3.36 (0.53)	1.03 (0.62)
Climate [Warming+ppt] * Site [Northern]									2.71 (0.40)	
Climate [Warming+ppt] * Site [Southern]									5.11 (0.53)	
Climate [Drought] * Year [2018]									0.51 (0.15)	
Climate [Warming] * Year [2018]									0.30 (0.20)	
Climate [Warming+ppt] * Year [2018]									0.43 (0.20)	
Site [Northern] * Year [2017]	5.25 (0.78)			-0.47 (0.23)		0.24 (0.55)	-1.13 (0.42)			
Site [Northern] * Year [2018]						0.09 (0.54)	-1.18 (0.43)		0.67 (0.13)	
Site [Southern] * Year [2018]									4.05 (0.26)	
Size * Year [2017]				-0.15 (0.08)			0.29 (0.16)			
Size * Year [2018]							-0.23 (0.17)			

Danthonia californica												
Predictors	**Seedling survival $_1$**	**Seedling growth $_2$**	**Adult survival $_1$**	**Adult growth μ_2**	**Adult growth σ^2_2**	**Reproduction $_1$**	**Spikelet production $_2$**	**Flag leaf production $_2$**	**Florets $_2$**	**Cleistogs $_2$**	**Germ (17/18) $_1$**	**Germ (2016) $_1$**
(Intercept)	0.21 (0.34)	-3.77 (0.31)	2.25 (0.57)	1.18 (0.32)	2.52 (0.59)	0.10 (0.73)	0.84 (0.31)	1.30 (0.24)	6.99 (0.37)	5.43 (0.57)	0.21 (0.21)	0.38 (0.23)
BmsTrt [Removal]		0.61 (0.21)					-0.18 (0.11)				1.26 (0.07)	
Climate [Drought]	1.09 (0.45)										0.88 (0.24)	0.61 (0.33)
Climate [Warming]	2.31 (0.47)										0.37 (0.24)	0.33 (0.29)
Climate [Warming+ppt]	0.85 (0.48)										0.37 (0.24)	
Site [Northern]	1.25 (0.42)	-1.72 (0.34)	0.19 (1.05)								0.50 (0.22)	0.07 (0.29)
Site [Southern]	1.33 (0.45)	-0.22 (0.50)	0.02 (1.24)								0.19 (0.23)	0.03 (0.45)
Size			1.57 (0.10)	0.53 (0.05)	-0.21 (0.12)	3.27 (0.17)	0.36 (0.05)	0.39 (0.05)				
$Size^2$				0.03 (0.02)								
Warming [Warming]		0.86 (0.32)		0.61 (0.37)		0.82 (0.90)	-0.36 (0.38)	-0.43 (0.33)				
Year [2017]	2.60 (0.31)	1.13 (0.22)	2.44 (0.60)			3.16 (0.66)	0.48 (0.19)					
Year [2018]						1.03 (0.50)	0.13 (0.18)				0.79 (0.10)	
BmsTrt [Removal] * Site [Northern]											2.47 (0.12)	
BmsTrt [Removal] * Site [Southern]											0.90 (0.14)	
Climate [Drought] * Year [2017]	0.42 (0.44)											
Climate [Drought] * Year [2018]											0.67 (0.14)	
Climate [Warming] * Year [2017]	0.19 (0.50)											
Climate [Warming] * Year [2018]											0.52 (0.18)	
Climate [Warming+ppt] * Year [2017]	0.81 (0.50)											
Climate [Warming+ppt] * Year [2018]											0.78 (0.17)	
Site [Northern] * Climate [Drought]												0.76 (0.52)
Site [Southern] * Climate [Drought]												2.19 (0.61)
Site [Southern] * Climate [Warming]												2.88 (0.55)
Site [Northern] * Year [2017]	0.97 (0.43)											
Site [Northern] * Year [2018]											0.13 (0.17)	
Site [Southern] * Year [2017]	0.06 (0.73)											
Site [Southern] * Year [2018]											2.09 (0.14)	
Size * Warming [Warming]						1.99 (0.34)	0.34 (0.08)	0.22 (0.07)				
Year [2017] * Warming [Warming]							-0.80 (0.26)					
Year [2018] * Warming [Warming]							-0.37 (0.25)					

APPENDIX C

SUPPLEMENTARY INFORMATION FOR CHAPTER IV

Supplemental Methods

Species descriptions:

All descriptions are based on information gathered from the Consortium of Pacific Northwest Herbaria (https://www.pnwherbaria.org/data/search.php), the USDA Plant Profiles databases (https://plants.usda.gov/), the CalFlora database (https://www.calflora.org/), *Flora of the Pacific Northwest: An Illustrated Manual* (Hitchcock et al., 2018), and authors' experience observing these species.

Plectritis congesta (shortspur seablush) is an annual forb in the Valerianaceae native to upland prairie habitat from California to the Vancouver Island region of British Columbia. It is within its current geographic range at all four experimental sites. *P. congesta* prefers open meadows and slopes but can be found in habitat ranging from wetlands to rocky balds. Its typical flowering period in Pacific Northwest prairies is early April through June. It often forms dense patches of slender plants up to ~60 cm tall, with one-seeded, keeled, and sometimes winged achenes that are dispersed by gravity and wind.

Collinsia grandiflora (giant blue-eyed Mary) is an annual forb in the Plantaginaceae native between northern California to Vancouver Island, British Columbia. It is within its current geographic range at all four experimental sites. C. *grandiflora* grows from the lowlands up to ~2,000 m in elevation in the Cascade mountains, and depending on elevation and latitude, flowers between late April and late June. It ranges in size from minute with a single whorl of flowers to ~40 cm tall with multiple whorls and hundreds of flowers. Flowers produce one fruit with ~2-7 seeds that are dispersed by gravity.

Clarkia purpurea (winecup Clarkia) is a slender annual forb in the Onagraceae, and is native from southern California to the Puget Trough of Washington. It is within its current geographic range at all four experimental sites. *C. purpurea* can tolerate a wide range of habitats, but often prefers low competition and relatively open areas. Its typical flowering period in the Pacific Northwest is May into early July. It can grow to ~1 m and produces large fruits with many small seeds that are dispersed by gravity.

Plagiobothrys nothofulvus (rusty popcorn flower) is a small annual forb in the Boraginaceae and is native from southern California to approximately the Columbia River Gorge between Oregon and Washington. It is within its current geographic range at the southern and central sites, but beyond its range at the two northern sites. *P. nothofulvus* is most often found in open, drier, low productivity meadows. It produces a clump of basal leaves with few, alternating stem leaves, and can grow to ~30 cm tall. It

blooms early, typically reaching peak before May in Pacific Northwest prairies. It produces between 1-4 nutlets per fruit that are dispersed by gravity.

Aristida oligantha (prairie threeawn) is a C4 annual grass in the Poaceae native to North America. West of the Cascade mountains in the Pacific Northwest, it naturally occurs as far north as the Willamette Valley. It is within its current geographic range at the southern and central sites, but beyond its range at the two northern sites. In this region, *A. oligantha* is generally found in drier, open habitat. It forms clumps of flowering stems and may reach ~70 cm tall. It is a late-season species, with seeds forming in July and August and dispersing via gravity and animals (ectozoochory).

Achyrachaena mollis (blow-wives) is an annual forb in the Asteraceae, native in low-elevation prairies west of the Sierra and Cascade mountain ranges from southern California to southwestern Oregon. It is within its current geographic range at the southern site but beyond its range at the three remaining sites. *A. mollis* produces a straight stem up to ~30 cm tall with a large bud producing a spherical cluster of flowers bearing a single seed each. It typically flowers in May and its seeds disperse shortly after their scales become exposed to the wind.

Thysanocarpus radians (ribbed fringepod) is a small annual forb in the Brassicaceae, native to low-elevation prairies from southern California to southwestern Oregon. It is within its current geographic range at the southern site but beyond its range at the three remaining sites. *T.* radians is generally found in low-productivity, open habitat and can grow up to ~60 cm tall. It generally blooms in April and May and its tiny flowers produce single large, round, disc-like fruits that hang from their pedicels and feature characteristic ribs radiating from the center seed to the thin marginal wings that aid in wind dispersal.

Navarretia pubescens (downy pincushion plant) is a small annual forb in the Polemoniaceae native from central California to southwestern Oregon. It is within its current geographic range at the southern site but beyond its range at the three remaining sites. *N. pubescens* can be found in open, mountainous habitat and generally reaches up to 30 cm in height. Its inflorescence is a cluster with few to many flowers surrounded by sharp, leaflike bracts. It typically flowers in May and June in southern Oregon region. Seeds develop inside the inflorescence mass and are dispersed by gravity.

Climate treatment implementation:

All plots were trenched and surrounded by 50 cm-deep aluminum flashing to isolate their soils and minimize lateral water flow. During both experiments 1 and 2 (hereafter Exp1 and Exp2), we collected continuous plot-level canopy temperatures (using SI-121 infrared radiometers; Campbell Scientific, Logan, Utah, USA) and volumetric water contents (at 0-30 cm depth using CS616-L water content reflectometers; Campbell Scientific) and recorded 30-minute averages using AM16/32B multiplexors connected to CR1000 dataloggers (Campbell Scientific). We used these data to regulate

our warming treatments during both experiments, as well as the automated irrigation system in Exp2.

To achieve our warming treatments, we used six 2000-W infrared heaters per plot (Kalglo Electronics, Bethlehem, Pennsylvania, USA) and controlled their radiation output using the mean control-plot canopy temperatures (Kimball et al. 2008). We sought a warming treatment of +2.5-3°C to be consistent with expectations for the region for the end of the 21st century (Mote and Salathé 2010). In Exp1, we achieved +3°C in 2010 but altered this to +2.5°C for 2011 and 2012 due to budget limitations (Pfeifer-Meister et al. 2016). In Exp2, we stayed consistent with +2.5°C during all three years (Reed et al. 2020).

For +20% precipitation in Exp1 (both precip and warming + precip treatment plots), we used a gauged hose to add additional rainfall (collected on site and stored in a cistern) within two weeks after each rainfall event. Because of the nature of the wet and dry seasons in this system, this effectively created more intense rainfall events during the wet winter months and is consistent with the expectation for an increase in winter precipitation (Mote and Salathé 2010).

In Exp2, we altered our warming + precip treatment so that we could deconfound the effects of warming from a strong reduction in soil moisture, which occurred even when we added +20% precipitation in Exp1 (Pfeifer-Meister et al. 2016). In addition, the +20% precipitation addition had very little plant effects (Pfeifer-Meister et al. 2013, 2016). To do this, we set up an automated irrigation system within the center of each warming + precip plot. Using rainfall collected and stored on site, these plots would be irrigated for 30 minutes each night that their volumetric water content dropped below 95% of the control plot average. This successfully caused these plots' soil moisture to roughly match that of the control plots (Reed et al. 2019).

Lastly, for the drought treatment in Exp2, we built rainout shelters (~1.5 m tall) that featured UV resistant, clear acrylic shingles (MultiCraft Plastics, Eugene, Oregon, USA), which intercepted rainfall above 40% of the plot area. We used a 40% reduction in precipitation as this represents an "extreme" event for each the three sites as determined by the Precipitation Trends and Manipulation tool from Drought-Net (Lemoine et al. 2016), and aligns with the expectation that regional drought potential will increase with climate change (Jung and Chang 2012).

Due to logistical constraints in receiving electricity and in writing the program to run the automated irrigation system, some of our treatments had delayed starting dates. In Exp1, +20% precipitation began by spring 2010 and warming by fall 2010. In Exp2, the drought treatment began in February 2016, while the warming treatments began in February, January, and June 2016 at the southern, central, and northern 2 sites, respectively. The automated irrigation for the warming + precip plots began in September 2016 at all three sites. Warming was turned off August-September 2016 and 2017 due to fire hazard and ended permanently in July 2018.

Methods for deriving climate variables for experimental treatments and site:

Before using climate data in our analyses, we had to contend with sporadic missing plot-level microclimate data. We were missing some microclimate data (e.g., canopy temperature and soil moisture) since these did not begin recording until after the experiments began, as well as sensor failures in some sites and months. In addition, we wished to convert our local measurements to correspond to macroclimatic indices and downscaled future climate predictions so that they could be interpreted beyond the local site measurements. To make this conversion, and to best estimate missing data, required us to process the microclimate data in a series of statistical models. The end results are seasonal measures of climate that are comparable to those derived from PRISM (PRISM Climate Group) or derived variables using PRISM data (e.g., climatic water deficit - CWD).

Step 1: Obtain monthly mean climate values from experimental microclimate monitoring.

We assembled monthly data on soil moisture and canopy temperature from the experimental plots (Pfeifer-Meister et al. 2013, Reed et al. 2020). For all analysis steps until a final aggregation into seasonal values, we used monthly climate variables. For both soil moisture and canopy temperature, we used the monthly mean value if more than 20 days of data were recorded. Otherwise, we assigned the value as NA.

Step 2: Determine the effective climate treatment for each plot in each month.

We used the treatment initiation and ending dates to determine the effective treatment in a given month for each treatment type in each site. This was especially an issue for Exp2, for which the staggered start dates of different treatments meant that a range of effective treatments occurred. Note that it was also an issue for Exp1 in the first year (late 2009 to early 2010), when there were no microclimate data recorded, requiring us to estimate microclimate data for each plot in the same way. There were a few months in spring 2010 when there were partial or complete treatments that also had to be filled in with Step 3 (below). Note that we assigned the actual treatment based on the effective treatment for the majority of the days in a month. For example, if warming in a warming treatment started on April 7th, we said that the treatment for that month was warming.

Step 3: Estimate plot-level microclimate values based on PRISM data and treatment-specific plot-level data.

We used data on monthly mean precipitation and temperature from PRISM (to determine climate variation across time), combined with monthly plot data (to estimate how treatments cause deviations from control conditions) to estimate plot- and treatment-

specific microclimate values from the experimental data sets. This was done separately for soil volumetric water content (VWC) and canopy temperature, and separately for Exp2 and Exp1. These relationships were then used in Step 4, below, to estimate missing plot-level climate values. These analyses are detailed below:

Exp2 VWC:

For the second experiment, we identified a predictive model for VWC using 'dredge' from the MuMIn package (Barton, 2018). While we generally prefer testing a small set of alternative causal models with a priori justification, in the case of climate variables and site effects, it is nearly certain that all possible causal links do exist, so there is not a clear limit on model complexity, just a question of which links are strong and consistent enough to improve model fit without overfitting. In this context, we feel that use of dredge is a reasonable approach. Exploratory analysis showed that inclusion of month + month^2 helped improve predictions considerably, while monthly precip^2 was not supported, nor was a random plot effect on the slope of precipitation. Using this information, the "global" model (the full model from which subsets are compared via dredge) includes linear and squared effects of monthly temperature, interactions of temperature and precipitation, as well as interactions with month, site, and realtrt (the effective treatment for a plot in a given month), as well as random plot intercepts. Due to the staggered treatment start dates, some interactions withrealtrt could not be estimated, and the global model reflects this limitation. We also found that log-transforming precipitation had higher explanatory power in these models than did untransformed precipitation, so all monthly precipitation values are included as log(monthly precip + 1):

```
global_model = lmer(VWC ~ (monthlytemp + I(monthlytemp^2)) *
logmonthlyprecip + (monthlytemp + I(monthlytemp^2) + logmonthlyprecip) *
(month + I(month^2) + site + realtrt) + (1 + monthlytemp | plotid), REML =
FALSE, data = vdats, na.action = 'na.fail')
```

We called dredge with several fixed main effects:

```
dredgemodsVWC_Exp2 = dredge(global_model, fixed = c('monthlytemp',
'logmonthlyprecip', 'site', 'realtrt', 'month', 'I(month^2)'), beta = 'none', trace = 2)
```

The most supported model included multiple interactions:

```
VWC ~ I(monthlytemp^2) + logmonthlyprecip + month + I(month^2) + monthlyt
emp +  realtrt + site + (1 + monthlytemp | plotid) + logmonthlyprecip:month + log
monthlyprecip:monthlytemp + logmonthlyprecip:site + month:monthlytemp + I(
monthlytemp^2):I(month^2) + logmonthlyprecip:I(month^2) + monthlytemp:I(m
onth^2) + monthlytemp:realtrt +
monthlytemp:site + I(monthlytemp^2):logmonthlyprecip + I(monthlytemp^2):mo
nth +
I(monthlytemp^2):realtrt + I(monthlytemp^2):site
```

This model has $r^2_{marginal}$ = 0.868 and $r^2_{conditional}$ = 0.890 and provides good predictions of o bserved VWC .

Exp2 Canopy Temp:

To model canopy temperatures for the second experiment, we used a global model of:

```
global_model = lmer(ctemp ~ monthlytemp * site * (month + (month^2)) +
monthlytemp * site * realtrt + (1 + monthlytemp | plotid), data = tdats, REML =
FALSE, na.action = 'na.fail')
```

Here, ctemp is measured canopy temperature. Note that the model includes random effects of plot on the intercept and also the monthly temp slope. We then called dredge with several fixed effects:

```
dredgemodsCTEMP_Exp2 = dredge(global_model, fixed = c('monthlytemp',
'realtrt'), beta = 'none')
```

The most supported model was:

```
ctemp ~ month + I(month^2) + site + monthlytemp + realtrt + month:monthlytem
p + month:site+ I(month^2):monthlytemp + monthlytemp:realtrt + site:monthlyte
mp + site:realtrt + month:site:monthlytemp + site:monthlytemp:realtrt + (1 + mon
thlytemp | plotid)
```

This model has $r^2_{marginal}$ = 0.974 and $r^2_{conditional}$ = 0.9773 and gave highly accurate predictions.

Exp1 VWC:

To estimate VWC in the first experiment, we called dredge using the same global model and fixed effects as for Exp2, but with Exp1 data. The most supported model includes multiple interactions:

```
VWC ~ logmonthlyprecip + I(monthlytemp^2) + month + I(month^2) + monthlyt
emp + realtrt + site + (1 + monthlytemp | plotid) + logmonthlyprecip:month + log
monthlyprecip:monthlytemp + logmonthlyprecip:site + month:monthlytemp + log
monthlyprecip:I(month^2) + monthlytemp:I(month^2) + monthlytemp:realtrt + m
onthlytemp:site +
logmonthlyprecip:I(monthlytemp^2) + I(monthlytemp^2):month + I(monthlytemp
^2):realtrt + I(monthlytemp^2):site
```

This model has $r^2_{marginal}$ = 0.810 and $r^2_{conditional}$ = 0.900 and provides good predictions of VWC.

Exp1 Canopy Temp:

To estimate canopy temperature for the first experiment, we called dredge using the same global model and fixed effects as for Exp2, but with Exp1 data. The most supported model was:

ctemp ~ month + I(month^2) + site + monthlytemp + realtrt + (1 + monthlytemp | plotid) + month:site + I(month^2):monthlytemp + I(month^2):site + monthlytemp:realtrt +
site:monthlytemp + site:realtrt + site:monthlytemp:realtrt

This model has $r^2_{marginal} = 0.987$ and $r^2_{conditional} = 0.988$ and gave highly accurate predictions.

Step 4: Estimate missing monthly microclimate values

With the final relationships from Step 3, we filled in estimates for each month for treatment and site-specific VWC and canopy temp where these data were missing, based upon monthly PRISM data. These dates included a considerable amount of time at the initiation of Exp2 (2015), at the beginning of the Exp1 experiment (end of 2009 and spring of 2010), as well as other missing values scattered through the data set.

Step 5: Translation of microclimate data into equivalent PRISM climate values

Using only directly measured data for the control plots, we established how to estimate PRISM values of temperature and precipitation from canopy temp and VWC. This was done separately for temperature and precipitation. We used plot-specific values for these analyses but did not include plot as a random effect, as these analyses were based only on control plots, and thus plot could not be included in a final model that was used to estimate PRISM-like climate variables from plot microclimate data. In these models, we included month of the year coded as an integer with January = 1. Inclusion of month substantially improved the fit of these models.

Temperature:

We began with a global model for PRISM-derived monthly temperature (monthlytemp) that included multiple interactions and effects of month, month^2, site, and canopy temp:

global_model = lm(monthlytemp ~ ctemp * site * (month + I(month^2)), data = Ctdats, na.action = 'na.fail')

We called dredge with one fixed effect to find the most-supported predictive model:

dredgetempmods = dredge(global_model, fixed = c('ctemp'), beta = 'none', trace = 2)

The most supported model retained all main effects and multiple interactions:

lm(formula = monthlytemp ~ month + I(month^2) + site + ctemp:month + ctemp: I(month^2) + ctemp:site + month:site + I(month^2):site + ctemp:month:site + ctemp:I(month^2):site + ctemp, data = Ctdats, na.action = "na.fail")

This model has $r^2 = 0.985$ and there is a linear relationship between predictions and observed PRISM temperatures.

Precipitation:

Exploratory analysis showed that inclusion of month + month^2 helped improve estimates of PRISM-derived monthly precipitation (monthlyprecip) considerably, and that both canopy temp and VWC effects were strong. We also found that models predicting log-transformed precipitation were more linear and provided overall better predictions, so as noted for the Step 3 analyses, we ran models using logged precipitation as the dependent variable.

We started with the following global model:

global_model = lm(logmonthlyprecip ~ (ctemp + I(ctemp^2)) * (VWC + I(VWC^2)) + (ctemp + I(ctemp^2) + VWC + I(VWC^2)) * (site + month + I(month^2)), data = Cpdats, na.action='na.fail')

We called dredge on this global model with several fixed effects:

dredgeprecipmods3 = dredge(global_model, fixed = c('ctemp', 'VWC', 'site', 'month', 'I(month^2)'), beta = 'none', trace = 2)

The most supported model from this search was:

lm(formula = logmonthlyprecip ~ I(ctemp^2) + I(VWC^2) + ctemp:I(month^2) + ctemp:site + I(ctemp^2):I(VWC^2) + I(ctemp^2):month + I(ctemp^2):site + ctem p + month + I(month^2) + site + VWC, data = Cpdats, na.action = "na.fail")

This model has $r^2 = 0.828$. This model also did a reasonably good job of predicting log(precip) values.

Step 6: Estimate PRISM-equivalent climate values for each month for each plot

Using plot- and treatment-specific VWCs and canopy temps, including all estimated values from Step 4, we estimated PRISM values for temperature and precipitation for each month for each plot.

Step 7: Estimate derived climate variables from PRISM-equivalent climate values

We used the treatment-specific estimates of temperature and precipitation for each month to estimate three additional climate variables: Potential Evapotranspiration (PET), Actual Evapotranspiration (AET) and Climatic Water Deficit (CWD, the difference between AET and PET: PET – AET). These estimates were made using the Redmond 2019 R function (using a modified Thornthwaite water balance model) and also used the soil water holding capacity from 0-30 cm depth from SSURGO USDA (https://www.nrcs.usda.gov/wps/portal/nrcs/detail/soils/survey/office/ssr12/tr/?cid=nrcs142p2_010596).

Step 8: Aggregate climate values into seasonal mean variables.

We aggregated monthly values into three 4-month mean seasonal values for each year. These periods were: winter (November – February), spring (March – June), and summer (July – October).

Supplemental Figures

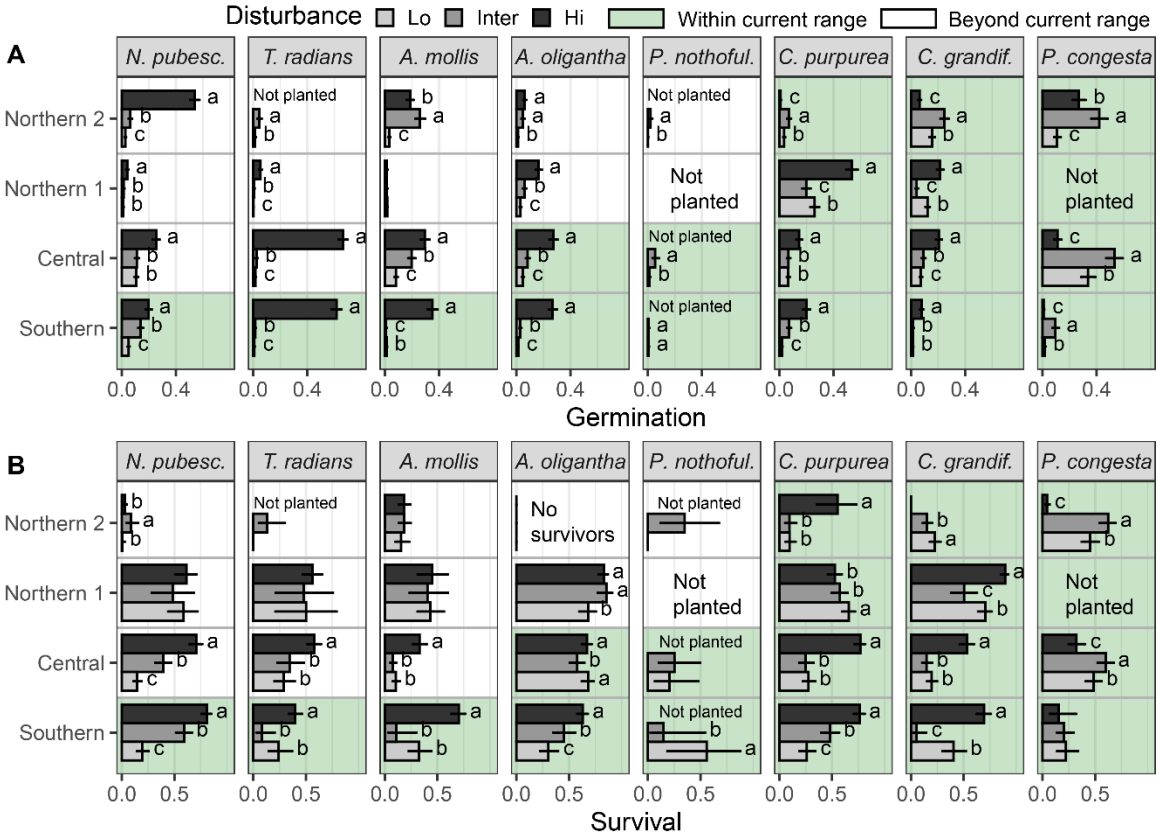

Figure S4.1. The role of disturbance (high, intermediate, low) on species' germination (A) and survival (B). Bars show estimated marginal means ± 95% confidence limits. "High" disturbance includes all data from 2010 and 2016; "intermediate" disturbance includes all data from the plot halves receiving the intermediate disturbance treatments of 2012 and 2017; "Low" disturbance includes all data from 2011 and 2018, as well as all data from the plot halves that did not receive the intermediate disturbance treatments in 2012 and 2017 (see methods). Letters indicate significant differences ($p < 0.05$) between disturbance levels for a given site and species. Species are arranged from left to right in ascending order of northern range limit.

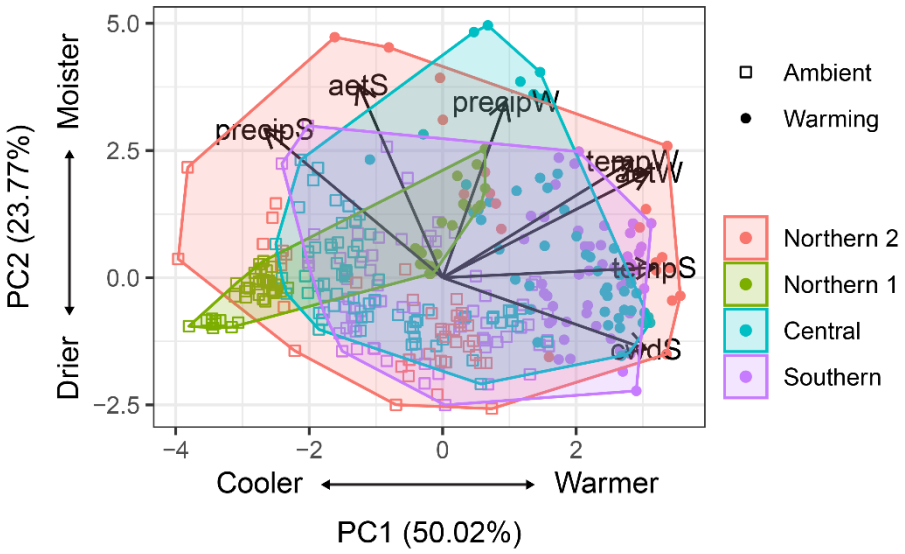

Figure S4.2. Principal components analysis of the seven climate variables used in the study, using all 360 unique replicates from Exp1 and Exp2. Polygons encapsulate the four sites. 'temp' = mean temperature, 'precip' = total precipitation, 'aet' = total actual evapotranspiration, 'cwd' = total climatic water deficit; 'W' = winter, 'S' = spring. PC1 is primarily driven by temperature (cooler to warmer from left to right) while PC2 reflects additional variation explained by moisture (drier to moister from bottom to top). There is considerable overlap in climatic space by site relative to the separation driven by the warming treatments (see Figure 3).

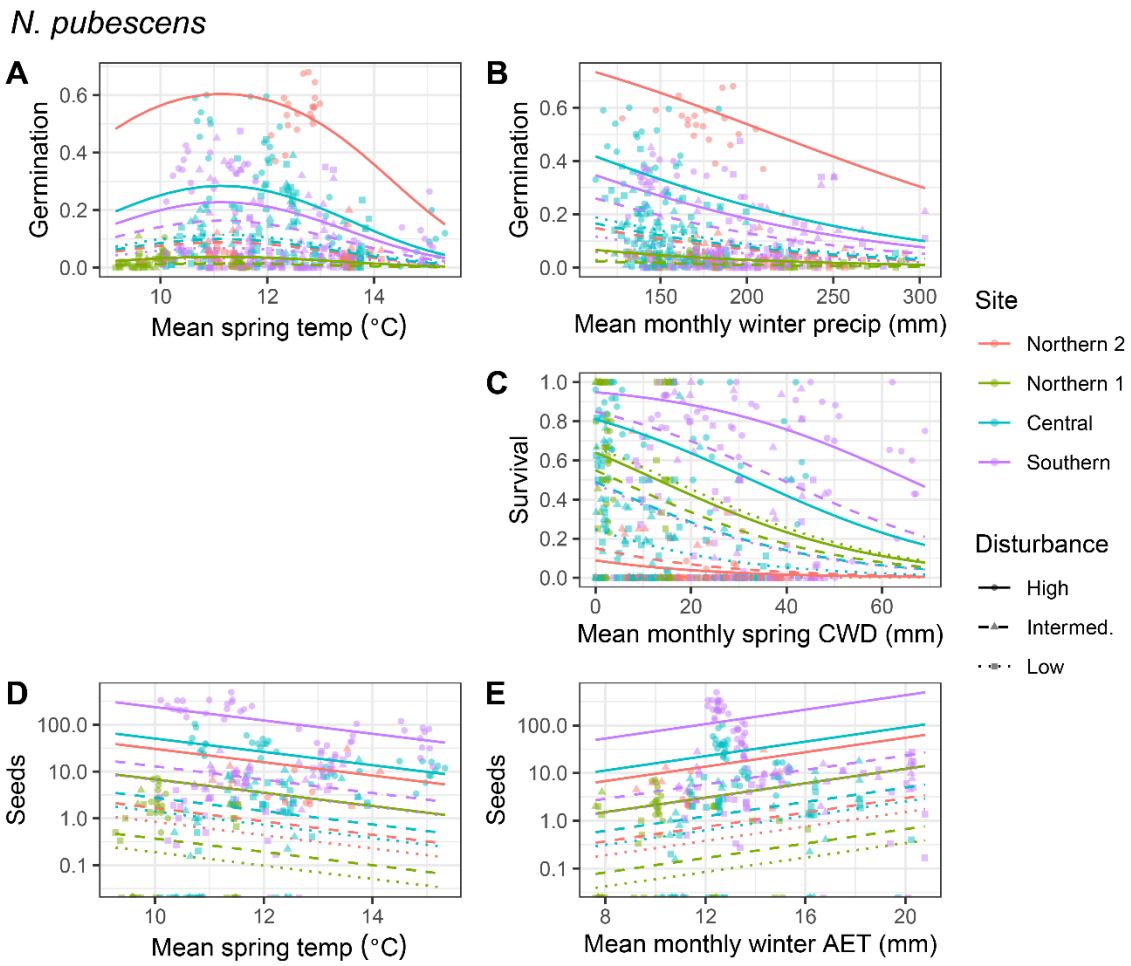

Figure S4.3. *Navarretia pubescens* germination (A, B), survival (C), and seed production (D, E) against climatic predictor variables in the models with the best predictive performance (Table S2). Lines depict model predictions for each site and disturbance combination while symbols show the plot-level datapoints used to fit the models.

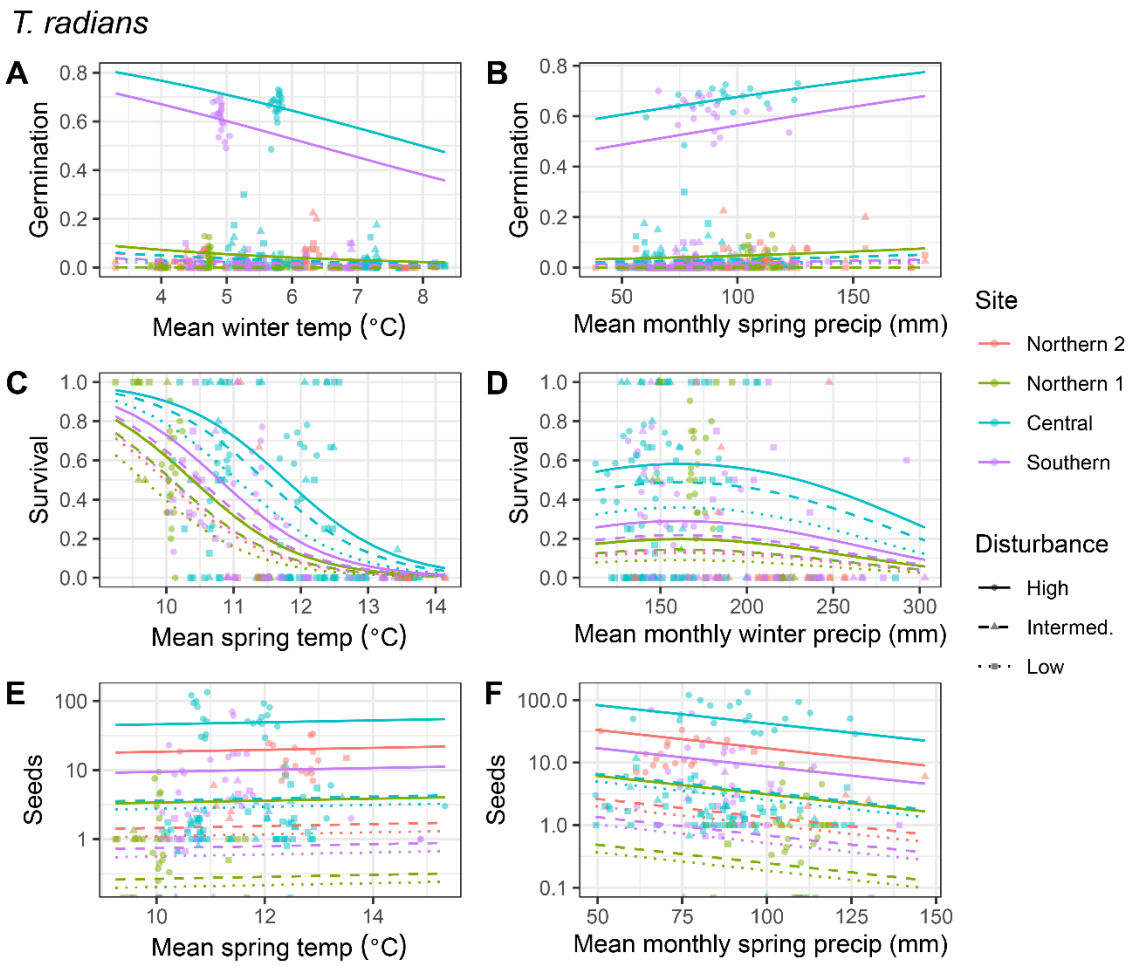

Figure S4.4. *Thysanocarpus radians* germination (A, B), survival (C, D), and seed production (E, F) against climatic predictor variables in the models with the best predictive performance (Table S2). Lines depict model predictions for each site and disturbance combination while symbols show the plot-level datapoints used to fit the models. The Northern 2 site under high disturbance is excluded from germination and survival figures since this species was not planted in fall 2015. However, this site-disturbance combination is depicted in the seed figures because there were some individuals that occurred throughout the plot matrix in spring 2016 as a result of the initial plot seed sowing.

A. mollis

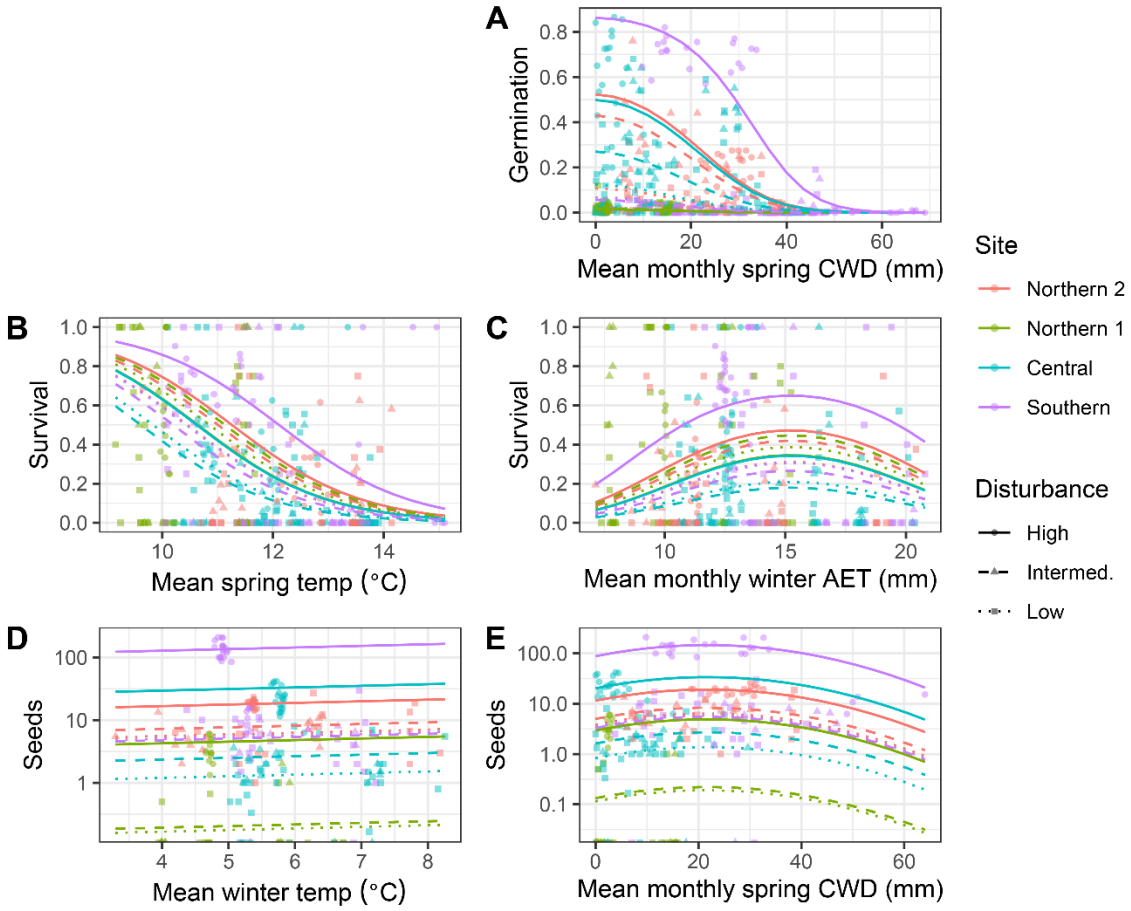

Figure S4.5. *Achyrachaena mollis* germination (A), survival (B, C), and seed production (D, E) against climatic predictor variables in the models with the best predictive performance (Table S2). Lines depict model predictions for each site and disturbance combination while symbols show the plot-level datapoints used to fit the models.

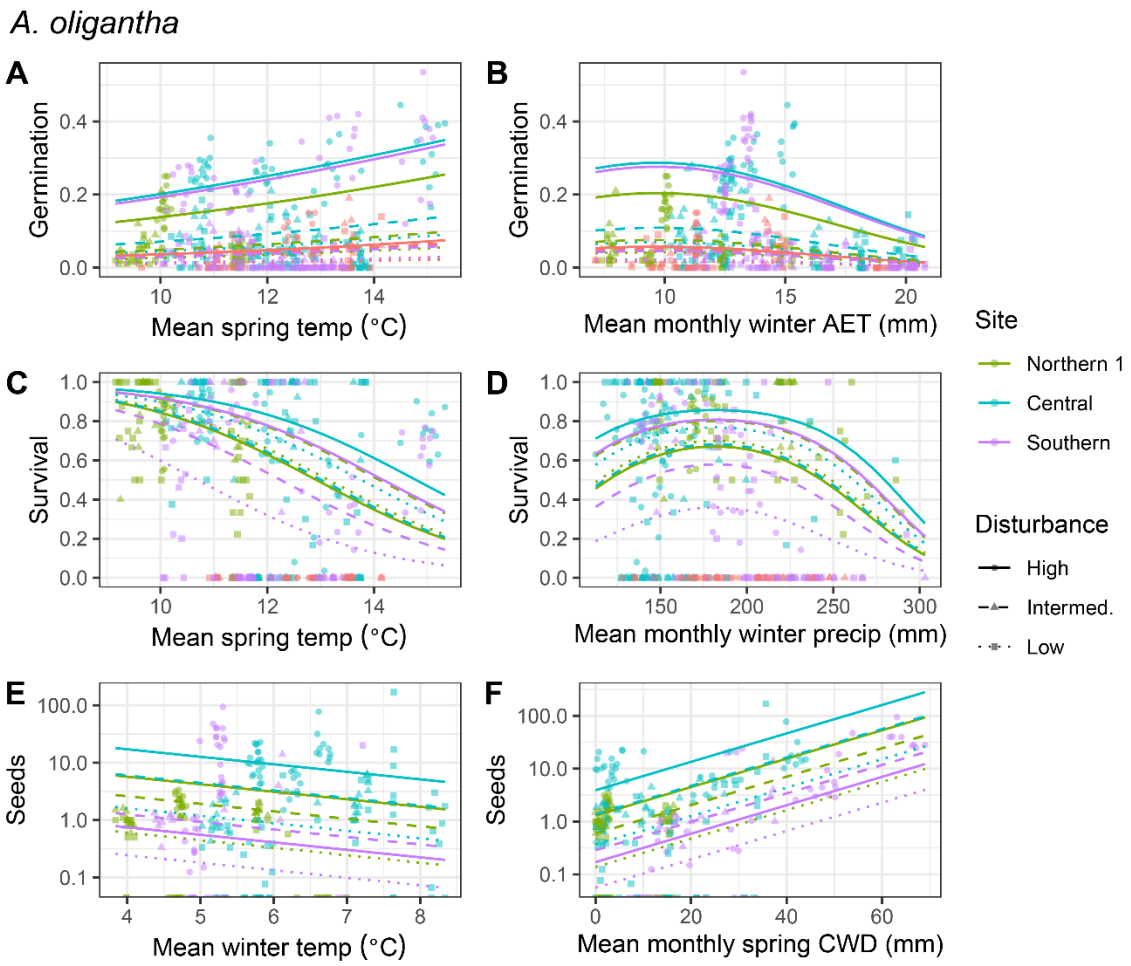

Figure S4.6. *Aristida oligantha* germination (A, B), survival (C, D), and seed production (E, F) against climatic predictor variables in the models with the best predictive performance (Table S2). Lines depict model predictions for each site and disturbance combination while symbols show the plot-level datapoints used to fit the models. Zero plants survived at the Northern 2 site, hence, it is absent from the survival and seed production figures.

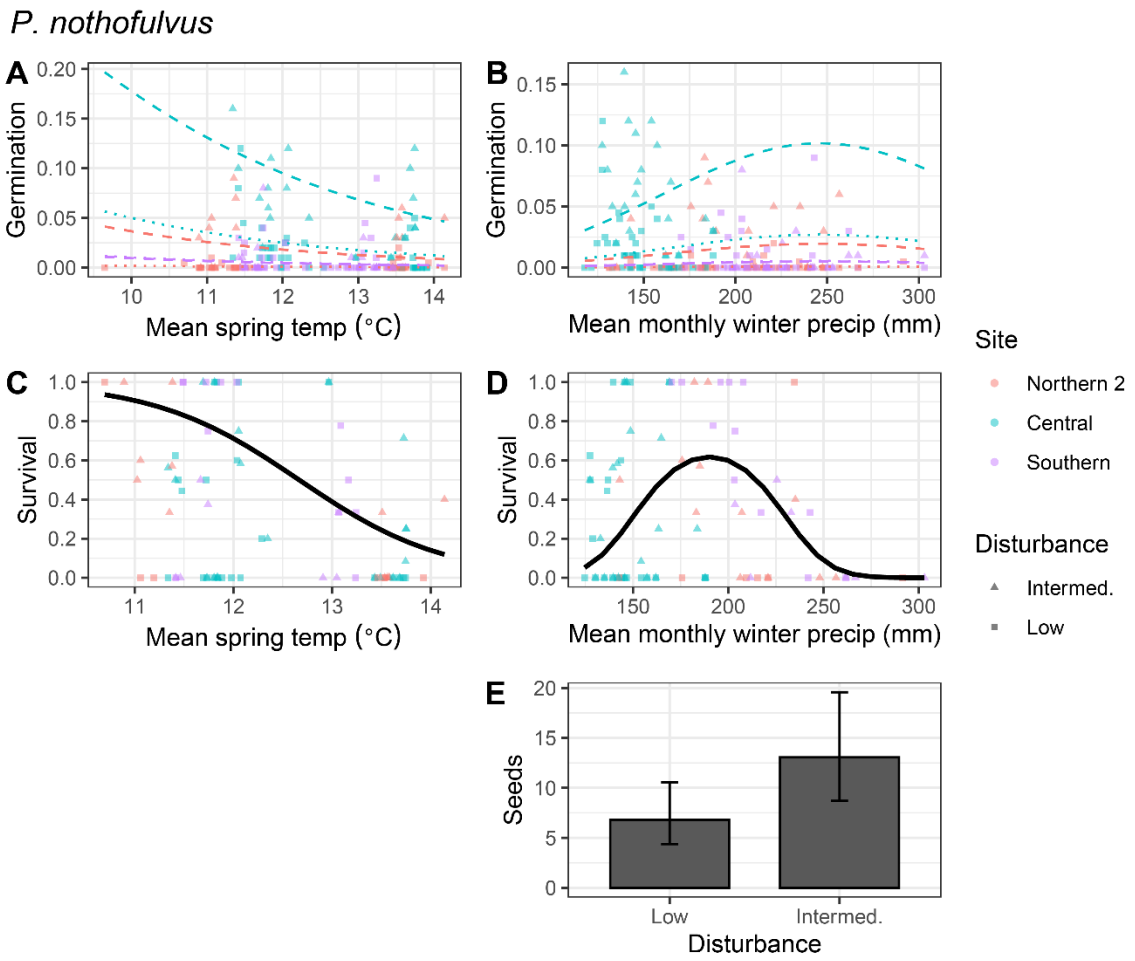

Figure S4.7. *Plagiobothrys nothofulvus* germination (A, B), survival (C, D), and seed production (E) against climatic predictor variables in the models with the best predictive performance (Table S2). For seeds, the most-supported model did not contain any climate variables or site, so predictions are depicted only against disturbance. Lines depict model predictions for site and disturbance combinations for germination and across all sites for survival while symbols show the plot-level datapoints used to fit the models. This species was never planted at the Northern 1 site nor under high disturbance.

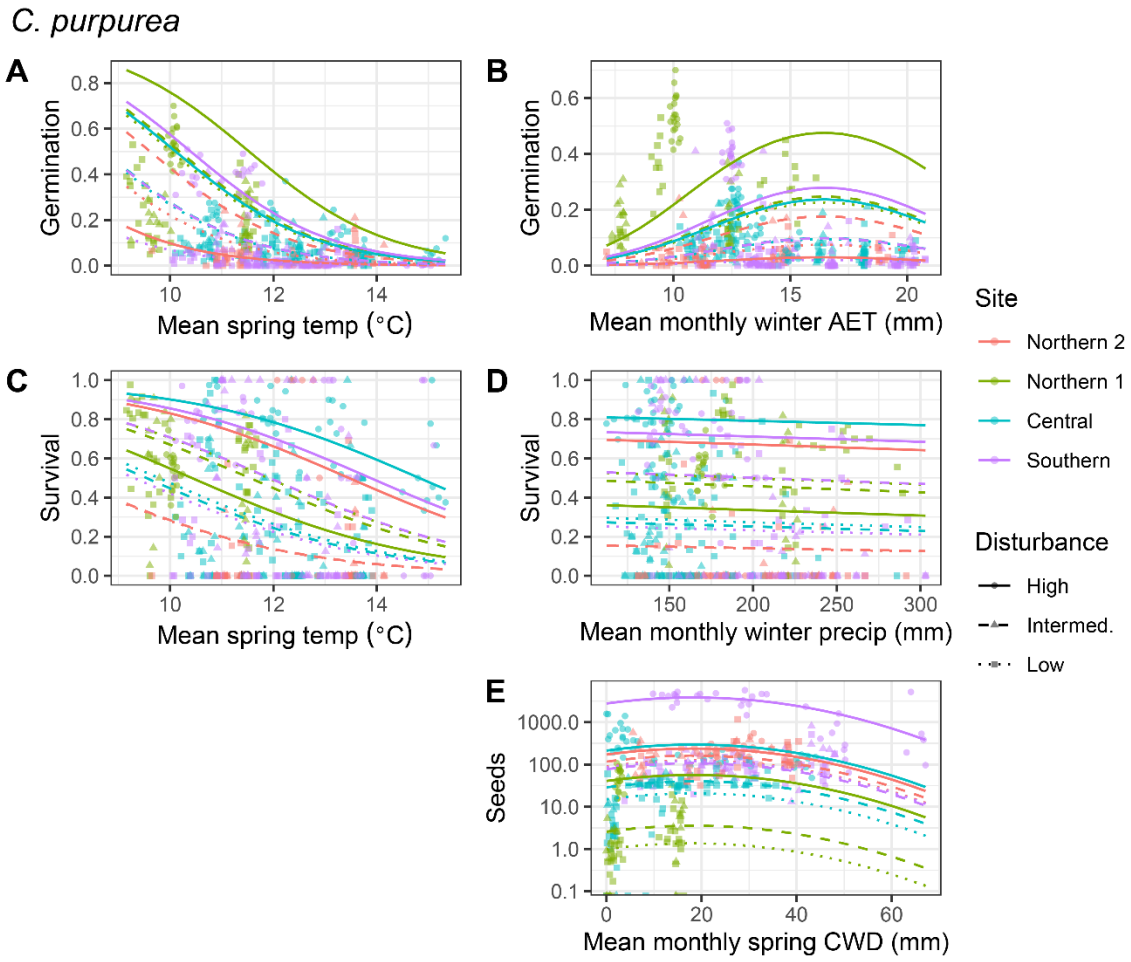

Figure S4.8. *Clarkia purpurea* germination (A, B), survival (C, D), and seed production (E) against climatic predictor variables in the models with the best predictive performance (Table S2). Lines depict model predictions for each site and disturbance combination while symbols show the plot-level datapoints used to fit the models.

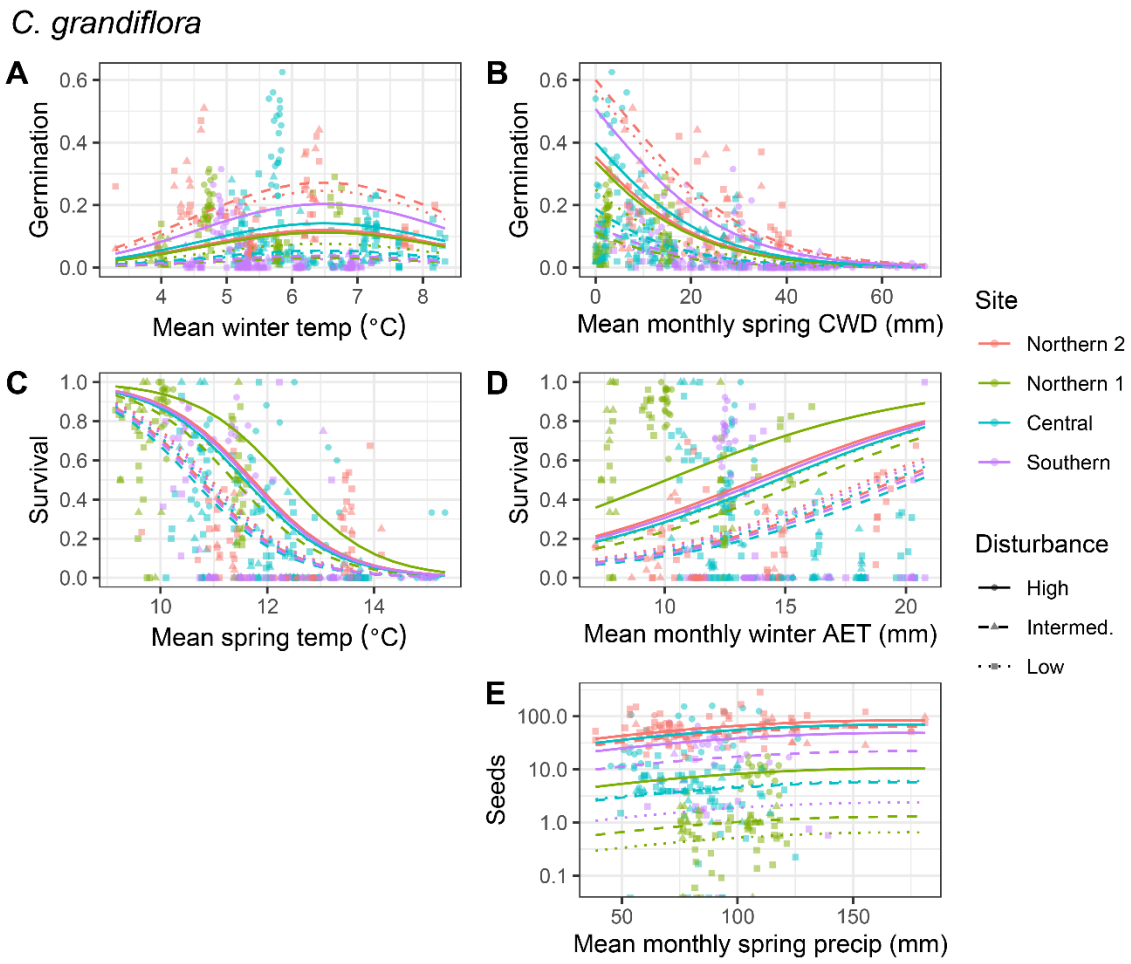

Figure S4.9. *Collinsia grandiflora* germination (A, B), survival (C, D), and seed production (E) against climatic predictor variables in the models with the best predictive performance (Table S2). Lines depict model predictions for each site and disturbance combination while symbols show the plot-level datapoints used to fit the models.

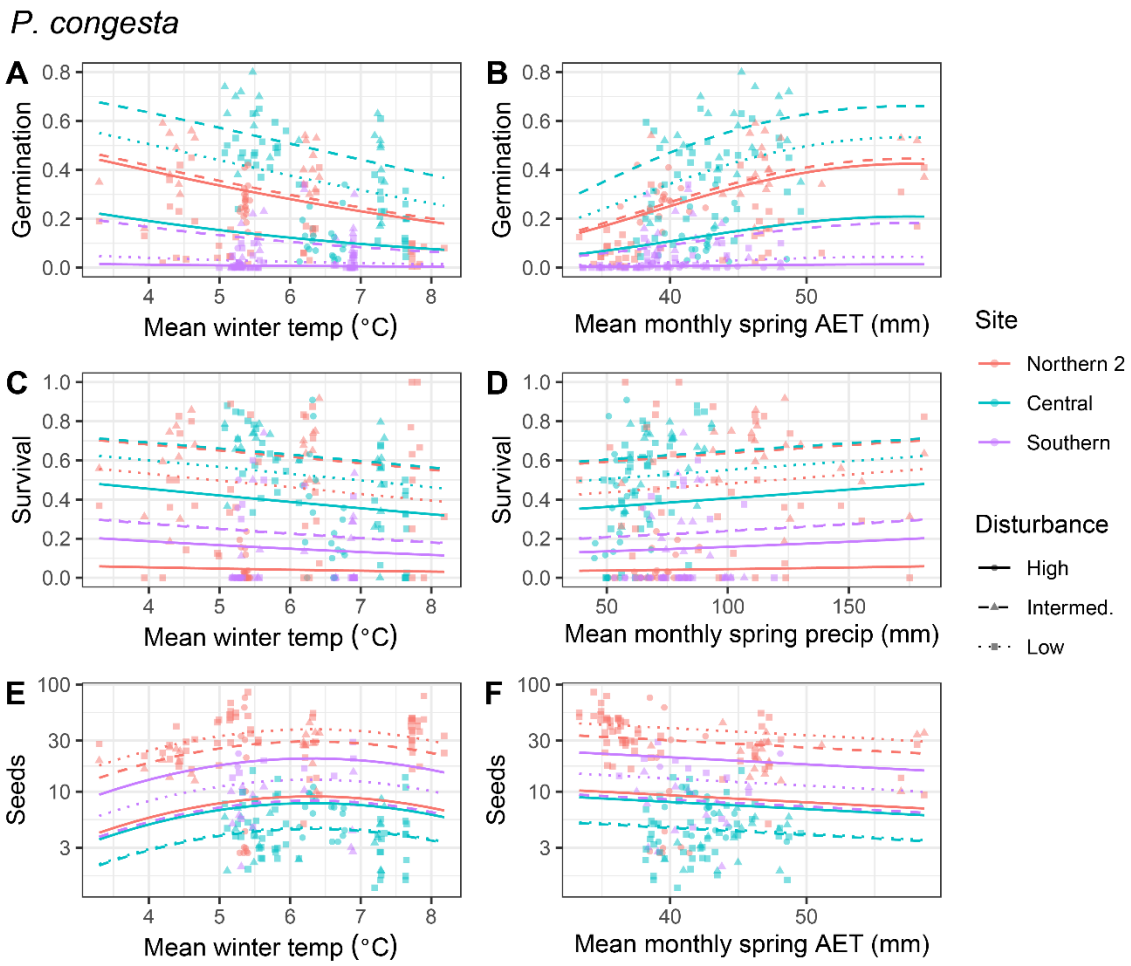

Figure S4.10. *Plectritis congesta* germination (A, B), survival (C, D), and seed production (E, F) against climatic predictor variables in the models with the best predictive performance (Table S2). Lines depict model predictions for each site and disturbance combination while symbols show the plot-level datapoints used to fit the models. This species was never planted at the Northern 1 site.

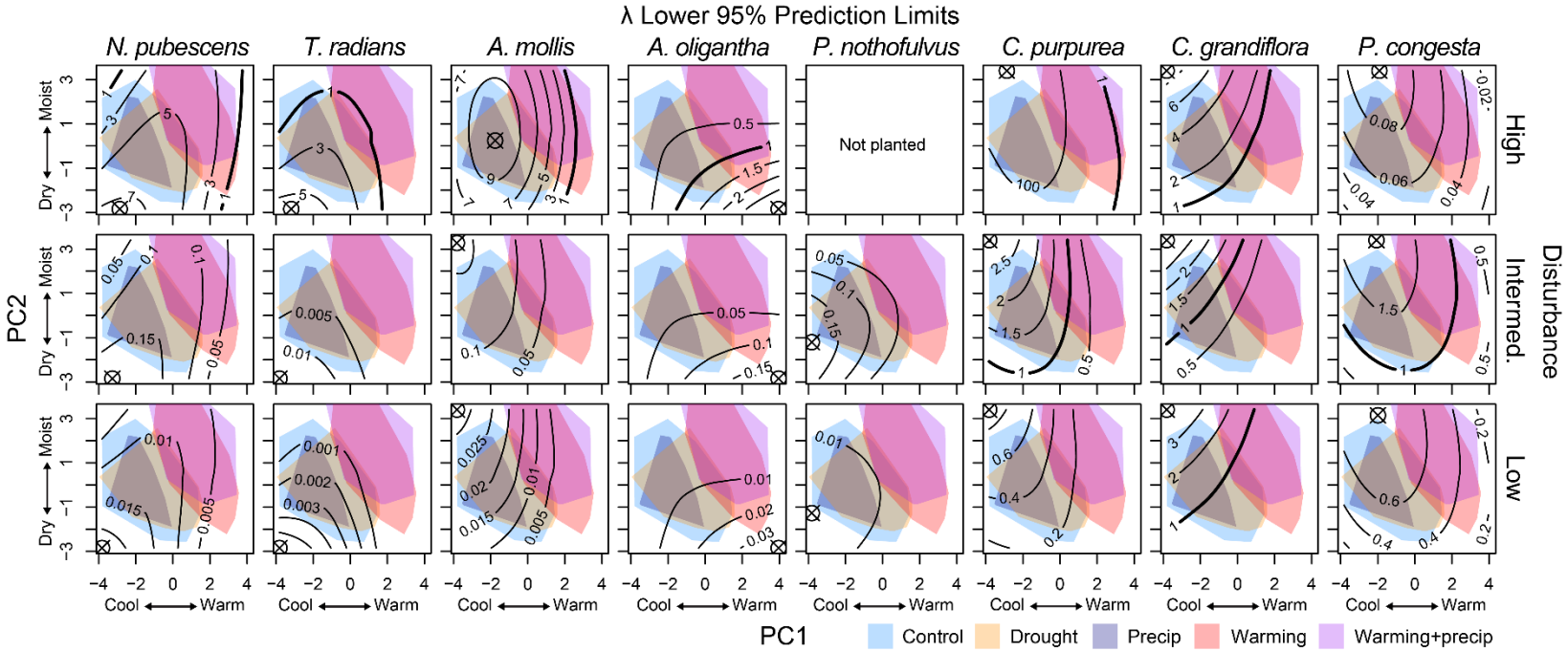

Figure S4.11. Contour plots of the lower 95% prediction limits in the estimated population growth rates (λ) as a function of climate (PC1 and PC2) and disturbance (low, intermediate, and high) averaged across sites for each of the eight focal species. Climate is depicted as the first two principal components of all seven climate variables used in the study, with PC1 reflecting temperature (cooler to warmer left to right) and PC2 reflecting moisture (drier to moister bottom to top). Colored polygons depict the range of climatic conditions that occurred in each broad climate treatment over the course of the experiments. ⊗ indicates the location of highest λ.

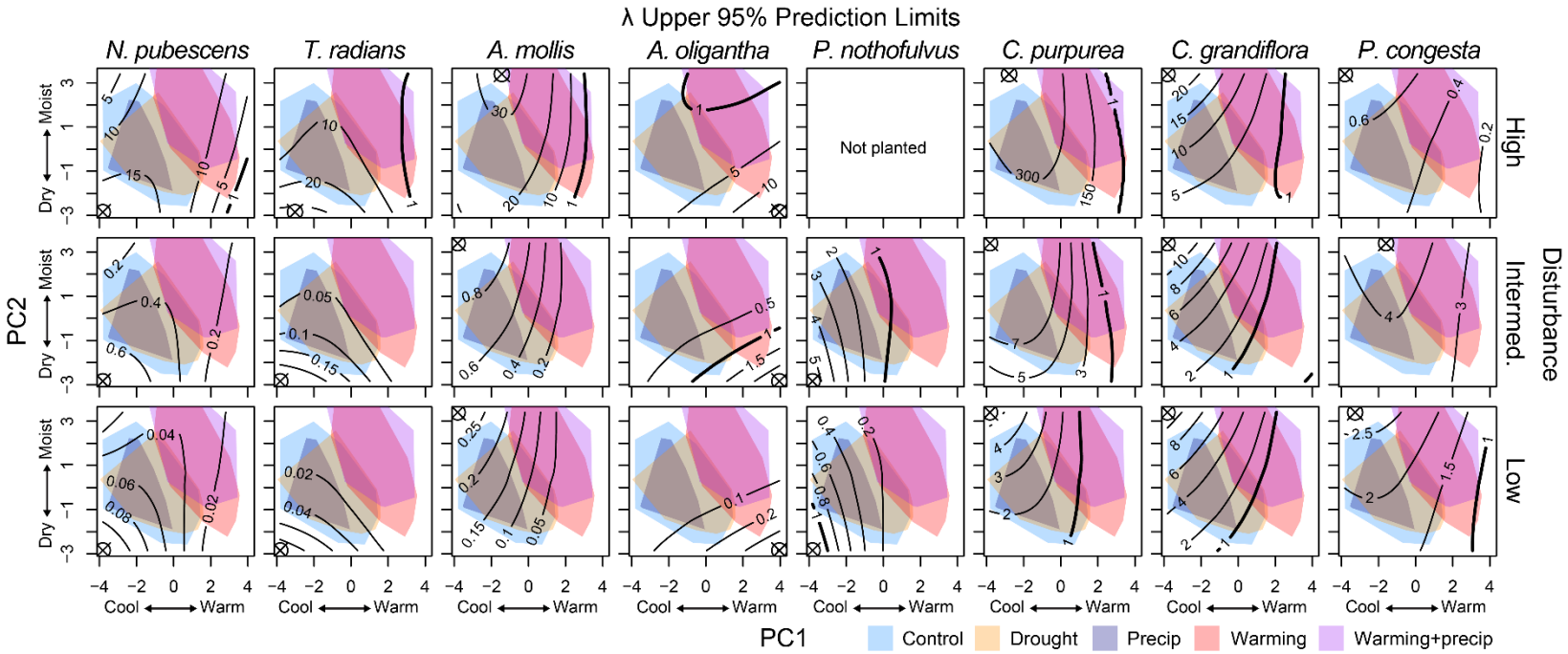

Figure S4.12. Contour plots of the upper 95% prediction limits in the estimated population growth rates (λ) as a function of climate (PC1 and PC2) and disturbance (low, intermediate, and high) averaged across sites for each of the eight focal species. Climate is depicted as the first two principal components of all seven climate variables used in the study, with PC1 reflecting temperature (cooler to warmer left to right) and PC2 reflecting moisture (drier to moister bottom to top). Colored polygons depict the range of climatic conditions that occurred in each broad climate treatment over the course of the experiments. ⊗ indicates the location of highest λ.

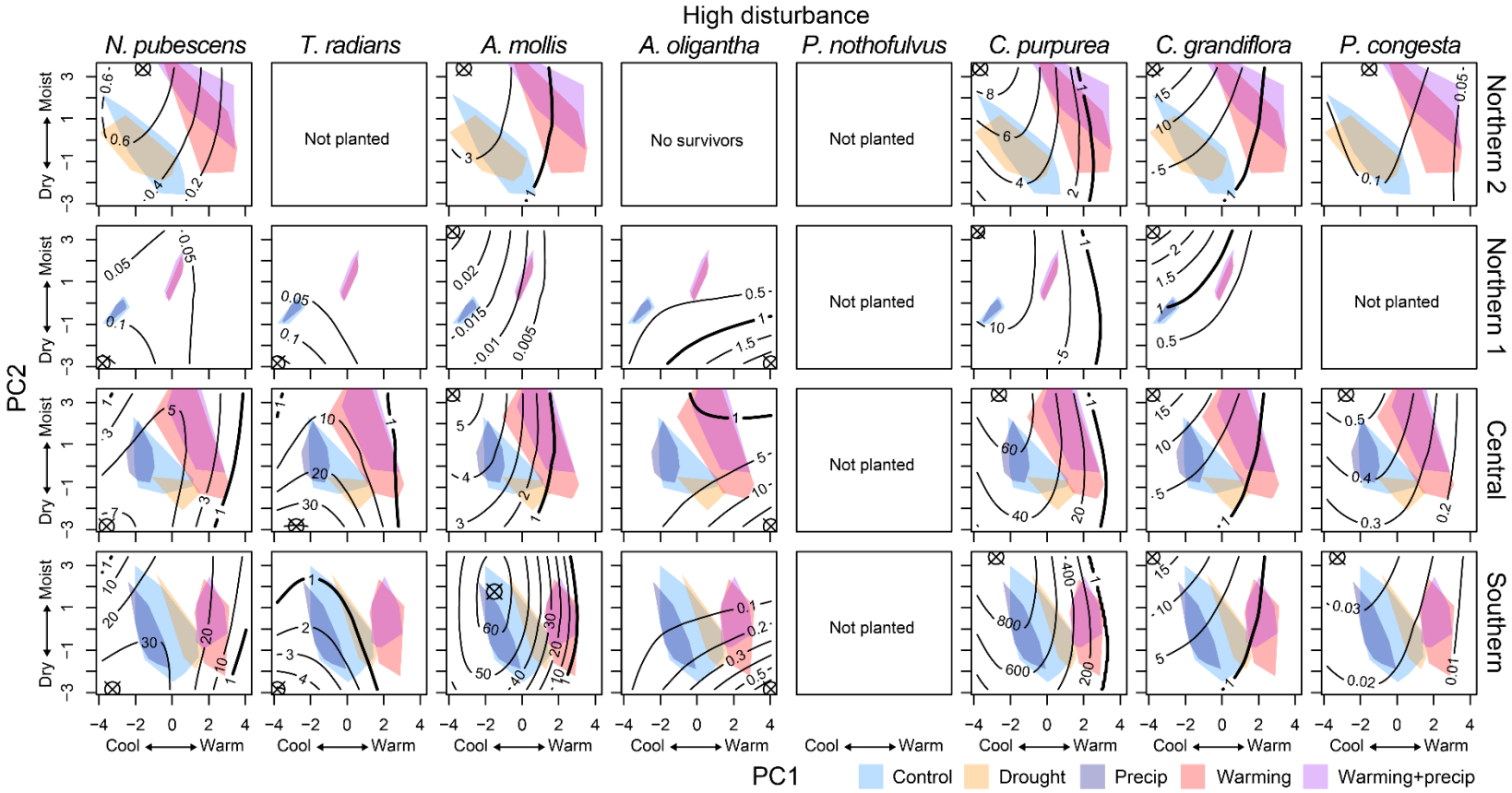

Figure S4.13. Contour plots of population growth rate (λ) as a function of climate (PC1 and PC2 axes) and site (rows) under high disturbance conditions for each of the eight focal species (columns). Climate is depicted as the first two principal components of all seven climate variables used in the study, with PC1 reflecting temperature (cooler to warmer left to right) and PC2 reflecting moisture (drier to moister bottom to top). Colored polygons depict the range of climatic conditions that occurred in each climate treatment at each site over the course of the experiments. ⊗ indicates the location where λ is highest.

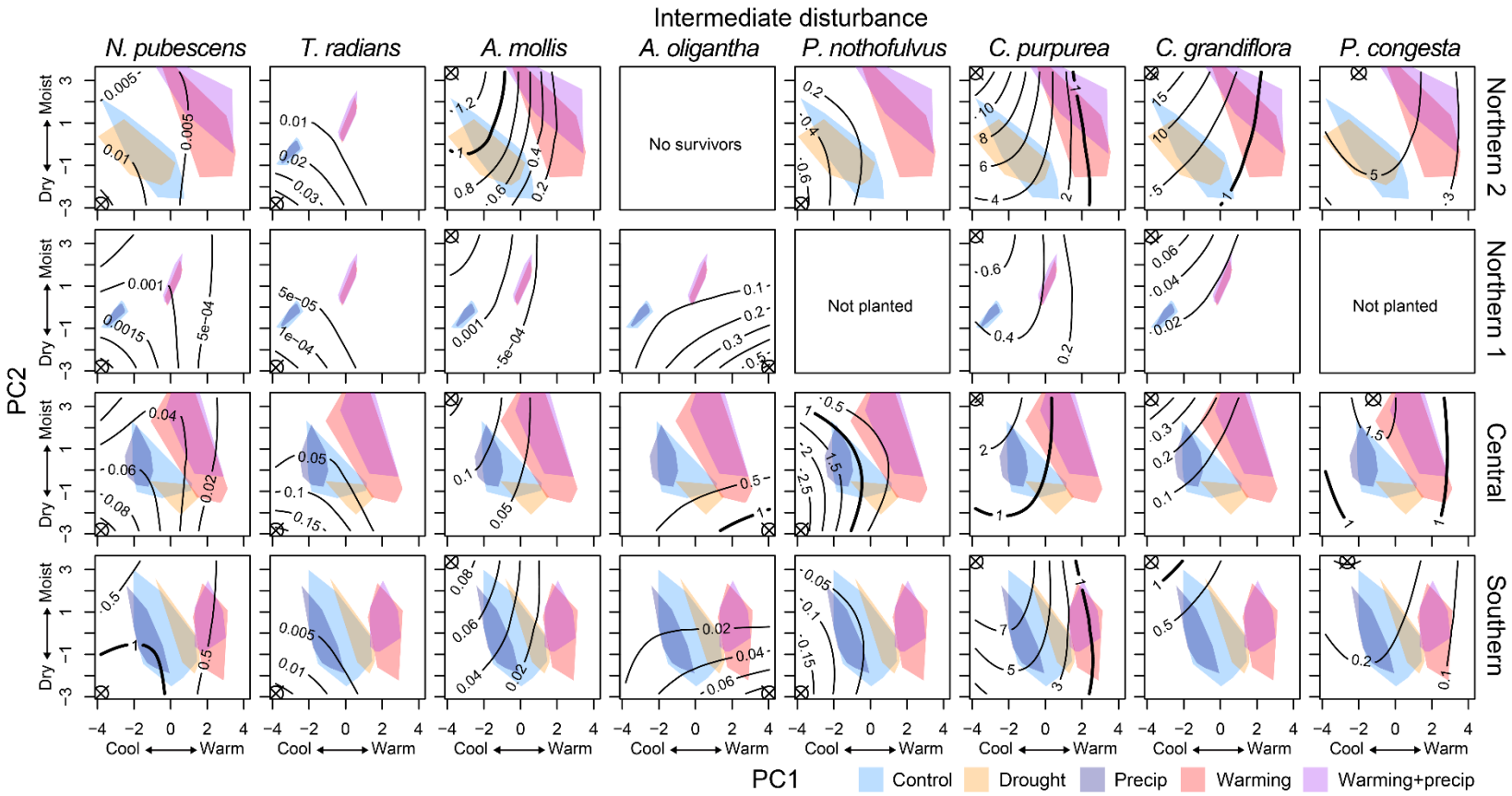

Figure S4.14. Contour plots of population growth rate (λ) as a function of climate (PC1 and PC2 axes) and site (rows) under intermediate disturbance conditions for each of the eight focal species (columns). Climate is depicted as the first two principal components of all seven climate variables used in the study, with PC1 reflecting temperature (cooler to warmer left to right) and PC2 reflecting moisture (drier to moister bottom to top). Colored polygons depict the range of climatic conditions that occurred in each climate treatment at each site over the course of the experiments. ⊗ indicates the location where λ is highest.

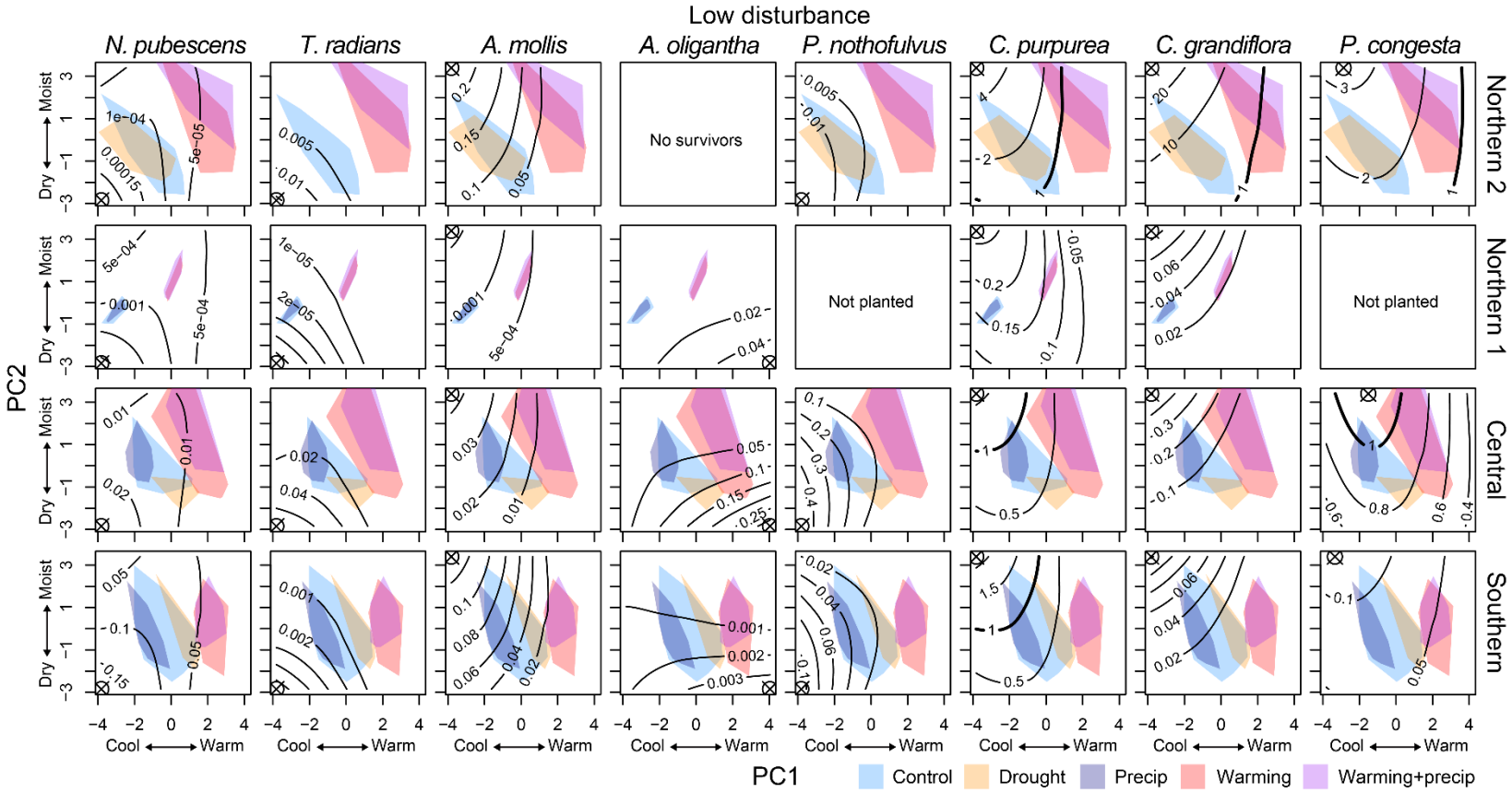

Figure S4.15. Contour plots of population growth rate (λ) as a function of climate (PC1 and PC2 axes) and site (rows) under low disturbance conditions for each of the eight focal species (columns). Climate is depicted as the first two principal components of all seven climate variables used in the study, with PC1 reflecting temperature (cooler to warmer left to right) and PC2 reflecting moisture (drier to moister bottom to top). Colored polygons depict the range of climatic conditions that occurred in each climate treatment at each site over the course of the experiments. ⊗ indicates the location where λ is highest.

Supplemental Tables

Table S4.1. Germination from the potential seedbanks in spring 2018 (potential meaning the maximum number of seeds that could still be in the seedbank, assuming no mortality). The 2nd year seedbank consists of seeds planted in fall 2016 that did not germinate in spring 2017, while the 3rd year seedbank consists of seeds planted in fall 2015 that did not germinate in spring 2016. *Germinant counts at the northern 2 site for *P. congesta*, *C. grandiflora*, and *C. purpurea* and at the central site for *P. congesta* are likely overestimated due to high seed rain from reproductive individuals in the previous spring. It is likely that seeds dropped within these subplot rings, and we therefore had low certainty that the germinants we found in these rings were from the seeds we planted in fall 2015 and 2016. *P. nothofulvus* and *T. radians* do not have 3rd year seedbank data as they were not planted in fall 2015.

	Species	**Site**	**2nd year seedbank**	**2nd year germs**	**2nd year % germ**	**3rd year seedbank**	**3rd year germs**	**3rd year % germ**
*	*P. congesta*	Northern 2	2,745	64	2.33%	2,909	12	0.41%
*	*C. grandiflora*	Northern 2	3,058	128	4.19%	3,738	66	1.77%
*	*C. purpurea*	Northern 2	3,788	32	0.84%	3,961	49	1.24%
	P. nothofulvus	Northern 2	3,942	1	0.03%	*NA*	*NA*	*NA*
	A. oligantha	Northern 2	3,818	0	0.00%	3,738	0	0.00%
	A. mollis	Northern 2	3,366	11	0.33%	3,229	2	0.06%
	T. radians	Northern 2	1,535	0	0.00%	*NA*	*NA*	*NA*
	N. pubescens	Northern 2	3,819	39	1.02%	1,838	14	0.76%
*	*P. congesta*	Central	2,155	68	3.16%	3,514	9	0.26%
	C. grandiflora	Central	3,481	19	0.55%	3,951	11	0.28%
	C. purpurea	Central	3,765	1	0.03%	3,650	9	0.25%
	P. nothofulvus	Central	3,829	14	0.37%	*NA*	*NA*	*NA*
	A. oligantha	Central	3,734	4	0.11%	2,839	5	0.18%
	A. mollis	Central	2,722	10	0.37%	3,997	0	0.00%
	T. radians	Central	1,522	2	0.13%	*NA*	*NA*	*NA*
	N. pubescens	Central	3,768	44	1.17%	3,704	5	0.13%
	P. congesta	Southern	3,660	0	0.00%	3,956	0	0.00%
	C. grandiflora	Southern	3,950	0	0.00%	3,978	1	0.03%
	C. purpurea	Southern	3,780	1	0.03%	3,959	0	0.00%
	P. nothofulvus	Southern	3,965	1	0.03%	*NA*	*NA*	*NA*
	A. oligantha	Southern	3,856	0	0.00%	2,675	0	0.00%
	A. mollis	Southern	3,960	0	0.00%	3,982	0	0.00%
	T. radians	Southern	1,569	0	0.00%	*NA*	*NA*	*NA*
	N. pubescens	Southern	3,581	7	0.20%	3,694	4	0.11%

Table S4.2. The models with the best predictive performance (lowest average mean-squared-error) for each vital rate based on *K*-fold cross-validation. The top part of the table provides coefficients, standard errors (in parentheses), and p-values, while the bottom part provides random effects. For germination and survival (binomial logistic regressions), coefficients are nontransformed log-odds values. For mean seed models, the response variable was log-transformed after adding a small constant (0.1). Categorical predictor variables (Disturbance and Site) are listed with factor level in brackets (reference levels being 'Low' disturbance and the 'Southern' site, respectively). Climate predictor variables = actual evapotranspiration (aet), climatic water deficit (cwd), precipitation (precip), and temperature (temp). 'W' and 'S' for each climate variable represent winter (November through February) and spring (March through June) values, respectively. * indicates an interaction.

Germination																
	N. pubescens		***T. radians***		***A. mollis***		***A. oligantha***		***P. nothofulvus***		***C. purpurea***		***C. grandiflora***		***P. congesta***	
Predictors	*Log-Odds*	*p*	*Log-Odds*	*p*	*Log-Odds*	*p*	*Log-Odds*	*p*	*Log-Odds*	*p*	*Log-Odds*	*p*	*Log-Odds*	*p*	*Log-Odds*	*p*
(Intercept)	-2.68 (0.09)	**<0.001**	-4.55 (0.10)	**<0.001**	-3.55 (0.17)	**<0.001**	-3.96 (0.11)	**<0.001**	-5.30 (0.31)	**<0.001**	-4.08 (0.12)	**<0.001**	-3.70 (0.13)	**<0.001**	-3.61 (0.15)	**<0.001**
Disturb. [Inter] * Site [Central]	-1.13 (0.08)	**<0.001**			1.16 (0.20)	**<0.001**	-0.24 (0.14)	0.087	1.49 (0.33)	**<0.001**	-1.59 (0.12)	**<0.001**	-0.21 (0.16)	0.191	-1.02 (0.13)	**<0.001**
Disturb. [Inter] * Site [Northern 1]	-1.18 (0.23)	**<0.001**			0.07 (0.27)	0.808	-0.11 (0.17)	0.527			-1.52 (0.11)	**<0.001**	-1.33 (0.19)	**<0.001**		
Disturb. [Inter] * Site [Northern 2]	0.05 (0.14)	0.69			2.03 (0.21)	**<0.001**	0.40 (0.19)	**0.038**	3.10 (0.48)	**<0.001**	-0.66 (0.14)	**<0.001**	-0.22 (0.16)	0.174	-0.45 (0.13)	**0.001**
Disturb. [High] * Site [Central]	-0.27 (0.07)	**<0.001**			-2.49 (0.10)	**<0.001**	-1.12 (0.10)	**<0.001**			-1.82 (0.09)	**<0.001**	-1.02 (0.10)	**<0.001**	-0.25 (0.19)	0.194
Disturb. [High] * Site [Northern 1]	-0.51 (0.15)	**0.001**			-4.78 (0.18)	**<0.001**	-1.04 (0.12)	**<0.001**			-1.78 (0.09)	**<0.001**	-1.79 (0.10)	**<0.001**		
Disturb. [High] * Site [Northern 2]	2.40 (0.11)	**<0.001**			-2.23 (0.12)	**<0.001**	-1.55 (0.15)	**<0.001**			-3.86 (0.19)	**<0.001**	-3.08 (0.12)	**<0.001**	2.24 (0.19)	**<0.001**
Site [Central]	0.56 (0.13)	**<0.001**	0.48 (0.11)	**<0.001**	0.66 (0.24)	**0.005**	1.18 (0.14)	**<0.001**	1.62 (0.56)	**0.004**	1.60 (0.16)	**<0.001**	0.58 (0.17)	**0.001**	3.19 (0.19)	**<0.001**
Site [Northern 1]	-1.49 (0.18)	**<0.001**	-3.25 (0.14)	**<0.001**	-1.25 (0.25)	**<0.001**	0.65 (0.15)	**<0.001**			2.63 (0.16)	**<0.001**	1.09 (0.17)	**<0.001**		
Site [Northern 2]	-0.75 (0.15)	**<0.001**	0.46 (0.18)	**0.013**	0.50 (0.24)	**0.042**	-0.29 (0.17)	0.098	-1.73 (0.49)	**<0.001**	1.34 (0.17)	**<0.001**	2.46 (0.17)	**<0.001**	1.73 (0.19)	**<0.001**
Disturb. [Inter]	0.97 (0.06)	**<0.001**	0.56 (0.11)	**<0.001**	-0.19 (0.19)	0.303	0.73 (0.12)	**<0.001**	-0.09 (0.30)	0.777	1.64 (0.09)	**<0.001**	0.36 (0.15)	**0.015**	1.56 (0.12)	**<0.001**
Disturb. [High]	1.39 (0.06)	**<0.001**	4.69 (0.08)	**<0.001**	4.44 (0.09)	**<0.001**	2.81 (0.09)	**<0.001**			2.91 (0.08)	**<0.001**	2.22 (0.09)	**<0.001**	-1.22 (0.18)	**<0.001**
aetW							-0.32 (0.04)	**<0.001**			0.50 (0.03)	**<0.001**				
$aetW^2$							-0.13 (0.03)	**<0.001**			-0.30 (0.02)	**<0.001**				
aetS															0.35 (0.03)	**<0.001**
$aetS^2$															-0.05 (0.01)	**<0.001**
cwdS					-1.38 (0.03)	**<0.001**							-1.16 (0.03)	**<0.001**		
$cwdS^2$					-0.51 (0.02)	**<0.001**										
precipW * tempS	0.33 (0.02)	**<0.001**							0.53 (0.18)	**0.004**						
precipS * tempW			0.18 (0.04)	**<0.001**												
precipW	-0.36 (0.02)	**<0.001**							0.19 (0.25)	0.436						
$precipW^2$									-0.11 (0.10)	0.291						
precipS			0.14 (0.05)	**0.006**												
tempW			-0.34 (0.06)	**<0.001**									0.23 (0.03)	**<0.001**	-0.27 (0.03)	**<0.001**
$tempW^2$													-0.18 (0.01)	**<0.001**		
tempS	-0.28 (0.03)	**<0.001**					0.20 (0.02)	**<0.001**	-0.65 (0.22)	**0.004**	-1.06 (0.03)	**<0.001**				
$tempS^2$	-0.24 (0.02)	**<0.001**														
Random Effects																
Residual variance (σ^2)	3.29		3.29		3.29		3.29		3.29		3.29		3.29		3.29	
Between-subject variance (τ_{00})	0.13_{plot}		0.09_{plot}		0.48_{plot}		0.10_{plot}		0.72_{plot}		0.20_{plot}		0.21_{plot}		0.24_{plot}	
Intraclass-correlation coefficient	0		0		0		0		0		0		0		0	
N	80_{plot}		80_{plot}		80_{plot}		80_{plot}		60_{plot}		80_{plot}		80_{plot}		60_{plot}	
Observations	480		420		480		480		180		480		480		240	
Marginal R^2 / Conditional R^2	0.323 / 0.323		0.553 / 0.553		0.533 / 0.534		0.293 / 0.293		0.349 / 0.350		0.345 / 0.345		0.345 / 0.345		0.437 / 0.437	

Table S4.2 (continued).

Survival																
	N. pubescens		***T. radians***		***A. mollis***		***A. oligantha***		***P. nothofulvus***		***C. purpurea***		***C. grandiflora***		***P. congesta***	
Predictors	Est.	p	Est.	p	Est.	p	Est.	p	Est.	p	Est.	p	Est.	p	Est.	p
(Intercept)	-1.00 (0.18)	**<0.001**	-2.41 (0.32)	**<0.001**	-1.21 (0.29)	**<0.001**	-0.72 (0.27)	**0.007**	0.98 (0.44)	**0.025**	-1.22 (0.22)	**<0.001**	-1.17 (0.19)	**<0.001**	-1.19 (0.27)	**<0.001**
Disturb. [Inter] * Site [Central]	-0.74 (0.19)	**<0.001**			0.01 (0.71)	0.988	-1.34 (0.32)	**<0.001**			-1.31 (0.26)	**<0.001**			0.42 (0.29)	0.153
Disturb. [Inter] * Site [Northern 1]	-2.31 (0.51)	**<0.001**			0.44 (0.82)	0.59	-0.35 (0.43)	0.417			-1.36 (0.24)	**<0.001**				
Disturb. [Inter] * Site [Northern 2]	1.00 (1.05)	0.343			0.67 (0.72)	0.352					-1.19 (0.40)	**0.003**			0.65 (0.30)	**0.033**
Disturb. [High] * Site [Central]	-0.43 (0.19)	**0.022**			-0.76 (0.28)	**0.006**	-1.42 (0.24)	**<0.001**			0.21 (0.23)	0.349			-0.06 (0.52)	0.904
Disturb. [High] * Site [Northern 1]	-3.12 (0.36)	**<0.001**			-1.62 (0.42)	**<0.001**	-2.15 (0.33)	**<0.001**			-2.78 (0.21)	**<0.001**				
Disturb. [High] * Site [Northern 2]	-0.79 (1.02)	0.438			-0.75 (0.34)	**0.025**					0.43 (0.49)	0.377			-2.48 (0.54)	**<0.001**
Site [Central]	-1.03 (0.24)	**<0.001**	1.23 (0.30)	**<0.001**	-0.51 (0.34)	0.133	1.78 (0.34)	**<0.001**			0.22 (0.28)	0.43	-0.11 (0.23)	0.651	1.35 (0.30)	**<0.001**
Site [Northern 1]	0.78 (0.36)	**0.031**	-0.51 (0.38)	0.185	0.36 (0.40)	0.371	1.42 (0.37)	**<0.001**			1.19 (0.26)	**<0.001**	0.80 (0.25)	**0.001**		
Site [Northern 2]	-4.45 (1.02)	**<0.001**	-0.12 (0.67)	0.862	0.02 (0.39)	0.959					-0.62 (0.34)	0.07	0.07 (0.26)	0.778	1.08 (0.31)	**<0.001**
Disturb. [Inter]	1.81 (0.15)	**<0.001**	0.53 (0.29)	0.07	-0.20 (0.69)	0.769	0.90 (0.28)	**0.001**			1.20 (0.21)	**<0.001**	-0.22 (0.10)	**0.03**	-0.01 (0.28)	0.96
Disturb. [High]	3.00 (0.15)	**<0.001**	0.91 (0.22)	**<0.001**	1.44 (0.25)	**<0.001**	2.02 (0.23)	**<0.001**			2.10 (0.20)	**<0.001**	0.93 (0.09)	**<0.001**	-0.52 (0.51)	0.305
aetW					0.29 (0.12)	**0.011**							0.65 (0.07)	**<0.001**		
$aetW^2$					-0.33 (0.07)	**<0.001**										
cwdS	-0.70 (0.05)	**<0.001**														
precipW * tempS			-0.83 (0.22)	**<0.001**							-0.25 (0.06)	**<0.001**				
precipS * tempW															0.15 (0.04)	**<0.001**
precipW			-0.36 (0.22)	0.103			0.02 (0.08)	0.749	0.62 (0.34)	0.067	-0.07 (0.06)	0.244				
$precipW^2$			-0.10 (0.08)	0.228			-0.26 (0.05)	**<0.001**	-1.12 (0.28)	**<0.001**						
precipS															0.05 (0.06)	0.384
tempW															-0.12 (0.08)	0.145
tempS			-1.86 (0.33)	**<0.001**	-1.20 (0.14)	**<0.001**	-0.81 (0.05)	**<0.001**	-1.91 (0.50)	**<0.001**	-0.65 (0.07)	**<0.001**	-1.67 (0.11)	**<0.001**		
Random Effects																
Residual variance (σ^2)	3.29		3.29		3.29		3.29		3.29		3.29		3.29		3.29	
Between-subject variance (τ_{00})	0.35_{plot}		0.62_{plot}		0.48_{plot}		0.58_{plot}		2.25_{plot}		0.36_{plot}		0.42_{plot}		0.30_{plot}	
Intraclass-correlation coefficient	0.01		0.02		0.01		0.01		0.13		0.01		0.01		0	
N	80_{plot}		78_{plot}		80_{plot}		60_{plot}		48_{plot}		80_{plot}		80_{plot}		60_{plot}	
Observations	424		222		329		318		81		416		399		211	
Marginal R^2 / Conditional R^2	0.518 / 0.522		0.556 / 0.563		0.296 / 0.302		0.239 / 0.248		0.523 / 0.586		0.298 / 0.304		0.387 / 0.392		0.244 / 0.246	

Table S4.2 (continued).

Seeds																
	N. pubescens		***T. radians***		***A. mollis***		***A. oligantha***		***P. nothofulvus***		***C. purpurea***		***C. grandiflora***		***P. congesta***	
Predictors	Est.	p	Est.	p	Est.	p	Est.	p	Est.	p	Est.	p	Est.	p	Est.	p
(Intercept)	1.33 (0.13)	**<0.001**	-0.49 (0.23)	**0.036**	1.77 (0.16)	**<0.001**	-1.65 (0.54)	**0.002**	1.93 (0.21)	**<0.001**	4.78 (0.14)	**<0.001**	0.51 (0.32)	0.112	2.54 (0.26)	**<0.001**
Disturb. [Inter] * Site [Central]					0.73 (0.58)	0.21	-0.32 (0.80)	0.686			0.76 (0.27)	**0.004**	-2.28 (1.12)	**0.041**	0.42 (0.33)	0.196
Disturb. [Inter] * Site [Northern 1]					0.21 (0.73)	0.78	-0.18 (0.87)	0.841			1.07 (0.26)	**<0.001**	-1.54 (1.15)	0.182		
Disturb. [Inter] * Site [Northern 2]					0.32 (0.59)	0.585					0.37 (0.21)	0.072	-2.50 (1.10)	**0.023**	0.19 (0.34)	0.579
Disturb. [High] * Site [Central]					-0.03 (0.26)	0.916	1.24 (0.59)	**0.036**			-0.82 (0.23)	**<0.001**	-0.57 (0.38)	0.134	0.07 (0.73)	0.92
Disturb. [High] * Site [Northern 1]					0.01 (0.43)	0.975	1.12 (0.68)	0.096			0.25 (0.23)	0.276	-0.24 (0.38)	0.52		
Disturb. [High] * Site [Northern 2]					-2.13 (0.27)	**<0.001**					-2.82 (0.20)	**<0.001**	-3.01 (0.36)	**<0.001**	-1.90 (0.76)	**0.013**
Site [Central]	-1.55 (0.13)	**<0.001**	1.59 (0.19)	**<0.001**	-1.44 (0.24)	**<0.001**	1.89 (0.59)	**0.001**			-1.75 (0.23)	**<0.001**	0.93 (0.35)	**0.008**	-1.04 (0.27)	**<0.001**
Site [Northern 1]	-3.55 (0.30)	**<0.001**	-1.02 (0.32)	**0.001**	-3.41 (0.30)	**<0.001**	0.90 (0.63)	0.149			-4.47 (0.22)	**<0.001**	-1.30 (0.35)	**<0.001**		
Site [Northern 2]	-2.06 (0.50)	**<0.001**	0.67 (0.30)	**0.024**	0.10 (0.25)	0.701					0.04 (0.20)	0.832	3.55 (0.33)	**<0.001**	1.08 (0.27)	**<0.001**
Disturb. [Inter]	0.68 (0.16)	**<0.001**	0.28 (0.31)	0.379	-0.06 (0.53)	0.913	1.64 (0.75)	**0.028**	0.64 (0.25)	**0.01**	-0.11 (0.14)	0.431	2.22 (1.09)	**0.042**	-0.45 (0.32)	0.154
Disturb. [High]	3.59 (0.16)	**<0.001**	2.81 (0.18)	**<0.001**	3.23 (0.19)	**<0.001**	1.12 (0.57)	0.05			3.47 (0.15)	**<0.001**	3.02 (0.35)	**<0.001**	0.46 (0.72)	0.523
aetW	0.57 (0.09)	**<0.001**														
aetS															-0.07 (0.04)	0.052
cwdS					0.03 (0.11)	0.755	0.98 (0.08)	**<0.001**			-0.07 (0.06)	0.256				
$cwdS^2$					-0.27 (0.10)	**0.007**					-0.24 (0.05)	**<0.001**				
precipS * tempS			0.53 (0.17)	**0.001**												
precipS			-0.06 (0.13)	0.633									0.18 (0.05)	**<0.001**		
$precipS^2$													-0.02 (0.02)	0.176		
tempW					0.06 (0.09)	0.496	-0.31 (0.13)	**0.017**							0.09 (0.05)	0.065
$tempW^2$															-0.09 (0.03)	**0.001**
tempS	-0.46 (0.08)	**<0.001**	-0.13 (0.16)	0.414												
Random Effects																
Residual variance (σ^2)			5.66				12.45		1.92		8.1		5.37		2.94	
Between-subject variance (τ_{00})			0.09_{plot}				0.05_{plot}		0.24_{plot}		0.13_{plot}		0.08_{plot}		0.07_{plot}	
Intraclass-correlation coefficient			0.02				0		0.11		0.02		0.01		0.02	
N			76_{plot}				60_{plot}		31_{plot}		80_{plot}		80_{plot}		55_{plot}	
Observations	278		183		221		257		49		396		330		203	
R^2 / R^2_{adj} or R^2_m / R^2_c	0.759 / 0.752		0.314 / 0.325		0.907 / 0.901		0.128 / 0.132		0.046 / 0.154		0.314 / 0.324		0.355 / 0.364		0.202 / 0.221	

Note: Seed models for *N. pubescens* and *A. mollis* were regular linear models since there were singular-fit issues when trying to include a random plot effect.

Table S4.3: The average mean-squared-error (MSE) of the best model and the two no-climate null models for each vital rate following a *K*-fold cross-validation procedure (*K* = 5). The model with the best predictive performance ("Best model") was the model with the lowest average MSE across the five folds. Null 1 = model with site x disturbance but no climate terms. Null 2 = model with site only as a fixed term. '% Reduced' columns provide the reduction in average MSE for the best models relative to the two null models.

Species	Vital rate	Avg. MSE: Best model	Avg. MSE: Null 1	Avg. MSE: Null 2	% Reduced: Null 1 - Best	% Reduced: Null 2 - Best
N. pubescens	Germination	0.0082	0.0111	0.0214	26.1%	61.8%
	Survival	0.0821	0.0897	0.1192	8.4%	31.1%
	Seeds	1494.8	2425.3	4713.9	38.4%	68.3%
T. radians	Germination	0.0013	0.0013	0.0334	4.1%	96.2%
	Survival	0.0962	0.1126	0.1296	14.6%	25.8%
	Seeds	198.3	230.2	486.0	13.9%	59.2%
A. mollis	Germination	0.0178	0.0297	0.0401	40.2%	55.7%
	Survival	0.0930	0.0997	0.1074	6.7%	13.4%
	Seeds	236.3	430.6	1297.9	45.1%	81.8%
A. oligantha	Germination	0.0026	0.0029	0.0105	10.4%	74.9%
	Survival	0.1169	0.1256	0.1419	6.9%	17.7%
	Seeds	194.4	211.2	219.1	8.0%	11.3%
P. nothofulvus	Germination	0.0005	0.0006	0.0008	9.3%	37.9%
	Survival	0.1080	0.1689	0.1638	36.1%	34.1%
	Seeds	302.6	306.7	325.3	2.5%	7.0%
C. purpurea	Germination	0.0047	0.0080	0.0136	41.2%	65.4%
	Survival	0.0796	0.0871	0.1259	8.6%	36.8%
	Seeds	182229.4	393360.6	868243.1	53.7%	79.0%
C. grandiflora	Germination	0.0060	0.0082	0.0107	26.5%	43.8%
	Survival	0.0588	0.0854	0.1069	31.1%	45.0%
	Seeds	663.0	681.5	862.0	2.7%	23.1%
P. congesta	Germination	0.0113	0.0139	0.0264	19.3%	57.4%
	Survival	0.0584	0.0593	0.0782	1.6%	25.3%
	Seeds	127.2	140.3	146.7	9.4%	13.3%

APPENDIX D

SUPPLEMENTARY INFORMATION FOR CHAPTER V

Supplemental Methods

Climate treatment implementation:

Over the course of the experiment, we regularly collected canopy temperatures (using SI-121 infrared radiometers; Campbell Scientific, Logan, Utah, USA), soil temperatures (at 10 cm depth using 107-L thermistor probes; Campbell Scientific), and volumetric water contents (at 0-30 cm depth using CS616-L water content reflectometers; Campbell Scientific) in each plot and logged these data using 30-minute averages (via AM16/32B multiplexors connected to CR1000 dataloggers; Campbell Scientific). We imposed the drought treatment using fixed rainout shelters built with clear acrylic shingles (MultiCraft Plastics, Eugene, Oregon, USA) that intercepted precipitation above 40% of the plot area. This 40% drought represents an "extreme" event for each the three sites as determined by the Precipitation Trends and Manipulation tools from Drought-Net (Lemoine *et al.* 2016), and aligns with the expectation that regional drought potential will increase with climate change (Jung & Chang 2012). The warming was achieved using six 2000-W infrared heaters per plot (Kalglo Electronics, Bethlehem, Pennsylvania, USA) with their radiation output regulated using the mean control-plot canopy temperature (Kimball *et al.* 2008). The target increase of +2.5°C is consistent with expectations for the Pacific Northwest for the end of the 21st century (Mote & Salathé 2010). During the growing season, using rainfall collected and stored on site, the warming + irrigation plots were automatically irrigated for 30 minutes each night that their volumetric water content dropped to <95% of the control plot average. This was largely successful in deconfounding warming from a reduction in soil moisture (Figure S5.2). Drought began in February 2016, warming in January, February, and June 2016 at the central, southern, and northern sites, respectively, and irrigation in September 2016 at all sites. Warming was turned off in August and September 2016 and 2017 due to fire hazard and (along with irrigation) ended permanently in July 2018.

Interpolating missing climate data:

Of the 1003 days between October 1, 2016 and June 30, 2019, canopy temperature data were missing from 5, 10, and 47 days, soil temperature data from 26, 9, and 65 days, and volumetric water content data from 26, 31, and 43 days at the southern, central, and northern sites, respectively. We filled in these missing data with predicted values using regressions described below.

We first downloaded daily site-level temperature and precipitation data for this time period from PRISM (PRISM Climate Group). Next, we determined the 'effective' climate treatment for each plot on any given day based on when warming and irrigation was active. We then aggregated all data to monthly values and eliminated values for which <20 days of the month were recorded. We assigned the actual treatment based on the effective treatment for the majority of the days in a month. For example, although

heaters were off at the central site between August and October 12, 2017 due to fire hazard, we still called the treatment 'warming' for the month of October.

We used the 'dredge' function from the MuMIn package (Barton 2020) to identify predictive models for canopy temperature, soil temperature, and volumetric water content. For canopy temperature, we built a global model containing linear and squared month terms interacting with site and PRISM temperature, as well as a three-way interaction between site, effective treatment, and PRISM temperature, with plot as a random effect. The best-supported canopy temperature model had $R^2_m = 0.969$ and $R^2_c = 0.972$ and provided highly accurate predictions of observed canopy temperature. The global model for soil temperature contained linear and squared month terms interacting with site and canopy temperature, as well as a three-way interaction between site, effective treatment, and canopy temperature, with plot as a random effect. The best-supported soil temperature model had $R^2_m = 0.983$ and $R^2_c = 0.986$ and provided highly accurate predictions of observed soil temperature. Lastly, the global model for volumetric water content included linear and squared PRISM temperature terms interacting with PRISM precipitation, as well as these terms interacting with site, effective treatment, and linear and squared month terms, with plot as a random effect. The best-supported volumetric water content model had $R^2_m = 0.852$ and $R^2_c = 0.872$ and provided good predictions of observed water content. The final set of daily soil temperature and matric potential data (averaged to the climate-treatment level) can be found in Figures S5.1 and S5.2, where dotted lines are the predictions from these regressions for the missing data and solid lines are recorded data.

Data Collection for Soil Matric Potential:

To compare moisture across sites with different soil characteristics, we calculated soil matric potential from volumetric water content and soil texture and carbon (Saxton & Rawls 2006). We collected soil from six cores at each site, dried it at 60°C for 48 h and sieved it to 2 mm, and then determined percent clay using the hydrometer method (Gee & Bauder 1986), percent sand from the weight after sieving to 53 µm, and soil carbon using a Costech Analytical Technologies 4010 elemental combustion analyzer (Valencia, CA, USA).

Supplemental Figures

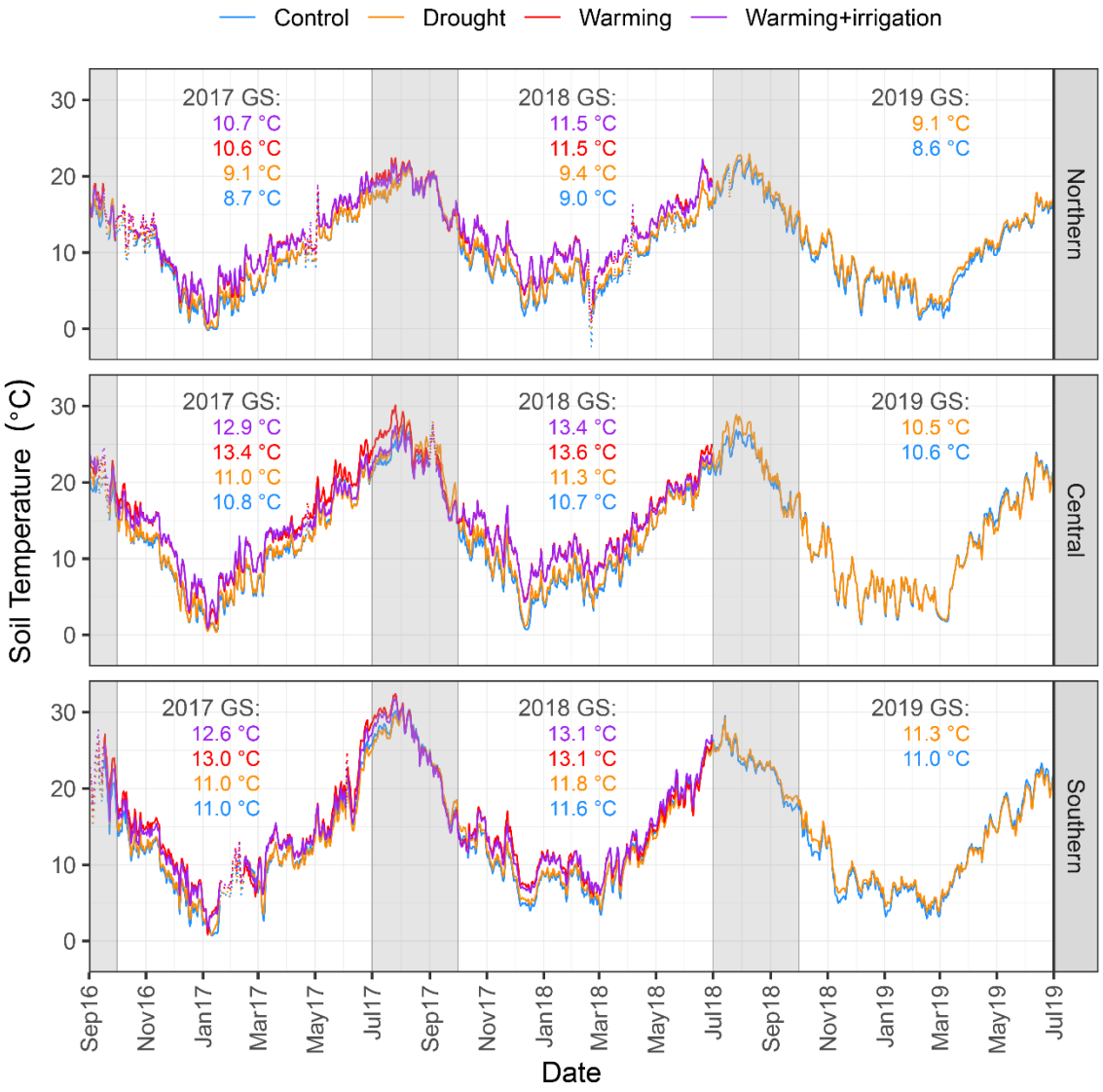

Figure S5.1. Lines indicate daily soil temperature data over the course of the study averaged to the climate-treatment level. Where lines are dotted, data were missing due to equipment malfunctions. These data were filled in with predicted values using regressions described in the supplemental methods. The text values indicate the mean growing season (Oct. 1 – Jun. 30) temperatures for each of the four treatments. Growing seasons are highlighted in white while the non-growing seasons are denoted with grey.

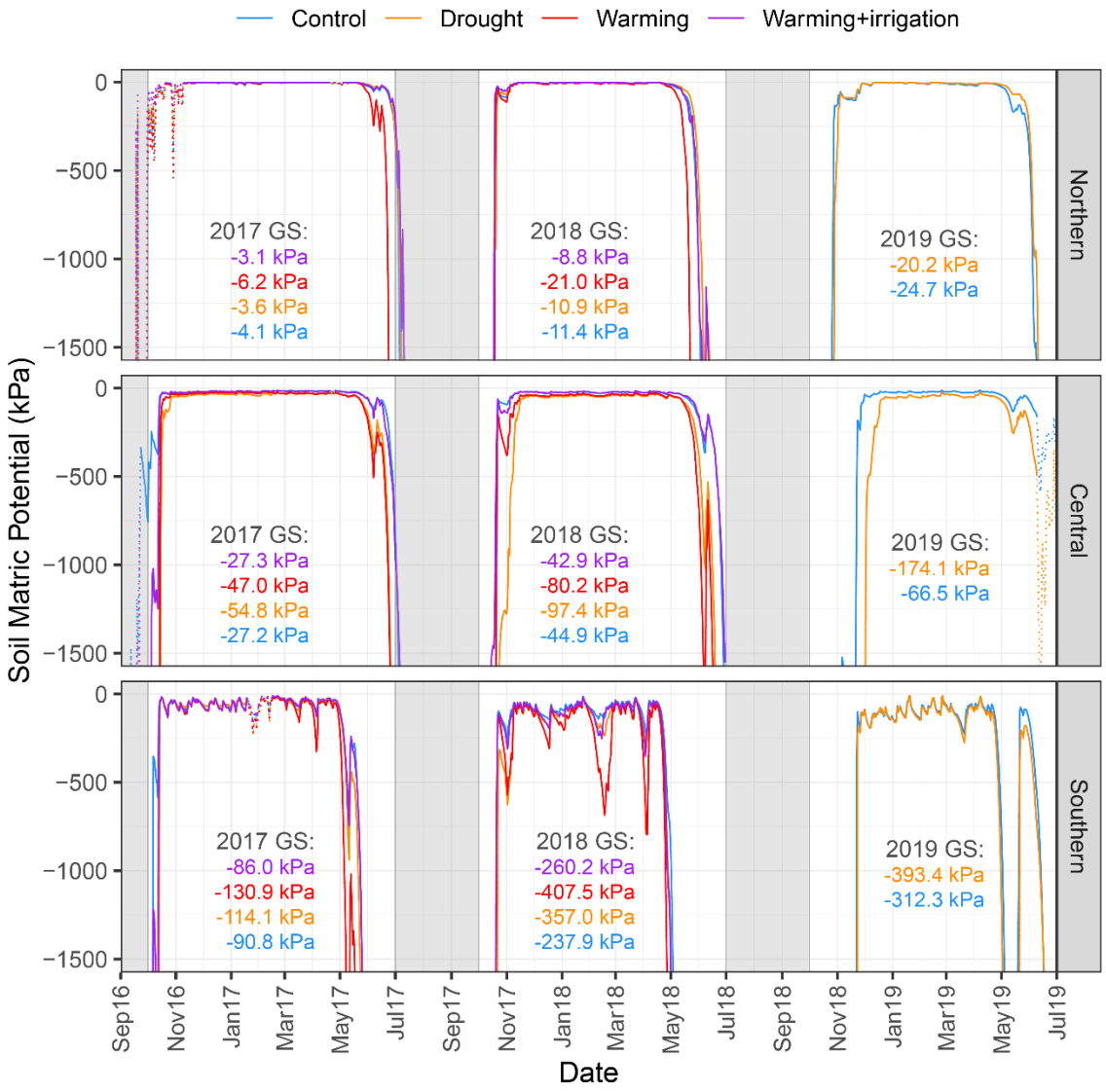

Figure S5.2. Lines indicate daily soil matric potential data over the course of the study averaged to the climate-treatment level. 0 kPa indicates saturation while -1500 kPa is the permanent wilting point. Where lines are dotted, volumetric water content data were missing due to equipment malfunctions. These data were filled in with predicted values using regressions described in the supplemental methods. The text values indicate the mean growing season (Oct. 1 – Jun. 30) soil matric potentials for each of the four treatments. Growing seasons are highlighted in white while the non-growing seasons are denoted with grey. This region is characterized by a Mediterranean-type climate, in which soils are nearly constantly saturated during the wet season and have no plant-available water during the summer drought. Matric potential was calculated using soil volumetric water content, soil % sand, % clay, and % organic matter as described in Saxton & Rawls (2006).

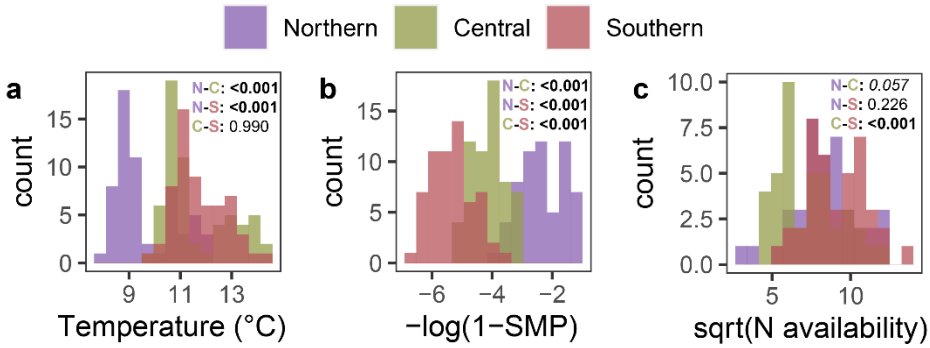

Figure S5.3. Histograms showing the distributions of mean growing season (a) soil temperature, (b) transformed soil moisture (-log[1-soil matric potential (kPa)]), and (c) square-root-transformed N availability (µg/10cm^2 strip/burial period) by site. Site had a significant effect on each variable ($p < 0.001$). Tukey's post-hoc comparisons are provided within each histogram.

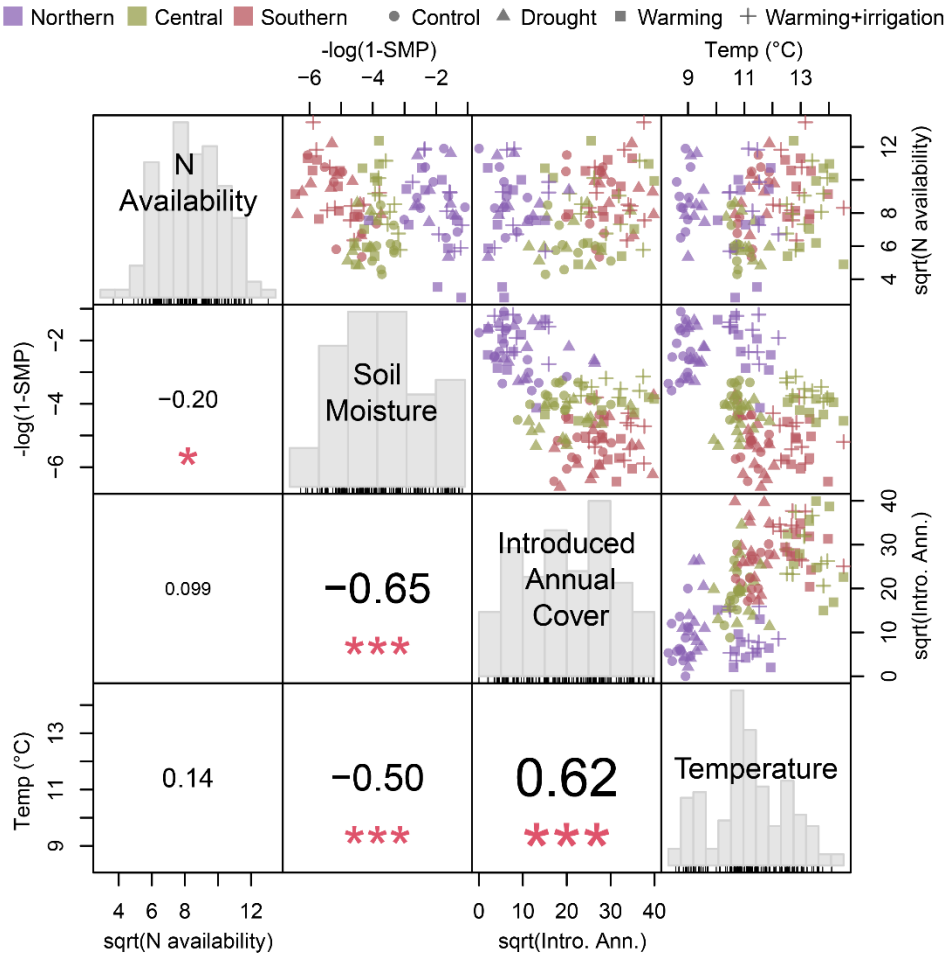

Figure S5.4. Pearson's correlation coefficients and bivariate scatterplots for the four predictor variables in the structural equation models. Axes labels indicate transformations. Stars indicate significant correlations (* <0.05, *** <0.001). SMP = soil matric potential.

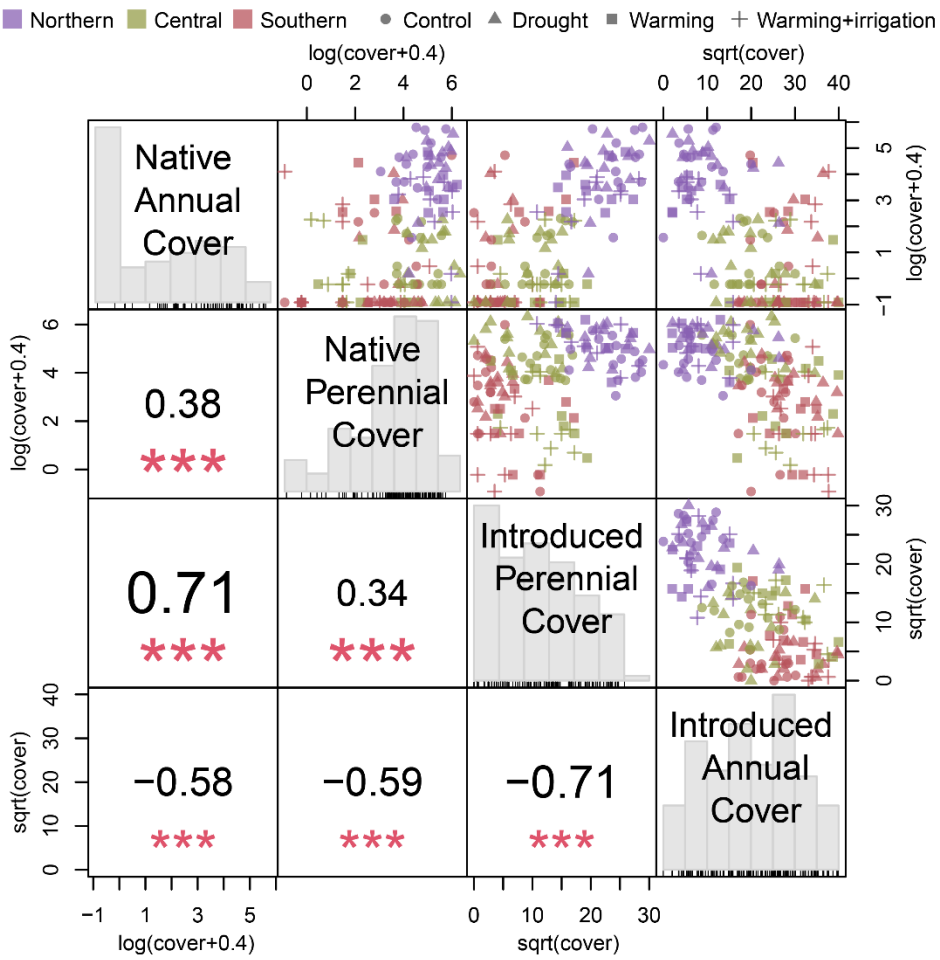

Figure S5.5. Pearson's correlation coefficients and bivariate scatterplots for the absolute cover of native annuals, native perennials, introduced perennials, and introduced annuals. Axes labels indicate transformations. Significance: *** <0.001.

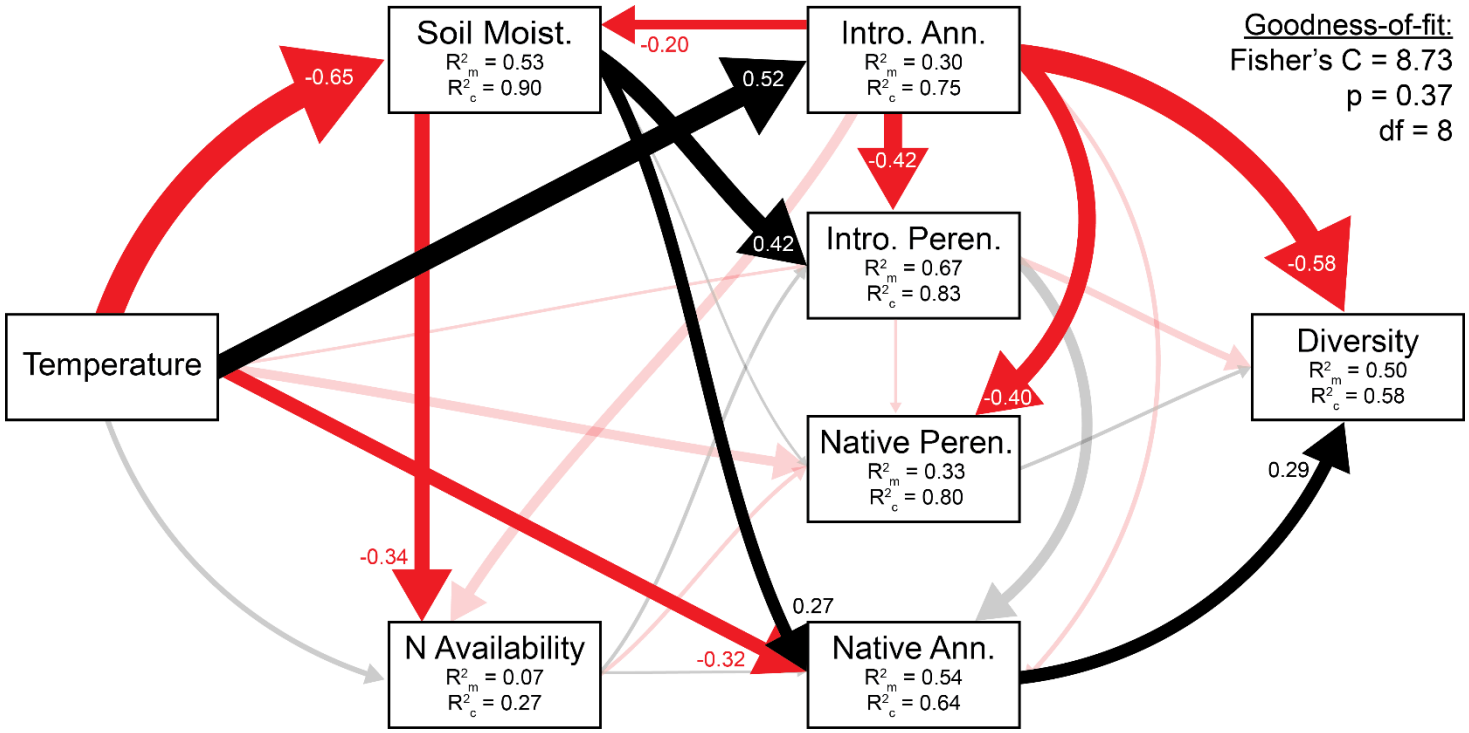

Figure S5.6. Structural equation model using 2017-2018 data (to include N availability) to determine how temperature, moisture, and nutrients control functional group cover and how functional groups control diversity. Values within/next to arrows are standardized estimates of coefficients and arrow thickness is scaled to their magnitude. Red = negative effects, black = positive effects, semi-transparent = non-significant effects ($p > 0.05$; Table S2). Within each response variable box (those at the receiving end of arrows), R^2_m provides the variance explained by the fixed effect(s) alone (boxes at the starting end of the arrows) and R^2_c provides the variance explained by both fixed and random effects (plot = random).

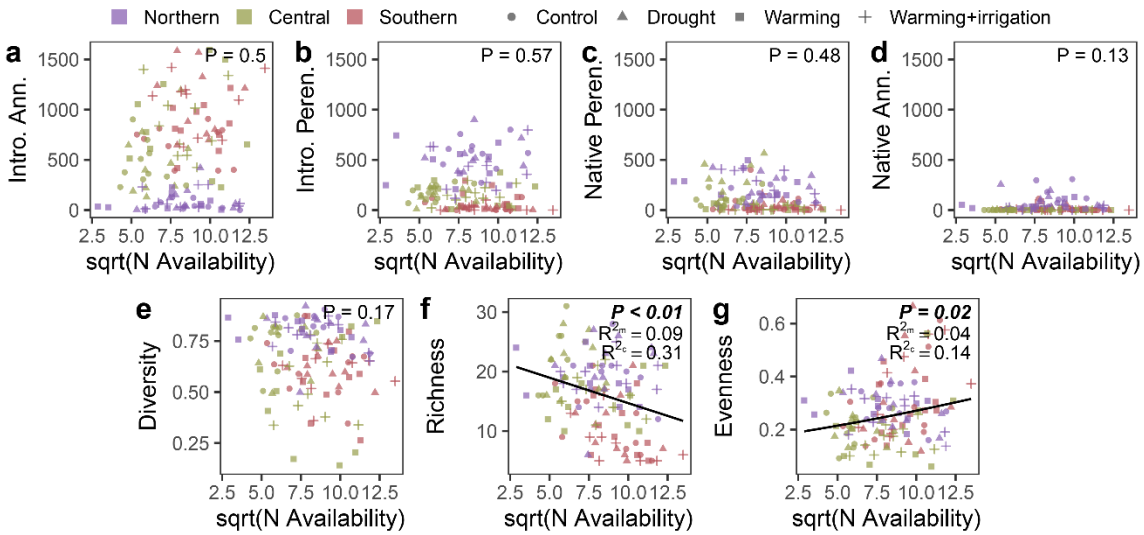

Figure S5.7. Bivariate regressions of the absolute cover of introduced annuals (a), introduced perennials (b), native perennials (c) and native annuals (d), as well as diversity (e), richness (f), and evenness (g) against mean growing season N availability (μg/10cm^2 strip/burial period), with plot as a random effect.

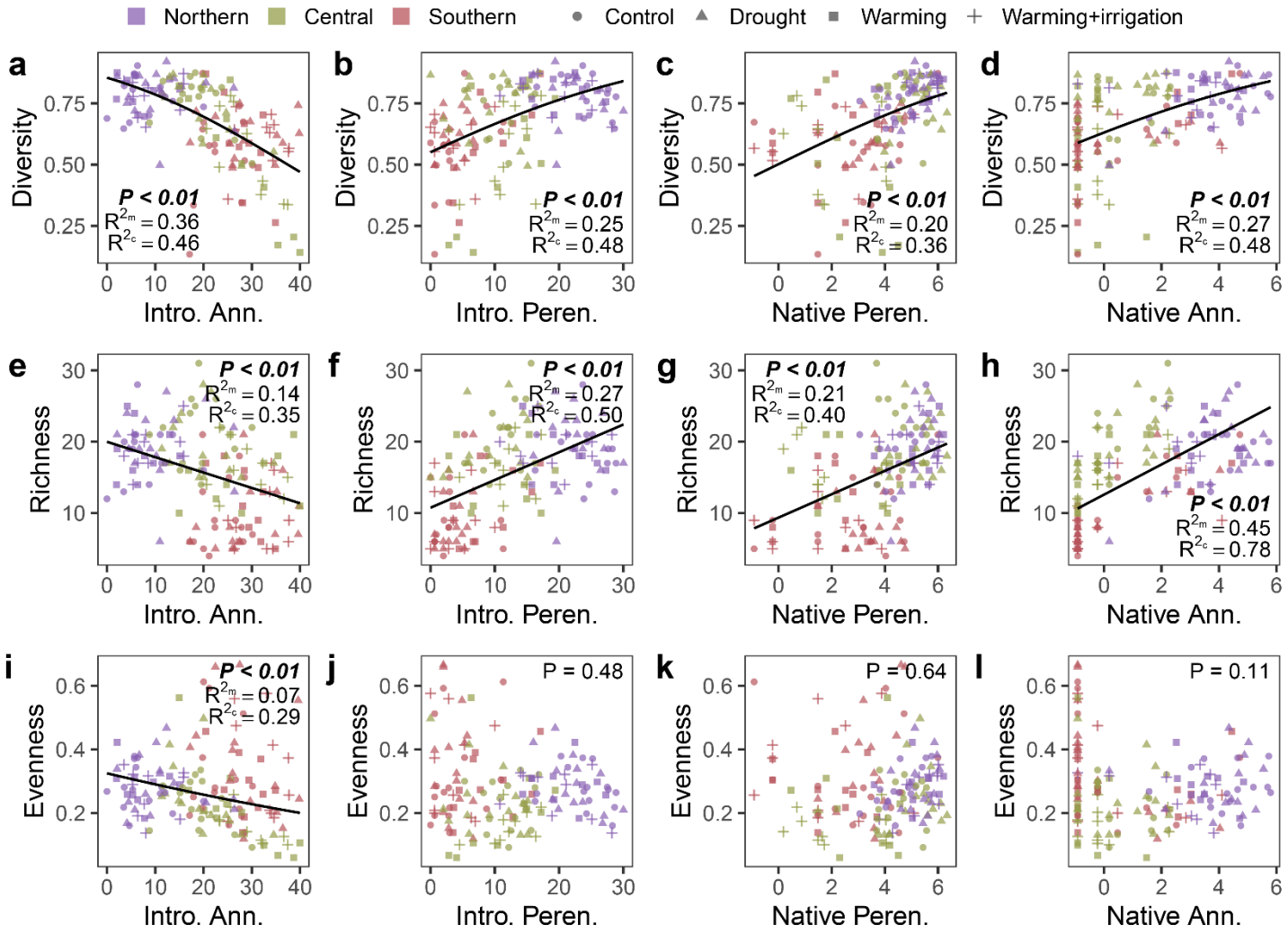

Figure S5.8. Bivariate regressions showing Simpson's index of diversity (a-d), richness (e-h), and evenness (i-l) against the (transformed) cover of the four functional groups, with plot as a random effect. See Methods for transformations.

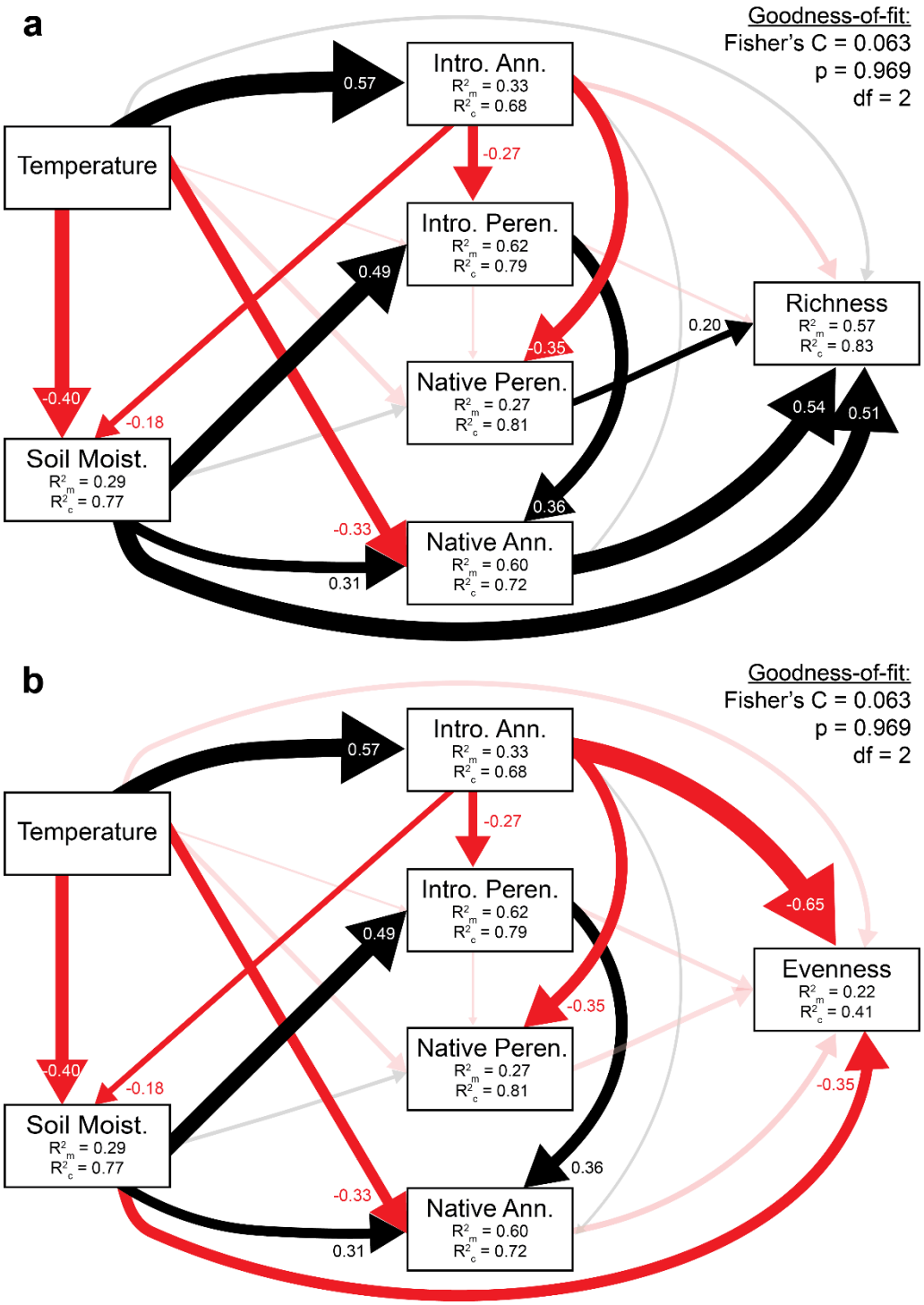

Figure S5.9. Structural equation model using 2017-2019 for richness (a) and evenness (b). Both richness and evenness had poor model fit based on our *a priori* hypotheses that they would be controlled exclusively by functional group cover, so we therefore added direct effects of soil moisture and temperature. Values within/next to arrows are standardized estimates of coefficients and arrow thickness is scaled to their magnitude. Red = negative effects, black = positive effects, semi-transparent = non-significant effects ($p > 0.05$; Table S2). Within each response variable box (those at the receiving end of

arrows), R^2_m provides the variance explained by the fixed effect(s) alone (boxes at the starting end of the arrows) and R^2_c provides the variance explained by both fixed and random effects (plot = random).

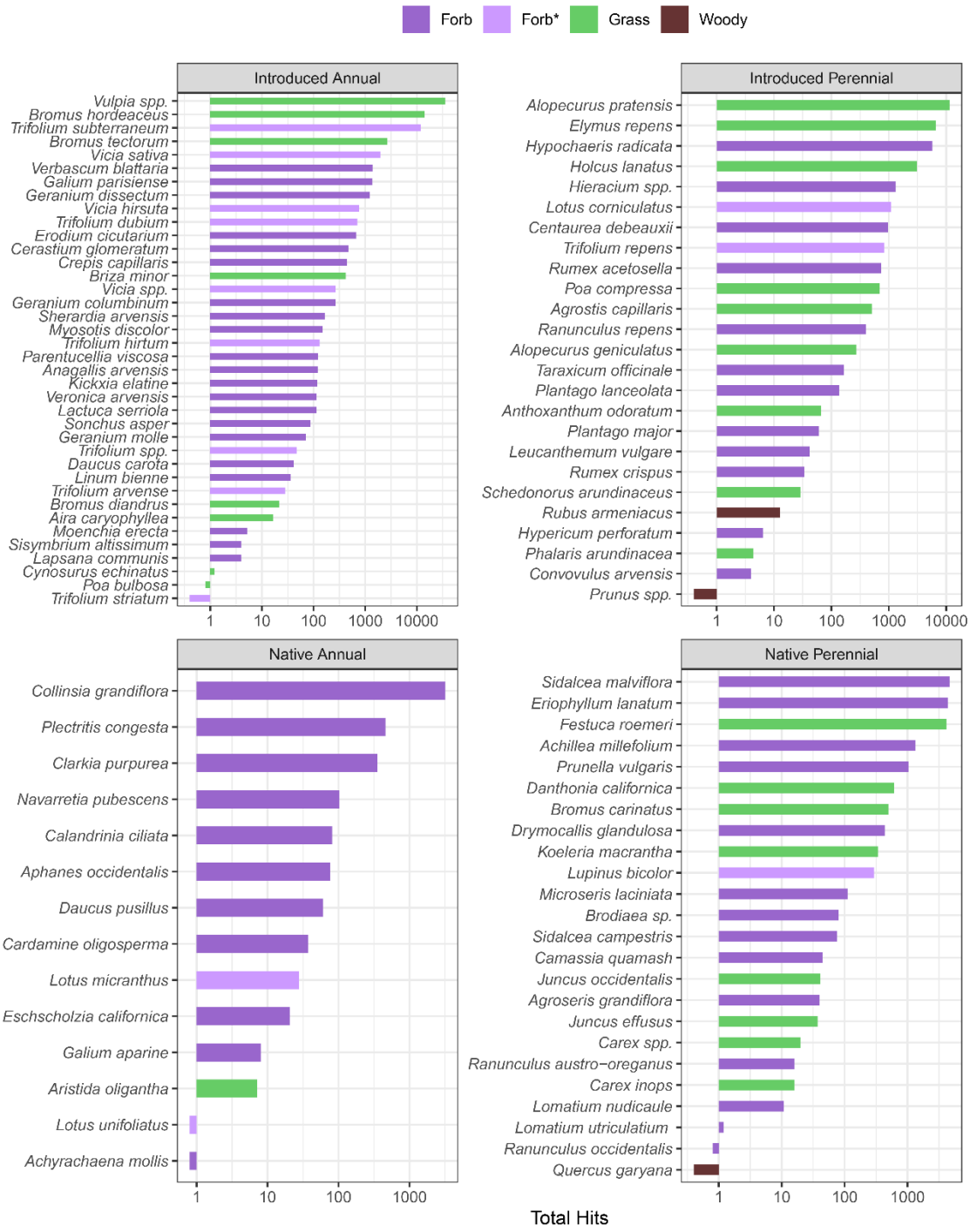

Figure S5.10. The breakdown of total hits (cover) by species across all plots and years organized into functional groups. Note the log-scale axes and different magnitudes by functional group. Forb* are legumes.

Supplemental Tables

Table S5.1. Variance inflation factors for each predictor variable in the SEMs. All variables besides temperature and richness were transformed prior to analyses (see Methods).

SEMs	Response	Temp.	Soil Moist.	Intro. Ann.	Intro. Peren.	Native Peren.	Native Ann.	N Avail.
2017-2019	Intro. Peren.	1.49	1.42	1.53	*NA*	*NA*	*NA*	*NA*
	Native Peren.	1.34	1.58	1.31	1.57	*NA*	*NA*	*NA*
	Native Ann.	1.55	2.2	1.93	2.45	*NA*	*NA*	*NA*
	Diversity	*NA*	*NA*	2.44	2.48	1.56	1.89	*NA*
	Richness	1.58	2	1.75	2	1.43	1.85	*NA*
	Evenness	1.9	2.54	2.41	2.96	1.69	2.18	*NA*
2017-2018 only	Intro. Peren.	1.75	2.15	1.83	*NA*	*NA*	*NA*	1.11
	Native Peren.	1.76	2.32	1.78	1.99	*NA*	*NA*	1.16
	Native Ann.	1.76	2.96	2.89	3.06	*NA*	*NA*	1.08
	Diversity	1.75	1.62	3.4	*NA*	*NA*	*NA*	2.81

Table S5.2. Summary results of the structural equation model using only 2017 and 2018 data to include N availability. All variables besides temperature and richness were transformed prior to analyses (see Methods).

Response	Predictor	Est.	Std. Err.	DF	Crit. Value	P-val.	Std. Est.
Intro. Ann.	Temperature	3.878	0.64	82	36	<**0.001**	0.525
Soil Moist.	Temperature	-0.611	0.081	114.9	55.5	<**0.001**	-0.646
Soil Moist.	Intro. Ann.	-0.026	0.01	110.1	6.7	**0.011**	-0.199
N availability	Temperature	0.122	0.188	67.2	0.4	0.519	0.086
N availability	Soil Moist.	-0.515	0.222	104.5	5.3	**0.024**	-0.341
N availability	Intro. Ann.	-0.042	0.028	115.7	2.1	0.146	-0.216
Intro. Peren.	Temperature	-0.109	0.424	71.3	0.1	0.799	-0.021
Intro. Peren.	Soil Moist.	2.364	0.474	108.6	24.3	<**0.001**	0.419
Intro. Peren.	N availability	0.142	0.181	107	0.6	0.44	0.038
Intro. Peren.	Intro. Ann.	-0.301	0.056	113.1	27.9	<**0.001**	-0.416
Native Peren.	Temperature	-0.236	0.138	80.7	2.9	*0.094*	-0.192
Native Peren.	Soil Moist.	0.015	0.151	113.7	0	0.924	0.011
Native Peren.	N availability	-0.04	0.049	88.5	0.7	0.422	-0.046
Native Peren.	Intro. Ann.	-0.067	0.017	94.2	15	<**0.001**	-0.402
Native Peren.	Intro. Peren.	-0.005	0.026	104.7	0	0.858	-0.021
Native Ann.	Temperature	-0.444	0.129	64.7	11.7	**0.001**	-0.316
Native Ann.	Soil Moist.	0.399	0.175	100.4	5.1	**0.026**	0.269
Native Ann.	N availability	0.012	0.064	114	0	0.859	0.012
Native Ann.	Intro. Ann.	-0.012	0.022	113.4	0.3	0.595	-0.063
Native Ann.	Intro. Peren.	0.058	0.032	104.3	3.3	*0.074*	0.221
Diversity	Intro. Ann.	0.113	0.035	114.9	10.1	**0.002**	0.289
Diversity	Intro. Peren.	0.016	0.04	85.3	0.2	0.686	0.037
Diversity	Native Peren.	-0.013	0.012	101.7	1.2	0.281	-0.129
Diversity	Native Ann.	-0.043	0.01	115	19.7	<**0.001**	-0.581

Table S5.3. Summary results of structural equation models using 2017-2019 data (without N availability). All variables besides temperature and richness were transformed prior to analyses (see Methods).

Response	Predictor	Est.	Std. Err.	DF	Crit. Value	P-val.	Std. Est.
Intro. Ann.	Temperature	3.915	0.568	79.6	46.9	<**0.001**	0.568
Soil Moist.	Temperature	-0.376	0.088	120.8	17.9	<**0.001**	-0.401
Soil Moist.	Intro. Ann.	-0.024	0.01	140.5	5.4	**0.022**	-0.177
Intro. Peren.	Temperature	-0.295	0.398	92.7	0.5	0.465	-0.053
Intro. Peren.	Soil Moist.	2.958	0.388	138.3	56.9	<**0.001**	0.495
Intro. Peren.	Intro. Ann.	-0.219	0.053	142	17.1	<**0.001**	-0.27
Native Peren.	Temperature	-0.177	0.109	119.5	2.6	0.111	-0.155
Native Peren.	Soil Moist.	0.13	0.106	135.3	1.5	0.224	0.107
Native Peren.	Intro. Ann.	-0.058	0.012	117.8	22.6	<**0.001**	-0.349
Native Peren.	Intro. Peren.	-0.012	0.019	130.9	0.4	0.522	-0.06
Native Ann.	Temperature	-0.467	0.112	86.3	17.2	<**0.001**	-0.325
Native Ann.	Soil Moist.	0.471	0.137	141.4	11.6	<**0.001**	0.307
Native Ann.	Intro. Ann.	0.016	0.017	143.8	0.9	0.354	0.076
Native Ann.	Intro. Peren.	0.092	0.025	141.5	13.7	<**0.001**	0.36
Diversity	Intro. Ann.	-0.03	0.008	145	12.6	<**0.001**	-0.374
Diversity	Intro. Peren.	0	0.011	128.5	0	0.975	-0.003
Diversity	Native Peren.	0.061	0.04	96.7	2.3	0.136	0.128
Diversity	Native Ann.	0.11	0.034	144.5	10	**0.002**	0.291
Richness	Temperature	0.395	0.396	116.9	1	0.326	0.096
Richness	Soil Moist.	2.249	0.423	142.6	27.6	<**0.001**	0.51
Richness	Intro. Ann.	0.088	0.051	124.6	3	*0.088*	0.146
Richness	Intro. Peren.	-0.059	0.074	135.4	0.6	0.438	-0.079
Richness	Native Peren.	0.709	0.301	138.2	5.4	**0.021**	0.197
Richness	Native Ann.	1.542	0.232	129.8	43.3	<**0.001**	0.536
Evenness	Temperature	-0.063	0.049	94.1	1.7	0.201	-0.152
Evenness	Soil Moist.	-0.152	0.058	133.1	6.7	**0.011**	-0.346
Evenness	Intro. Ann.	-0.039	0.008	142.7	25.9	<**0.001**	-0.647
Evenness	Intro. Peren.	-0.01	0.011	142.3	0.8	0.369	-0.132
Evenness	Native Peren.	-0.06	0.039	109	2.3	0.131	-0.166
Evenness	Native Ann.	-0.053	0.034	142.4	2.4	0.125	-0.184

Table S5.4. Bivariate regression results. All variables besides temperature and richness were transformed prior to analyses (see Methods). R^2_m = marginal R^2; R^2_c = conditional R^2. τ_{00} plot = variance by random plot effect; σ^2 = residual variance.

Response	Predictor	N	Estimate	SE	P-val.	R^2_m	R^2_c	τ_{00} plot	σ^2
Introduced	Temperature	150	3.915	0.568	**<0.001**	0.333	0.683	36.40	32.95
Annual	Soil moist.	150	-3.900	0.539	**<0.001**	0.315	0.582	25.64	40.08
Cover	N supply	120	-0.194	0.289	0.502	0.001	0.815	101.52	23.03
Introduced	Temperature	150	-1.908	0.497	**<0.001**	0.133	0.788	40.62	13.16
Perennial	Soil moist.	150	3.653	0.361	**<0.001**	0.471	0.763	16.41	13.36
Cover	N supply	120	-0.103	0.182	0.571	0.001	0.862	55.44	8.86
Native	Temperature	150	-0.385	0.104	**<0.001**	0.124	0.795	1.81	0.56
Perennial	Soil moist.	150	0.224	0.092	**0.015**	0.035	0.820	2.25	0.51
Cover	N supply	120	-0.031	0.044	0.477	0.001	0.847	2.85	0.52
Native	Temperature	150	-0.867	0.112	**<0.001**	0.367	0.603	1.10	1.84
Annual	Soil moist.	150	1.034	0.109	**<0.001**	0.444	0.704	1.24	1.42
Cover	N supply	120	-0.124	0.082	0.129	0.016	0.477	2.07	2.35
	Temperature	150	-0.264	0.046	**<0.001**	0.230	0.459	0.16	0.37
	Soil moist.	150	0.291	0.048	**<0.001**	0.241	0.519	0.19	0.34
	N supply	120	-0.046	0.034	0.171	0.014	0.347	0.23	0.44
Diversity	Intro. Ann.	150	-0.047	0.005	**<0.001**	0.363	0.455	0.06	0.36
	Intro. Peren.	150	0.049	0.008	**<0.001**	0.245	0.482	0.16	0.36
	Native Peren.	150	0.211	0.038	**<0.001**	0.202	0.362	0.11	0.42
	Native Ann.	150	0.195	0.028	**<0.001**	0.267	0.480	0.14	0.35
	Temperature	150	-1.735	0.373	**<0.001**	0.173	0.475	11.88	20.64
	Soil moist.	150	3.251	0.326	**<0.001**	0.468	0.716	11.14	12.73
	N supply	120	-0.855	0.247	**0.001**	0.088	0.313	8.49	26.01
Richness	Intro. Ann.	150	-0.216	0.049	**<0.001**	0.136	0.354	8.05	23.77
	Intro. Peren.	150	0.389	0.060	**<0.001**	0.274	0.497	8.72	19.68
	Native Peren.	150	1.637	0.287	**<0.001**	0.212	0.401	7.06	22.47
	Native Ann.	150	2.115	0.189	**<0.001**	0.448	0.785	15.75	10.05
	Temperature	150	-0.046	0.038	0.222	0.012	0.193	0.07	0.32
	Soil moist.	150	-0.078	0.040	**0.049**	0.030	0.228	0.08	0.30
	N supply	120	0.062	0.026	**0.019**	0.044	0.138	0.04	0.34
Evenness	Intro. Ann.	150	-0.016	0.005	**0.002**	0.071	0.294	0.09	0.28
	Intro. Peren.	150	-0.005	0.007	0.481	0.004	0.195	0.07	0.32
	Native Peren.	150	0.015	0.032	0.640	0.002	0.192	0.07	0.32
	Native Ann.	150	-0.041	0.025	0.110	0.019	0.262	0.10	0.30

REFERENCES CITED

CHAPTER I

Bayly, M. J., & Angert, A. L. (2019). Niche models do not predict experimental demography but both suggest dispersal limitation across the northern range limit of the scarlet monkeyflower (Erythranthe cardinalis). *Journal of Biogeography*, *46*(7), 1316–1328. https://doi.org/10.1111/jbi.13609

Boyd, R. (1999). Indians, fire, and the land. In *Oregon State University Press*. Retrieved from https://ecoshare.info/uploads/ccamp/synthesis_paper_tools/huckleberry/Boyd_1999.pdf

Brooker, R. W. (2006). Plant-plant interactions and environmental change. *New Phytologist*, *171*(2), 271–284. Retrieved from http://onlinelibrary.wiley.com/doi/10.1111/j.1469-8137.2006.01752.x/abstract

Chen, I.-C., Hill, J. K., Ohlemuller, R., Roy, D. B., & Thomas, C. D. (2011). Rapid range shifts of species associated with high levels of climate warming. *Science*, *333*, 1024–1026.

Cleland, E. E., Chuine, I., Menzel, A., Mooney, H. A., & Schwartz, M. D. (2007). Shifting plant phenology in response to global change. *Trends in Ecology and Evolution*, *22*(7), 357–365. https://doi.org/10.1016/j.tree.2007.04.003

Dai, A. (2013). Increasing drought under global warming in observations and models. *Nature Climate Change*, *3*, 52–58. https://doi.org/10.1038/NCLIMATE1633

Dalton, M., & Fleishman, E. (2021). *Fifth Oregon Climate Assessment*. Retrieved from https://blogs.oregonstate.edu/occri/oregon-climate-assessments/

Dennehy, C., Alverson, E. R., Anderson, H. E., Clements, D. R., Gilbert, R., & Kaye, T. N. (2011). Management strategies for invasive plants in Pacific Northwest prairies, savannas, and oak woodlands. *Northwest Science*, *85*(2), 329–351. https://doi.org/10.3955/046.085.0219

Dunwiddie, P. W., & Bakker, J. D. (2011). The future of restoration and management of prairie-oak ecosystems in the Pacific Northwest. *Northwest Science*, *85*(2), 83–92. https://doi.org/10.3955/046.085.0201

Hargreaves, A. L., Samis, K. E., & Eckert, C. G. (2014). Are species' range limits simply niche limits writ large? A review of transplant experiments beyond the range. *The American Naturalist*, *183*(2), 157–173. https://doi.org/10.1086/674525

Inouye, D. W. (2008). Effects of climate change on phenology, frost damage, and floral abundance of montane wildflowers. *Ecology*, *89*(2), 353–362.

Inouye, D. W. (2008). Effects of climate change on phenology, frost damage, and floral abundance of montane wildflowers. *Ecology*, *89*(2), 353–362.

IPCC, 2014: Climate Change 2014: Synthesis Report. Contributions of Working Groups I, II, and II to the Fifth Assessment Report of the Intergovernmental Panel on Climate Change [Core Writing Team, R.K. Pachauri and L.A. Meyers (eds.)]. IPCC, Geneva, Switzerland, 151 pp.

IPCC, 2018: Summary for Policymakers. In: Global Warming of 1.5°C. An IPCC Special Report on the impacts of global warming of 1.5°C above pre-industrial levels and related global greenhouse gas emission pathways, in the context of strengthening the global response to the threat of climate change, sustainable development, and efforts to eradicate poverty [Masson-Delmotte, V., P. Zhai, H.-O. Pörtner, D. Roberts, J. Skea, P.R. Shukla, A. Pirani, W. Moufouma-Okia, C. Péan, R. Pidcock, S. Connors, J.B.R. Matthews, Y. Chen, X. Zhou, M.I. Gomis, E. Lonnoy, T. Maycock, M. Tignor, and T. Waterfield (eds.)]. World Meteorological Organization, Geneva, Switzerland, 32 pp.

Jung, I. W., & Chang, H. (2012). Climate change impacts on spatial patterns in drought risk in the Willamette River Basin, Oregon, USA. *Theoretical and Applied Climatology*, *108*, 355–371.

Koteen, L. E., Baldocchi, D. D., & Harte, J. (2011). Invasion of non-native grasses causes a drop in soil carbon storage in California grasslands. *Environmental Research Letters*, *6*(4). https://doi.org/10.1088/1748-9326/6/4/044001

Kottek, M., Grieser, J., Beck, C., Rudolf, B., & Rubel, F. (2006). World map of the Köppen-Geiger climate classification updated. *Meteorologische Zeitschrift*, *15*(3), 259–263. https://doi.org/10.1127/0941-2948/2006/0130

Kremen, C. (2005). Managing ecosystem services: What do we need to know about their ecology? *Ecology Letters*, *8*(5), 468–479. https://doi.org/10.1111/j.1461-0248.2005.00751.x

Lemoine, N. P., Sheffield, J., Dukes, J. S., Knapp, A. K., & Smith, M. D. (2016). Terrestrial Precipitation Analysis (TPA): A resource for characterizing long-term precipitation regimes and extremes. *Methods in Ecology and Evolution*, *7*(11), 1396–1401. https://doi.org/10.1111/2041-210X.12582

MacArthur, R. H. (1972). *Geographic Ecology* (H. and Row, ed.). New York, NY.

McLaren, J. R., & Turkington, R. (2010). Ecosystem properties determined by plant functional group identity. *Journal of Ecology*, *98*(2), 459–469. https://doi.org/10.1111/j.1365-2745.2009.01630.x

Miller-Rushing, A. J., Høye, T. T., Inouye, D. W., & Post, E. (2010). The effects of phenological mismatches on demography. *Philosophical Transactions of the Royal Society B*, *365*, 3177–3186. https://doi.org/10.1098/rstb.2010.0148

Miller, M. E., Belote, R. T., Bowker, M. A., & Garman, S. L. (2011). Alternative states of a semiarid grassland ecosystem: Implications for ecosystem services. *Ecosphere*, *2*(5), 1–18. https://doi.org/10.1890/ES11-00027.1

Mote, P. W., & Salathé, E. P. (2010). Future climate in the Pacific Northwest. *Climatic Change*, *102*(1), 29–50. https://doi.org/10.1007/s10584-010-9848-z

Noss, R. F., LaRoe, E. T., & Scott, J. M. (1995). *Endangered ecosystems of the United States: A preliminary assessment of loss and degradation*.

Pendergrass, A. G., Knutti, R., Lehner, F., Deser, C., & Sanderson, B. M. (2017). Precipitation variability increases in a warmer climate. *Scientific Reports*, *7*(1), 1–9. https://doi.org/10.1038/s41598-017-17966-y

Pereira, H. M., Leadley, P. W., Proença, V., Alkemade, R., Scharlemann, J. P. W., Fernandez-Manjarrés, J. F., … Walpole, M. (2010). Scenarios for global biodiversity in the 21st century. *Science*, *330*, 1496–1501.

Rehm, E. M., Olivas, P., Stroud, J., & Feeley, K. J. (2015). Losing your edge: Climate change and the conservation value of range-edge populations. *Ecology and Evolution*, *5*(19), 4315–4326. https://doi.org/10.1002/ece3.1645

Sinclair, M., Alverson, E., Dunn, P., Dunwiddie, P., & Gray, E. (2006). Bunchgrass Prairies. In D. Apostol, M. Sinclair, & E. Higgs (Eds.), *Restoring the Pacific Northwest: The Art and Science of Ecological Restoration in Cascadia* (pp. 22–62). Washington, DC: Island Press.

Thomas, C. D. (2010). Climate, climate change and range boundaries. *Diversity and Distributions*, *16*(3), 488–495. https://doi.org/10.1111/j.1472-4642.2010.00642.x

Vitt, P., Havens, K., Kramer, A. T., Sollenberger, D., & Yates, E. (2010). Assisted migration of plants: Changes in latitudes, changes in attitudes. *Biological Conservation*, *143*(1), 18–27. https://doi.org/10.1016/j.biocon.2009.08.015

Walther, G.-R. (2010). Community and ecosystem responses to recent climate change. *Philosophical Transactions of the Royal Society B: Biological Sciences*, *365*(1549), 2019–2024. https://doi.org/10.1098/rstb.2010.0021

Wang, Y., Fang, Q., Dissanayake, S. T. M., & Önal, H. (2020). Optimizing conservation planning for multiple cohabiting species. *PLoS ONE*, *15*(6), 1–14. https://doi.org/10.1371/journal.pone.0234968

CHAPTER II

Amano, T., Smithers, R. J., Sparks, T. H., & Sutherland, W. J. (2010). A 250-year index of first flowering dates and its response to temperature changes. *Proceedings of the Royal Society B: Biological Sciences*, *277*(1693), 2451–2457.

Bachelet, D., Johnson, B. R., Bridgham, S. D., Dunn, P. V, Anderson, H. E., & Rogers, B. M. (2011). Climate change impacts on western Pacific Northwest prairies and savannas. *Northwest Science*, *85*(2), 411–429.

Barton, K. 2018. MuMIn: Multi-Model Inference. R package version 1.40.4. https://CRAN.R-project.org/package=MuMIn.

Bernal, M., Estiarte, M., & Peñuelas, J. (2011). Drought advances spring growth phenology of the Mediterranean shrub Erica multiflora. *Plant Biology*, *13*(2), 252–257.

Burnham, K. P., & Anderson, D. R. (2002). *Model selection and multimodel inference: a practical information-theoretic approach (second edition)*. *Ecological Modelling* (Vol. 172).

Chuine, I., & Beaubien, E. G. (2001). Phenology is a major determinant of tree species range. *Ecology Letters*, *4*, 500–510.

Cleland, E. E., Chuine, I., Menzel, A., Mooney, H. A., & Schwartz, M. D. (2007). Shifting plant phenology in response to global change. *Trends in Ecology and Evolution*, *22*(7), 357–365.

Crawford, R., & Hall, H. (1997). *Changes in the south Puget prairie landscape*. In P. Dunn and K. Ewing (editors), Ecology and Conservation of the South Puget Sound Prairie Landscape. The Nature Conservancy, Seattle, Washington, 11-15.

Crimmins, T. M., Crimmins, M. A., & David Bertelsen, C. (2010). Complex responses to climate drivers in onset of spring flowering across a semi-arid elevation gradient. *Journal of Ecology*, *98*(5), 1042–1051.

Cui, T., Martz, L., & Guo, X. (2017). Grassland phenology response to drought in the Canadian prairies. *Remote Sensing*, *9*(1258), 1–21.

Dennehy, C., Alverson, E. R., Anderson, H. E., Clements, D. R., Gilbert, R., & Kaye, T. N. (2011). Management Strategies for Invasive Plants in Pacific Northwest Prairies, Savannas, and Oak Woodlands. *Northwest Science*, *85*(2).

Diez, J. M., Ibáñez, I., Miller-Rushing, A. J., Mazer, S. J., Crimmins, T. M., Crimmins, M. A., … Inouye, D. W. (2012). Forecasting phenology: From species variability to community patterns. *Ecology Letters*, *15*(6), 545–553.

Dunne, J. A., Harte, J., & Taylor, K. J. (2003). Subalpine meadow flowering phenology responses to climate change: integrating experimental and gradient methods. *Ecological Monographs*, *73*(1), 69–86.

Dunne, J. A., Saleska, S. R., Fischer, M. L., & Harte, J. (2004). Integrating experimental and gradient methods in ecological climate change research. *Ecology*, *85*(4), 904–916.

ELP (Environmental Leadership Program) 2016 and 2018 Teams. University of Oregon. *Unpublished data*. https://blogs.uoregon.edu/phenology/results/.

Fitter, A. H., & Fitter, R. S. R. (2002). Rapid changes in flowering time in British plants. *Science*, *296*, 1689–1691.

Forrest, J., & Miller-Rushing, A. J. (2010). Toward a synthetic understanding of the role of phenology in ecology and evolution. *Philosophical Transactions of the Royal Society B*, *365*, 3101–3112.

Frenne, P. De, Graae, B. J., Rodríguez-Sanchez, F., Kolb, A., Chabrerie, O., Decocq, G., … Verheyen, K. (2013). Latitudinal gradients as natural laboratories to infer species' responses to temperature. *Journal of Ecology*, *101*, 784–795.

Galipaud, M., Gillingham, M. A. F., David, M., & Dechaume-Moncharmont, F. X. (2014). Ecologists overestimate the importance of predictor variables in model averaging: a plea for cautious interpretations. *Methods in Ecology and Evolution*, *5*, 983–991.

Gherardi, L. A., & Sala, O. E. (2013). Automated rainfall manipulation system: a reliable and inexpensive tool for ecologists. *Ecosphere*, *4*(2), 1–10.

Gordo, O., & Sanz, J. J. (2009). Long-term temporal changes of plant phenology in the Western Mediterranean. *Global Change Biology*, *15*, 1930–1948.

Gordo, O., & Sanz, J. J. (2010). Impact of climate change on plant phenology in Mediterranean ecosystems. *Global Change Biology*, *16*, 1082–1106.

Hamman, S. T., Dunwiddie, P. W., Nuckols, J. L., & Mckinley, M. (2011). Fire as a restoration tool in Pacific Northwest prairies and oak woodlands: challenges, successes, and future directions. *Northwest Science*, *85*(2), 317–328.

Hänel, S., & Tielbörger, K. (2015). Phenotypic response of plants to simulated climate change in a long-term rain-manipulation experiment: a multi-species study. *Oecologia*, *177*, 1015–1024.

Havens, K., Vitt, P., Still, S., Kramer, A. T., Fant, J. B., & Schatz, K. (2015). Seed sourcing for restoration in an era of climate change. *Natural Areas Journal*, *35*(1), 122–133.

Henry, G. H. R., & Molau, U. (1997). Tundra plants and climate change: the International Tundra Experiment (ITEX). *Global Change Biology*, *3*(S1), 1–9.

Ibáñez, I., Primack, R. B., Miller-Rushing, A. J., Ellwood, E., Higuchi, H., Lee, S. D., … Silander, J. A. (2010). Forecasting phenology under global warming. *Philosophical Transactions of the Royal Society B*, *365*, 3247–3260.

Inouye, D. W. (2008). Effects of climate change on phenology, frost damage, and floral abundance of montane wildflowers. *Ecology*, *89*(2), 353–362.

Jaster, T., Meyers, S., & Sundberg, S. eds. 2017. Oregon Vascular Plant Checklist. [Family]. http://www.oregonflora.org/checklist.php. Version 1.7.

Kanner, M., McCullough, L., & Nock, K. (2017). Springing forward: changes in phenology of native plant species in Southern Oregon prairies as a result of experimental climate change. *Oregon Undergraduate Research Journal*, *11*(1).

Klausmeyer, K. R., & Shaw, M. R. (2009). Climate change, habitat loss, protected areas and the climate adaptation potential of species in mediterranean ecosystems worldwide. *PLOS One*, *4*(7).

Kottek, M., Grieser, J., Beck, C., Rudolf, B., & Rubel, F. (2006). World map of the Köppen-Geiger climate classification updated. *Meteorologische Zeitschrift*, *15*(3), 259–263.

Lemoine, N. P., Sheffield, J., Dukes, J. S., Knapp, A. K., & Smith, M. D. (2016). Terrestrial Precipitation Analysis (TPA): A resource for characterizing long-term precipitation regimes and extremes. *Methods in Ecology and Evolution*, *7*(11), 1396–1401.

Lindh, B. C., McGahan, K. A., & Bluhm, W. L. (2018). Changes in urban plant phenology in the Pacific Northwest from 1959 to 2016: anthropogenic warming and natural oscillation. *International Journal of Biometeorology*.

Menzel, A., Sparks, T. H., Estrella, N., Koch, E., Aaasa, A., Ahas, R., … Zust, A. (2006). European phenological response to climate change matches the warming pattern. *Global Change Biology, 12*, 1969–1976.

Miller-Rushing, A. J., Høye, T. T., Inouye, D. W., & Post, E. (2010). The effects of phenological mismatches on demography. *Philosophical Transactions of the Royal Society B*, *365*, 3177–3186.

Moore, L. M., & Lauenroth, W. K. (2017). Differential effects of temperature and precipitation on early- vs . late-flowering species. *Ecosphere*, *8*(5), 1–18.

Moore, L. M., Lauenroth, W. K., Bell, D. M., & Schlaepfer, D. R. (2015). Soil water and temperature explain canopy phenology and onset of spring in a semiarid steppe. *Great Plains Research*, *25*(2), 121–138.

Mote, P. W., & Salathé, E. P. (2010). Future climate in the Pacific Northwest. *Climatic Change*, *102*(1), 29–50.

Mueller, K. E., Blumenthal, D. M., Pendall, E., Carrillo, Y., Dijkstra, F. A., Williams, D. G., … Penuelas, J. (2016). Impacts of warming and elevated CO2 on a semi-arid grassland are non-additive, shift with precipitation, and reverse over time. *Ecology Letters*, *19*(8), 956–966.

Noss, R. F., Laroe, E. T., & Scott, J. M. (1995). *Endangered Ecosystems of the United States: A Preliminary Assessment of Loss and Degradation*.

Olsson, K., & Agren, J. (2002). Latitudinal population differentiation in phenology, life history and flower morphology in the perennial herb Lythrum salicaria. *Journal of Evolutionary Biology*, *15*, 983–996.

Parmesan, C. (2007). Influences of species, latitudes and methodologies on estimates of phenological response to global warming. *Global Change Biology*, *13*, 1860–1872.

Parmesan, C., & Yohe, G. (2003). A globally coherent fingerprint of climate change impacts across natural systems. *Nature*, *421*, 37–42.

Peñuelas, J., Filella, I., Zhang, X., Llorens, L., Ogaya, R., Lloret, F., … Terradas, J. (2004). Complex spatiotemporal phenological shifts as a response to rainfall changes. *New Phytologist*, *161*(3), 837–846.

Pettorelli, N., Vik, J. O., Mysterud, A., Gaillard, J., Tucker, C. J., Stenseth, N. C., & Lyon, C. B. (2005). Using the satellite-derived NDVI to assess ecological responses to environmental change. *Trends in Ecology and Evolution*, *20*(9), 503–510.

Pfeifer-Meister, L., Bridgham, S. D., Little, C. J., Reynolds, L. L., Goklany, M. E., & Johnson, B. R. (2013). Pushing the limit: Experimental evidence of climate effects on plant range distributions. *Ecology*, *94*(10), 2131–2137.

Pfeifer-Meister, L., Bridgham, S. D., Reynolds, L. L., Goklany, M. E., Wilson, H. E., Little, C. J., … Johnson, B. R. (2016). Climate change alters plant biogeography in Mediterranean prairies along the West Coast, USA. *Global Change Biology*, *22*, 845–855.

Prevéy, J. S., & Seastedt, T. R. (2014). Seasonality of precipitation interacts with exotic species to alter composition and phenology of a semi-arid grassland. *Journal of Ecology*, *102*, 1549–1561.

Prevéy, J., Vellend, M., Ruger, N., Hollister, R. D., Bjorkman, A. D., Myers-Smith, I. H., … Rixen, C. (2017). Greater temperature sensitivity of plant phenology at colder sites: implications for convergence across northern latitudes. *Global Change Biology*, *23*, 2660–2671.

Prieto, P., Peñuelas, J., Niinemets, Ü., Ogaya, R., Schmidt, I. K., Beier, C., … Estiarte, M. (2009). Changes in the onset of spring growth in shrubland species in response to experimental warming along a north-south gradient in Europe. *Global Ecology and Biogeography*, *18*(4), 473–484.

PRISM Climate Group, Oregon State University, http://prism.oregonstate.edu, created 4 Feb 2004.

R Core Team (2016). R: A language and environment for statistical computing. R Foundation for Statistical Computing, Vienna, Austria. URL https://www.R-project.org/.

Rafferty, N. E., Caradonna, P. J., & Bronstein, J. L. (2015). Phenological shifts and the fate of mutualisms. *Oikos*, *124*(1), 14–21.

Rathcke, B., & Lacey, E. P. (1985). Phenological patterns of terrestrial plants. *Annual Review of Ecology, Evolution, and Systematics*, *16*, 179–214.

Reynolds, L. L., Johnson, B. R., Pfeifer-Meister, L., & Bridgham, S. D. (2015). Soil respiration response to climate change in Pacific Northwest prairies is mediated by a regional Mediterranean climate gradient. *Global Change Biology*, *21*, 487–500.

Rosa, R. K., Oberbauer, S. F., Starr, G., La Puma, I. P., Pop, E., Ahlquist, L., & Baldwin, T. (2015). Plant phenological responses to a long-term experimental extension of growing season and soil warming in the tussock tundra of Alaska. *Global Change Biology*, *21*, 4520–4532.

Sala, O. E., Chapin III, F. S., Armesto, J. J., Berlow, E., Bloomfield, J., Dirzo, R., … Wall, D. H. (2000). Global biodiversity scenarios for the year 2100. *Science*, *287*, 1770–1774.

Saxton, K. E., & Rawls, W. J. (2006). Soil water characteristic estimates by texture and organic matter for hydrologic solutions. *Soil Science Society of America Journal*, *1578*, 1569–1578.

Schultz, C. B., Hammond, P. C., & Wilson, M. V. (2003). Biology of the Fender's blue butterfly (Icaricia icarioides fenderi Macy), an endangered species of western Oregon native prairies. *Natural Areas Journal*, *23*(1), 61–71.

Schultz, C. B., Henry, E., Carleton, A., Hicks, T., Thomas, R., Potter, A., … Reader, B. (2011). Conservation of prairie-oak butterflies in Oregon, Washington, and British Columbia. *Northwest Science*, *85*(2), 361–388.

Sherry, R. A., Zhou, X., Gu, S., Arnone, J. A., Schimel, D. S., Verburg, P. S., … Luo, Y. (2007). Divergence of reproductive phenology under climate warming. *Proceedings of the National Academy of Sciences*, *104*(1), 198–202.

Tang, J., Körner, C., Muraoka, H., Piao, S., Shen, M., Thackeray, S. J., & Yang, X. (2016). Emerging opportunities and challenges in phenology: A review. *Ecosphere*, *7*(8), 1–17.

Theobald, E. J., Breckheimer, I., & Hille Ris Lambers, J. (2017). Climate drives phenological reassembly of a mountain wild flower meadow community. *Ecology*, *98*(11), 2799–2812.

Tielbörger, K., Bilton, M. C., Metz, J., Kigel, J., Holzapfel, C., Lebrija-Trejos, E., … Sternberg, M. (2014). Middle-Eastern plant communities tolerate 9 years of drought in a multi-site climate manipulation experiment. *Nature Communications*, *5*(5102), 1–9.

Tucker, C. J., Slayback, D. A., Pinzon, J. E., Los, S. O., Myneni, R. B., & Taylor, M. G. (2001). Higher northern latitude normalized difference vegetation index and growing season trends from 1982 to 1999. *International Journal of Biometeorology*, *45*(4), 184–190.

U.S. Fish and Wildlife Service, (2010). *Recovery plan for the prairie species of western Oregon and southwestern Washington.*

Wang, H., Ge, Q., Dai, J., & Tao, Z. (2015). Geographical pattern in first bloom variability and its relation to temperature sensitivity in the USA and China. *International Journal of Biometeorology*, *59*(8), 961–969.

Westerling, A. L., Hidalgo, H. G., Cayan, D. R., & Swetnam, T. W. (2006). Warming and earlier spring increase Western U.S. forest wildfire activity. *Science*, *313*(5789), 940–943.

Whittington, H. R., Tilman, D., Wragg, P. D., & Powers, J. S. (2015). Phenological responses of prairie plants vary among species and year in a three-year experimental warming study. *Ecosphere*, *6*(10), 1–15.

Wolf, A. A., Zavaleta, E. S., & Selmants, P. C. (2017). Flowering phenology shifts in response to biodiversity loss. *Proceedings of the National Academy of Sciences*, *114*(13), 3463–3468.

Wolkovich, E. M., Cook, B. I., Allen, J. M., Crimmins, T. M., Betancourt, J. L., Travers, S. E., … Cleland, E. E. (2012). Warming experiments underpredict plant phenological responses to climate change. *Nature*, *485*, 8–12.

Yahdjian, L., & Sala, O. E. (2002). A rainout shelter design for intercepting different amounts of rainfall. *Oecologia*, *133*, 95–101.

Yang, L. H., & Rudolph, V. H. W. (2010). Phenology, ontogeny and the effects of climate change on the timing of species interactions. *Ecology Letters*, *13*, 1–10.

Zelikova, T. J., Williams, D. G., Hoenigman, R., Blumenthal, D. M., Morgan, J. A., & Pendall, E. (2015). Seasonality of soil moisture mediates responses of ecosystem phenology to elevated CO_2 and warming in a semi-arid grassland. *Journal of Ecology*, *103*(5), 1119–1130.

CHAPTER III

Abatzoglou, J. T., Rupp, D. E., & Mote, P. W. (2014). Seasonal climate variability and change in the Pacific Northwest of the United Dtates. *Journal of Climate*, *27*(5), 2125–2142. doi: 10.1175/JCLI-D-13-00218.1

Angert, A. L., Sheth, S. N., & Paul, J. R. (2011). Incorporating population-level variation in thermal performance into predictions of geographic range shifts. *Integrative and Comparative Biology*, *51*(5), 733–750. doi: 10.1093/icb/icr048

Araújo, M. B., & Rozenfeld, A. (2014). The geographic scaling of biotic interactions. *Ecography*, *37*(5), 406–415. doi: 10.1111/j.1600-0587.2013.00643.x

Baer, K. C., & Maron, J. L. (2018). Declining demographic performance and dispersal limitation influence the geographic distribution of the perennial forb Astragalus utahensis (Fabaceae). *Journal of Ecology*, (October 2018), 1250–1262. doi: 10.1111/1365-2745.13086

Barton, K. (2018). *MuMIn: Multi-Model Inference*. R package version 1.40.4. Retrieved from https://CRAN.R-project.org/package=MuMIn.

Burnham, K. P., & Anderson, D. R. (2004). Multimodel inference: understanding AIC and BIC in model selection. *Sociological Methods and Research*, *33*(2), 261–304. doi: 10.1177/0049124104268644

Cahill, A. E., Aiello-Lammens, M. E., Fisher-Reid, M. C., Hua, X., Karanewsky, C. J., Yeong Ryu, H., … Wiens, J. J. (2012). How does climate change cause extinction? *Proceedings of the Royal Society B: Biological Sciences*, *280*(1750). doi: 10.1098/rspb.2012.1890

Caswell, H. (1989). Analysis of life table response experiments I: decomposition of effects on population growth rate. *Ecological Modelling*, *46*, 221–237.

Caswell, H. (2001). *Matrix population models* (Second; S. A. Inc., ed.). Sunderland, Massachusetts, USA.

Chen, I.-C., Hill, J. K., Ohlemuller, R., Roy, D. B., & Thomas, C. D. (2011). Rapid range shifts of species associated with high levels of climate warming. *Science*, *333*, 1024–1026.

Dawson, T. P., Jackson, S. T., House, J. I., Prentice, I. C., & Mace, G. M. (2011). Beyond predictions: biodiversity conservation in a changing climate. *Science*, *332*, 53–58. doi: 10.1126/science.1200303

Dibner, R. R., Peterson, M. L., Louthan, A. M., & Doak, D. F. (2019). Multiple mechanisms confer stability to isolated populations of a rare endemic plant. *Ecological Monographs*, *89*(2), 1–16. doi: 10.1002/ecm.1360

Doak, D. F., & Morris, W. F. (2010). Demographic compensation and tipping points in climate-induced range shifts. *Nature*, *467*, 959–962.

Dunne, J. A., Saleska, S. R., Fischer, M. L., & Harte, J. (2004). Integrating experimental and gradient methods in ecological climate change research. *Ecology*, *85*(4), 904–916. doi: 10.1890/03-8003

Easterling, M. R., Ellner, S. P., Dixon, P. M., & Mar, N. (2000). Size-specific sensitivity: applying a new structured population model. *Ecology*, *81*(3), 694–708. Retrieved from http://www.esajournals.org/doi/abs/10.1890/0012-9658(2000)081[0694:SSSAAN]2.0.CO;2

Ellner, S. P., & Rees, M. (2006). Integral projection models for species with complex demography. *The American Naturalist*, *167*(3), 410–428.

Ettinger, A., & HilleRisLambers, J. (2017). Competition and facilitation may lead to asymmetric range shift dynamics with climate change. *Global Change Biology*, *23*(9), 3921–3933. doi: 10.1111/gcb.13649

Gaston, K. J. (2009). Geographic range limits: Achieving synthesis. *Proceedings of the Royal Society B: Biological Sciences*, *276*(1661), 1395–1406. doi: 10.1098/rspb.2008.1480

Griffith, A. B. (2017). Perturbation approaches for integral projection models. *Oikos*, *126*, 1675–1686. doi: 10.1111/oik.04458

Hargreaves, A. L., Samis, K. E., & Eckert, C. G. (2014). Are species' range limits simply niche limits writ large? A review of transplant experiments beyond the range. *The American Naturalist*, *183*(2), 157–173. doi: 10.1086/674525

Hitchcock, C., Cronquist, A., Janish, J., Rumely, J., Shin, C., & Porcino, N. (2018). *Flora of the Pacific Northwest: An Illustrated Manual* (Giblin D., Legler B., Zika P., & Olmstead R., Eds.). Seattle: University of Washington Press.

Kimball, B. A., Conley, M. M., Wang, S., Lin, X., Luo, C., Morgan, J., & Smith, D. (2008). Infrared heater arrays for warming ecosystem field plots. *Global Change Biology*, *14*(2), 309–320. doi: 10.1111/j.1365-2486.2007.01486.x

Lemoine, N. P., Sheffield, J., Dukes, J. S., Knapp, A. K., & Smith, M. D. (2016). Terrestrial Precipitation Analysis (TPA): A resource for characterizing long-term precipitation regimes and extremes. *Methods in Ecology and Evolution*, *7*(11), 1396–1401. doi: 10.1111/2041-210X.12582

Lesica, P., & Crone, E. E. (2017). Arctic and boreal plant species decline at their southern range limits in the Rocky Mountains. *Ecology Letters*, *20*(2), 166–174. doi: 10.1111/ele.12718

MacArthur, R. H. (1972). *Geographic Ecology* (H. and Row, ed.). New York, NY.

MacLean, S. A., & Beissinger, S. R. (2017). Species' traits as predictors of range shifts under contemporary climate change: a review and meta-analysis. *Global Change Biology*, *23*(10), 4094–4105. doi: 10.1111/gcb.13736

Merow, C., Dahlgren, J. P., Metcalf, C. J. E., Childs, D. Z., Margaret, E. K., Jongejans, E., … Mcmahon, S. M. (2014). Advancing population ecology with integral projection models: a practical guide. *Methods in Ecology and Evolution*, *5*, 99–110. doi: 10.1111/2041-210X.12146

Mlynarek, J. J., Moffat, C. E., Edwards, S., Einfeldt, A. L., Heustis, A., Johns, R., … Heard, S. B. (2017). Enemy escape: a general phenomenon in a fragmented literature? *Facets*, *2*(2), 1015–1044. doi: 10.1139/facets-2017-0041

Mote, P. (2003). Trends in temperature and precipitation in the Pacific Northwest during the twentieth century. *Northwest Science*, *77*(4), 271–282.

Mote, P. W., & Salathé, E. P. (2010). Future climate in the Pacific Northwest. *Climatic Change*, *102*(1), 29–50. doi: 10.1007/s10584-010-9848-z

Norton, L. R., Firbank, L. G., Scott, A., & Watkinson, A. R. (2005). Characterising spatial and temporal variation in the finite rate of population increase across the northern range boundary of the annual grass Vulpia fasciculata. *Oecologia*, *144*(3), 407–415. doi: 10.1007/s00442-005-0102-8

Oldfather, M. F., & Ackerly, D. D. (2019). Microclimate and demography interact to shape stable population dynamics across the range of an alpine plant. *New Phytologist*, *222*(1), 193–205. doi: 10.1111/nph.15565

Olsen, S. L., Töpper, J. P., Skarpaas, O., Vandvik, V., & Klanderud, K. (2016). From facilitation to competition: Temperature-driven shift in dominant plant interactions affects population dynamics in seminatural grasslands. *Global Change Biology*, *22*(5), 1915–1926. doi: 10.1111/gcb.13241

Panetta, A. M., Stanton, M. L., & Harte, J. (2018). Climate warming drives local extinction: evidence from observation and experimentation. *Science Advances*, *4*(2), 1–9. doi: 10.1126/sciadv.aaq1819

Parmesan, C. (2006). Ecological and evolutionary responses to recent climate change. *Annual Review of Ecology, Evolution, and Systematics*, *37*, 637–669. doi: 10.2307/annurev.ecolsys.37.091305.30000024

Parmesan, C., & Yohe, G. (2003). A globally coherent fingerprint of climate change impacts across natural systems. *Nature*, *421*, 37–42.

Pecl, G. T., Araújo, M. B., Bell, J. D., Blanchard, J., Bonebrake, T. C., Chen, I. C., … Williams, S. E. (2017). Biodiversity redistribution under climate change: impacts on ecosystems and human well-being. *Science*, *355*(6332). doi: 10.1126/science.aai9214

Peterson, M. L., Doak, D. F., & Morris, W. F. (2018). Both life-history plasticity and local adaptation will shape range-wide responses to climate warming in the tundra plant Silene acaulis. *Global Change Biology*, *24*(4), 1614–1625. doi: 10.1111/gcb.13990

Peterson, M. L., Doak, D. F., & Morris, W. F. (2019). Incorporating local adaptation into forecasts of species' distribution and abundance under climate change. *Global Change Biology*, *25*(3), 775–793. doi: 10.1111/gcb.14562

Pfeifer-Meister, L., Bridgham, S. D., Little, C. J., Reynolds, L. L., Goklany, M. E., & Johnson, B. R. (2013). Pushing the limit: experimental evidence of climate effects on plant range distributions. *Ecology*, *94*(10), 2131–2137. doi: 10.1890/13-0284.1

Pfeifer-Meister, L., Bridgham, S. D., Reynolds, L. L., Goklany, M. E., Wilson, H. E., Little, C. J., … Johnson, B. R. (2016). Climate change alters plant biogeography in Mediterranean prairies along the West Coast, USA. *Global Change Biology*, *22*, 845–855. doi: 10.1111/gcb.13052

Prince, S. D., & Carter, R. N. (1985). The geographical distribution of prickly lettuce (Lactuca serriola): III. Its performance in transplant sites beyond its distribution limit in Britain. *The Journal of Ecology*, *73*(1), 49–64. doi: 10.2307/2259767

R Core Team (2016). *R: A language and environment for statistical computing*. Vienna, Austria: R Foundation for Statistical Computing. Retrieved from https://www.R-project.org/.

Reed, P. B., Peterson, M. L., Pfeifer-Meister, L. E., Morris, W. F., Doak, D. F., Roy, B. A., Johnson, B. R., Bailes, G. T., Nelson, A. A., Bridgham, S. D. (2020). Data from: Climate manipulations differentially affect plant population dynamics within versus beyond northern range limits. Dryad Digital Repository. https://doi.org/10.5061/dryad.rxwdbrv5d.

Reed, P. B., Pfeifer-Meister, L. E., Roy, B. A., Johnson, B. R., Bailes, G. T., Nelson, A. A., … Bridgham, S. D. (2019). Prairie plant phenology driven more by temperature than moisture in climate manipulations across a latitudinal gradient in the Pacific Northwest, USA. *Ecology and Evolution*, *9*(6), 3637–3650. doi: 10.1002/ece3.4995

Rees, M., Childs, D. Z., & Ellner, S. P. (2014). Building integral projection models: a user's guide. *Journal of Animal Ecology*, *83*, 528–545. doi: 10.1111/1365-2656.12178

Rehm, E. M., Olivas, P., Stroud, J., & Feeley, K. J. (2015). Losing your edge: Climate change and the conservation value of range-edge populations. *Ecology and Evolution*, *5*(19), 4315–4326. doi: 10.1002/ece3.1645

Reynolds, L. L., Johnson, B. R., Pfeifer-Meister, L., & Bridgham, S. D. (2015). Soil respiration response to climate change in Pacific Northwest prairies is mediated by a regional Mediterranean climate gradient. *Global Change Biology*, *21*, 487–500. doi: 10.1111/gcb.12732

Richards, C. M. (2000). Inbreeding depression and genetic rescue in a plant metapopulation. *The American Naturalist*, *155*(3), 383–394. doi: 10.2307/3078873

Rustad, L. E., Campbell, J. L., Marion, G. M., Norby, R. J., Mitchell, M. J., Hartley, A. E., … Wright, R. (2001). A meta-analysis of the response of soil respiration, net nitrogen mineralization, and aboveground plant growth to experimental ecosystem warming. *Oecologia*, *126*(4), 543–562. doi: 10.1007/s004420000544

Samis, K. E., & Eckert, C. G. (2009). Ecological correlates of fitness across the northern geographic range limit of a Pacific coast dune plant. *Ecology*, *90*(11), 3051–3061. doi: 10.1890/08-1914.1

Sexton, J. P., Mcintyre, P. J., Angert, A. L., & Rice, K. J. (2009). Evolution and ecology of species range limits. *Annual Review of Ecology, Evolution, and Systematics*, *40*, 415–436. doi: 10.1146/annurev.ecolsys.110308.120317

Sheth, S. N., & Angert, A. L. (2018). Demographic compensation does not rescue populations at a trailing range edge. *Proceedings of the National Academy of Sciences*, *115*(10), 201715899. doi: 10.1073/pnas.1715899115

Thomas, C. D. (2010). Climate, climate change and range boundaries. *Diversity and Distributions*, *16*(3), 488–495. doi: 10.1111/j.1472-4642.2010.00642.x

Trask, M. M., & Pyke, D. A. (1998). Variability in seed dormancy of three Pacific Northwestern grasses. *Seed Science and Technology*, *26*, 179–191.

Villellas, J., Doak, D. F., García, M. B., & Morris, W. F. (2015). Demographic compensation among populations: What is it, how does it arise and what are its implications? *Ecology Letters*, *18*(11), 1139–1152. doi: 10.1111/ele.12505

Wallin, L., Svensson, B. M., & Lönn, M. (2009). Artificial dispersal as a restoration tool in meadows: sowing or planting? *Restoration Ecology*, *17*(2), 270–279. doi: 10.1111/j.1526-100X.2007.00350.x

Walther, G.-R. (2010). Community and ecosystem responses to recent climate change. *Philosophical Transactions of the Royal Society B: Biological Sciences*, *365*(1549), 2019–2024. doi: 10.1098/rstb.2010.0021

Young-Mathews, A. (2012). *Plant guide for rose checker-mallow (Sidalcea virgata)*. Corvallis, Oregon.

CHAPTER IV

Adams, D. E., and L. L. Wallace. 1985. Nutrient and biomass allocation in five grass species in an Oklahoma tallgrass prairie. The American Midland Naturalist 113:170–181.

Bachelet, D., B. R. Johnson, S. D. Bridgham, P. V Dunn, H. E. Anderson, and B. M. Rogers. 2011. Climate change impacts on western Pacific Northwest prairies and savannas. Northwest Science 85:411–429.

Barton, K. 2018. *MuMIn: Multi-Model Inference*. R package version 1.40.4. Retrieved from https://CRAN.R-project.org/package=MuMIn.

Bayly, M. J., and A. L. Angert. 2019. Niche models do not predict experimental demography but both suggest dispersal limitation across the northern range limit of the scarlet monkeyflower (Erythranthe cardinalis). Journal of Biogeography 46:1316–1328.

Bazzaz, F. A. 1979. The physiological ecology of plant succession. Annual Review of Ecology and Systematics 10:351–371.

Bickford, D., S. D. Howard, D. J. J. Ng, and J. A. Sheridan. 2010. Impacts of climate change on the amphibians and reptiles of Southeast Asia. Biodiversity and Conservation 19:1043–1062.

Boyd, R. 1999. Indians, fire, and the land. Page Oregon State University Press. Corvallis, Oregon.

Bradford, J. B., and W. K. Lauenroth. 2006. Controls over invasion of *Bromus tectorum*: The importance of climate, soil, disturbance and seed availability. Journal of Vegetation Science 17:693.

Burnham, K. P., and D. R. Anderson. 2002. Model selection and multimodel inference: a practical information-theoretic approach (second edition). Ecological Modelling. Springer.

Calflora: Information on California plants for education, research, and conservation. 2021. The Calflora Database. Berkeley, California, USA. https://www.calflora/org/. Accessed: Feb 04, 2021.

Consortium of Pacific Northwest Herbaria. 2021. University of Washington Herbarium, Burke Museum of Natural History and Culture. Seattle, Washington, USA. www.pnwherbaria.org/. Accessed: Feb 04, 2021.

Coates, F., I. D. Lunt, and R. L. Tremblay. 2006. Effects of disturbance on population dynamics of the threatened orchid *Prasophyllum correctum* D.L. Jones and implications for grassland management in south-eastern Australia. Biological Conservation 129:59–69.

Connell, J. H., and R. O. Slatyer. 1977. Mechanisms of succession in natural communities and their role in community stability and organization. The American Naturalist 111:1119–1144.

Cruzan, M. B., and E. C. Hendrickson. 2020. Landscape genetics of plants: Challenges and opportunities. Plant Communications 1:1–15.

Dalton, M., and E. Fleishman. 2021. Fifth Oregon climate assessment. Oregon Climate Change Research Institute, Oregon State University, Corvallis, Oregon. https://blogs.oregonstate.edu/occri/oregon-climate-assessments/

Davison, C., and K. Kindscher. 1999. Tools for diversity: Fire, grazing and mowing on tallgrass prairies. Ecological Restoration 17:136–143.

Dennehy, C., E. R. Alverson, H. E. Anderson, D. R. Clements, R. Gilbert, and T. N. Kaye. 2011. Management strategies for invasive plants in Pacific Northwest prairies, savannas, and oak woodlands. Northwest Science 85:329–351.

Doak, D. F., and W. F. Morris. 2010. Demographic compensation and tipping points in climate-induced range shifts. Nature 467:959–962.

Dunne, J. A., S. R. Saleska, M. L. Fischer, and J. Harte. 2004. Integrating experimental and gradient methods in ecological climate change research. Ecology 85:904–916.

Dunwiddie, P. W., E. R. Alverson, R. A. Martin, and R. Gilbert. 2014. Annual species in native prairies of South Puget Sound, Washington. Northwest Science 88:94–105.

Dunwiddie, P. W., and J. D. Bakker. 2011. The future of restoration and management of prairie-oak ecosystems in the Pacific Northwest. Northwest Science 85:83–92.

Edwards, E. J., and C. J. Still. 2008. Climate, phylogeny and the ecological distribution of C4 grasses. Ecology Letters 11:266–276.

Gremer, J. R., and D. L. Venable. 2014. Bet hedging in desert winter annual plants: Optimal germination strategies in a variable environment. Ecology Letters 17:380–387.

Hargreaves, A. L., K. E. Samis, and C. G. Eckert. 2014. Are species' range limits simply niche limits writ large? A review of transplant experiments beyond the range. The American Naturalist 183:157–173.

Hitchcock, C., Cronquist, A., Janish, J., Rumely, J., Shin, C., & N. Porcino. 2018) *Flora of the Pacific Northwest: An Illustrated Manual* (Giblin D., Legler B., Zika P., & Olmstead R., Eds.). Seattle: University of Washington Press.

Holl, K. D., and G. F. Hayes. 2006. Challenges to introducing and managing disturbance regimes for *Holocarpha macradenia*, an endangered annual grassland forb. Conservation Biology 20:1121–1131.

Kimball, B. A., M. M. Conley, S. Wang, X. Lin, C. Luo, J. Morgan, and D. Smith. 2008. Infrared heater arrays for warming ecosystem field plots. Global Change Biology 14:309–320.

Knowles, J. E., and C. Frederick. 2020. merTools: Tools for Analyzing Mixed Effect Regression Models. R package version 0.5.2. https://CRAN.R-project.org/package=merTools

James, G., D. Witten, T. Hastie, and R. Tibshirani. 2013. An Introduction to Statistical Learning with Applications in R. Page (G. Casella, S. Fienberg, and I. Olkin, Eds.). 1st edition. Springer, New York, NY.

Jung, I. W., and H. Chang. 2012. Climate change impacts on spatial patterns in drought risk in the Willamette River Basin, Oregon, USA. Theoretical and Applied Climatology 108:355–371.

Lembrechts, J. J., A. Pauchard, J. Lenoir, M. A. Nuñez, C. Geron, A. Ven, P. Bravo-Monasterio, E. Teneb, I. Nijs, and A. Milbau. 2016. Disturbance is the key to plant invasions in cold environments. Proceedings of the National Academy of Sciences of the United States of America 113:14061–14066.

Lemoine, N. P., J. Sheffield, J. S. Dukes, A. K. Knapp, and M. D. Smith. 2016. Terrestrial Precipitation Analysis (TPA): A resource for characterizing long-term precipitation regimes and extremes. Methods in Ecology and Evolution 7:1396–1401.

Lesica, P., and E. E. Crone. 2017. Arctic and boreal plant species decline at their southern range limits in the Rocky Mountains. Ecology Letters 20:166–174.

Linares, C., and D. F. Doak. 2010. Forecasting the combined effects of disparate disturbances on the persistence of long-lived gorgonians: A case study of *Paramuricea clavata*. Marine Ecology Progress Series 402:59–68.

Loarie, S. R., P. B. Duffy, H. Hamilton, G. P. Asner, C. B. Field, and D. D. Ackerly. 2009. The velocity of climate change. Nature 462:1052–1055.

Macdougall, A. S., and R. Turkington. 2007. Does the type of disturbance matter when restoring disturbance-dependent grasslands? Restoration Ecology 15:263–272.

Montero-Serra, I., J. Garrabou, D. F. Doak, J. B. Ledoux, and C. Linares. 2019. Marine protected areas enhance structural complexity but do not buffer the consequences of ocean warming for an overexploited precious coral. Journal of Applied Ecology 56:1063–1074.

Moritz, C., and R. Agudo. 2013. The future of species under climate change: resilience or decline? Science 341.

Morris, W. F., C. A. Pfister, S. Tuljapurkar, C. V Haridas, C. L. Boggs, M. S. Boyce, E. M. Bruna, D. R. Church, T. Coulson, D. F. Doak, S. Forsyth, J.-M. Gaillard, C. C. Horvitz, S. Kalicz, B. E. Kendall, T. M. Knight, C. T. Lee, and E. S. Menges. 2008. Longevity can buffer plant and animal populations against changing climatic variability. Ecology 89:19–25.

Mote, P. W., and E. P. Salathé. 2010. Future climate in the Pacific Northwest. Climatic Change 102:29–50.

Noss, R. F., E. T. LaRoe, and J. M. Scott. 1995. Endangered ecosystems of the United States: A preliminary assessment of loss and degradation.

Nunney, L. 2002. The effective size of annual plant populations: The interaction of a seed bank with fluctuating population size in maintaining genetic variation. American Naturalist 160:195–204.

Pagel, J., M. Treurnicht, W. J. Bond, T. Kraaij, H. Nottebrock, A. L. Schutte-Vlok, J. Tonnabel, K. J. Esler, and F. M. Schurr. 2020. Mismatches between demographic niches and geographic distributions are strongest in poorly dispersed and highly persistent plant species. Proceedings of the National Academy of Sciences of the United States of America 117:3663–3669.

Palmer, M. A., R. F. Ambrose, and N. L. Poff. 1997. Ecological theory and community restoration ecology. Restoration Ecology 5:291–300.

Panetta, A. M., M. L. Stanton, and J. Harte. 2018. Climate warming drives local extinction: evidence from observation and experimentation. Science Advances 4:1–9.

Parmesan, C. 2006. Ecological and evolutionary responses to recent climate change. Annual Review of Ecology, Evolution, and Systematics 37:637–669.

Pereira, H. M., P. W. Leadley, V. Proença, R. Alkemade, J. P. W. Scharlemann, J. F. Fernandez-Manjarrés, M. B. Araújo, P. Balvanera, R. Biggs, W. W. L. Cheung, L. Chini, H. D. Cooper, E. L. Gilman, S. Guénette, G. C. Hurtt, H. P. Huntington, G. M. Mace, T. Oberdorff, C. Revenga, P. Rodrigues, R. J. Scholes, U. R. Sumaila, and M. Walpole. 2010. Scenarios for global biodiversity in the 21st century. Science 330:1496–1501.

Peterson, M. L., G. Bailes, L. B. Hendricks, L. Pfeifer-Meister, P. B. Reed, S. D. Bridgham, B. R. Johnson, R. Shriver, E. Waddle, H. Wroton, D. F. Doak, B. A. Roy, and W. F. Morris. 2020. Latitudinal gradients in population growth do not reflect demographic responses to climate. Ecological Applications. 0(0), 2021, e02242. doi.org/10.1002/eap.2242

Peterson, M. L., D. F. Doak, and W. F. Morris. 2018. Both life-history plasticity and local adaptation will shape range-wide responses to climate warming in the tundra plant *Silene acaulis*. Global Change Biology 24:1614–1625.

Pfeifer-Meister, L., S. D. Bridgham, C. J. Little, L. L. Reynolds, M. E. Goklany, and B. R. Johnson. 2013. Pushing the limit: experimental evidence of climate effects on plant range distributions. Ecology 94:2131–2137.

Pfeifer-Meister, L., S. D. Bridgham, L. L. Reynolds, M. E. Goklany, H. E. Wilson, C. J. Little, A. Ferguson, and B. R. Johnson. 2016. Climate change alters plant biogeography in Mediterranean prairies along the West Coast, USA. Global Change Biology 22:845–855.

PRISM Climate Group. 2020. https://prism.oregonstate.edu/

R Core Team. 2020. R: A language and environment for statistical computing. R Foundation for Statistical Computing, Vienna, Austria. https://www.R-project.org/.

Reed, P. B., M. L. Peterson, L. E. Pfeifer-Meister, W. F. Morris, D. F. Doak, B. A. Roy, B. R. Johnson, G. T. Bailes, A. A. Nelson, and S. D. Bridgham. 2021. Climate manipulations differentially affect plant population dynamics within versus beyond northern range limits. Journal of Ecology 109:664–675.

Reed, P. B., L. E. Pfeifer-Meister, B. A. Roy, B. R. Johnson, G. T. Bailes, A. A. Nelson, M. C. Boulay, S. T. Hamman, and S. D. Bridgham. 2019. Prairie plant phenology driven more by temperature than moisture in climate manipulations across a latitudinal gradient in the Pacific Northwest, USA. Ecology and Evolution 9:3637–3650.

Rees, M., and M. J. Long. 1992. Germination biology and the ecology of annual plants. The American Naturalist 139:484–508.

Rehm, E. M., P. Olivas, J. Stroud, and K. J. Feeley. 2015. Losing your edge: Climate change and the conservation value of range-edge populations. Ecology and Evolution 5:4315–4326.

Reynolds, L. L., B. R. Johnson, L. Pfeifer-Meister, and S. D. Bridgham. 2015. Soil respiration response to climate change in Pacific Northwest prairies is mediated by a regional Mediterranean climate gradient. Global Change Biology 21:487–500.

Román-Palacios, C., and J. J. Wiens. 2020. Recent responses to climate change reveal the drivers of species extinction and survival. Proceedings of the National Academy of Sciences of the United States of America 117:4211–4217.

Sheth, S. N., and A. L. Angert. 2014. The evolution of environmental tolerance and range size: A comparison of geographically restricted and widespread Mimulus. Evolution 68:2917–2931.

Sheth, S. N., and A. L. Angert. 2018. Demographic compensation does not rescue populations at a trailing range edge. Proceedings of the National Academy of Sciences 115:201715899.

Storm, L., and D. Shebitz. 2006. Evaluating the purpose, extent, and ecological restoration applications of indigenous burning practices in southwestern Washington. Ecological Restoration 24:256–268.

The PLANTS Database. 2021. National Plant Data Team, USDA, NRCS. Greensboro, North Carolina, USA. http://plants.usda.gov. Accessed: Feb 04, 2021.

Thomson, D. M., R. Cruz-de Hoyos, K. Cummings, and E. L. Schultz. 2016. Why are native annual abundances low in invaded grasslands? Testing the effects of competition and seed limitation. Plant Ecology 217:431–442.

Tilman, D. 1990. Constraints and tradeoffs: toward a predictive theory of competition and succession. Oikos 58:3–15.

Tredennick, A. T., G. Hooker, S. P. Ellner, and P. B. Adler. 2021. A practical guide to selecting models for exploration, understanding, and prediction in ecology. Ecology. https://doi.org/10.1002/ecy.3336

Ulrey, C., P. F. Quintana-Ascencio, G. Kauffman, A. B. Smith, and E. S. Menges. 2016. Life at the top: long-term demography, microclimatic refugia, and responses to climate change for a high-elevation southern Appalachian endemic plant. Biological Conservation 200:80–92.

Villellas, J., M. B. García, and W. F. Morris. 2019. Geographic location, local environment, and individual size mediate the effects of climate warming and neighbors on a benefactor plant. Oecologia 189:243–253.

Vitt, P., K. Havens, A. T. Kramer, D. Sollenberger, and E. Yates. 2010. Assisted migration of plants: Changes in latitudes, changes in attitudes. Biological Conservation 143:18–27.

Wang, Y., Q. Fang, S. T. M. Dissanayake, and H. Önal. 2020. Optimizing conservation planning for multiple cohabiting species. PLoS ONE 15:1–14.

Young-Mathews, A. 2012. Plant fact sheet for shortspur seablush (*Plectritis congesta*). Corvallis, Oregon.

Chapter V

Adler, P.B. & HilleRisLambers, J. (2008). The influence of climate and species composition on the population dynamics of ten prairie forbs. *Ecology*, 89, 3049–3060.

Adler, P.B., Leiker, J. & Levine, J.M. (2009). Direct and indirect effects of climate change on a prairie plant community. *PLoS One*, 4, 1–6.

Adler, P.B. & Levine, J.M. (2007). Contrasting relationships between precipitation and species richness in space and time. *Oikos*, 116, 221–232.

Allen, E.B. & Knight, D.H. (1984). The effects of introduced annuals on secondary succession in sagebrush-grassland, Wyoming. *Southwest. Nat.*, 29, 407–421.

Avolio, M.L., La Pierre, K.J., Houseman, G.R., Koerner, S.E., Grman, E., Isbell, F., *et al.* (2015). A framework for quantifying the magnitude and variability of community responses to global change drivers. *Ecosphere*, 6, 1–14.

Barton, K. (2020). MuMIn: Multi-Model Inference. R package version 1.43.17. https://CRAN.R-project.org/package=MuMIn

Bates, D., Mächler, M., Bolker, B.M. & Walker, S.C. (2015). Fitting linear mixed-effects models using lme4. *J. Stat. Softw.*, 67, 1–48.

Blumenthal, D.M., Kray, J.A., Ortmans, W., Ziska, L.H. & Pendall, E. (2016). Cheatgrass is favored by warming but not CO2 enrichment in a semi-arid grassland. *Glob. Chang. Biol.*, 22, 3026–3038.

Brambila, A., Reed, P.B., Bridgham, S.D., Roy, B.A., Johnson, B.R., Pfeifer-Meister, L., *et al.* (In prep). Disturbance: a double-edged sword for restoration in a changing climate.

Brooker, R.W. (2006). Plant-plant interactions and environmental change. *New Phytol.*, 171, 271–284.

Brooks, M.L. (2003). Effects of increased soil nitrogen on the dominance of alien annual plants in the Mojave Desert. *J. Appl. Ecol.*, 40, 344–353.

Chu, C., Kleinhesselink, A.R., Havstad, K.M., McClaran, M.P., Peters, D.P., Vermeire, L.T., *et al.* (2016). Direct effects dominate responses to climate perturbations in grassland plant communities. *Nat. Commun.*, 7, 1–10.

Clary, J. (2012). Determinants of perennial and annual grass distribution in Mediterranean-climate California. *Plant Ecol.*, 213, 1203–1208.

Cleland, E.E., Chiariello, N.R., Loarie, S.R., Mooney, H.A. & Field, C.B. (2006). Diverse responses of phenology to global changes in a grassland ecosystem. *Proc. Natl. Acad. Sci. U. S. A.*, 103, 13740–13744.

Corbin, J.D. & D'Antonio, C.M. (2004). Competition between native perenial and exotic annual grasses: implications for an historical invasion. *Ecology*, 85, 1273–1283.

D'Antonio, C.M. & Vitousek, P.M. (1992). Biological invasions by exotic grasses, the grass/fire cycle, and global change. *Annu. Rev. Ecol. Syst.*, 23, 63–87.

Dalton, M. & Fleishman, E. (2021). *Fifth Oregon Climate Assessment*. Oregon Climate Change Research Institute, Oregon State University, Corvallis, Oregon. https://blogs.oregonstate.edu/occri/oregon-climate-assessments/.

Dennehy, C., Alverson, E.R., Anderson, H.E., Clements, D.R., Gilbert, R. & Kaye, T.N. (2011). Management strategies for invasive plants in Pacific Northwest prairies, savannas, and oak woodlands. *Northwest Sci.*, 85, 329–351.

Dunwiddie, P.W., Alverson, E.R., Martin, R.A. & Gilbert, R. (2014). Annual species in native prairies of South Puget Sound, Washington. *Northwest Sci.*, 88, 94–105.

Dunwiddie, P.W. & Bakker, J.D. (2011). The future of restoration and management of prairie-oak ecosystems in the Pacific Northwest. *Northwest Sci.*, 85, 83–92.

Dunwiddie, P.W. & Rogers, D.L. (2017). Rare species and aliens: reconsidering non-native plants in the management of natural areas. *Restor. Ecol.*, 25, S164–S169.

Dyer, A.R. & Rice, K.J. (1999). Effects of competition on resource availability and growth of a California bunchgrass. *Ecology*, 80, 2697–2710.

Elzinga, C.L., Salzer, D.W. & Willoughby, J.W. (1998). *Measuring & monitoring plant populations*. *U.S. Dep. Inter. Bur. L. Manag.*

Everard, K., Seabloom, E.W., Harpole, W.S. & De Mazancourt, C. (2010). Plant water use affects competition for nitrogen: Why drought favors invasive species in California. *Am. Nat.*, 175, 85–97.

Franklin, J., Serra-Diaz, J.M., Syphard, A.D. & Regan, H.M. (2016). Global change and terrestrial plant community dynamics. *Proc. Natl. Acad. Sci. U. S. A.*, 113, 3725–3734.

Friddle, M. (2018). *Plant guide for subterranean clover (Trifolium subterraneum)*. Corvallis.

Gee, G. & Bauder, J. (1986). Particle-size analysis. In: *Methods of Soil Analysis. Part 1. Physical and Mineralogical Methods* (ed. Klute, A.). American Society of Agronomy, Madison, Wisconsin, USA, pp. 383–411.

Gornish, E.S. & Tylianakis, J.M. (2013). Community shifts under climate change: Mechanisms at multiple scales. *Am. J. Bot.*, 100, 1422–1434.

Hallett, L.M., Hsu, J.S., Cleland, E.E., Collins, S.L., Dickson, T.L., Farrer, E.C., *et al.* (2014). Biotic mechanisms of community stability shift along a precipitation gradient. *Ecology*, 95, 1693–1700.

Harrison, S. (2020). Plant community diversity will decline more than increase under climatic warming. *Philos. Trans. R. Soc. B Biol. Sci.*, 375.

Harrison, S.P., Gornish, E.S., Copeland, S. & Levine, J.M. (2015). Climate-driven diversity loss in a grassland community. *Proc. Natl. Acad. Sci.*, 112, 1–6.

Harrison, S.P., LaForgia, M.L. & Latimer, A.M. (2018). Climate-driven diversity change in annual grasslands: Drought plus deluge does not equal normal. *Glob. Chang. Biol.*, 24, 1782–1792.

James, G., Witten, D., Hastie, T. & Tibshirani, R. (2013). *An Introduction to Statistical Learning with Applications in R*. 1st editio. Springer, New York, NY.

Jung, I.W. & Chang, H. (2012). Climate change impacts on spatial patterns in drought risk in the Willamette River Basin, Oregon, USA. *Theor. Appl. Climatol.*, 108, 355–371.

Kimball, B.A., Conley, M.M., Wang, S., Lin, X., Luo, C., Morgan, J., *et al.* (2008). Infrared heater arrays for warming ecosystem field plots. *Glob. Chang. Biol.*, 14, 309–320.

Klausmeyer, K.R. & Shaw, M.R. (2009). Climate change, habitat loss, protected areas and the climate adaptation potential of species in mediterranean ecosystems worldwide. *PLoS One*, 4.

Kottek, M., Grieser, J., Beck, C., Rudolf, B. & Rubel, F. (2006). World map of the Köppen-Geiger climate classification updated. *Meteorol. Zeitschrift*, 15, 259–263.

LaForgia, M.L., Harrison, S.P. & Latimer, A.M. (2020). Invasive species interact with climatic variability to reduce success of natives. *Ecology*, 101, 1–10.

Lefcheck, J.S. (2016). piecewiseSEM: Piecewise structural equation modelling in R for ecology, evolution, and systematics. *Methods Ecol. Evol.*, 7, 573–579.

Lemoine, N.P., Sheffield, J., Dukes, J.S., Knapp, A.K. & Smith, M.D. (2016). Terrestrial Precipitation Analysis (TPA): A resource for characterizing long-term precipitation regimes and extremes. *Methods Ecol. Evol.*, 7, 1396–1401.

Levine, J.M., McEachern, A.K. & Cowan, C. (2010). Do competitors modulate rare plant response to precipitation change? *Ecology*, 91, 130–140.

Lindh, B.C. (2018). Tipping the native-exotic balance: Succession in restored upland prairies in Oregon's willamette valley. *Ecol. Restor.*, 36, 28–40.

Ma, M., Collins, S.L. & Du, G. (2020). Direct and indirect effects of temperature and precipitation on alpine seed banks in the Tibetan Plateau. *Ecol. Appl.*, 30, 1–13.

Mariotte, P., Spotswood, E.N., Farrer, E.C. & Suding, K.N. (2017). Positive litter feedbacks of an introduced species reduce native diversity and promote invasion in Californian grasslands. *Appl. Veg. Sci.*, 20, 28–39.

Melgoza, G., Nowak, R.S. & Tausch, R.J. (1990). Soil water exploitation after fire: competition between Bromus tectorum (cheatgrass) and two native species. *Oecologia*, 83, 7–13.

Morris, E.K., Caruso, T., Buscot, F., Fischer, M., Hancock, C., Maier, T.S., *et al.* (2014). Choosing and using diversity indices: insights for ecological applications from the German Biodiversity Exploratories. *Ecol. Evol.*, 4, 3514–3524.

Mote, P.W. & Salathé, E.P. (2010). Future climate in the Pacific Northwest. *Clim. Change*, 102, 29–50.

Nakagawa, S., Johnson, P.C.D. & Schielzeth, H. (2017). The coefficient of determination R2 and intra-class correlation coefficient from generalized linear mixed-effects models revisited and expanded. *J. R. Soc. Interface*, 14.

Noss, R.F., LaRoe, E.T. & Scott, J.M. (1995). *Endangered ecosystems of the United States: A preliminary assessment of loss and degradation*.

Oksanen, J., Blanchet, F.G., Friendly, M., Kindt, R., Legendre, P., McGlinn, D., *et al.* (2019). vegan: Community Ecology Package. R package version 2.5-6. https://CRAN.R-project.org/package=vegan

Pecl, G.T., Araújo, M.B., Bell, J.D., Blanchard, J., Bonebrake, T.C., Chen, I.C., *et al.* (2017). Biodiversity redistribution under climate change: Impacts on ecosystems and human well-being. *Science (80-.).*, 355.

Pendergrass, A.G., Knutti, R., Lehner, F., Deser, C. & Sanderson, B.M. (2017). Precipitation variability increases in a warmer climate. *Sci. Rep.*, 7, 1–9.

Pfeifer-Meister, L., Bridgham, S.D., Little, C.J., Reynolds, L.L., Goklany, M.E. & Johnson, B.R. (2013). Pushing the limit: experimental evidence of climate effects on plant range distributions. *Ecology*, 94, 2131–2137.

Pfeifer-Meister, L., Bridgham, S.D., Reynolds, L.L., Goklany, M.E., Wilson, H.E., Little, C.J., *et al.* (2016). Climate change alters plant biogeography in Mediterranean prairies along the West Coast, USA. *Glob. Chang. Biol.*, 22, 845–855.

Prevéy, J.S. & Seastedt, T.R. (2014). Seasonality of precipitation interacts with exotic species to alter composition and phenology of a semi-arid grassland. *J. Ecol.*, 102, 1549–1561.

R Core Team (2020). R: A language and environment for statistical computing. R Foundation for Statistical Computing, Vienna, Austria. URL https://www.R-project.org/.

Reed, P.B., Bridgham, S.D., Pfeifer-Meister, L.E., Peterson, M.L., Johnson, B.R., Roy, B.A., *et al.* (In review). Climate warming threatens the persistence of a community of disturbance-adapted native annual plants.

Reed, P.B., Peterson, M.L., Pfeifer-Meister, L.E., Morris, W.F., Doak, D.F., Roy, B.A., *et al.* (2021). Climate manipulations differentially affect plant population dynamics within versus beyond northern range limits. *J. Ecol.*, 109, 664–675.

Reed, P.B., Pfeifer-Meister, L.E., Roy, B.A., Johnson, B.R., Bailes, G.T., Nelson, A.A., *et al.* (2019). Prairie plant phenology driven more by temperature than moisture in climate manipulations across a latitudinal gradient in the Pacific Northwest, USA. *Ecol. Evol.*, 9, 3637–3650.

Sala, O.E., Chapin Iii, F.S., Armesto, J.J., Berlow, E., Bloomfield, J., Dirzo, R., *et al.* (2000). Global biodiversity scenarios for the year 2100. *Science (80-.).*, 287, 1770–1774.

Saxton, K.E. & Rawls, W.J. (2006). Soil water characteristic estimates by texture and organic matter for hydrologic solutions. *Soil Sci. Soc. Am. J.*, 1578, 1569–1578.

Simpson, E.H. (1949). Measurement of diversity. *Nature*, 163, 688.

Sinclair, M., Alverson, E., Dunn, P., Dunwiddie, P. & Gray, E. (2006). Bunchgrass Prairies. In: *Restoring the Pacific Northwest: The Art and Science of Ecological Restoration in Cascadia* (eds. Apostol, D., Sinclair, M. & Higgs, E.). Island Press, Washington, DC, pp. 22–62.

Stanley, A.G., Kaye, T.N. & Dunwiddie, P.W. (2011). Multiple treatment combinations and seed addition increase abundance and diversity of native plants in Pacific Northwest prairies. *Ecol. Restor.*, 29, 35–44.

Thuiller, W., Richardson, D.M. & Midgley, G.F. (2008). Will climate change promote alien plant invasions? In: *Biological Invasions* (ed. Nentwig, W.). Springer, Berlin, Heidelberg, pp. 197–211.

USDA-Natural Resources Conservation Service. (2012). *'Zorro' annual fescue (Vulpia myuros)*. California Plant Materials Center, Lockeford, CA.

USDA-Natural Resources Conservation Service. (2014). *Conservation Plant Release Brochure for 'Blando' brome (Bromus hordeaceus subsp. hordeaceus)*. California Plant Materials Center, Lockeford, CA.

Warton, D.I. & Hui, F.K.C. (2011). The arcsine is asinine: the analysis of proportions in ecology. *Ecology*, 92, 3–10.

Chapter VI

Bachelet, D., Johnson, B. R., Bridgham, S. D., Dunn, P. V, Anderson, H. E., & Rogers, B. M. (2011). Climate change impacts on western Pacific Northwest prairies and savannas. *Northwest Science*, *85*(2), 411–429. https://doi.org/10.3955/046.085.0224

Boyd, R. (1999). Indians, fire, and the land. In *Oregon State University Press*. Retrieved from https://ecoshare.info/uploads/ccamp/synthesis_paper_tools/huckleberry/Boyd_1999.pdf

Dunwiddie, P. W., Alverson, E. R., Martin, R. A., & Gilbert, R. (2014). Annual species in native prairies of South Puget Sound, Washington. *Northwest Science*, *88*(2), 94–105. https://doi.org/10.3955/046.088.0205

Koteen, L. E., Baldocchi, D. D., & Harte, J. (2011). Invasion of non-native grasses causes a drop in soil carbon storage in California grasslands. *Environmental Research Letters*, *6*(4). https://doi.org/10.1088/1748-9326/6/4/044001

Noss, R. F., LaRoe, E. T., & Scott, J. M. (1995). *Endangered ecosystems of the United States: A preliminary assessment of loss and degradation*.

Pfeifer-Meister, L., Bridgham, S. D., Reynolds, L. L., Goklany, M. E., Wilson, H. E., Little, C. J., … Johnson, B. R. (2016). Climate change alters plant biogeography in Mediterranean prairies along the West Coast, USA. *Global Change Biology*, *22*(2), 845–855. https://doi.org/10.1111/gcb.13052